Investigating the interplay of diet and inflammation on cerebral ischaemia

A thesis submitted to The University of Manchester for the degree of Doctor of Philosophy in the Faculty of Biology, Medicine and Health

2020

Claire Stephanie White

School of Biological Sciences

Division of Neuroscience and Experimental Psychology

Contents

Word count: 67914

Abstract

Cerebral ischaemia occurs when cerebral blood flow (CBF) is compromised and brain tissue becomes starved of oxygen and nutrients, leading to cell death and neurological deficits. Ischaemic events in the brain can be either focal or global, and are major pathological features of age-related diseases, such as stroke and dementia. Several modifiable risk factors, such as diet, can exacerbate ischaemic damage. The aim of this thesis was to investigate how different dietary states, obesity and high sugar, affect inflammation and ischaemic outcomes in murine models of global and focal ischaemia.

In order to investigate global ischaemic pathology, we sought to characterise a mouse model of chronic cerebral hypoperfusion, bilateral common carotid artery occlusion (BCAS). We demonstrated a sustained reduction in CBF at 3 months in BCAS animals; however, consequent neuropathology and cognitive deficits were absent. Additionally, we measured clinically validated markers of hypoperfusion (vascular endothelial growth factor, myelin associated protein, and proteolipid protein 1), that had not previously been investigated in the context of the BCAS, but found that there was no change in tissue oxygenation. We hypothesise that the reduction in CBF was not severe enough to induce global ischaemia and subsequent neuropathology.

Turning our focus to focal ischaemic pathology, we used middle cerebral artery occlusion (MCAo) to investigate how diet affects ischaemic injury. We found that stroke induced long-term changes in depressive/anxiety-like behaviours, and also altered the levels of plasma lipids and adipokines, which may have negative impacts on vascular health. Obese mice also had long-term alterations in depressive and anxiety-like behaviours after stroke, but these changes did not differ significantly from lean mice that had equivalent lesion volumes.

Next, we investigated how hyperglycaemia affects stroke outcomes. We found that hyperglycaemia exacerbates ischaemic brain damage by augmenting interleukin (IL)-1β dependent post-stroke inflammation. We showed that macrophage production of IL-1β post-stroke is glycolysis dependent, and in the context of hyperglycaemic conditions, is potentiated by increased substrate availability. Furthermore, we identify pyruvate as an essential metabolite downstream of glycolysis that regulates IL-1β production, and we hypothesise that this is mediated via succinate accumulation.

This thesis produces mechanistic insight into the inflammatory pathology of focal and global ischaemia. Specifically, we have shown that obese and hyperglycaemic states have distinct impacts on post-stroke outcomes, primarily by regulating inflammatory and metabolic processes in immune cells. Ultimately, gaining a better mechanistic insight into how diet-related diseases and dietary factors modulate ischaemic pathology may help identify new therapeutic targets, increase health and lifestyle education, and improve public awareness.

Declaration

Work included in Chapter 3 of this thesis has previously been submitted as part of MSci (Kelly O'Toole and Daisy Roberts) and BSc dissertations (Conor Lane and Oliver Heaney), where I supervised students throughout their projects. I declare that no other portion of the work referred to in the thesis has been submitted in support of an application for another degree or qualification of this or any other university or other institute of learning.

Claire White

26/03/2020

Copyright Statement

Thesis Format

This thesis has been submitted in journal format to allow the inclusion of published papers. This consists of a general introduction, three results chapters, general discussion and references. This format has been approved by the University of Manchester Doctoral Academy (presentation of theses policy, section 9).

Acknowledgements

Firstly I would like to thank my incredible supervisory team, Stuart, Cath and Pat. It has been a privilege to have supervisors with exceptional knowledge and passion for science, but are also an absolute pleasure to be around and to work alongside. It has been particularly great to have Pat join my supervisory team half way through my project, and kicking off the immunometabolism madness that this PhD has turned into - you're a bloody good bloke, and I am certain you are going to have an incredible academic career. Thank you to my collaborators Karen Horsburgh and Scott Miners whose time and contributions have significantly shaped the work presented in this thesis. Importantly, none of this work would be possible without the generous donation and continued support of my funder, Edward Bonham-Carter – thank you so much for the opportunity to do my PhD, and funding much-needed research into mechanisms of cerebrovascular disease. Other funding bodies which supported this work include Alzheimer's Research UK and Kohn Foundation.

I would like to make a special mention to a number of senior members of the group whose expertise, advice and patience have been invaluable. First, Dr. Michael exHaley for designing the stroke study, conducting all stroke surgeries and imparting invaluable *in vivo* research knowledge. Secondly, Dr. Jack Auty for intense statistical and behavioural consultation - you rock. Last, but not least, Dr. Elena Redondo-Castro, the proud co-founder of the sisters in science, *come back please*. To all the other BIG members, I consider myself very lucky to have ended up in such a social and supportive group. In particular those that I have shared many, many, pints with in Big Hands, the ladz (Siddhu and Bad Jack) and the sassy gals (Victor, Hannah, Tess, Siobhan and Ohud); you're bloody brilliant. I would like to do a big shout out to all the masters and undergraduate students I have worked with throughout my PhD and that have contributed to this work: Kelly, Daisy, Connor, and Ollie. I would also like to acknowledge the contribution of excellent core facilities units at the university: Bioimaging, BSF, and Genomics.

My life in Manchester would not be complete without my gorgeous and amazing friends who fill every day with laughter and happiness. Every. Single. Central road hun (Caitlin, Catrin, July, Imi, Billy, Jack and Josh) is a hun of ginormous magnitude. Thanks for every gourmet dinner, quick cuppa, and all the boozy weekends. And especially to the QTs, Ellie and Becky, coming home to you every day is a delight. Our little home is a sanctuary, thank you for being there through all the peaks and pits.

My family are my rock. My supportive unit: Mom, Dad, Laura and Hannah; have always made me believe that I can do anything. You have supported me through everything, and will continue to always be there for me. I can't thank you enough for everything you have done to get me here. I dedicate this thesis to my loving Grandmothers, Barbara and Kath, who weren't around to see this through to the end.

Finally to Dr COB. With all the incredible experiences I have had throughout this PhD, hands down the best thing to come out of it was you. Thank you for constantly reassuring me and supporting me, and importantly, thank you for never calling HR on me. Sharing this PhD journey with you has been so special, and now it's time to start some new journeys.

List of Figures

List of Tables

Abbreviations

2DG	2-Deoxyglucose
2-VO	2 vessel occlusion
AC	Ameroid microconstrictors
ACAS	AC arterial stenosis
AD	Alzheimer’s disease
ADNI	Alzheimer’s disease Neuroimaging Initiative
AIM2	Absent in melanoma 2
ALT	Alanine aminotransferase
AMPA	α-amino-3-hydroxy-5-methyl-4-isoxazole propionic acid
ANOVA	One-way analysis of variance
APOE	Apolipoprotein E
ASC	Apoptosis-associated speck-like protein containing a CARD
ATP	Adenosine triphosphate
BBB	Blood brain barrier
BCA	Bicinchoninic protein assay
BCAS	Bilateral carotid artery stenosis
BMDM	Bone marrow derived macrophages
BMI	Body mass index
BPTES	Bis-2-(5-phenylacetamido-1,3,4-thiadiazol-2-yl)ethyl sulfide
BSA	Bovine serum albumin
CAA	Cerebral amyloid angiopathy
CADASIL	Cerebral autosomal dominant arteriopathy with subcortical infarcts and leukoencephalopathy
CARASIL	Cerebral autosomal recessive arteriopathy with subcortical infarcts and leukoencephalopathy
CBF	Cerebral blood flow
CCA	Common carotid artery
CCL	C-C Motif Chemokine Ligand
CCR	C-C Motif Chemokine Receptor
CRP	C-reactive protein
CSF	Cerebrospinal fluid
CT	Computerized tomography
CXCL	C-X-C motif ligand
DAMP	Danger-associated molecular patterns
DASH	Dietary Approaches to Stop Hypertension
DBM	Diethyl butylmalonate
dMCAo	Distal middle cerbral artery occulusion
DMEM	Dulbecco's Modified Eagle Medium
DNA	Deoxyribonucleic acid
DS	Diethyl succinate
ECAR	Extracellular acidification rate
ELISA	Enzyme-linked immunosorbent assay

EtOp	Etoposide
FAO	Fatty acid oxidation
FBS	Fetal bovine serum
FFA	Free fatty acids
FINGER	Finnish Geriatric Intervention Study to Prevent Cognitive Impairment and Disability
GABA	Gamma aminobutyric acid
GCAS	Gradual carotid artery stenosis
GFAP	Glial fibrillary acidic protein
GIST-UK	UK Glucose Insulin in Stroke Trial
Glc	Glucose
GLMM	Generalised linear mixed modelling
HIF	Hypoxia-inducible factor
HighGlc	High glucose containing DMEM
HMGB1	High mobility group box 1
i.p	Intraperitoneal
i.v.	Intravenously
Iba1	Ionized calcium binding adaptor molecule-1
ICAM	Intercellular adhesion molecule
IFNγ	Interferon-gamma
IgG	Immunoglobulin G
IL	Interleukin
IL-1R1	IL-1 receptor 1
IL-1RA	IL-1 receptor antagonist
IL-1RAcP	IL-1 receptor accessory protein
IL-1α	Interleukin-1α
IL-1β	Interleukin-1β
IQ	Interquartile range
KEAP1	Kelch-like ECH-associated protein 1
LDH	Lactate dehydrogenase
LDH_A	Lactate dehydrogenase A
LPS	Lipopolysaccharide
LSCI	Laser speckle contrast imaging
MAG	Myelin-associated glycoprotein
MAPT	French Multidomain Alzheimer Preventive Trial
MCA	Middle cerebral artery
MCAo	Middle cerebral artery occlusion
MIND	Mediterranean-Dietary Approaches to Stop Hypertension Intervention for Neurodegenerative Delay
MMP	Matrix metalloproteinases
MRI	Magnetic resonance imaging
MTT	3-(4,5-dimethylthiazol-2-yl)-2,5-diphenyltetrazolium bromide
MWM	Morris water maze
NFκB	Nuclear factor kappa-light-chain-enhancer of activated B cells
NLR	NOD-like receptor

NLRC4	NOD-, LRR- and CARD-containing 4
NLRP	NOD-, LRR- and pyrin domain-containing
NMDA	N-methyl-d-aspartic acid
NO	Nitric oxide
NOR	Novel object recognition
NormGlc	Normal glucose containing DMEM
NRF2	Nuclear factor erythroid 2-related factor 2
OCR	Oxygen consumption rate
OXPHOS	Oxidative phosphorylation
PAMP	Pathogen associated molecular patterns
PBS	Phosphate buffered saline
PBST	Phosphate-buffered saline, 1% Tween 20
PCR	Polymerase chain reaction
PDGFR-β	Platelet Derived Growth Factor Receptor Beta
PenStrep	Penicillin streptomycin
PFA	Paraformaldehyde
PFKFB3	6-phosphofructo-2-kinase/fructose-2,6-biphosphatase-3
PHD	Prolyl hydroxylase domain
PLP	Proteolipid protein 1
PMSF	Phenylmethylsulfonyl fluoride
pO_2	Partial pressure of oxygen
PreDIVA	Dutch Prevention of Dementia by Intensive Vascular Care
PRRs	Pattern recognition receptors
RCT	Randomised control trial
RNA	Ribonucleic acid
RNA-seq	Ribonucleic acid sequencing
ROS	Reactive oxygen species
RT	Room temperature
rtPA	Recombinant tissue plasminogen activator
SD	Standard deviation
SDH	Succinate dehydrogenase
SDS	Sodium dodecyl sulfate
SEM	Standard error of mean
SHR	Spontaneously hypertensive rats
SPRINT	Systolic Blood Pressure Intervention Trial
SPSHR	Stroke prone spontaneously hypertensive rats
SVD	Small vessel disease
TBST	Tris-buffered saline-TWEEN
TCA	Tricarboxylic acid cycle
TLR	Toll-like receptors
TNFα	Tumor necrosis factor
tPA	Tissue plasminogen activator
TrisEDTA	Ethylenediaminetetraacetic acid
Tris-HCl	Tris hydrochloride

TTC	Triphenyltetrazolium
UCCAo	Unilateral common carotid artery occlusion
VCAM	Vascular cell adhesion molecule
VEGF	Vascular endothelial growth factor
VWF	von Willebrand factor
WML	White matter lesions

Chapter 1. Introduction

1.1. Cerebral ischaemia

The brain is the body's most energetically demanding organ, accounting for over 20% of the total energy consumption and requiring a constant supply of blood to sustain metabolic activity (Magistretti and Allaman, 2015). Disruption to this cerebral blood flow (CBF) can result in an ischaemic state, which can have potentially devastating effects on brain function. There are two types of cerebral ischaemia, focal ischaemia and global ischaemia; these are major pathological events central to the aetiologies of common vascular and age-related diseases, such as stroke and dementia. Focal ischaemia occurs as a result of the complete cessation of blood flow in a specific region of the brain, with large cerebral vessels most typically affected. Global ischaemia, on the other hand, is the result of diminished CBF to many brain regions, and can be caused by cardiac insufficiency (heart failure, cardiac arrhythmias), peripheral and cranial vessel stenosis, and small vessel disease (SVD) (Ciacciarelli et al., 2020); SVD in particular is a major contributor to vascular dementia and has a growing global burden (O'Brien and Thomas, 2015). During cerebral ischaemia, the brain is subject to hypoxic conditions that initiate an irreversible cascade of events of cell death, inflammation, tissue damage, and distinct functional and cognitive deficits.

1.2. Ischaemic stroke

There are two broad classifications of stroke: ischaemic and haemorrhagic. Ischaemic stroke accounts for approximately 70% of overall stroke cases and occurs in response to a blockage in cerebral blood vessels (Campbell et al., 2019). The remaining stroke cases are haemorrhagic, caused by the rupture of cerebral blood vessels. For the purposes of this thesis, attention will be focused on ischaemic stroke. Combined, ischaemic and haemorrhagic stroke affect over 13 million people worldwide, with stroke being the second leading cause of death after ischaemic heart disease (Campbell et al., 2019; GBD 2016 Stroke Collaborators, 2019). As well as being a major cause of mortality, stroke is also the third most common cause of morbidity; there are over 80 million stroke survivors worldwide, many of whom are left with significant disabilities (GBD 2016 Stroke Collaborators, 2019). In addition, stroke-related mortality and morbidity is associated with a huge economic burden, where it is estimated to cost approximately £26 billion a year in the UK alone (Stroke Association, 2015). Improved prevention strategies and treatments have resulted in reduced incidence and mortality rates in developing

countries, though prevalence is still increasing because of the ageing population. Consequently, there are many stroke survivors living with stroke-induced disabilities and post-stroke dementia, which are major unmet clinical needs (Pollock et al., 2012).

1.2.1. Aetiology of ischaemic stroke

Ischaemic strokes are most commonly associated with thromboemboli that result from large artery atherosclerosis (23%) or cardioembolism (22%) (Adams et al., 1993). During atherosclerosis, plaques that are rich in low-density lipoprotein build up in vessel walls (Bentzon et al., 2014). Over a long period of time, plaque burden can advance to completely occlude the affected blood vessel or, more commonly, lead to the formation of emboli that occlude vessels distal to the plaque. Embolism of atherosclerotic plaques in peripheral vessels, such as the common carotid, is a major contributor to ischaemic stroke (Marulanda-Londoño and Chaturvedi, 2016), whereas intracranial atherosclerosis is less common. The latter is more commonly observed in Asian populations than in western populations (Holmstedt et al., 2013; Kim et al., 2018). Cardioembolic strokes commonly occur due to atrial fibrillation, a process in which thrombi form in the atrium due to arrhythmias, and can subsequently travel as emboli in the circulation to occlude cerebral vessels. Anticoagulation strategies for atrial fibrillation have been used to reduced risk of cardioembolic stroke; however, this has been associated with increased risk of haemorrhage (Best et al., 2019). Furthermore, stroke is associated with increased risk of atrial fibrillation, as stroke damage in turn can promote dysrhythmia (Kamel et al., 2016). Other causes of stroke include: SVD (22%) and genetic forms (3%), although in one quarter of cases, the aetiology is unknown (Adams et al., 1993). All of the described stroke aetiologies can contribute to transient ischaemic attacks, which are characterised by temporary blockage of CBF, spontaneous resolution, and no permanent cerebral damage. However, transient ischaemic attacks are associated with a 10% increased risk of having a recurring stroke (Coutts, 2017), as well as an increased risk of dementia (Pendlebury and Rothwell, 2019).

1.2.2. Ischaemic stroke treatment

Currently approved therapies for ischaemic stroke aim to promote vessel recanalisation by breaking down or removing the clot. Alteplase is a recombinant form of tissue plasminogen activator (tPA) administered intravenously (i.v.), functioning via cleavage of plasminogen to plasmin which in turn degrades fibrin-rich clots and restores CBF (Campbell et al., 2019). Tenecteplase is a genetically modified version of tPA with longer half-life, and has greater specificity for fibrin than alteplase (Tanswell et al., 2002). Currently, tenecteplase is only licensed for use in India; however, ongoing clinical trials have demonstrated that the efficacy and safety profile is superior to alteplase (Coutts et al., 2018; Campbell et al., 2019). The major limitation of i.v. thrombolytic therapies is that they are only efficacious in a short time window, within approximately 4.5 hours after stroke onset (Emberson et al., 2014); the efficacy of these treatments decreases markedly with delayed administration (Muchada et al., 2014). A short therapeutic time window, combined with delayed disease presentation and lengthy hospital admission times, has resulted in only 10% of stroke admissions in the UK qualifying for thrombolysis treatment (McMeekin et al., 2017). Furthermore, the main adverse effect of thrombolysis is an increased risk of haemorrhage, and with it, worse outcomes (Campbell et al., 2019). Therefore, before thrombolytic treatment can be administered, neuroimaging must confirm ischaemic rather than haemorrhagic aetiology, and patients with history of uncontrolled hypertension and systemic bleeding are excluded from treatment (Powers et al., 2018). Apart from tPA, no other drugs to date have been effective for treating ischaemic stroke, despite an estimated $1 billion dollars to date being spent on developing new pharmacological therapies(Feuerstein and Chavez, 2009).

In the past 5 years, vessel recanalisation approaches in stroke have been revolutionised through the development of endovascular thrombectomy to surgically remove thromboemboli and restore CBF. Several clinical trials have reported high efficacy compared with tPA, and an extended therapeutic window of 6 hours (Goyal et al., 2016); in addition, some trials have even demonstrated efficacy up to 24 hours after onset (Albers et al., 2018; Nogueira et al., 2018). Mechanical thrombectomy is also not associated with subsequent risk of haemorrhage, meaning that more patients are eligible for this treatment (Campbell et al., 2019). Despite these advantages, the technically demanding nature of this

procedure and lack of skilled operators are major obstacles preventing more widespread utilisation. Indeed, it has been estimated that although 10% of ischaemic stroke patients are eligible for thrombectomy, less than 1% of patients receive this treatment (McMeekin et al., 2017). With more specialists being trained and the expansion of thrombectomy services in stroke centres worldwide, the number of patients receiving treatment should increase significantly in the coming years.

Independent of pharmacologic and mechanical approaches, the greatest overall benefit for stroke patients is being admitted into a specialised stroke unit (Langhorne, 1997). This ensures patients are treated by dedicated staff who manage the prevention of secondary complications and instigate early rehabilitation. A further extension of specialised stroke care is the introduction of mobile stroke units, which comprise ambulances equipped with CT scanners to facilitate rapid diagnosis and early thrombolytic treatment; these units have been shown to be effective in Germany (Ebinger et al., 2014). Despite specialised stroke units providing better care, they are limited by the lack of effective therapies available. Current treatments are restricted to a subset of patients, and there are no therapeutics that modulate damage or improve recovery following ischaemia. Consequently, there is an unmet need to develop new treatments that reduce ischaemic injury acutely and facilitate neurological repair.

1.2.3. Pathophysiology of ischaemic stroke

Prolonged cessation of blood flow in the brain triggers an ischaemic cascade that ultimately results in neuronal death. The tissue in the core, the area most deprived of CBF, becomes deficient in oxygen and glucose, which halts cellular metabolism and adenosine triphosphate (ATP) generation (Dirnagl et al., 1999). A lack of energy results in an ionic imbalance; the resting membrane potential cannot be maintained via ATP-dependent channels and neurons become depolarised and release neurotransmitters such as glutamate (Martin et al., 1994; Dirnagl et al., 1999). Glutamate is an excitatory neurotransmitter and initiates the next stage of the ischaemic cascade, excitotoxicity. Glutamate can induce neuronal cell death both directly and indirectly (the latter by cytotoxic oedema). Glutamate activates AMPA and NMDA receptors to further exacerbate the ionic imbalance, facilitating cytotoxic oedema by increasing osmolarity (Lipton, 1999), and the next wave of

damage via Ca^{2+}. Intracellular Ca^{2+} contributes to a loss of cellular integrity by activating of proteases, lipases and nucleases (Lipton, 1999), and mediates the accumulation of reactive oxygen species (ROS) (Dirnagl et al., 1999). Oxidative stress induces further cellular injury and contributes to induction of an inflammatory response. In addition, ATP insufficiency leads to necrotic (ATP-independent) rather than apoptotic (ATP-dependent) cell death, wherein cell membrane rupture and the release of cellular contents, drives inflammatory responses. Inflammation is critical in determining the extent of ischaemic injury, and will be discussed further in later sections. Oxidative stress and inflammatory mediators both promote increased blood brain barrier (BBB) permeability through transcellular and paracellular routes (Iadecola and Anrather, 2011). BBB opening exacerbates oedema, and facilitates entry of immune cells and blood serum proteins into the parenchyma further impacting neuronal cell death. Even in the event that normal CBF is restored, such as following clot thrombolysis, further vascular damage, known as reperfusion injury, can occur (Eltzschig and Eckle, 2011).

1.3. Small vessel disease

In contrast to the aforementioned large-vessel strokes, SVD affects the small vessels of the brain: arterioles, capillaries and venules. SVD has an extremely heterogeneous presentation that is dependent on the extent of the pathology, and which vessels are affected (Wardlaw et al., 2013). Neuroimaging techniques (MRI and CT) can detect various SVD-related lesions, including white matter hyperintensities, lacunes, small subcortical infarcts, enlarged perivascular spaces and microbleeds (*Fig. 1.1*) (Wardlaw et al., 2019). These lesions can be asymptomatic, or manifest as a broad range of clinical symptoms such as cognitive impairment, mood disturbances and abnormal gait (Rajani and Williams, 2017). SVD directly contributes to both ischaemic stroke and dementia; it has been reported that 1 in 5 strokes are caused by SVD (Pantoni et al., 2010) and SVD also results in worse outcome after stroke (IST-3 collaborative group, 2015). Moreover, neuropathological examinations of brains of Alzheimer's disease (AD) patients found that 80% had distinct vascular pathology (Toledo et al., 2013; Power et al., 2018). Given the heterogenous phenotype of SVD, and its role in other age-related diseases, the prevalence is difficult to ascertain.

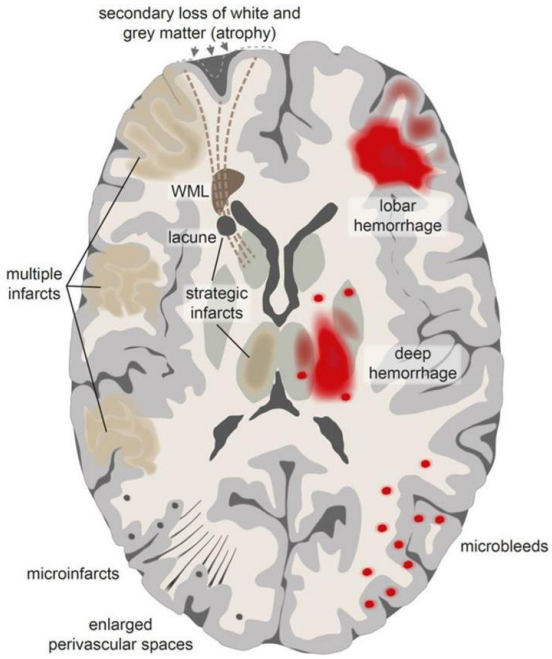

Figure 1.1 - Distinct cerebrovascular pathologies underly the heterogeneous clinical manifestations of SVD.
Figure adapted from Dichgans and Leys (2017).

1.3.1. Aetiology of small vessel disease

There are 3 major aetiopathogenic classifications of SVD: arteriolosclerosis, cerebral amyloid angiopathy (CAA) and rare familial forms; of which, arteriolosclerosis and CAA are most prevalent (Pantoni et al., 2010). Arteriolosclerosis, also known as hypertensive arteriopathy, is characterised by thickening of the arteriole vessel wall and vessel lumen stenosis. Histopathological features of arteriolosclerosis include microatheromas (small lipid-containing vascular lesions), lipohyalinosis (asymmetric thickening of vessel wall with deposits of hyaline) and fibrinoid necrosis (necrosis of smooth muscle cell and subsequent fibrin deposition) (Pantoni et al., 2010; Wardlaw et al., 2013). Vessels become tortuous and lose integrity, becoming dysfunctional (Román and Benavente, 2004). The pathogenesis of these vascular lesions is not well understood, but is strongly associated with ageing, hypertension, diabetes and atherosclerosis (Pantoni et al., 2010). The second subcategory of SVD pathology is CAA, characterised by amyloid-β accumulation around arterioles and capillaries, namely the leptomeningeal vessels (Werring, 2018). Amyloid accumulation results in vessel dilation and subsequent vessel rupture, which manifests as microbleeds

and large lobular haemorrhages (Smith and Eichler, 2006). The development of CAA is predominantly sporadic in nature and it is extremely common; it is reported that over 90% of individuals with dementia have CAA (Arvanitakis et al., 2011). In addition to sporadic forms, rare familial CAA-related mutations have also been identified (Banerjee et al., 2017). This third category of small vessel pathology encompasses rare genetic forms of SVD, including: cerebral autosomal dominant arteriopathy with subcortical infarcts and leukoencephalopathy (CADASIL) (Joutel et al., 1996); cerebral autosomal recessive arteriopathy with subcortical infarcts and leukoencephalopathy (CARASIL) (Fukutake, 2011); Col4A1 mutations (Lanfranconi and Markus, 2010); and Fabry's disease (Kolodny et al., 2015). Ultimately, these microangiopathies impede cerebral perfusion and contribute to both focal and global ischaemic events, the progression of white matter lesions (WML), and neurodegeneration and cortical thinning (Wardlaw et al., 2019).

Current therapies for the treatment and prevention of SVD are limited, and are predominantly targeted at managing risk factors. Randomised control trials (RCT) to test the efficacy of anti-hypertensive (Dufouil et al., 2005; Weber et al., 2012) and lipid-lowering drugs (Ten Dam et al., 2005) to reduce WML have not found any clinical benefit for patients. Additionally, the recent Systolic Blood Pressure Intervention Trial (SPRINT) MIND trial found that reducing systolic blood pressure to <120 mm Hg, compared to <140 mm Hg, did not reduce the risk of dementia, but did reduce the incidence of mild cognitive impairment by 19% (Williamson et al., 2019). These results demonstrate that SVD is poorly understood, and a better understanding of the underlying disease mechanisms may drive the development of novel and more effective therapeutics.

1.3.2. Pathophysiology of small vessel disease

In contrast to the well-defined sequence of events that occur before, during and after ischaemic stroke, SVD pathophysiology has not been fully elucidated. WMLs are the major pathology observed in patients with SVD, and are indicated by MRI as white matter hyperintensities which are predominantly subcortical or periventricular (Alber et al., 2019). White matter hyperintensities that contribute to SVD are presumed to be of vascular origin, although exactly how microvasculopathies cause WMLs and contribute to SVD is not well understood.

The current literature proposes two major theories for how SVD-related WML develop. The first theory proposes that chronic hypoperfusion contributes to WML progression and SVD. Distinct WMLs have been associated with chronic hypoperfusion due to cranial atherosclerosis and cardiac insufficiency (Román and Benavente, 2004). However, the contribution of microvascular stenosis to WML formation is not as clearly defined (Fisher, 1982). Several neuroimaging studies have demonstrated that subjects with WMLs have lower resting CBF than those with normal-appearing white matter (Sam et al., 2016; Van Dalen et al., 2016). A further study assessing WMLs and histopathological markers of hypoxia (hypoxia-inducible factor (HIF)-1α and HIF-2α) in post-mortem tissue found that WMLs were associated with a hypoxic environment (Fernando et al., 2006); this indicates that reduced perfusion may be a causative factor in the development of WMLs. However, a systematic review of the literature surrounding CBF and WML, which excluded studies without appropriate age-matched controls, found there was no longer a strong association between CBF and WML (Shi et al., 2016). Additionally, patients with a genetic form of SVD, CADASIL, have no change in CBF in white matter (Chabriat et al., 2000). Consequently, it is suspected that rather than having a causal role in WML progression, hypoperfusion is a downstream response to tissue damage that is caused through other mechanisms.

The second theory proposes that distinct vascular pathology causes endothelial dysfunction and BBB permeability that consequently drives SVD-related WML formation (Wardlaw et al., 2003). Endothelial dysfunction can facilitate the disruption of endothelial tight junctions, the basement membrane and key cells that make up the neurovascular unit (astrocyte and pericytes). Ultimately, disruption of any of these factors can facilitate the passage of blood serum proteins into the brain parenchyma, which can have deleterious effects on homeostatic brain function (Joutel and Chabriat, 2017). Firstly, BBB permeability facilitates fluid accumulation in the interstitial space, which causes oedema and contributes to further vascular changes, such as thickened and stiff vessel walls (Wardlaw et al., 2019). Secondly, the extravasation of fibrinogen has been shown to contribute to WMLs and perivascular tissue damage by: activating microglia and perivascular macrophages; impairing myelin repair by inhibiting oligodendrocyte precursor cell maturation; and impairing amyloid-β clearance (which has relevance for CAA pathology) (Petersen et al., 2018; Wardlaw et al., 2019). Ultimately, BBB leakage

contributes to demyelination and a loss of white matter integrity; this can have direct effects on cognition through impaired signal transmission, and further indirect effects on cognition through secondary neurodegeneration and cortical thinning (Duering et al., 2015; Wardlaw et al., 2019).

The association between BBB permeability and WMLs has been demonstrated by multiple methodologies, including biomarker and histopathological analyses, and by neuroimaging techniques. Levels of serum albumin in cerebrospinal fluid (CSF) can be used as a biomarker for BBB permeability. A systematic review found that an elevated CSF/serum albumin ratio correlates with vascular dementia and WML burden in patients (Farrall and Wardlaw, 2009). Histopathological studies have demonstrated BBB permeability by immunostaining for extravasated serum proteins (immunoglobulin G (IgG), complement and fibrinogen) in white matter regions (periventricular and deep white matter) (Akiguchi et al., 1997; Hainsworth et al., 2017). Finally, neuroimaging studies show that SVD patients have increased BBB permeability (Huisa et al., 2015; Muñoz Maniega et al., 2017). Additionally, BBB leakage increases with proximity to WMLs (Wardlaw et al., 2017), and increased BBB permeability is a prognostic predictor of WML evolution (Van Leijsen et al., 2018). Combined, this evidence supports that endothelial dysfunction and subsequent BBB permeability drives WML progression and SVD.

Downstream consequences of endothelial disruption and BBB breakdown are reduced CBF, and reduced cerebrovascular reactivity (Joutel and Chabriat, 2017). Thickened vessel walls through fluid accumulation will negatively impact vessel function, impairing CBF and promoting hypoperfusion (Wardlaw et al., 2019). Moreover, tissue damage and cellular loss reduce metabolic demand, further decreasing CBF (Joutel and Chabriat, 2017). Consequently, reduced perfusion promotes a hypoxic environment that further exacerbates BBB permeability. Indeed, oligodendrocyte precursor cells are reported to express matrix metallopeptidase (MMP)-9 in hypoxic conditions, which disrupts BBB integrity and leads to a self-perpetuating cycle of damage (Seo et al., 2013).

1.4. Risk factors of cerebral ischaemia

The pathological mechanisms and clinical presentations of cerebral ischaemia can be extremely heterogeneous, in part due to the wide array of risk factors associated with the initiation and progression of the disease. Age, sex and genetics are the most important non-modifiable risk factors for stoke; stroke risk doubles every decade from the age of 55 onwards (Wolf et al., 1992), and there is a 33% greater incidence of stroke in men than women (Appelros et al., 2009). The INTERSTROKE trial identified 10 modifiable risk factors that accounted for 90% of all strokes (O'Donnell et al., 2010). These factors were: hypertension; physical inactivity; dysregulated apolipoproteins; poor diet; elevated waist-to-hip ratio; psychosocial factors; smoking; cardiovascular events; alcohol consumption; and diabetes mellitus. Hypertension was the most important risk factor, accounting for 35% of all strokes (O'Donnell et al., 2010). These risk factors were almost identical to those identified in the INTERHEART trial as contributors to myocardial infarction, further demonstrating the importance of vascular health (Yusuf et al., 2004). Impressively, O'Donnell *et al* extended this trial to investigate these risk factors globally in 32 countries, and were able to identify precise regional differences that may help influence country-specific stroke prevention strategies (GBD 2016 Stroke Collaborators, 2016).

In light of these modifiable risk factors, the concept of a polypill, containing a low dosage of blood pressure-lowering agents (aspirin and statins) has been proposed to prevent ischaemic events (Campbell et al., 2019). Although this has been trialled for heart disease, it has not yet been investigated for stroke (Castellano et al., 2014). In the context of dementia, studies of lifestyle-based preventions have attempted to reduce the impact of modifiable risk factors on disease development. For example, the Finnish Geriatric Intervention Study to Prevent Cognitive Impairment and Disability (FINGER) trial implemented multidomain interventions consisting dietary counselling, exercise, cognitive training, social activities, and the monitoring and movement of vascular and metabolic risk factors; the trial showed a 25% improvement in cognitive performance in patients with a high dementia risk score (Ngandu et al., 2015). Currently, this multidomain intervention strategy is being extended into a worldwide RCT (Kivipelto et al., 2018).

1.4.1. Dietary risk factors and cerebral ischaemia

Interestingly, of the 10 modifiable risk factors identified in the INTERSTROKE study, 7 (hypertension, dysregulated apolipoproteins, poor diet, elevated waist-to-hip ratio, cardiovascular events, alcohol consumption, and diabetes mellitus) are directly influenced by diet (O'Donnell et al., 2010; GBD 2016 Stroke Collaborators, 2016); this highlights the importance of dietary influences on modulating the likelihood of cerebral ischaemia. Indeed, it has been estimated that dietary interventions may decrease stroke risk by 19% (Rees et al., 2013).

Diet-related diseases, such as obesity, are huge social and economic burdens. The global prevalence of obesity is rapidly increasing; it was estimated that in 2016 there were >1.9 billion adults overweight, and 650 million were obese (Nyberg et al., 2018), and this is associated with $2 trillion related health costs a year globally (Dobbs et al., 2014). Simply, obesity is a result of a long-term energy imbalance, when more calories are consumed than are expended, and is clinically defined as a body mass index (BMI) >30 kg/m^2, or a waist-to-hip ratio of >0.8 women or >0.9 for men (Blüher, 2019). In the INTERSTROKE trial, waist-to-hip ratio was directly implicated with increased risk of stroke. Obesity also directly affects the development of hypertension and hyperlipidemia, impacting on subsequent cardiovascular events such as atrial fibrillation and atherosclerosis, which are both critical in ischaemic stroke pathogenesis (Rocha and Libby, 2009; Vyas and Lambiase, 2019). Moreover, increased BMI has been shown to reduce CBF, contributing to chronic hypoperfusion (Alosco et al., 2012), and is also associated with increased risk of dementia (Kivimäki et al., 2018).

High-salt diets are strongly linked with hypertension (Rose et al., 1988) and reducing salt intake is effective to lower blood pressure (He and MacGregor, 2002). Hypertension as a result of a high-salt diet is associated with a significantly increased risk of cardiovascular disease and stroke (Strazzullo et al., 2009); it has been estimated that a reduction in sodium intake by 100 mmol/day would lower blood pressure and reduce stroke mortality by 25% (Stamler et al., 1989). Lifestyle approaches to reduce dietary salt using the Dietary Approaches to Stop Hypertension (DASH) diet (a diet rich in vegetables, fruits, and low-fat dairy products) demonstrated substantial reductions in blood pressure (Sacks et al., 2001). Moreover, the DASH diet has been associated with decreased risk of stroke

(Feng et al., 2018). A modified DASH diet, the Mediterranean DASH (MIND) diet, which is designed to be rich in fruit and vegetables that have reported neuroprotective effects, is associated with a reduced rate of cognitive decline (Morris et al., 2015). Consequently, the American Heart Association recommend a reduced sodium intake of 1500 mg/day (Appel et al., 2011).

Glucose is another dietary component that contributes to poorer outcome after cerebral ischaemia. High-sugar diets are associated with the development of type 2 diabetes mellitus (Ley et al., 2014), which is characterised by insulin resistance and uncontrolled blood glucose levels (DeFronzo et al., 2015). Diabetes has well-established atherosclerotic manifestations that are attributable to the chronic effects of hyperglycaemia, insulin resistance and free fatty acids on the vascular endothelium; this promotes vasoconstriction, inflammation and thrombosis (Creager et al., 2003). In line with this, diabetes mellitus was identified as a modifiable risk factor in the INTERSTROKE trial; however, controlling diabetes via glycaemic control has not shown any benefit for preventing stroke in 3 major RCTs (Hewitt et al., 2012). Moreover, diabetes has been associated with dementia, and AD has been referred to as “type 3 diabetes”, due to shared pathological features. Alongside profound effects on the vasculature, insulin resistance in neurons may play an important role in memory decline (Willette et al., 2015; Zhao et al., 2017), and phase II trials of an insulin nasal spray has improved cognitive decline (Claxton et al., 2013). Independent of diabetes status, hyperglycaemia alone has been associated with increased mortality and morbidity after stroke (Kruyt et al., 2010); however, the underlying mechanisms have not been elucidated. Additionally, high glucose-containing diets have been associated with an unfavourable apolipoprotein profile (a modifiable risk factor identified in the INTERSTROKE trial) (Frondelius et al., 2017), and may suggest an interplay between hyperglycaemic and high-cholesterol diets that may influence outcomes after stroke.

In addition to its profound effects on hypertension, atherosclerosis and insulin sensitivity, diet may increase the risk of stroke through other mechanisms, such as inflammation, thrombosis, endothelial dysfunction, and oxidation (Ding and Mozaffarian, 2006). Thus, there is the need for preclinical research to fully elucidate the mechanisms by which dietary components contribute to cerebral ischaemia, in order to contribute to new therapeutic approaches and enhanced dietary interventions.

1.5. Inflammation

Inflammation is a physiological host defence response, designed to prevent infection to invading pathogens and to promote repair. However, inflammation has been shown to be a major contributor to a plethora of non-communicable diseases from cancer and diabetes to stroke and dementia (Sobowale et al., 2016). In these disease states, an immune response is commonly initiated to endogenous stimuli (referred to as sterile inflammation) leading to tissue damage. Indeed, sterile inflammation is central to the pathophysiology of both cerebral ischaemia and dementia, and represents an important therapeutic target for the treatment of both diseases (Chamorro et al., 2012; White et al., 2017). Moreover, prominent risk factors such as aging (Goldberg and Dixit, 2015), diabetes (Donath, 2014), and hypertension (Solak et al., 2016) have been described to have inflammatory components.

1.5.1. Post-stroke inflammation

A complex inflammatory cascade is initiated following an ischaemic event, and this persists for days to months after the initial injury. It is becoming increasingly clear that this inflammatory component contributes to both tissue damage and resolution, which can potentially be modulated therapeutically to prevent tissue damage or to enhance repair.

After initial occlusion, the inflammatory cascade starts in the intravascular compartment, where hypoxia and changes in shear stress cause ROS production (Iadecola and Anrather, 2011). ROS activates endothelial cells to produce adhesion molecules and proinflammatory cytokines, and has an important role in initiating the coagulation cascade in platelets (Iadecola and Anrather, 2011). CBF is compromised as oxidative stress inhibits the production of nitric oxide (NO) dependending, a potent vasodilator, and promotes the constriction of pericytes (Yemisci et al., 2009; Iadecola and Anrather, 2011). The BBB also becomes compromised in this process, as oxidative stress and inflammation upregulate transcellular transport through pinocytotic vesicles, and downregulate tight junction protein expression, which facilitates paracellular permeability (Engelhardt and Sorokin, 2009).

Minutes to hours after vessel occlusion, necrotic cells release damage-associated molecular patterns (DAMPS), which are endogenous intracellular entities that provoke immune responses, and include high mobility group box 1 (HMGB1), ATP, ribonucleic acid (RNA), deoxyribonucleic acid (DNA), and heat shock proteins (Chamorro et al., 2012). DAMPS activate local innate immune cells (microglia and perivascular macrophages) via pattern recognition receptors (PRRs), such as toll-like receptors (TLR), to produce proinflammatory cytokines (interleukin (IL)-1, tumor necrosis factor α (TNFα) and IL-6) and chemokines (C-X-C motif ligand (CXCL)-1 and C-C Motif Chemokine Ligand (CCL)-2) to recruit circulating immune cells (Chamorro et al., 2012). The importance of PRR activation in stroke has been demonstrated using toll-like receptor (TLR)-$4^{-/-}$ (Caso et al., 2007) and TLR-$2^{-/-}$ mice (Lehnardt et al., 2007); after stroke, animals had reduced lesion volumes, improve neurological outcomes, and reduced proinflammatory cytokine production. Put simply, the activation of glial and endothelial cells recruits circulating inflammatory leukocytes and lymphocytes to the site of injury along a chemotactic gradient mediated by cytokines, chemokines and adhesion molecules.

Neutrophils are the first leukocyte to migrate to the brain after stroke, where they have been detected within the first hour, and peak at 1-3 days (Jickling et al., 2015). Neutrophils are associated with mediating stroke damage; blockade of neutrophil infiltration or depletion of neutrophils is associated with reduced lesion volumes and better behavioural outcomes in experimental animal models (Neumann et al., 2015). Clinically, elevated neutrophils are associated with larger infarcts after stroke (Buck et al., 2008); however, therapeutic attempts to block neutrophil recruitment in stroke have generated mixed results (Jickling et al., 2015). Following neutrophil recruitment, monocytes infiltrate the brain. Monocytes are first detected at 24 hours, and peak at 4 days (Planas, 2018), before differentiating into macrophages (Miró-Mur et al., 2016). Interestingly, depletion of monocytes/macrophages in CD11b-diphtheria toxin receptor mice (Perego et al., 2016), or inhibition of monocyte recruitment with C-C Motif Chemokine Receptor (CCR)-2 inhibitors have led to increased lesion volumes (Chu et al., 2015). Thus, monocyte recruitment into the brain may be beneficial during stroke, as it has been postulated that monocytes convert from a proinflammatory phenotype to an anti-inflammatory one, aiding tissue repair and recovery.

Alongside a prominent innate immune response, the adaptive immune response is also critical in stroke pathology, and B cells and T cells can modulate outcomes after stroke. T cells rapidly increase in the brain within 24 hours after stroke, where they play an important role in promoting thromboinflammation and exacerbating stroke damage (Stoll and Nieswandt, 2019). After the first 24 hours, different T cell subsets emerge, and these have been shown to have both detrimental and beneficial effects. $CD8^+$ cytotoxic T cells rapidly infiltrate the parenchyma after 24 hours (Chu et al., 2014) and mediate neuronal death (Mracsko et al., 2014). Infiltrating γδ T cells have been shown to contribute to stroke injury through the production of IL-17 (Shichita et al., 2009). In contrast, regulatory T cells accumulate at later timepoints and secrete IL-10, which is essential for post-stroke repair (Liesz et al., 2009). B cells have also been shown to have neuroprotective effects, through the secretion of IL-10 (Bodhankar et al., 2013), and more recently have been shown to promote neurogenesis and functional improvements (Ortega et al., 2020). However, a detrimental role for B cells after stroke has also been demonstrated, as B cell follicles form in the brain parenchyma and contribute to cognitive decline through the production of IgG (Doyle and Buckwalter, 2017).

1.5.2. Hypoperfusion-related inflammation

In comparison to ischaemic stroke, a well-defined inflammatory cascade has not been described for SVD-related ischaemia. Hypoperfusion-related ischaemia is chronic and consequently, the temporal dynamics of the inflammatory response are likely to be different. Chronic hypoperfusive neurodegeneration occurs over an extended period of time, from months to years, and neurons die via apoptosis rather than necrosis (Broughton et al., 2009; Park et al., 2019). In contrast to necrosis, apoptosis is an energy-dependent programmed cell death that results in damaged cells being phagocytosed before DAMPS are released and a large inflammatory response can be initiated (Taylor et al., 2008). Despite this, a neuroinflammatory response has been observed in SVD, and is likely to contribute to pathology.

In line with the widely accepted hypothesis that BBB permeability causes WMLs and SVD, pathological studies have demonstrated neuroinflammation in the regions of WML around blood vessels (Akiguchi et al., 1997). Post-mortem examinations have shown astrocyte and microglia activation, with increased

expression of cyclooxygenase-2 (Tomimoto et al., 2000) and MMPs (Rosenberg, 2009), which can further degrade basic myelin protein, and facilitate demyelination (Cammer et al., 1978; Chandler et al., 1995). These findings are consistent with animal studies that have shown microglia and astrocyte activation in white matter (Farkas et al., 2004). A recent systematic review critically assessing the literature associating SVD and inflammation found that markers of vascular inflammation (intercellular adhesion molecule (ICAM)-1, vascular cell adhesion molecule (VCAM)-1, homocysteine, von Willebrand factor (VWF)) were strongly associated with SVD pathology (WMLs, enlarged perivascular spaces and cerebral microbleeds) (Low et al., 2019). Further analysis assessing the regional distribution of SVD found stronger associations between vascular inflammation and SVD in regions associated with arteriosclerotic vessels, which are a major histopathological feature of SVD. These data indicate that endothelial dysfunction in arteriosclerotic vessels can lead to BBB permeability that drives SVD pathology. However, due to a lack of data, it was not possible to establish whether inflammation contributes to SVD pathogenesis, or is a consequence of SVD. In the same review, the authors assessed how markers of peripheral inflammation were associated with SVD. Although the association between peripheral inflammation and SVD was not as strong as that of vascular inflammation, peripheral markers of inflammatory were associated with CAA-related SVD.

1.6. Interleukin-1

IL-1 has a major role in orchestrating immune responses and consequently has been strongly linked with poorer outcomes in cerebrovascular disease. The IL-1 cytokine family consists of 11 members in total and has been shown to have pleiotropic functions in innate and adaptive immunity (Dinarello, 2018). The most widely studied IL-1 family cytokines are IL-1α, IL-1β and IL-1RA. All 3 cytokines signal through the receptor IL-1 receptor (IL-1R)-1; however, IL-1RA is a naturally occurring antagonist that binds to IL-1R1 and prevents IL-1α/β signalling (Sims and Smith, 2010; Dinarello, 2018). Although IL-1α and IL-1β both signal via IL-1R1, IL-1α/β biology is vastly different (Dinarello, 2018); this thesis will focus on the regulatory mechanisms that control IL-1β, as IL-1β has been shown to be highly relevant both in stroke (Sobowale et al., 2016; Barrington et al., 2017) and in AD (White et al., 2017). The release of IL-1β from monocytes and macrophages is a key driver of inflammatory responses and therefore it is tightly regulated at multiple

biological checkpoints, from expression to maturation, to secretion (Schroder and Tschopp, 2010).

1.6.1. IL-1β expression

Under basal conditions, IL-1β is expressed at low levels (Vitkovic et al., 2001), and following an inflammatory stimulus is rapidly up-regulated (Dinarello, 2009). IL-1β expression is regulated by the major proinflammatory transcription factor, nuclear factor kappa-light-chain-enhancer of activated B cells (NFκB), which is activated following TLR (Dinarello, 2018), or IL-1R1 (Dinarello et al., 1987) stimulation. As previously discussed, TLRs can be activated in response to DAMPs in the context of sterile inflammation, and in response to pathogen associated molecular patterns (PAMP), such as bacterial lipopolysaccharide (LPS) (Chow et al., 1999). More recently, IL-1β expression has also been shown to be regulated by HIF-1α (Tannahill et al., 2013). IL-1β is expressed as a biologically inactive 31 kDa protein, pro IL-1β, which requires post-translational proteolytic cleavage into its 17 kDa mature form (Mosley et al., 1987).

1.6.2. IL-1β maturation

Pro IL-1β cleavage is mediated by caspase-1 (Kostura et al., 1989); mice deficient in caspase-1 are resistant to LPS-induced endotoxic shock and have decreased serum IL-1β (Kuida et al., 1995; Li et al., 1995). However, caspase-1 is also expressed in cells as an inactive form, pro-caspase-1, which also requires activation via further post-translational modification (Afonina et al., 2015). Caspase-1 requires proximity-induced self-cleavage for activation, which is mediated by the assembly of large multimeric protein structures, known as inflammasomes (Lamkanfi and Dixit, 2014). Inflammasomes are molecular scaffolds comprised of 3 proteins: an inflammasome sensor molecule, an adaptor molecule known as ASC and the pro-caspase-1; which interact via homotypic interactions (Schroder and Tschopp, 2010). Multiple inflammasome sensor molecules have been identified; majority are from the NOD-like receptor (NLR) family and include NLRP (NOD-, LRR- and pyrin domain-containing)1, NLRP3, NLRP6, NLRP7, NLRP12 and NLRC4 (NOD-, LRR- and CARD-containing 4) (Latz et al., 2013). These intracellular PRRs have been shown to be activated in response to a broad range of endogenous and exogenous signals. For example,

NLRP1 is activated in response to anthrax toxin (Boyden and Dietrich, 2006), NLRP7 is activated in response to bacterial LPS (Khare et al., 2012), and NLRC4 is activated in response to cytosolic flagellin (Abdelaziz et al., 2010) Another inflammasome, absent in melanoma 2 (AIM2), has been shown to bind directly to cytosolic DNA (Bürckstümmer et al., 2009). Following activation, inflammasome sensor molecules oligomerise with the adaptor protein, apoptosis-associated speck-like protein containing a CARD (ASC), to form large ASC specks; ASC speck formation recruits pro-caspase-1 to the inflammasome and initiates caspase-1 activation and subsequent IL-1β maturation (Fernandes-Alnemri et al., 2007; Latz et al., 2013; Proell et al., 2013). The most extensively studied inflammasome is the NLRP3 inflammasome and this has been strongly implicated in AD pathology (Heneka et al., 2014), but there have been conflicting findings about NLRP3 involvement in stroke (Yang et al., 2014; Denes et al., 2015; Ye et al., 2017; Lemarchand et al., 2019) .

1.6.3. IL-1β secretion

The final checkpoint of IL-1β regulation is secretion. Once cleaved, IL-1β is secreted from cells through a non-conventional pathway, where it can bypass the Golgi-endoplasmic reticulum network and be secreted by either the shedding of microvesicles, or by cell membrane permeabilisation and lytic cell death. It is generally considered that IL-1β secretion by shredding or permeabilisation is a continuum that is dependent on the strength of the stimulus; a weak stimuli facilitates shredding of microvesicles, whereas a strong stimulus results in cell permeabilisation and IL-1β release (Lopez-Castejon and Brough, 2011). Predominantly, IL-1β release is associated with membrane permeabilisation and cell death, referred to as pyroptosis (Denes et al., 2012). Pyroptosis is a proinflammatory form of cell death that causes an infected macrophage to die and at the same time release proinflammatory cytokines such as IL-1β, and DAMPs, essential for propagating an immune response (Bergsbaken et al., 2009). In addition, caspase-1 also facilitates cell death through gasdermin D cleavage, which releases the N-terminal fragment that consequently associates with the cell membrane and facilitates membrane permeabilisation, cell death and IL-1β release (Shi et al., 2015).

1.6.4. IL-1 signalling

As previously discussed, IL-1β and IL-1α signal via IL-1R1, which is expressed on several cell types. IL-1R1 is a membrane-bound receptor which, upon IL-1α/β binding, recruits the IL-1 receptor accessory protein (IL-1RAcP) (Weber et al., 2010). An IL-1R1/IL-1RAcP complex activates intracellular signalling cascades that ultimately activates NF-κB, which translocates to the nucleus to upregulate the expression of proinflammatory genes, such as cytokines (IL-1, IL-6), chemokines (CXCL1, IL-8), eicosanoids (prostaglandin E) and adhesion molecules (ICAM-1 and VCAM-1) (Libermann and Baltimore, 1990; Mantovani et al., 2019). IL-1β cleavage to the 17 kDa form is essential for activity at IL-1R1 (Garlanda et al., 2013), although pro IL-1α has been shown to demonstrate activity at the IL-R1 receptor with marked potency compared to the mature IL-1α (Kim et al., 2013).

Further regulatory mechanisms of IL-1 signalling are IL-1RA, and the decoy receptor, IL-1R2. IL-1RA binds to IL-1R1 to prevent IL-1α/β binding, and does not recruit IL-1RAcP to prevent NF-κB activation (Arend et al., 1998). Moreover, IL-1RA expression is induced by IL-1, serving as an endogenous negative feedback loop to dampen IL-1 signalling (Arend et al., 1998). IL-1R2 has been shown to bind IL-1α/β and recruit IL-1RAcP, although it does not have an intracellular signalling domain and therefore cannot activate NF-κB signalling (Colotta et al., 1993).

1.6.5. IL-1 in ischaemic stroke

IL-1 was first implicated in stroke pathology in the early 1990s when IL-1RA was found to be protective in a rat model of stroke (Relton and Rothwell, 1992; Garcia et al., 1995). A myriad of preclinical studies since then have reported the protective effects of blocking IL-1 signalling in stroke, through varying mechanisms, such as intracerebroventricular injection of anti-IL-1β antibodies in rats (Yamasaki et al., 1995), delayed IL-1RA administration in rats (Loddick and Rothwell, 1996), IL-1RA administration in mice (Nawashiro et al., 1997) and the use of IL-1α/$\beta^{-/-}$ mice (Boutin et al., 2001). Impressively, the protective effects of IL-1RA in individual laboratories have been recapitulated in a multicentre preclinical study (Maysami et al., 2016), and verified in a meta-analysis (Banwell et al., 2009; McCann et al., 2016). Additionally, systemic administration of IL-1β has been found to potentiate ischaemic stroke damage (McColl et al., 2007). Similar neuroprotective effects

have been reported when investigating upstream of IL-1 signalling, as inhibiting IL-1β processing via capase-1 with inhibitors Ac-YVAD-cmk (Hara et al., 1997; Rabuffetti et al., 2000) or VRT-018858 (Ross et al., 2007) has also reduced stroke-induced brain damage. More recent preclinical studies have focused on identifying which inflammasome sensor molecules facilitate IL-1β production after stroke. Initial studies identified AIM2 and NLRC4 as mediators of IL-1β production after stroke, and not NLRP3 (Denes et al., 2015). Subsequent studies suggested a role for NLRP3 in stroke damage (Yang et al., 2014; Ismael et al., 2018); however, Lemarchand *et al* (2019) contradict these results and replicate the initial findings that NLRP3 does not contribute to ischaemic damage.

Recent preclinical studies have attempted to map IL-1 signalling in the brain to identify which cell types respond to IL-1. Two independent groups have comprehensively demonstrated that IL-1 signalling in brain endothelial cells is critical for the propagation of neuroinflammation (Liu et al., 2019; Wong et al., 2019). Wong *et al* (2019) also demonstrated that conditional deletion of interleukin-1 receptor 1 (IL-1R1) in brain endothelial cells caused a significant reduction in lesion volume and immune cell infiltration. Furthermore, IL-1 signalling through cholinergic neurons was an important contributor to neuronal cell death after stroke, through as yet unidentified mechanisms (Wong et al., 2019). In the context of fever, Liu *et al* (2019) demonstrated that brain endothelial IL-1R1$^{-/-}$ mice did not experience sickness behaviour and immune cell recruitment was impaired.

Following the successes of IL-1RA in preclinical models, recombinant IL-1RA (anakinra) has subsequently been evaluated in clinical trials for the treatment of ischaemic stroke and subarachnoid haemorrhage. Anakinra is currently approved for the treatment of rheumatoid arthritis, and therefore a well-tolerated safety profile has previously been demonstrated, which permitted phase II clinical trials to assess efficacy for stroke (Mertens and Singh, 2009). The first small phase II study investigating i.v. anakinra in acute ischaemic stroke demonstrated a good safety profile, a reduction in inflammatory markers (IL-6 and C-reactive protein) and a trend for improved clinical outcome at 3 months for anakinra-treated patients (Emsley et al., 2005). In a subsequent second phase II clinical trial with subcutaneous anakinra, IL-6 and C-reactive protein were also reduced, but IL-1RA

treatment was not associated with better clinical outcomes (Smith et al., 2018), highlighting the enormous complexity of the role of IL-1 in stroke.

1.6.6. IL-1 in small vessel disease

Though there is a well-defined role for IL-1 in the context of stroke, its role in SVD is not as clear. SVD predominantly affects the elderly, and it is widely recognised that low-grade chronic inflammation contributes to age-related diseases (Youm et al., 2013). However, the mechanisms responsible for driving this inflammation remain unclear. It is hypothesised that inflammasomes are central to this chronic inflammatory state, especially as they have been directly implicated in vascular diseases (Lénárt et al., 2016) and in neurodegeneration (Freeman and Ting, 2016; White et al., 2017).

The most common risk factor for SVD is hypertension (Heye et al., 2016; Ihara and Yamamoto, 2016); elevated levels of IL-1β have been reported with patients with hypertension (Dalekos et al., 1997; Dörffel et al., 1999; Fearon and Fearon, 2008). Additionally, genetic polymorphisms have been identified: within NLRP3 (Kunnas et al., 2015), in the non-coding region of NLRP3 (Omi et al., 2006) and in NLRP3-associated genes (Zhao et al., 2016), which are all linked to hypertension susceptibility. Moreover, a recent paper, published by Furman *et al* (2017) demonstrated that inflammasomes are pivotal regulators of age-related disease, contributing to the development of hypertension and increased mortality. Specifically, by using gene expression data accumulated from a longitudinal population cohort, they identified NLRC4 and NLRP5 to be highly expressed with increased age, and patients that highly express these inflammasome components were associated with increased IL-1β serum levels, hypertension and mortality. The authors showed that the metabolites (N^4-acetylcytidine) NA4 and adenosine activate NLRC4 *in vitro,* and *in vivo,* NA4 exacerbated hypertension in angiotensin-II treated mice. Thus, this study directly implicates NLRC4 in the chronic low-grade inflammation that occurs in aging and hypertension.

Atherosclerosis is also a major risk factor for SVD. A major component of atherosclerotic plaques is cholesterol crystals that activate NLRP3 in circulating immune cells and drive inflammation (Duewell et al., 2010; Rajaṁaki et al., 2010). Another key cell type in plaque formation is platelets, which constitutively express

inflammasome components (NLRP3, NLRC4 and ASC), and are major sources of circulating IL-1β. It has been demonstrated *in vitro* that NLRP3 activation contributes to platelet activation, aggregation, and thrombus formation (Murthy et al., 2017). In addition, NA4 and adenosine, activators of the NLRC4, can also activate platelets (Furman et al., 2017). Another risk factor associated with the development of SVD is obesity, which is associated with worse outcome after stroke (McColl et al., 2009; Maysami et al., 2015) and accelerated memory decline in AD (Knight et al., 2014). Saturated fatty acids such as palmitate have been shown to activate NLRP3 in endothelial cells (Mohamed et al., 2014) and NLRC4 in astrocytes (Liu and Chan, 2014). Arteriosclerosis that affects cerebral microvessels in SVD is often lipid, so it remains unclear whether pathophysiological mechanisms observed in atherosclerosis are directly relevant.

As previously mentioned, the NLRP3 inflammasome has been strongly implicated in AD pathology. Heneka *et al* (2013) showed that APP/PS1xNLRP3$^{-/-}$ mice have reduced neuroinflammation, decreased amyloid burden, and are protected from cognitive decline. Furthermore, NLRP3 and NLRP1 gene expression has been shown to be upregulated in monocytes from patients with severe AD compared to age-matched healthy controls, and these monocytes also exhibited augmented responses to LPS and amyloid-β stimulation (Saresella et al., 2016). In the context of CAA, amyloid-β accumulation around arterioles may mediate inflammasome activation and contribute to SVD pathology; however, this has yet to be investigated.

1.7. Immunometabolism

In past decade there has been a considerable shift in our understanding of how cellular metabolic systems support and alter immune cell functions; this has resulted in the establishment of the immunometabolism field. Classically, the 6 main cellular metabolic pathways, (glycolysis, the citric acid cycle (TCA), pentose phosphate, fatty acid oxidation (FAO), fatty acid synthesis and amino acid metabolic pathways) were considered for their anabolic and catabolic actions, and the generation of ATP. However, a surge of evidence has shown that metabolic processes are key regulators of an inflammatory responses, and that nutrient availability (e.g. diet) can dominantly regulate cellular metabolism. Thus, immunometabolism may be an important pathophysiological mechanism that underlies the association between diet, inflammation and outcomes in cerebrovascular disease.

Early studies which first suggested that metabolic shifts were important for immune cell function showed that activated macrophages and T cells had increased glucose uptake (Alonso and Nungester, 1956; Newsholme et al., 1986), and preventing glycolysis with 2-deoxyglucose (2DG) inhibited activation (Michl et al., 1976; Hamilton et al., 1986). Initially these findings were controversial because glycolytic production of ATP is inferior to oxidative phosphorylation (OXPHOS)/TCA ATP production, with 2 molecules of ATP and 36 molecules of ATP being produced respectively from 1 molecule of glucose (O'Neill et al., 2016). However, it is now appreciated that while a switch to glycolysis does maintain ATP generation, it also supports effector cell function, such as cytokine production in macrophages (Viola et al., 2019), and cellular growth and proliferation in T cells (Pearce, 2010). Whereas glycolysis is associated with proinflammatory cell phenotypes, a switch to FAO metabolism has been associated with reparative immunity, mediated by T_{reg} cells and memory T cells (O'Neill et al., 2016). However, this stratification is a vast oversimplification, as glycolysis is not solely associated with inflammatory cellular functions, and FAO is not only associated with repair. In fact, all metabolic pathways are closely interconnected and have been shown to be important in supporting a vast array of cellular functions, depending on the stimulus (Van den Bossche et al., 2017). Indeed, all immune cells are sentinel cells that respond to an array of signals within the extracellular milieu, to fight infection and promote repair. The rapidly expanding field of

immunometabolism is currently characterising the underlying metabolic fluxes that support immune cell function, in response to specific signals. Alongside this, the field is further highlighting aberrant metabolic states in diseases with a distinct inflammatory component, and identifying new therapeutic targets to modulate immune responses. Within the scope of this thesis, we will review specifically how metabolic reprogramming supports macrophage function.

1.7.1. Macrophage immunometabolism

In physiological conditions, tissue-resident macrophages maintain tissue integrity and remove apoptotic cells. Following tissue damage or pathogen invasion, tissue-resident macrophages are among the first cells to respond, initiating an inflammatory signalling cascade of proinflammatory chemokines to recruit circulating immune cells, including bone marrow-derived monocytes. At the site of inflammation, monocytes differentiate into macrophages to maintain the immune response or to promote resolution and tissue regeneration. Involvement across the entirety of the inflammatory response suggests that macrophages are extremely plastic cells with vast phenotypic heterogeneity. Broadly speaking, macrophage activation has been simplified into M1 (proinflammatory) and M2 (anti-inflammatory) phenotypes. However, this is a vast over-simplification that does not account for the full breadth of macrophage activation states which have been characterised in multi-dimensional models of macrophage polarisation (Gordon et al., 2014; Martinez and Gordon, 2014). Stark differences in the underlying metabolic processes that support M1 and M2 activation have been described (*Fig. 1.2*); however, the full extent of metabolic reprogramming for the full breadth of macrophage polarisation has not yet been elucidated.

M1 macrophages are critical for initiating and sustaining inflammatory responses, secreting proinflammatory cytokines to recruit infiltrating immune cells, alongside phagocytosing damaged or infected cells (Viola et al., 2019). Glycolysis facilitates sufficient and rapid ATP generation, and increased biosynthesis for cytokine production. Inhibiting glycolysis prevents cytokine production (Tannahill et al., 2013) and impairs macrophage migration (Semba et al., 2016). This metabolic switch to glycolysis is commonly referred to as the Warburg effect (Warburg, 1956), which was first described in cancer cells and is characterised by increased glucose uptake, increased lactate production and decreased OXPHOS. Indeed, M1

macrophages have been found to exhibit all of these metabolic changes (Freemerman et al., 2014). *In vitro* M1 polarisation has been described in response to a wide array of stimuli, including LPS and interferon-γ (IFNγ) (Wang et al., 2018). Furthermore, it has been shown that enzymes in the glycolytic pathway influence the proinflammatory phenotype, with the enzymes pyruvate kinase muscle (Palsson-McDermott et al., 2015) and glyceraldehyde-3-phosphate dehydrogenase (Millet et al., 2016) upregulating IL-1β and TNFα production, respectively. Additionally, 6-phosphofructo-2-kinase/fructose-2,6-biphosphatase-3 (PFKFB3) has been shown to promote the phagocytosis of virus-infected cells (Jiang et al., 2016).

At the other end of the spectrum, M2 macrophages are associated with resolution of inflammation, and have been shown to release anti-inflammatory cytokines (IL-1RA, transforming growth factor β, and insulin-like growth factor-1), phagocytose apoptotic cells and mediate collagen deposition (Mantovani et al., 2013; Viola et al., 2019). M2 macrophages have been shown to be polarised in response to IL-4 (Stein et al., 1992) or IL-33 (Doyle et al., 1994; White et al., 2017), and utilise OXPHOS as their primary energy source (O'Neill et al., 2016). Initially, FAO and fatty acid synthesis was shown to be upregulated in metabolic pathways that support TCA anaplerosis and OXPHOS (Huang et al., 2014). Interestingly, this was shown in the context of efferocytosis, where lipids absorbed by phagocytosis are metabolised by fatty acid oxidation to support OXPHOS (Zhang et al., 2019). More recently, however, a role for glycolysis in M2 activation has also been demonstrated, where it also is required for early IL-4 responses to support the TCA and OXPHOS (Tan et al., 2015).

Studies have demonstrated that alongside the dynamic shift in metabolic pathways, the accumulation of specific metabolites modulates macrophage functions, adding a new layer of understanding to the way in which metabolism supports cellular function and shapes immune responses. During LPS stimulation, cellular metabolism switches from OXPHOS to glycolysis and two breaks in the TCA occur, resulting in the accumulation of citrate and succinate (Jha et al., 2015). Initially, citrate accumulates due to suppression of isocitrate dehydrogenase, which mediates citrate metabolism in the TCA cycle (Van den Bossche et al., 2017). Subsequently, citrate moves into the cytosol where it is a substrate for fatty acid

synthesis to support the production of NO and prostaglandins, which have prominent effects on vascular inflammation and endothelial cell activation (Infantino et al., 2011). Moreover, citrate is a substrate for immunoresponsive gene 1 which converts citrate to itoconate (Strelko et al., 2011; O'Neill and Artyomov, 2019). Interestingly, itoconate has been shown to have anti-inflammatory properties by promoting nuclear factor erythroid 2-related factor 2 (NRF2). NRF2 is a transcription factor that upregulates the expression of cytoprotective genes (Hayes and Dinkova-Kostova, 2014), and has been shown to inhibit the expression of inflammatory cytokines, IL-6 and IL-1β (Kobayashi et al., 2016). Itoconate activates NRF2 signalling by interacting Kelch-like ECH-associated protein 1 (KEAP1), which targets NRF2 for proteosomal degradation, thereby enabling NRF2 activity (Mills et al., 2018). Moreover, itoconate links citrate and succinate accumulation, where it has been shown to inhibit succinate dehydrogenase which mediates succinate metabolism (Cordes et al., 2016; Lampropoulou et al., 2016). Succinate has also been demonstrated to be a critical immunometabolite in shaping immune cell function. The accumulation of succinate has been shown to stabilise HIF-1α expression, which can directly upregulate IL-1β expression (Tannahill et al., 2013). Succinate has been shown to stabilise HIF-1α expression via two mechanisms: (i) inhibition of cytosolic prolyl hydroxylase domain (PHD) enzymes which continually degrade HIF-1α during normoxia (Tannahill et al., 2013), and (ii) succinate dehydrogenase can oxidise succinate which generates ROS and stabilises HIF-1α expression (Mills et al., 2016). Combined, citrate, itoconate, and succinate are key metabolites which have been shown to have distinct roles in regulating both pro- and anti-inflammatory macrophage responses.

Despite metabolic reprogramming being well-described in peripheral macrophages, the metabolic changes that occur in the brain's tissue-resident macrophage population, the microglia, are not as well understood. It has been shown that in response to various proinflammatory stimuli, such as LPS (Voloboueva et al., 2013; Orihuela et al., 2016) and LPS + IFNγ (Gimeno-Bayón et al., 2014), microglia become polarised to an inflammatory M1-like phenotype, and a shift from OXPHOS to glycolysis. This has been demonstrated by an increase in extracellular acidification rate and a decrease in oxygen consumption rate in cultured microglia (Holland et al., 2018), alongside the production of inflammatory cytokines (Lynch, 2019). Interestingly, M1-like polarisation and

glycolytic flux has also been demonstrated in response to AD-related stimuli, amyloid-β (Rubio-Araiz et al., 2018; Baik et al., 2019). Similarly, microglia polarisation with IL-4 is associated with OXPHOS, with an increased oxygen consumption rate and ATP production (Holland et al., 2018). Importantly, there is a paucity of research investigating the consequences of metabolic reprogramming in ischaemic injury, highlighting an important area of investigation.

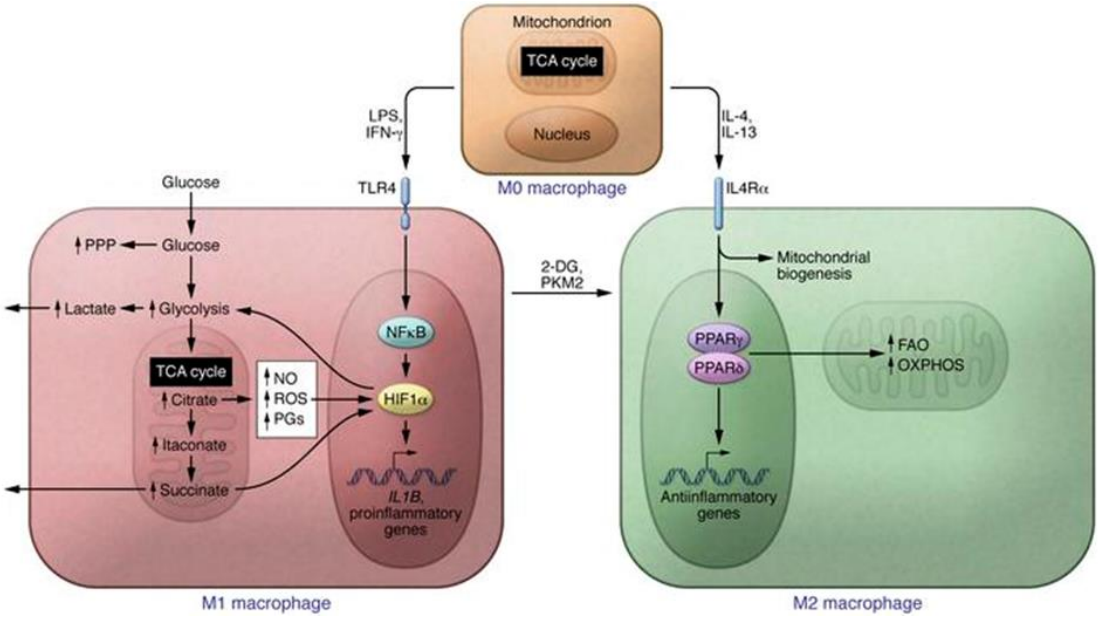

Figure 1.2 - Metabolic reprogramming supports macrophage M1/M2 polarisation. Following an M1 stimulus (LPS or IFNγ) via TLR4 glycolytic and PPP pathways are upregulated to facilitate the production of inflammatory mediators, such as: cytokines, nitric oxide and prostaglandins. Inflammatory profile is further supported by specific immunometabolites, such as glycolytic enzymes and TCA cycle intermediates. Alternatively, following an M2 stimulus (IL-4 or IL-13) OXPHOS and FAO pathways are upregulated. Figure taken from Corcoran and O'Neill (2016). *Abbreviations - FAO: fatty acid oxidation; IFN: interferon; IL: interleukin; LPS: lipopolysaccharide; NO: nitric oxide; OXPHOS: oxidative phosphorylation; PG: prostaglandins; PPP: pentose phosphate pathway; ROS: reactive oxygen species; TCA: tricarboxylic acid cycle; TLR: toll like* receptor.

1.8. Animal models of cerebral ischaemia

Post-mortem tissue is critical for validating the clinical relevance of preclinical findings; however, access to human tissue is challenging, and is limited to a single timepoint. To better explore the temporal dynamics of ischaemic events, longitudinal clinical studies can be conducted; however, due to the inaccessible nature of the brain, experimental read-outs are limited. Therefore, the use of animal models in ischaemic research has been invaluable for understanding pathophysiological mechanisms which occur in response to hypoxic events. Combined, animal and clinical studies are a powerful tool to better understand disease mechanisms, and to explore new therapeutic strategies. A number of animal models have been developed to recapitulate both focal and global ischaemia in humans, with some of these described below.

1.8.1. Focal cerebral ischaemia

It has been shown that over 50% of strokes originate from an occlusion in the middle cerebral artery (MCA) (Ng et al., 2007). Consequently, many different techniques have been developed to manipulate the MCA in experimental animal models of stroke. MCA occlusion (MCAo) is the most widely used experimental technique, whereby an intraluminal filament is inserted into the common carotid artery (CCA), advanced to the Circle of Willis to occlude the MCA for a given period, before subsequent removal. There are two major variations of this surgery, the Koizumi or the Longa method. An important difference in these methods is that the Koizumi method inserts the filament directly into the CCA, which subsequently requires permanent ligation (Koizumi et al., 1986), whereas the Longa method inserts the filament into the external carotid artery, and the CCA does not require permanent ligation (Longa et al., 1989). Both of these methods produce striato-cortical lesions, bordered by a partially ischaemic penumbra region, but have different reperfusion profiles. Large ischaemic lesions affect white and grey matter (Arakawa et al., 2006), resulting in significant contra-lateral motor deficits (MacRae, 2011), and cognitive deficits (Ryan et al., 2006; Carmo et al., 2014). Furthermore, following MCAo, a well-defined inflammatory response is initiated, involving activation of neuroimmune cells, infiltration of peripheral immune cells and production of cytokines and chemokines (Chamorro et al., 2012). Another inducible model of focal cerebral ischaemia is the distal MCAo (dMCAo) model. This model requires a craniotomy to expose the distal branches of the MCA, which can subsequently be occluded by different experimental techniques, such as

photothrombosis (Labat-gest and Tomasi, 2013), or electrocoagulation (Llovera et al., 2014), or by initiating endogenous clot formation by application of thrombin (Orset et al., 2007) or $FeCl_3$ (Karatas et al., 2011). dMCAo produces small and consistent cortical lesions, with associated contra-lateral motor deficits. Non MCA-related models of focal ischaemia include CCA injections of particulates to induce multi-infarct lesions, such as micro-spheres (Miyake et al., 1993; Fukatsu et al., 2002), suspended cholesterol crystals (Rapp et al., 2008) or autologous blood clots (Zhang et al., 2013).

1.8.2. Global cerebral ischaemia

Global cerebral ischaemia has been modelled in animals by manipulating the CCA to induce chronic hypoperfusion. These models have recapitulated SVD-related pathology, such as, white matter damage, vascular pathology, BBB breakdown and neuroinflammation, alongside distinct cognitive deficits. However, the major criticism of these models is that they do not model human disease, as carotid stenosis does not widely contribute to SVD progression (Potter et al., 2012), and it is speculated that reduced CBF is secondary to BBB breakdown (Wardlaw et al., 2017). However, global hypoperfusion (due to atherosclerosis in the Circle of Willis, cardiac insufficiency, orthostatic hypotension, and impaired autoregulatory responses following hypertension) has still been implicated in the formation of WMLs and cognitive impairments. Moreover, neuropathology induced by these models phenocopies pathology caused by alternate SVD pathophysiological mechanisms. Therefore, these preclinical models are invaluable tools to study the effects of reduced perfusion and global ischaemia on cerebral function.

The most frequently used model of global hypoperfusion is the 2-vessel occlusion (2-VO) in rats (Jiwa et al., 2010; Madigan et al., 2016) which involves the surgical ligation of the common CCA to produce a sustained drop in CBF. After ligation, CBF rapidly drops to around 30-40% of baseline for 3-4 days (Tomimoto et al., 2003), and then begins to gradually increase. However, CBF has been shown to remain lower than baseline up to 3 months after surgery (Otori et al., 2003). Robust white matter damage is induced during 2-VO, notably extensive white matter rarefaction along the optic tract and moderate damage in the corpus callosum (Wakita et al., 1994; Farkas et al., 2007). Vasculopathy has been demonstrated in rats 14 months post-surgery by electron microscopic examination, identified by the

thickening and fibrosis of capillaries (De Jong et al., 1999). Neuroinflammation has been demonstrated through the activation of inflammatory glial cells, astrocytes (Wakita et al., 1994; Pappas et al., 1996; Schmidt-Kastner et al., 2005; Farkas et al., 2007) and microglia (Wakita et al., 1994; Abrahám and Lázár, 2000; Farkas et al., 2007). Furthermore, 2-VO animals treated with cyclosporine A, an immunosuppressant drug, had significantly less activated microglia and reduced white matter rarefaction (Wakita et al., 1995). Alongside the histopathological features, cognitive loss is also observed in this experimental model of SVD. Impaired learning and memory has been identified in multiple cognitive tests, including the Morris water maze (MWM) (Pappas et al., 1996; Vicente et al., 2009; Wang et al., 2010), radial arm maze (Pappas et al., 1996) and Y-maze (Sarti et al., 2002). These cognitive deficits have largely been attributed to white matter dysfunction; however, some studies have identified dysfunction in the hippocampus (Pappas et al., 1996; Jiwa et al., 2010). Variations of the 2-VO model can be implemented to attain a more severe reduction in CBF; 3-vessel occlusion bilaterally ligates the CCAs and one vertebral artery (De La Torre and Fortin, 1994; Horecký et al., 2009), whereas a 4-vessel occlusion model ligates one CCA and the opposite vertebral artery is ligated in one surgical procedure, followed by a second procedure 7 days later ligating the remaining CCA and vertebral artery (Plaschke et al., 1999). Both models generate chronic hypoperfusion and impaired memory; however, mortality is high and there is significant reduced locomotor activity (Jiwa et al., 2010). A major limitation of these models is the extensive damage which occurs along the optic tract, which induces impaired vision (Farkas et al., 2007). Consequently, animals with impaired vision will not perform as well in cognitive tests, such as MWM or novel object recognition (NOR), as both require responses to visual cues, and thus the validity of the behavioural assessment is compromised (Ihara and Tomimoto, 2011). Furthermore, 2-VO is restricted to rats. Some strains of mice lack fully developed posterior communicating arteries in their Circle of Willis and therefore cannot withstand this surgical procedure (Farkas et al., 2007), thereby limiting the model's suitability for more sophisticated molecular technologies, such as transgenic mice (Ihara and Tomimoto, 2011). Finally, the rapid drop in CBF observed in the acute phase of this model is not representative of clinical SVD; therefore, future models will need to be developed to replicate the gradual reduction in CBF and allow the use of transgenic animals (Ihara and Tomimoto, 2011; Kitamura et al., 2016).

Shibata *et al* (2004) developed a chronic model of hypoperfusion for use in mice, bilateral carotid artery stenosis (BCAS), which uses metal coils to narrow the CCA by 50%. It was found that that using these microcoils with a diameter of 0.18 mm, the stenosis of the CCAs produced selective white matter lesions, with no grey matter damage, and these have been shown to persist for up to 6 months post-surgery (Shibata et al., 2004; Nishio et al., 2010). CBF has been shown to drop acutely at day 1, gradually increasing by 1 month (Shibata et al., 2004) but remaining below baseline at 3 months (Nishio et al., 2010). BCAS animals develop impaired memory with sustained hypoperfusion, progressing from deficits in working memory at early timepoints (1 month) (Shibata et al., 2007; Coltman et al., 2011; Hou et al., 2015), to deficits in reference memory at later timepoints (6 months) (Nishio et al., 2010; Holland et al., 2015). Alongside cognitive impairments, progressive neuropathology has been described: WMLs in the corpus callosum at 1 month (Shibata et al., 2004, 2007; Saggu et al., 2016); decreased metabolism in the hippocampus at 6 months (Nishio et al., 2010); and pyknotic and apoptotic neurons in the hippocampus and cerebral cortex at 8 months (Nishio et al., 2010). Other pathological features of SVD that have been observed in BCAS mice include increased BBB permeability (Ihara and Tomimoto, 2011), thickened endothelial basement membrane (Holland et al., 2015), activated glial cells (Shibata et al., 2004; Holland et al., 2015; Saggu et al., 2016) and subcortical haemorrhagic lesions at 6 months (Holland et al., 2015).

Similar to 2-VO, CBF rapidly drops after BCAS surgery and gradually recovers and therefore does not reliably replicate clinically relevant chronic cerebral hypoperfusion. To represent a more physiological relevant stenosis of the vessels, the BCAS model has been modified to introduce a gradual narrowing of the vessels using ameroid microconstrictors (AC) made of hygroscopic casein which swell when water is absorbed. In this model, there is a gradual reduction in CBF over 2-3 days, impaired working memory at 28 days, and the presence of WMLs and a neuroinflammatory response (Kitamura et al., 2012). ACs can also be surgically implanted in mice to initiate gradual hypoperfusion in mice, commonly referred to as gradual carotid artery stenosis (GCAS). ACs with an internal diameter of 0.5 mm produced a phenotype that is too severe, with a mortality rate of 58.8% at 28 days post-surgery, and cerebral infarctions in both grey and white matter (Hattori

et al., 2014). However, using ACs with an internal diameter of 0.75 mm can model features of SVD and has a much-improved survival rate of 91% at 28 days post-surgery (Hattori et al., 2016). Mice surgically implanted with bilateral ACs exhibit a sustained reduction of CBF (50%) after 28 days, WMLs, microglial and astrocyte proliferation, and impaired working memory (Y-maze) and motor impairments (rotarod) (Hattori et al., 2016). Moreover, the GCAS has been further adapted to elicit a slightly different disease phenotype. The surgical placement of an AC on one CCA artery and a microcoil on the other CCA is a novel mouse model of chronic hypoperfusion referred to as AC arterial stenosis (ACAS) (Hattori et al., 2015). Arterial spin labelling has shown a gradual reduction of CBF over 28 days, with differences in CBF between the two different hemispheres and impairments in both working and spatial memory observed in Y-maze and MWM tests, respectively (Hattori et al., 2015). Interestingly, ACAS mice also exhibit motor deficits, with motor coordination and balance impairments identified in multiple behavioural tests: rotarod, wire hang and Y-maze (Hattori et al., 2015). Histopathological analysis have also identified distinct differences between the two hemispheres. In the right hemisphere (the AC side), multiple ischaemic strokes develop in the right subcortical area by day 14, with activation of astrocytes and microglia and hippocampal neuronal loss. In the left hemisphere (microcoil side) ischaemic infarcts are absent, but there is extensive white matter rarefaction by day 32, and glial cell activation (Hattori et al., 2015).

Another mouse model of global hypoperfusion that is commonly performed is unilateral ligation of the right CCA, known as unilateral CCA occlusion (UCCAo). CBF drops acutely in the ipsilateral hemisphere after surgery, with no change in contralateral CBF (Yoshizaki et al., 2008; Nishino et al., 2016) and has been shown to remain reduced in the ipsilateral hemisphere up to 4 months post-surgery (Zuloaga et al., 2015). Alongside a reduction in CBF, UCCAo elicits cognitive impairment in non-spatial working memory and spatial memory. Deficits in non-spatial working memory, as assessed by NOR, have been identified at 1 month (Yoshizaki et al., 2008; Ma et al., 2015; Zhou et al., 2017) and 3 months post-surgery (Zuloaga et al., 2015). Spatial memory impairment has been identified up to 1 month post-surgery (Ma et al., 2015; Zhou et al., 2017) but this was not seen at 3 months (Zuloaga et al., 2015) in the MWM task. Furthermore, no changes in motor activity or anxiety have been found (Yoshizaki et al., 2008; Zuloaga et al.,

2015). Cognitive decline in the UCCAo model has been attributed to hippocampal atrophy and ventricular enlargement observed at 4 months post-surgery (Zuloaga et al., 2015); however, no changes in neuronal density have been identified at 28 days in the hippocampus and neocortex (Nishino et al., 2016). Histopathological analysis has identified extensive WMLs in the corpus callosum and striatum (Yoshizaki et al., 2008; Ma et al., 2015; Zhou et al., 2017), in addition to activated glial cells and increased proinflammatory cytokines (Yoshizaki et al., 2008). Moreover, it has recently been identified that IL-1β plays a critical role in progenitor oligodendrocyte cell recruitment and white matter repair after UCCAo, where IL-1R1$^{-/-}$ and IL-1RA treated animals had improved re-myelination and prevented cognitive decline (Zhou et al., 2017).

1.9. Summary and aims

Cerebral ischaemia occurs in response to a marked reduction in blood flow to the brain, which can be a result of complete cessation of blood flow in vessels, or an accumulative effect of diminished flow. Reduced CBF can occur due to a multitude of aetiologies, and as a consequence, can produce an array of pathological manifestations. This heterogeneity has ultimately resulted in a poor understanding of the disease mechanisms, limited therapeutic targets, and a distinct lack of treatments. A further added complexity is how modifiable risk factors contribute to, and interact with ischaemic pathology. Of interest to this thesis is how dietary risk factors affect cerebral ischaemia, with a focus on obesity and hyperglycaemia. Ultimately, gaining a better understanding of the pathophysiology of cerebral ischaemia may reduce risk and also improve outcomes and aid recovery.

The overarching aim of this thesis was to investigate how diet influences inflammatory responses and the subsequent neuropathological and functional outcomes after global and focal cerebral ischaemia. Within this overall aim, we set out to address three specific objectives:

1. **Develop and characterise the BCAS model of global cerebral hypoperfusion, which will be used for the first time at the University of Manchester.**

2. **Investigate how obesity regulates inflammatory responses and long-term functional outcomes in mice following experimental stroke.**

3. **Determine how hyperglycaemia regulates inflammatory responses and neuropathological outcome in mice following experimental stroke.**

Chapter 2. Neuropathological characterisation of the murine bilateral common carotid artery stenosis model of hypoperfusion

Neuropathological characterisation of the murine bilateral common carotid artery stenosis model of hypoperfusion

Claire S White[1], Patrick Strangward[1], Scott Miners[2], Karen Horsburgh[3], Stuart M Allan[1]

[1]Faculty of Biology, Medicine and Health, Manchester Academic Health Science Centre, The University of Manchester, Manchester, M13 9PT, UK.

[2]Dementia Research Group, Clinical Neurosciences, Bristol Medical School, University of Bristol, Level 1, Learning and Research Building, Southmead Hospital, Bristol BS10 5NB, UK.

[3]Centre for Discovery Brain Science, University of Edinburgh, Chancellor's Building. 49 Little France Crescent. Edinburgh. EH16 4SB, UK.

Manuscript in preparation

2.1. Authors contributions

Experiments were planned in collaboration with CW, SA and PS. Surgeries were conducted equally by CW and PS, who were trained by KH. Laser speckle imaging, behavioural assessment and immunohistochemical analysis were conducted by CW. Biochemical assessment was conducted by SM at University of Bristol. All data and statistical analyses were conducted by CW. The manuscript was prepared by CW and reviewed by SA, PS and SMA.

2.2. Abstract

Global hypoperfusion is a key pathological process that contributes to cerebral ischaemia and has been associated with small vessel disease (SVD). Despite this, the pathophysiological consequences of global hypoperfusion are poorly understood. In order to investigate these phenomena, we used a mouse model of chronic cerebral hypoperfusion, bilateral common carotid artery stenosis (BCAS), to characterise changes in: cerebral blood flow (CBF), memory, blood brain barrier (BBB) breakdown and neuroinflammation. It has previously been shown that myelin-associated glycoprotein:proteolipid protein 1 (MAG:PLP) and vascular endothelial growth factor (VEGF) are robust markers of tissue hypoperfusion in human post-mortem tissue. These markers have not previously been investigated in the context of the BCAS model, and so were included in this study to assess changes in cerebral perfusion.

Mice had 0.18 mm microcoils applied bilaterally to the common carotid arteries and were recovered for 1 or 3 months. CBF was assessed by laser speckle contrast imaging at days 0 and 1, 1 and 3 months, and spatial working memory was assessed at 1 and 3 months. Neuroinflammation was assessed on post-mortem brains by microglia and astrocyte activation, and BBB breakdown was assessed by levels of fibrinogen and pericyte marker (PDGFR-β). Overall, BCAS induced a modest reduction in CBF, but no change in tissue oxygenation markers, MAG:PLP and VEGF. A lack of changes in these clinical markers of tissue hypoperfusion indicates that despite a modest reduction in CBF, the BCAS model was not severe enough to induce tissue hypoxia. Concomitantly, we did not observe hypoxia-related pathology, such as memory impairment, BBB breakdown, and neuroinflammation. These findings suggest that 0.18mm microcoils induce cerebral hypoperfusion of an insufficient magnitude to promote measurable pathology and cognitive decline.

2.3. Introduction

Cerebrovascular disease is increasingly considered a central pathological feature of dementia. Alois Alzheimer first described the histopathology in a dementia brain as “arteriosclerotic brain atrophy”, although this became overshadowed by the “Alzheimerization” of dementia, and the focus shifted to the molecular basis of amyloid and tau (Libon et al., 2006; Drouin and Drouin, 2017). However, there has been a recent resurgence in evidence that identifies vascular disease as a major contributor to dementia. Histopathological studies have highlighted that up to 80% of Alzheimer’s disease (AD) patients have vascular pathology, and that cerebrovascular disease is the most common neuropathological feature in aged subjects with dementia (Toledo et al., 2013; Power et al., 2018). Statistical modelling using the Alzheimer’s Disease Neuroimaging Initiative (ADNI) dataset to study the temporal ordering of disease progression has also identified vascular dysregulation as an early and important factor associated with the development of AD (Iturria-Medina et al., 2016), highlighting the need to better understand how cerebrovascular disease contributes to dementia.

Cerebral ischaemia is the principle pathological feature of cerebrovascular disease, of which there are two major types, focal ischaemia (i.e. stroke) and global ischaemia. Global ischaemia/hypoperfusion is caused by multiple disease states, including cardiac insufficiency (heart failure, cardiac arrhythmias or hypotension), peripheral and cranial vessel stenosis, and small vessel disease (Ciacciarelli et al., 2020); however, SVD is considered to have the largest contribution to chronic hypoperfusion. SVD affects the small vessels of the brain (arterioles, capillaries and venules) and has extremely heterogeneous pathology. The underlying pathophysiological mechanisms are not well understood, however, it is proposed that microvascular pathology causes endothelial dysfunction and BBB permeability, and hypoperfusion is a secondary consequence of BBB breakdown (Joutel and Chabriat, 2017). Eventually, the blood supply is unable to meet the brain’s metabolic demands. Consequently, tissue oxygenation is reduced, and an ischaemic environment develops over an extended period of time, which drives tissue damage. Clinically, SVD manifests as white matter hyperintensities, lacunes, microinfarcts and enlarged perivascular spaces that can be observed on magnetic resonance imaging (MRI) scans. Patients may be asymptomatic or they may present with cognitive dysfunction (Ciacciarelli et al., 2020). Indeed, reduced

CBF has been closely associated with cognitive decline (Shi et al., 2016; De La Torre, 2017) and is used as a predictive marker for dementia progression (Farkas et al., 2007). Furthermore, low resting CBF correlates with increased frequency of white matter hyperintensities (Fernando et al., 2006; Shi et al., 2016; Bahrani et al., 2017) and reduced cerebrovascular reactivity (a more sensitive indicator of tissue-level CBF), and it predicts the progression from normal white matter to the formation of white matter lesions (WML) (Sam et al., 2016).

WMLs are a key pathological feature associated with SVD and cerebral hypoperfusion and can be clearly delineated via MRI. However, histopathological methods to assess ischaemic white matter damage have historically been less sensitive than modern neuroimaging techniques. Barker *et al* (2013) recently developed a reliable post-mortem assay for ischaemic white matter damage by comparing myelin-associated glycoprotein (MAG) and proteolipid protein 1 (PLP). MAG is sensitive to ischaemia, whereas PLP is resistant to ischaemia; consequently, the MAG:PLP ratio declines with increasing SVD and cerebral amyloid angiopathy severity. MAG:PLP has also been shown to be a relevant indicator of hypoperfusion in different regions of the AD brain (Barker et al., 2014; Thomas et al., 2015). Further investigation of vasoregulatory factors that may contribute to ischaemia has highlighted that the angiogenic factor, vascular endothelial growth factor (VEGF), strongly correlates with MAG:PLP (Barker et al., 2014; Thomas et al., 2015). It is thought that VEGF is increased in response to hypoperfusion via hypoxia-inducible factor (HIF)1-alpha stabilisation and this upregulates VEGF expression to drive angiogenesis and restore CBF (Forsythe et al., 1996; Zhang et al., 2000; Rey and Semenza, 2010). Indeed, elevated VEGF expression has been demonstrated in preclinical models of stroke (Kalaria et al., 1998; Sun et al., 2003) and human post-mortem stroke tissue (Issa et al., 1999), and HIF staining is increased in human ischaemic white matter (Fernando et al., 2006).

BBB disruption has been proposed to be a major driving factor for WML progression (Wardlaw et al., 2003) and BBB permeability correlates with increased WML frequency (Wardlaw et al., 2017; Zhang et al., 2019; Freeze et al., 2020). BBB permeability permits serum proteins such as fibrinogen, albumin, and immunoglobulin G (IgG), to move from the blood vessels into the parenchyma.

Specifically, fibrinogen extravasation has been demonstrated in both preclinical AD models and in human AD brains; this has been shown to be a proinflammatory process that drives microglia-mediated neurodegeneration and cognitive decline (Merlini et al., 2019). In addition, fibrinogen has been shown to prevent oligodendrocyte precursor cell maturation, and this may further contribute to WML progression by preventing myelin repair (Petersen et al., 2018). Pericytes have also been shown to be critical regulators of CBF and the maintenance of BBB integrity; it has been widely reported that pericyte dysfunction and a loss of pericytes occurs in AD (Sengillo et al., 2013; Halliday et al., 2016; Miners et al., 2018, 2019; Nortley et al., 2019) and during stroke (Yemisci et al., 2009; Hall et al., 2014). The Atwell lab has shown that pericytes can constrict in response to ischaemia (Hall et al., 2014) and amyloid-β (Nortley et al., 2019), resulting in reduced CBF in the contexts of stroke and AD respectively. Further work from the Love group has shown that fibrinogen and the pericyte marker, platelet derived growth factor receptor beta (PDGFR-β), have a strong relationship with the MAG:PLP ratio and VEGF, further highlighting BBB breakdown as a key pathophysiological event in chronic cerebral hypoperfusion (Miners et al., 2018).

To investigate cerebral hypoperfusion in a preclinical setting, various rodent models have been used in which the circulatory system is manipulated to restrict blood flow to the brain; the most widely used model is the bilateral common carotid artery stenosis (BCAS) in mice. Shibata et al (2004) first characterised the BCAS model of global hypoperfusion, whereby CBF is restricted via the bilateral application of microcoils to the common carotid arteries (Nishio et al., 2010). They demonstrated that using 0.18 mm microcoils to narrow the common carotid arteries by 50% could produce SVD-related pathology (selective WML with no grey matter damage), which was detectable up to 6-months post-surgery. Subsequently, this model has been widely employed and multiple research groups have shown that CBF is significantly altered, with a peak reduction observed at acute timepoints (1 day) (Shibata et al., 2004) that slowly recovers over time (1 – 3 months), but never returns to baseline levels (Nishio et al., 2010). Alongside changes in CBF, impairments in both short-term (Shibata et al., 2007; Coltman et al., 2011; Hou et al., 2015) and long-term memory (Nishio et al., 2010; Holland et al., 2015) have been identified. Other neuropathological features of SVD have been observed in BCAS mice, including: white matter damage (Holland et al., 2011, 2015); blood

brain barrier (BBB) permeability (Ihara and Tomimoto, 2011); extra cellular matrix remodelling (Holland et al., 2015); neuroinflammation (Shibata et al., 2004; Holland et al., 2015; Saggu et al., 2016); and subcortical haemorrhagic lesions (Holland et al., 2015). A drawback of this model is that it does not accurately reflect the human disease, as carotid stenosis is not common in SVD (Potter et al., 2012), and reduced CBF is proposed to be secondary to BBB leakage (Wardlaw et al., 2017). Despite this, the BCAS model is an invaluable tool to study the effects of reduced perfusion and global ischaemia on cerebral function.

In this study, we performed neuropathological and cognitive assessments of mice subjected to BCAS or sham surgery, and assessed changes in CBF, short-term working memory, BBB breakdown, and neuroinflammation. We also performed biochemical assays to measure clinically validated markers of hypoperfusion, MAG, PLP, and VEGF, to determine whether these markers could reliably quantify ischaemic white matter damage in murine models of global hypoperfusion.

2.4. Materials and Methods

2.4.1. Animals

Male C57BL/6J mice (Charles River) were used for all studies. All animals were housed in groups (2–5 per cage) in individually ventilated cages in standard housing conditions (temperature 21 ± 2°C; humidity 55% ± 5%; 12-hour light/12-hour dark cycle), with access to food and water *ad libitum*. All experiments were conducted in accordance with the UK Animals (Scientific Procedures) Act 1986 and approved by the Home Office under relevant personal and project licenses at The University of Manchester, Biological Sciences Facility. All reporting of animal experiments complied with the ARRIVE guidelines (Animal Research: Reporting in In Vivo Experiments) (Kilkenny et al., 2010).

2.4.2. Bilateral common carotid artery stenosis

Chronic cerebral hypoperfusion was induced as previously described in 15–16 week old mice (Shibata et al., 2004). Briefly, anaesthesia was induced with 4% isoflurane and maintained with 1.5% (in a mix of 30% O_2 and 70% N_2O). Core body temperature was monitored using a rectal probe and maintained at 37±0.5°C with a homoeothermic blanket (Harvard Apparatus) throughout surgery. A midline incision was made at the neck, with submandibular glands and overlying connective tissue retracted to expose the common carotid arteries and microcoils (0.18 mm internal diameter; Sawane Spring Co) were applied permanently to both common carotid arteries, with a 30-min interval between each microcoil insertion. Sham animals underwent identical surgical interventions without application of microcoils. Animals were numbered and randomly allocated surgical group using Excel's randbetween function. Mice were given subcutaneous injections of saline (0.5 mL) and analgesia (Buprenorphine, 0.5 mg/kg) immediately after surgery. Animals were kept at 30°C, monitored until fully recovered from the effects of anaesthesia, and subsequently placed back in general housing. Mash was provided post-surgery and general behaviour, appearance and body weight were monitored regularly.

As this was the first time this model was used in our hands we did not have any pilot data on which to base power calculations. 22 animals were used for BCAS surgery and 20 animals were used for sham surgeries. 2 animals died during BCAS surgery, and 1 animal was euthanised at day 1 due to animal reaching humane endpoints. 1 death occurred in sham-operated group. Final group sizes were sham $n = 19$ and BCAS $n = 19$. Breakdown of group sizes for IHC and biochemical assessment at different time points can be found in Table 2.1, and are detailed in figure legends.

Table 2.1 - Final group sizes for animals used for IHC and biochemical assessment at different time points.

Surgery	Analysis	1 month	3 month
Sham	IHC	5	7
	Biochemistry	-	7
BCAS	IHC	4	7
	Biochemistry	-	8

2.4.3. Laser speckle imaging

Relative CBF was recorded by laser speckle contrast imaging (LSCI), performed using a moorFLPI-2 imager (Moor Instruments). Mice were anaesthetised with isoflurane 1.5% (in a mix of 30% O_2 and 70% N_2O) and core body temperature was monitored using a rectal probe and maintained at 37±0.5°C with a homoeothermic blanket (Harvard Apparatus). Mice were fixed in a stereotaxic frame and a midline incision in the scalp was made to expose the skull. An imaging window was made using ultrasound gel (to prevent the skull drying out) and a 16 mm cover slip to ensure a smooth flat surface. CBF was measured in all animals at baseline, day 1, and at 1- and 3-months. At baseline, day 1 and 1 month, animals were imaged for 4 min with a 250 frame temporal filter. At 3 months, animals were imaged for 4 min with a 1500 frame temporal filter. CBF was analysed by the MoorFLPI software and shown with arbitrary units in a 256-color palette. Briefly, for each animal all frames were averaged, and 2 regions of interest were placed over the somatosensory cortex on the left and right hemisphere, avoiding large draining veins. Average flux values for both regions of interest were taken. All analysis was performed blinded to experimental groups by randomising file names. Acquired images which were deemed to be of poor quality (patches of calcification or incorrect positioning) were not included in analysis.

2.4.4. Y-maze spontaneous alternation test

To assess short-term working memory, the Y-maze spontaneous alternation test was performed as previously described (Martin et al., 2014) at 1 and 3 months. Briefly, animals were placed in a white opaque Perspex maze with three arms containing different visual cues and allowed to explore for 8 min before being returned to their home cage. All tests were recorded by video and entries into arms were recorded (arm entries were defined as four paws crossing the threshold of a respective arm). Spontaneous alternation was defined as successive entry into three different arms. Subsequently, percent of correct alternation was calculated as:$\left(\frac{number\ of\ alternations}{total\ arm\ entries-2}\right) \times 100$. Mice with less than 8 arm entries during the 5 min trial were excluded from the analysis. All videos were scored randomised and blinded by randomising file names. Equipment was thoroughly cleaned between mice, screens placed around the test areas and white noise played throughout the test duration to minimise sensory cues. All testing was conducted during the light phase.

2.4.5. Tissue preparation

At 1- and 3-months post-surgery, mice were culled for histological and biochemical analysis. Animals culled for histological assessment were terminally anaesthetised with 4–5% isoflurane (in a mix of 30% O_2 and 70% N_2O) and transcardially perfused with phosphate buffered saline (PBS) followed by 4% paraformaldehyde (PFA). Brains were further immerse-fixed in PFA for 24 hours and gross sectioned into 2 mm thick sections using a metal brain matrix. All tissue was then embedded in paraffin wax using a Shadon Citadel 2000 tissue processor (Thermo Fisher Scientific), and subsequently sectioned into 5 µm sections using a Leica RM 2155 Microtome (Leica Microsystems Ltd) and mounted on SuperFrost Plus slides (Thermo Fisher Scientific). Animals culled for biochemical assessment were terminally anaesthetised with 4-5% isoflurane (in a mix of 30% O_2 and 70% N_2O) and transcardially perfused with PBS. Brains were removed and microdissections of white matter (corpus callosum, internal capsule and optic tract) and grey matter (cortex) were performed, and the tissue subsequently flash frozen with liquid nitrogen. Tissue was homogenised in 1% sodium dodecyl sulfate (SDS) buffer (100 µM NaCl, 10mM Tris pH 6, 1µM phenylmethylsulfonyl fluoride (PMSF), 1µg/ml aprotinin (Sigma Aldrich) and 1% SDS in distilled water) in a Precellys homogeniser (Stretton Scientific).

2.4.6. Immunohistochemistry

To further investigate microglia and astrocyte activation, Ionized calcium binding adaptor molecule 1 (Iba1) and Glial fibrillary acidic protein (GFAP) immunohistochemistry was performed. Slides were dewaxed and serially rehydrated in graded ethanol, followed by antigen retrieval with Tris-EDTA (pH9) for 30 min at 95 °C. Slides were left to cool for 20 min before being inserted into Shandon™ Sequenza™ slide racks (Thermo Fisher Scientific) and washed (3x) before primary antibodies were applied for 1 hour at room temperature (RT). Slides were washed (3x) and then secondary antibodies applied for 1 hour at RT: biotinylated goat anti-rabbit (1:200, Vector Laboratories). Slides were washed (3x) and ABC-Alkaline Phosphatase (Vector Laboratories) was added for 30 min at RT. Slides were washed (3x) and Vector Red Substrate (Vector Laboratories) was added to slides for 30 min at RT. Slides were washed (3x) and counter stained with haematoxylin. Coverslips were then mounted onto slides using DPX mounting medium (Sigma Aldrich). Images were taken on a 3D-Histech Pannoramic-250 microscope slide-scanner using a 0.30 Plan Achromat objective (Zeiss). Primary antibodies used were anti-Iba1 (1:1000, Abcam, ab178846) and anti-GFAP (1:1000, Abcam, ab68428). Wash steps were performed throughout using wash buffer (0.1 % TWEEN20 in Tris-buffered saline) and all antibodies were diluted in 0.1% BSA TBST. Specificity controls were performed on additional sections with omission of the primary antibodies, and no staining was observed. The frequency of Iba1- and GFAP-positive cells were determined in 3 regions: internal capsule, hippocampus and cortex. For each brain region, 1–3 regions of interest were selected in both the left and right hemispheres, and an average frequency of positive cells was calculated. All image analysis was conducted blinded using QuPath (Bankhead et al., 2017). Images which were deemed to be of poor quality, or not acquired correctly were not included in analysis.

2.4.7. ELISA

To assess tissue oxygenation, neuroinflammation and BBB breakdown, the levels of various markers in both grey and white matter tissue homogenate were analysed by ELISA. The concentration of MAG was determined using an in-house direct ELISA, as previously described (Barker et al., 2013, 2014; Miners et al., 2018). Proteins levels of PLP (Aviva Biosystems, OKEH05831), VEGF (R&D systems, DY493-05), Fibrinogen (Cloud Clone, SEA193Mu), PDGFR-β (Aviva Biosystems,

OKEH03442), GFAP (Cloud Clone, SEA068Mu) and CD11b (My Biosource, MBS934157), were determined according to the manufacturer's guidelines. Absorbance was read at 450 nM in a FLUOstar Optima plate reader (BMG Labtech). Absolute concentrations were determined for each analyte by interpolating against a standard curve of recombinant protein (supplied in kits). All concentrations were calculated from the average of duplicate measurements for each sample.

2.4.8. Data Analysis

Data collection and analysis was performed by experimenters in a blinded and randomised manner. Equal variance and normality were assessed with the Brown-Forsythe and Shapiro-Wilk test respectively and appropriate transformations were applied when necessary. Where appropriate, data are presented as mean ± standard error (SEM), or individual points plotted with best-fit linear regression and 95% confidence intervals. Statistical analyses performed were one-sample *t*-tests, linear regression and linear mixed effects models followed by Sidak-Holmes *post hoc* analysis. p values <0.05 were considered statistically significant. All statistical analyses were performed using GraphPad Prism v8 (GraphPad Software Inc). Further details on statistical analyses used are stated in the figure legends.

2.5. Results

2.5.1. BCAS reduced CBF but did not result in changes in working memory

This study aimed to replicate previous findings that have shown that BCAS causes a sustained reduction in CBF and memory impairments (Shibata et al., 2004; Nishio et al., 2010). C57BL/6 mice underwent BCAS or sham surgery and were recovered for either 1 or 3 months; CBF and memory were assessed at various timepoints throughout the study (*Fig. 2.1A*). We found that BCAS had no adverse effects on body weight (*Fig. 2.1B*); all animals increased body mass by 20% throughout the study. Using LSCI to measure CBF changes, BCAS resulted in a 20% decrease in CBF at Day 1 post-surgery, with no difference in CBF at 1 month (*Fig. 2.1C*). After optimisation of the LSCI procedure at 3 months (*Fig. 2.1D*) (to reduce the appearance of artefacts on the surface of the skull), we found that BCAS animals exhibited a 30% reduction in CBF compared to sham animals. These changes in CBF are demonstrated in representative images (*Fig. 2.1E*). No changes in short-term working memory were found in the Y-maze spontaneous alternation test at 1- and 3-months (*Fig. 2.1F*), and there was no difference in the total number of arm entries between groups (data not shown). Furthermore, we did not find a correlation between the frequency of spontaneous alternations and CBF (*Fig. 2.1G*). Combined, our results show that, despite a reduction in CBF at 3 months post-surgery, BCAS did not induce deficits in working memory.

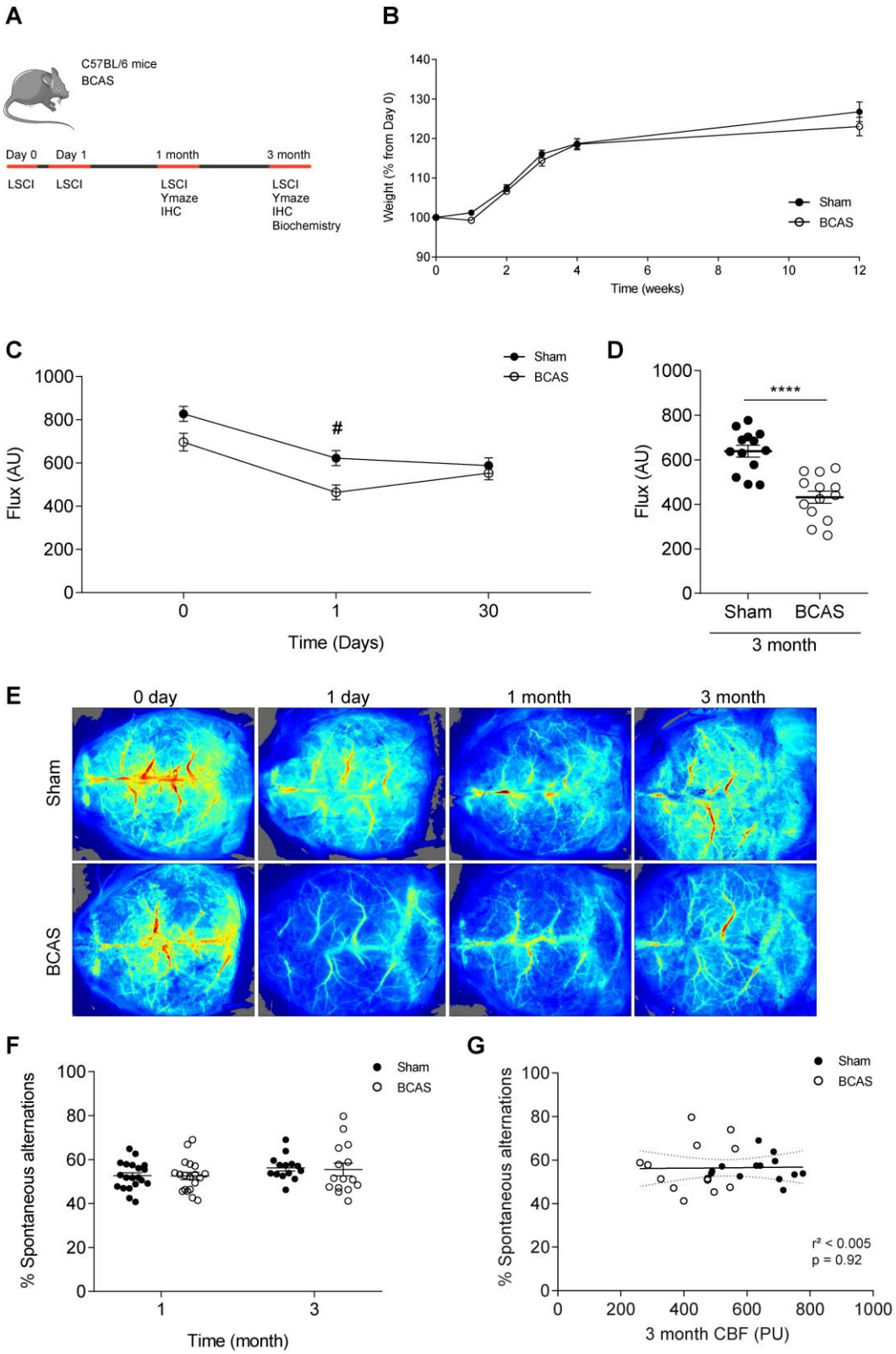
A
C57BL/6 mice
BCAS
Day 0
Day 1
1 month
3 month
LSCI
LSCI
LSCI
Ymaze
IHC
LSCI
Ymaze
IHC
Biochemistry
B
Weight (% from Day 0)
Time (weeks)
Sham
BCAS
C
Flux (AU)
Time (Days)
Sham
BCAS
#
D
Flux (AU)
****
Sham
BCAS
3 month
E
0 day
1 day
1 month
3 month
Sham
BCAS
F
% Spontaneous alternations
Time (month)
Sham
BCAS
G
% Spontaneous alternations
3 month CBF (PU)
Sham
BCAS
r² < 0.005
p = 0.92

Figure 2.1 - BCAS causes a modest drop in CBF with no changes in working memory.
Schematic diagram depicts the experimental design (A). Body weight was assessed throughout the study (B). Laser speckle contrast imaging was conducted at: Days 0 and 1, and at 1 and 3 months post-surgery. Relative CBF was quantified at days 0-30 (C) and at 3 months (D). Flux values are presented as mean ± SEM (n=13-20). #*P*<0.05, sham vs BCAS at Day 1, determined using linear mixed effects models followed by Sidak-Holmes *post hoc* analysis. ****P<0.0001 sham vs BCAS, determined using an unpaired t-test. Representative images show laser speckle contrast imaging speckle patterns at different timepoints (E). Working memory was assessed at 1- and 3-months, using the Y-maze spontaneous alternation test (F); data are presented as mean ± SEM (n=13-20). The correlation between working memory vs CBF was also assessed (G). Solid lines indicate best-fit linear regression and the interrupted lines indicate the 95% confidence intervals. r^2 and p values are detailed in the figure. Individual points represent separate animals.

2.5.2. BCAS does not cause changes in tissue oxygenation

As BCAS induced a modest reduction in CBF, we next assessed tissue oxygenation in both grey and white matter tissues via clinical markers of tissue oxygenation (Barker et al., 2014), MAG:PLP and VEGF (*Fig. 2.2*). In the white matter, MAG:PLP ratio (*Fig. 2.2A*) and VEGF levels (*Fig. 2.2C*) were not different between sham and BCAS animals. In addition, there were no correlations between MAG:PLP and CBF (*Fig. 2.2B*), or VEGF and CBF (*Fig. 2.2D*). Similarly, in the grey matter, no differences in MAG:PLP ratio (*Fig. 2.2E*) or VEGF levels (*Fig. 2.2G*) were found between sham and BCAS animals, and there were no correlations between MAG:PLP and CBF (*Fig. 2.2F*) or VEGF and CBF (*Fig. 2.2H*). These data suggest that the CBF reduction caused by BCAS at 3 months did not lead to a significant reduction in tissue oxygenation.

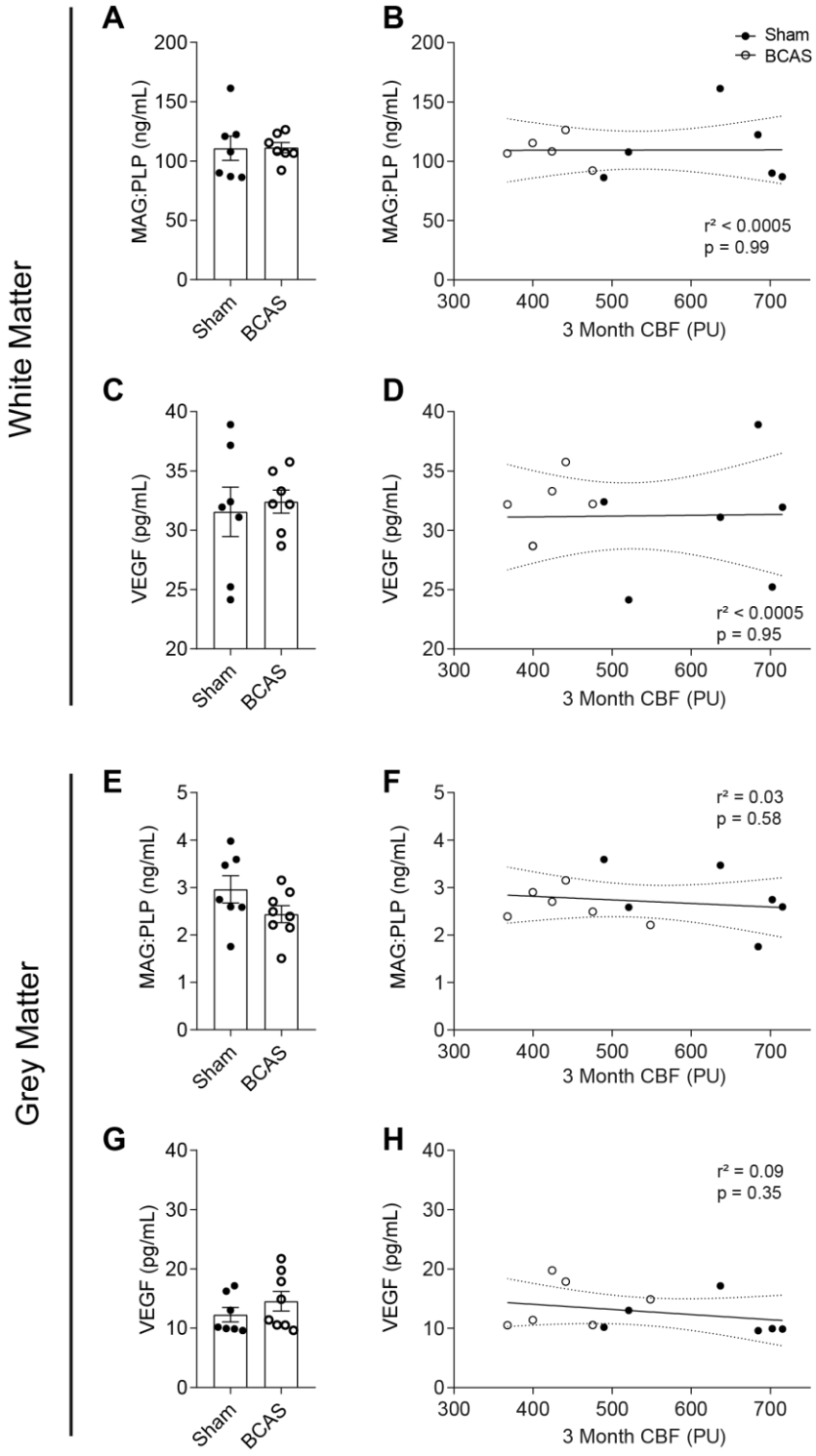

Figure 2.2 - BCAS does not cause a reduction in brain tissue oxygenation.
Tissue oxygenation was assessed using MAG:PLP and VEGF levels in both the white (A-D) and grey matter (E-H) . MAG:PLP (A & E) and VEGF (C & G) levels were determined by ELISA. Data are presented as mean ± SEM (n=6-7). Correlations between MAG:PLP vs CBF were assessed in white (B) and grey matter (F), and the correlations between VEGF vs CBF assessed in white (D) and grey matter (H). Solid lines indicate best-fit linear regression and the interrupted lines indicate the 95% confidence intervals. r^2 and p values are detailed in the figure. Individual points represent separate animals.

2.5.3. BCAS does not induce BBB disruption

As BCAS did not cause a reduction in tissue oxygenation, we next assessed other pathological indicators of ischaemia. BBB disruption is a consequence of ischaemic brain damage, resulting in the leakage of blood serum proteins into the parenchyma and loss of pericytes. In this study we assessed BBB breakdown by analysing fibrinogen and PDGFR-β levels in the cortex at 3 months (*Fig. 2.3*). Fibrinogen levels were not significantly different between sham and BCAS animals (*Fig. 2.3A*), and no correlation was established between fibrinogen levels and CBF (*Fig. 2.3B*). A trend of increased PDGFR-β was observed in BCAS animals (*Fig. 2.3C*); however, this did not reach statistical significance. Furthermore, there was no correlation between PDGFR-β and CBF (*Fig. 2.3D*). These data show that despite a modest CBF reduction at 3 months post-surgery, the BBB may not be disrupted in BCAS animals, suggesting that this model did not induce global brain ischaemia.

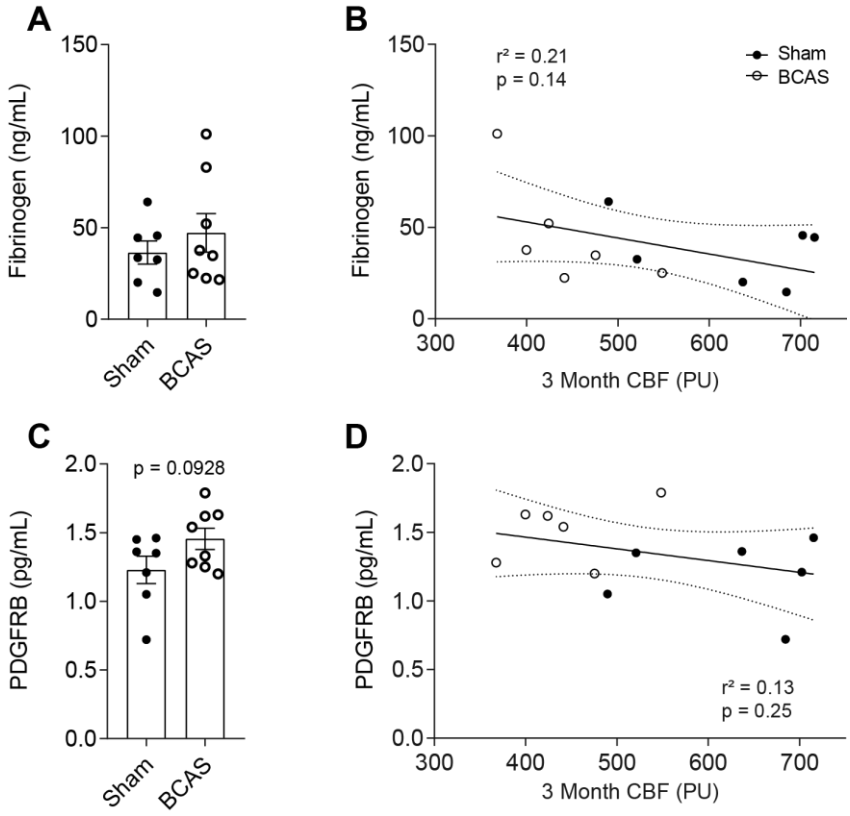

Figure 2.3 - BCAS does not cause BBB breakdown at 3 months post-surgery.
BBB breakdown in the grey matter was assessed by ELISA at 3 months. BBB disruption was assessed by fibrinogen (A), and PDGFR-β (C) levels. Data are presented as mean ± SEM (n=6-7). Correlations between fibrinogen vs CBF (B) and PDGFR-β vs CBF (D) were also determined. Solid lines indicate best-fit linear regression and the interrupted lines indicate the 95% confidence intervals. r^2 and p values are detailed in the figure. Individual points represent separate animals.

2.5.4. BCAS does not induce a microglia or astrocyte response

As ischaemia induces an inflammatory response, we also assessed neuroinflammation in BCAS and sham mice. To assess spatial and temporal microglial activation, immunostaining for Iba1 was conducted. Representative images show uniform Iba1 staining in the cortex (*Fig. 2.4A*), hippocampus (*Fig. 2.4D*) and internal capsule (*Fig. 2.4G*) at 1- and 3-months post-surgery. Iba1$^+$ cells displayed ramified morphologies that are indicative of a resting state, and not the amoeboid morphology associated with activation (Karperien et al., 2013). Quantification of the frequency of Iba1$^+$ cells in the cortex (*Fig. 2.4B*), hippocampus (*Fig. 2.4E*) and internal capsule (*Fig. 2.4H*) identified no differences between sham and BCAS animals at 1- or 3-months. A linear regression was performed to assess the correlation between CBF and the frequency of Iba1$^+$ cells. However, there was no relationship between CBF and the frequency of Iba1$^+$ cells in the cortex (*Fig. 2.4C*), hippocampus (*Fig. 2.4F*) or internal capsule (*Fig. 2.4I*). We also investigated CD11b, a marker of microglia and macrophages by ELISA. No difference in CD11b levels in the cortex at 3 months was found between sham and BCAS animals (*Fig. 2.4J*), and no correlation was established between CD11b and CBF (*Fig. 2.4K*).

GFAP immunostaining was conducted to assess spatial and temporal astrocyte activation after BCAS. Representative images show minimal GFAP staining in the cortex (*Fig. 2.5A*), and uniform staining in the hippocampus (*Fig. 2.5D*) and internal capsule (*Fig. 2.5G*) at 1- and 3- months. Quantification of the frequency of GFAP$^+$ cells in the cortex (*Fig. 2.5B*), hippocampus (*Fig. 2.5E*) and internal capsule (*Fig. 2.5H*) identified no differences between sham and BCAS animals at 1- or 3-months. Linear regression was performed to assess the correlation between CBF and the frequency of GFAP$^+$ cells. A significant correlation between CBF and the frequency of GFAP$^+$ cells was established in the cortex (*Fig. 2.5C*). However, no relationship between CBF and the frequency of GFAP$^+$ cells was found in the hippocampus (*Fig. 2.5F*) or internal capsule (*Fig. 2.5I*). Levels of GFAP in the cortex at 3 months were also assessed by ELISA. A trend of increased GFAP was observed in BCAS animals; however, this did not achieve statistical significance (*Fig. 2.5J*). Furthermore, there was no correlation between GFAP levels and CBF (*Fig. 2.5K*). Combined, these data imply that BCAS does not induce a neuroinflammatory response. In line with the tissue oxygenation and BBB disruption data, these data imply that BCAS did not induce global brain ischaemia.

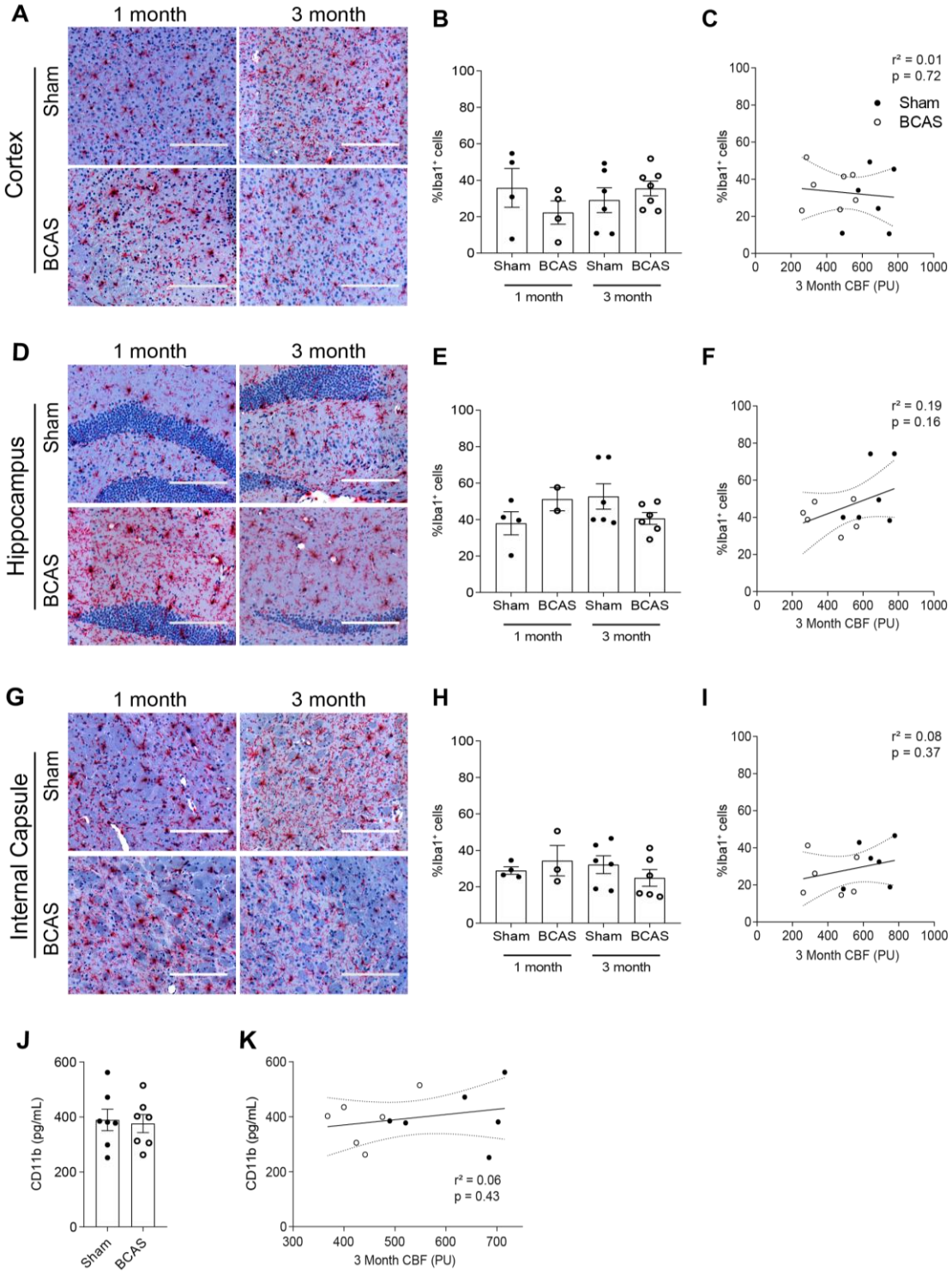
A
1 month
3 month
Cortex
Sham
BCAS
B
%Iba1+ cells
Sham BCAS Sham BCAS
1 month
3 month
C
r² = 0.01
p = 0.72
Sham
BCAS
%Iba1+ cells
3 Month CBF (PU)
D
1 month
3 month
Hippocampus
Sham
BCAS
E
%Iba1+ cells
Sham BCAS Sham BCAS
1 month
3 month
F
r² = 0.19
p = 0.16
%Iba1+ cells
3 Month CBF (PU)
G
1 month
3 month
Internal Capsule
Sham
BCAS
H
%Iba1+ cells
Sham BCAS Sham BCAS
1 month
3 month
I
r² = 0.08
p = 0.37
%Iba1+ cells
3 Month CBF (PU)
J
CD11b (pg/mL)
Sham
BCAS
K
CD11b (pg/mL)
r² = 0.06
p = 0.43
3 Month CBF (PU)

Figure 2.4 - BCAS does not cause microglial activation at 1- or 3-months post-surgery.

Immunostaining for Iba1 was conducted and number of activated microglia were determined in 3 different regions: cortex (A-C), hippocampus (D-F) and internal capsule (G-I). Representative images show Iba1 staining from sham and BCAS animals at 1- and 3-months in the cortex (A), hippocampus (D) and internal capsule (G). Scale bar = 200 µm. The frequency of Iba1-positive cells was quantified in the cortex (B), hippocampus (E) and internal capsule (H); data are presented as mean ± SEM (n=2-7). The correlation between the frequency of Iba1-positive cells vs CBF was assessed in the cortex (C), hippocampus (F) and internal capsule (I). Microglial activation was also assessed in the cortex at 3 months by ELISA for CD11b (J); data are presented as mean ± SEM (n=6-7). The correlation between CD11b vs CBF (K) was also determined. Solid lines indicate best-fit linear regression and the interrupted lines indicate the 95% confidence intervals. r^2 and p values are detailed in the figure. Individual points represent separate animals.

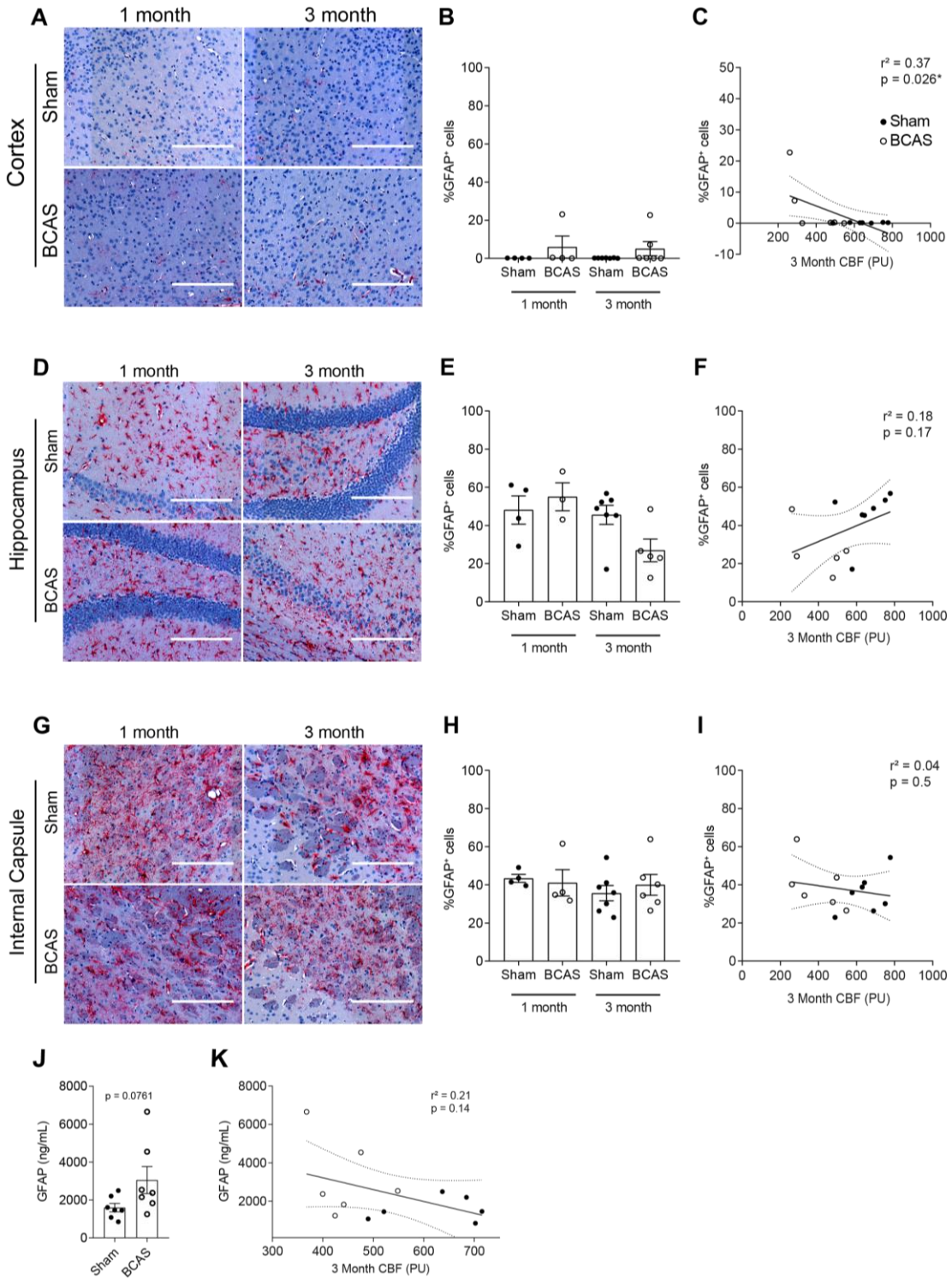
A
1 month
3 month
Cortex
Sham
BCAS
B
%GFAP⁺ cells
Sham BCAS Sham BCAS
1 month
3 month
C
r² = 0.37
p = 0.026*
Sham
BCAS
%GFAP⁺ cells
3 Month CBF (PU)
D
1 month
3 month
Hippocampus
Sham
BCAS
E
%GFAP⁺ cells
Sham BCAS Sham BCAS
1 month
3 month
F
r² = 0.18
p = 0.17
%GFAP⁺ cells
3 Month CBF (PU)
G
1 month
3 month
Internal Capsule
Sham
BCAS
H
%GFAP⁺ cells
Sham BCAS Sham BCAS
1 month
3 month
I
r² = 0.04
p = 0.5
%GFAP⁺ cells
3 Month CBF (PU)
J
p = 0.0761
GFAP (ng/mL)
Sham
BCAS
K
r² = 0.21
p = 0.14
GFAP (ng/mL)
3 Month CBF (PU)

Figure 2.5 - BCAS does not cause astrocyte activation at 1- or 3- months post-surgery.
Immunostaining for GFAP was conducted and the number of astrocytes were determined in 3 different regions: cortex (A-C), hippocampus (D-F) and internal capsule (G-I). Representative images show GFAP staining from sham and BCAS animals at 1- and 3-months in the cortex (A), hippocampus (D) and internal capsule (G). Scale bar = 200 µm. The frequency of GFAP-positive cells was quantified in the cortex (B), hippocampus (E) and internal capsule (H); data are presented as mean ± SEM (n=3-7). The correlation between the frequency of GFAP-positive cells vs CBF was assessed in the cortex (C), hippocampus (F) and internal capsule (I). Astrocyte activation was also assessed by ELISA for GFAP in the cortex at 3 months (J); data are presented as mean ± SEM (n=6-7). The correlation between GFAP vs CBF (K) was also determined. Solid lines indicate best-fit linear regression and the interrupted lines indicate the 95% confidence intervals. r^2 and p values are detailed in the figure. Individual points represent separate animals. *P<0.05.

2.6. Discussion

This study aimed to elaborate on previous studies using the BCAS model to induce global hypoperfusion, a key pathological process underlying SVD and dementia. Following surgical application of 0.18 mm microcoils to the common carotid arteries, we monitored the long-term changes in CBF and cognition. In addition, we characterised aspects of ischaemic pathology, with a focus on tissue oxygenation, BBB disruption, and neuroinflammation.

Chronic cerebral hypoperfusion has been heavily associated with cognitive decline in dementia (Shi et al., 2016; De La Torre, 2017) and is often used as a predictive marker for dementia progression (Farkas et al., 2007). To model cerebral hypoperfusion experimentally, we used the murine BCAS model. Assessment of CBF in this model using LSCI or laser Doppler flowmetry has shown previously that CBF drops by 30-40% at Day 1, before partially recovering to 20% below baseline by 1 month (Shibata et al., 2004), and this does not return to baseline levels by 3 months (Nishio et al., 2010). A similar trend in CBF was detected using arterial spin labelling where CBF is reduced by 50% at Day 1 and slowly increases over 1 month, but never returns to baseline (Hattori et al., 2016; Boehm-Sturm et al., 2017). In the present study, we observed similar changes in CBF; a peak reduction at Day 1 and a gradual increase in CBF by 1 month. Whilst we observed similar trends in CBF over time, the magnitude in peak reduction differed from other reports. Previous studies have demonstrated a peak reduction in CBF of 40-50%, which is in stark contrast to our study where the drop in CBF was modest (~20% at Day 1). During the LSCI procedure, technical issues arose due to the development of calcified patches on the skull. To account for these confounding artefacts, a new LSCI approach was adopted to more accurately assess CBF at 3 months. With this optimised protocol, we were able to detect a modest reduction in CBF compared with sham controls, in line with reports from other groups at this timepoint (Nishio et al., 2010). It is important to note that the data show a wide range of CBF values. It is well described that C57/B6 mice have large variability in the anatomy of the Circle of Willis. In a study by McColl *et al* (2004), only 10% of B6 mice were found to have a complete Circle of Willis, 60% were missing a single posterior communicating artery and 30% were missing both the left and the right single posterior communicating artery. This anatomical diversity may account for the CBF variability in our data; animals with an incomplete Circle of Willis will have

no compensatory flow mechanisms and experience more severe hypoperfusion. To take into account this variation in CBF, further pathological markers investigated in this study were assessed in relation to individual changes in CBF.

The BCAS model has also been widely used to study cognitive impairments in response to global hypoperfusion. At early timepoints (1 month), working memory is impaired in the 8-arm radial maze (Shibata et al., 2007; Coltman et al., 2011; Hou et al., 2015) and Y-maze (Dong et al., 2011; Hou et al., 2015). Cognitive dysfunction advances with time, and deficits in reference memory develop by 6 months in the Morris water maze (Holland et al., 2015) and at 8 months in the Barnes maze (Nishio et al., 2010). Working memory impairment may be attributable to frontal WMLs, whereas impairment in reference memory is largely associated with disruption of hippocampal integrity (Ihara and Tomimoto, 2011), with the observed impairments in cognition correlating with neuropathologic changes. One month post-surgery, WMLs are present in the corpus callosum, whilst no histological changes have been identified in the cerebral cortex or hippocampus (Shibata et al., 2004, 2007; Saggu et al., 2016). Six months post-surgery, fluorodeoxyglucose positron emission tomography indicates hippocampal dysfunction with a decrease in hippocampal glucose utilisation (Nishio et al., 2010). These metabolic changes progress by 8 months, with pyknotic and apoptotic neurons being identified in the hippocampus and cerebral cortex (Nishio et al., 2010). Despite other groups demonstrating a deficit in working memory via Y-maze, the current study did not detect any impairment at 1- or 3-months after surgery. Furthermore, there was no relationship between CBF and Y-maze performance. These results suggest that the modest reduction in CBF observed was not severe enough to induce cognitive decline.

It has previously been shown that MAG:PLP is a robust post-mortem marker of tissue hypoperfusion in AD and vascular dementia brains, in both white matter (Barker et al., 2013) and the cerebral cortex (Thomas et al., 2015; Miners et al., 2016). Another post-mortem marker of hypoperfusion is VEGF, which has been shown to increase in the frontal cortex of AD brains (Thomas et al., 2015) and correlates positively with MAG:PLP (Barker et al., 2014; Thomas et al., 2015). In the current study, we sought to investigate these clinically validated markers of hypoperfusion to back-translate these indices into our preclinical models, ensuring

we are recreating translational pathology. No changes in MAG:PLP or VEGF were identified in either the white or grey matter, and there was no relationship between these markers and CBF. These results support our other findings that the reduction in CBF was not severe enough to induce tissue hypoxia. To further investigate whether BCAS induced tissue ischaemia, assessment of tissue levels of oxygen (pO_2) could be assessed. Using this approach, Duncombe *et al* (2017) show that pO_2 is significantly reduced in the corpus callosum of BCAS mice for up to 6 weeks. Previous work has shown that the BCAS model increases expression of hypoxia-related genes in the white matter, 3 days after hypoperfusion (Reimer et al., 2011). An alternative method of determining whether BCAS induces pathologically hypoxic conditions is to investigate white matter damage. Indeed, white matter rarefaction and vacuolation had been reported in the initial characterisation of the model (Shibata et al., 2004), which has since been replicated (Holland et al., 2015), alongside loss of oligodendrocytes (McQueen et al., 2014). Subtle white matter pathology has also been detected by diffusion tensor imaging at 1 month (Holland et al., 2011) and is more pronounced at 6 months (Holland et al., 2015). These further analyses could also support our findings relating to working memory; if we do not identify WMLs, it would support the hypothesis that hypoperfusion did not induce hypoxia, axonal degeneration did not occur and memory was not impaired.

BBB disruption is a key pathological feature which has been widely demonstrated in neurodegenerative diseases (Zlokovic, 2008), and has been proposed to drive WML progression in SVD (Wardlaw et al., 2003). Clinically, BBB damage has been widely demonstrated by either measurement of the cerebrospinal fluid (CSF)/blood albumin ratio or post-mortem histopathological analysis. Advances in live-imaging techniques have uncovered subtle increases in BBB permeability in patients with dementia (van de Haar et al., 2015), and increased BBB leakage within white matter hyperintensities (Wardlaw et al., 2017). Whilst multiple studies assessing the CSF/blood albumin ratio suggest that BBB permeability increases in dementia (Skoog et al., 1998; Wada, 1998; Taheri et al., 2011), they demonstrate that increased CSF/blood albumin does not related to amyloid pathology, but does relate to diabetes and brain microvascular damage (Janelidze et al., 2017). Post-mortem analyses of the extravasation of serum proteins from the blood vessels into the brain classically assess the serum proteins, fibrinogen, albumin and IgG (Sengillo et al., 2013; Cortes-Canteli et al., 2015). A previous study that examined

fibrinogen levels in post-mortem AD brains showed an increase compared with controls, and an increase in fibrinogen levels was associated with increased cerebral amyloid angiopathy severity and end-stage disease in the Braak tangle stage (Miners et al., 2018). The authors also demonstrated that PDGFR-β levels decreased in AD brains and that this was associated with higher fibrinogen levels (Miners et al., 2018). To assess BBB breakdown in this study, we measured the levels of fibrinogen and PDGFR-β. We showed that BCAS did not alter levels of fibrinogen or PDGFR-β and that there was no relationship between CBF and fibrinogen or PDGFR-β. Previous studies have shown fibrinogen extravasation (Holland et al., 2015) and PDGFR-β loss (Liu et al., 2019) in response to BCAS; however, fibrinogen extravasation was observed at a later timepoint (6 months) (Holland et al., 2015), and PDGFR-β loss was observed acutely (Day 3) (Liu et al., 2019). Other groups have reported extravasation of Evans blue dye (Roberts et al., 2018; Liu et al., 2019) and IgG (Seo et al., 2013; Liu et al., 2019) at early timepoints (3, 7, and 14 days). In essence, the majority of studies reporting BBB disruption demonstrate that it occurs early on, implying that it may not be observed at the 3-month timepoint investigated here. Studies have shown that hypoxia can modulate BBB permeability directly by modulating endothelial cell tight junction protein expression (Engelhardt et al., 2014), and indirectly by TGFβ signalling from oligodendrocyte precursor cells (Seo et al., 2014). Moreover, oligodendrocyte precursor cells have been shown to express matrix metallopeptidase (MMP)-9 in response to hypoperfusion, driving BBB leakage (Seo et al., 2013). Combined, our data suggests that a modest reduction in CBF did not induce tissue hypoxia and subsequent BBB permeability did not occur.

It is hypothesised that following BBB disruption, the entry of blood serum proteins into the parenchyma further exacerbates hypoxia-induced damage by promoting an inflammatory response (Duncombe et al., 2017). The majority of clinical histopathological studies highlight that inflammation drives the development of white matter damage. Neuroinflammation is largely observed in WMLs around blood vessels (Akiguchi et al., 1997), where activated astrocytes and microglia (Simpson et al., 2007) express increased levels of cyclooxygenase-2 (Tomimoto et al., 2000) and MMPs (Rosenberg et al., 2001; Rosenberg, 2009). MMPs exacerbate damage and promote BBB breakdown through degradation of myelin protein and demyelination (Cammer et al., 1978; Chandler et al., 1995). Moreover,

transcriptomic analysis of post-mortem tissue from WMLs found that genes associated with immune regulation were significantly increased (Simpson et al., 2009). Another key neuroinflammatory component identified in vascular dementia pathogenesis is oxidative stress (Iadecola, 2013; Gorelick et al., 2016). Aberrant proinflammatory signalling by angiotensin II (Marchesi et al., 2008) has been shown to upregulate NADPH oxidase and the subsequent production of harmful reactive oxygen species (Faraci, 2011). In the BCAS model, a plethora of inflammatory markers have been used to investigate neuroinflammation, including: increased number of microglia (Wakita et al., 1994; Shibata et al., 2004; McQueen et al., 2014; Holland et al., 2015; Hase et al., 2017; Manso et al., 2018) and astrocytes (Holland et al., 2015; Saggu et al., 2016); endothelial cell activation (Kitamura et al., 2017); leukocyte rolling (Yata et al., 2014); proinflammatory (TNFα, IL-1 and IL6) cytokine production (Reimer et al., 2011; Yuan et al., 2017); and MMP expression (Ihara et al., 2001; Nakaji et al., 2006). In this study, we did not observe a neuroinflammatory response to BCAS. There was no difference in Iba1 staining in the different regions of the brains at 1- or 3-months, no difference in CD11b, and no relationship between these markers and CBF changes. Similarly, no difference in GFAP staining in the different regions of the brains was found, although a relationship between CBF and GFAP was identified in the cortex. This finding would suggest that the animals that experienced severe hypoperfusion had an inflammatory astrocytic response. However, this appears to be contraindicated by a lack of a significant increase in GFAP levels by ELISA, although this may be due to differences in CBF between the two groups. A previous study reported an astrocyte and microglial response in the optic tract and corpus callosum, but not in the internal capsule (Sigfridsson et al., 2018). Therefore, further analysis of these regions which are sensitive to hypoperfusion may have identified a neuroinfammatory response. Combined, these results show that in this study, BCAS-induced hypoperfusion did not provoke a neuroinflammatory response. This supports the hypothesis whereby BCAS did not induce tissue hypoxia, which in turn did not cause BBB breakdown and a subsequent neuroinflammatory response.

In conclusion, we have not been able to replicate the BCAS-related pathology that has been reported in previous studies. Despite a modest reduction in CBF, there were no corresponding changes in cognition, tissue oxygenation, neuroinflammation, BBB breakdown, or white matter damage after BCAS. We postulate that the reduction in CBF was not severe enough to cause tissue hypoxia and induce hypoxia-related pathology, and tighter coils are required to achieve a pathological reduction in CBF. These data suggest further work is required to identify the magnitude in CBF reduction required to reliably induce ischaemic white matter damage (and consequently cognitive decline). Defining this threshold would ultimately reduce inter-laboratory variability and make the BCAS model more reproducible.

2.7. References

Akiguchi, I., Tomimoto, H., Suenaga, T., Wakita, H. and Budka, H. (1997). Alterations in Glia and Axons in the Brains of Binswanger's Disease Patients. *Stroke*, 28(7), 1423–1429.

Bahrani, A. A., Powell, D. K., Yu, G., Johnson, E. S., Jicha, G. A. and Smith, C. D. (2017). White Matter Hyperintensity Associations with Cerebral Blood Flow in Elderly Subjects Stratified by Cerebrovascular Risk. *Journal of Stroke and Cerebrovascular Diseases*, 26(4), 779–786.

Bankhead, P., Loughrey, M. B., Fernández, J. A., Dombrowski, Y., McArt, D. G., Dunne, P. D., McQuaid, S., Gray, R. T., Murray, L. J., Coleman, H. G., James, J. A., Salto-Tellez, M. and Hamilton, P. W. (2017). QuPath: Open source software for digital pathology image analysis. *Scientific Reports*, 7(1), 16878.

Barker, R., Ashby, E. L., Wellington, D., Barrow, V. M., Palmer, J. C., Kehoe, P. G., Esiri, M. M. and Love, S. (2014). Pathophysiology of white matter perfusion in Alzheimer's disease and vascular dementia. *Brain*, 137(5), 1524–1532.

Barker, R., Wellington, D., Esiri, M. M. and Love, S. (2013). Assessing white matter ischemic damage in dementia patients by measurement of myelin proteins. *Journal of Cerebral Blood Flow & Metabolism*, 33(7), 1050–1057.

Boehm-Sturm, P., Füchtemeier, M., Foddis, M., Mueller, S., Trueman, R. C., Zille, M., Rinnenthal, J. L., Kypraios, T., Shaw, L., Dirnagl, U. and Farr, T. D. (2017). Neuroimaging Biomarkers Predict Brain Structural Connectivity Change in a Mouse Model of Vascular Cognitive Impairment. *Stroke*, 48(2), 468–475.

Cammer, W., Bloom, B. R., Norton, W. T. and Gordon, S. (1978). Degradation of basic protein in myelin by neutral proteases secreted by stimulated macrophages: A possible mechanism of inflammatory demyelination. *Proceedings of the National Academy of Sciences of the United States of America*, 75(3), 1554–1558.

Chandler, S., Coates, R., Gearing, A., Lury, J., Wells, G. and Bone, E. (1995). Matrix metalloproteinases degrade myelin basic protein. *Neuroscience letters*, 201(3), 223–6.

Ciacciarelli, A., Sette, G., Giubilei, F. and Orzi, F. (2020). Chronic cerebral hypoperfusion: An undefined, relevant entity. *Journal of Clinical Neuroscience*, 73(1), 8–12.

Coltman, R., Spain, A., Tsenkina, Y., Fowler, J. H., Smith, J., Scullion, G., Allerhand, M., Scott, F., Kalaria, R. N., Ihara, M., Daumas, S., Deary, I. J., Wood, E., McCulloch, J. and Horsburgh, K. (2011). Selective white matter pathology induces a specific impairment in spatial working memory. *Neurobiology of Aging*, 32(12), 7–12.

Cortes-Canteli, M., Mattei, L., Richards, A. T., Norris, E. H. and Strickland, S. (2015). Fibrin deposited in the Alzheimer's disease brain promotes neuronal degeneration. *Neurobiology of Aging*, 36(2), 608–617.

Dong, Y.-F., Kataoka, K., Toyama, K., Sueta, D., Koibuchi, N., Yamamoto, E., Yata, K., Tomimoto, H., Ogawa, H., Kim-Mitsuyama, S. and Therapeutics, M. (2011). Attenuation of Brain Damage and Cognitive Impairment by Direct Renin Inhibition in Mice With Chronic Cerebral Hypoperfusion. *Hypertension*, 58(4), 635–42.

Drouin, E. and Drouin, G. (2017). The first report of Alzheimer's disease. *The Lancet Neurology*, 16(9), 687.

Duncombe, J., Kitamura, A., Hase, Y., Ihara, M., Kalaria, R. N. and Horsburgh, K. (2017). Chronic cerebral hypoperfusion: A key mechanism leading to vascular cognitive impairment and dementia. Closing the translational gap between rodent models and human vascular cognitive impairment and dementia. *Clinical Science*, 131(19), 2451–2468.

Engelhardt, S., Al-Ahmad, A. J., Gassmann, M. and Ogunshola, O. O. (2014). Hypoxia selectively disrupts brain microvascular endothelial tight junction complexes through a hypoxia-inducible factor-1 (HIF-1) dependent mechanism. *Journal of Cellular Physiology*, 229(8), 1096–1105.

Faraci, F. M. (2011). Protecting against vascular disease in brain. *Am J Physiol Heart Circ Physiol*, 300(5), 1566–1582.

Farkas, E., Luiten, P. G. M. and Bari, F. (2007). Permanent, bilateral common carotid artery occlusion in the rat: A model for chronic cerebral hypoperfusion-related neurodegenerative diseases. *Brain Research Reviews*, 54(1), 162–180.

Fernando, M. S., Simpson, J. E., Matthews, F., Brayne, C., Lewis, C. E., Barber, R., Kalaria, R. N., Forster, G., Esteves, F., Wharton, S. B., Shaw, P. J., O'Brien, J. T., Ince, P. G. and MRC Cognitive Function and Ageing Neuropathology Study Group (2006). White Matter Lesions in an Unselected Cohort of the Elderly: Molecular Pathology Suggests Origin From Chronic Hypoperfusion Injury. *Stroke*, 37(6), 1391–1398.

Forsythe, J. A., Jiang, B. H., Iyer, N. V, Agani, F., Leung, S. W., Koos, R. D. and Semenza, G. L. (1996). Activation of vascular endothelial growth factor gene transcription by hypoxia-inducible factor 1. *Molecular and Cellular Biology*, 16(9), 4604–4613.

Freeze, W. M., Jacobs, H. I. L., de Jong, J. J., Verheggen, I. C. M., Gronenschild, E. H. B. M., Palm, W. M., Hoff, E. I., Wardlaw, J. M., Jansen, J. F. A., Verhey, F. R. and Backes, W. H. (2020). White matter hyperintensities mediate the association between blood-brain barrier leakage and information processing speed. *Neurobiology of Aging*, 85(1), 113–122.

Gorelick, P. B., Counts, S. E. and Nyenhuis, D. (2016). Vascular cognitive impairment and dementia. *Biochimica et Biophysica Acta*, 1862(5), 860–868.

van de Haar, H. J., Burgmans, S., Hofman, P. A. M., Verhey, F. R. J., Jansen, J. F. A. and Backes, W. H. (2015). Blood-brain barrier impairment in dementia: Current and future in vivo assessments. *Neuroscience and Biobehavioral Reviews*, (49) 71–81.

Hall, C. N., Reynell, C., Gesslein, B., Hamilton, N. B., Mishra, A., Sutherland, B. A., Oâ Farrell, F. M., Buchan, A. M., Lauritzen, M. and Attwell, D. (2014). Capillary pericytes regulate cerebral blood flow in health and disease. *Nature*, 508(1), 55–60.

Halliday, M. R., Rege, S. V, Ma, Q., Zhao, Z., Miller, C. A., Winkler, E. A. and Zlokovic, B. V (2016). Accelerated pericyte degeneration and blood-brain barrier breakdown in apolipoprotein E4 carriers with Alzheimer's disease. *Journal of Cerebral Blood Flow & Metabolism*, 36(1), 216–227.

Hase, Y., Craggs, L., Hase, M., Stevenson, W., Slade, J., Lopez, D., Mehta, R., Chen, A., Liang, D., Oakley, A., Ihara, M., Horsburgh, K. and Kalaria, R. N. (2017). Effects of environmental enrichment on white matter glial responses in a mouse model of chronic cerebral hypoperfusion. *Journal of Neuroinflammation*, 14(1), 81.

Hattori, Y., Enmi, J. I., Iguchi, S., Saito, S., Yamamoto, Y., Nagatsuka, K., Iida, H. and Ihara, M. (2016). Substantial Reduction of Parenchymal Cerebral Blood Flow in Mice with Bilateral Common Carotid Artery Stenosis. *Scientific Reports*, 6(32179), 1–6.

Holland, P. R., Bastin, M. E., Jansen, M. A., Merrifield, G. D., Coltman, R. B., Scott, F., Nowers, H., Khallout, K., Marshall, I., Wardlaw, J. M., Deary, I. J., McCulloch, J. and Horsburgh, K. (2011). MRI is a sensitive marker of subtle white matter pathology in hypoperfused mice. *Neurobiology of Aging*, 32(12), 2325.e1-e6.

Holland, P. R., Searcy, J. L., Salvadores, N., Scullion, G., Chen, G., Lawson, G., Scott, F., Bastin, M. E., Ihara, M., Kalaria, R., Wood, E. R., Smith, C., Wardlaw, J. M. and Horsburgh, K. (2015). Gliovascular disruption and cognitive deficits in a mouse model with features of small vessel disease. *Journal of Cerebral Blood Flow & Metabolism*, 35(10), 1005–1014.

Hou, X., Liang, X., Chen, J.-F. and Zheng, J. (2015). Ecto-5′-nucleotidase (CD73) is involved in chronic cerebral hypoperfusion-induced white matter lesions and cognitive impairment by regulating glial cell activation and pro-inflammatory cytokines. *Neuroscience*, 297(1), 118–126.

Iadecola, C. (2013). The Pathobiology of Vascular Dementia. *Neuron*, 80(4), 844–866.

Ihara, M. and Tomimoto, H. (2011). Lessons from a Mouse Model Characterizing Features of Vascular Cognitive Impairment with White Matter Changes. *Journal of Aging Research*, 2011(1), 978761.

Ihara, M., Tomimoto, H., Kinoshita, M., Oh, J., Noda, M., Wakita, H., Akiguchi, I. and Shibasaki, H. (2001). Chronic cerebral hypoperfusion induces MMP-2 but not MMP-9 expression in the microglia and vascular endothelium of white matter. *Journal of Cerebral Blood Flow & Metabolism*, 21(7), 828–834.

Issa, R., Krupinski, J., Bujny, T., Kumar, S., Kaluza, J. and Kumar, P. (1999). Vascular endothelial growth factor and its receptor, KDR, in human brain tissue after ischemic stroke. *Laboratory investigation; a journal of technical methods and pathology*, 79(4), 417–25.

Iturria-Medina, Y., Sotero, R. C., Toussaint, P. J., Mateos-Pérez, J. M. and Evans, A. C. (2016). Early role of vascular dysregulation on late-onset Alzheimer's disease based on multifactorial data-driven analysis. *Nature Communications*, 7(11934), 1–14.

Janelidze, S., Hertze, J., Nägga, K., Nilsson, K., Nilsson, C., Wennström, M., van Westen, D., Blennow, K., Zetterberg, H. and Hansson, O. (2017). Increased blood-brain barrier permeability is associated with dementia and diabetes but not amyloid pathology or APOE genotype. *Neurobiology of Aging*, 51(1), 104–112.

Joutel, A. and Chabriat, H. (2017). Pathogenesis of white matter changes in cerebral small vessel diseases: Beyond vessel-intrinsic mechanisms. *Clinical Science*, 131(8), 635–651.

Kalaria, R. N., Cohen, D. L., Premkumar, D. R. D., Nag, S., LaManna, J. C. and Lust, W. D. (1998). Vascular endothelial growth factor in Alzheimer's disease and experimental cerebral ischemia. *Molecular Brain Research*, 62(1), 101–105.

Karperien, A., Ahammer, H. and Jelinek, H. F. (2013). Quantitating the subtleties of microglial morphology with fractal analysis. *Frontiers in Cellular Neuroscience*, 7(3), 1–18.

Kilkenny, C., Browne, W. J., Cuthill, I. C., Emerson, M. and Altman, D. G. (2010). Improving Bioscience Research Reporting: The ARRIVE Guidelines for Reporting Animal Research. *PLoS Biology*, 8(6), e1000412.

Kitamura, A., Manso, Y., Duncombe, J., Searcy, J., Koudelka, J., Binnie, M., Webster, S., Lennen, R., Jansen, M., Marshall, I., Ihara, M., Kalaria, R. N. and Horsburgh, K. (2017). Long-term cilostazol treatment reduces gliovascular damage and memory impairment in a mouse model of chronic cerebral hypoperfusion. *Scientific Reports*, 7(4299), 1–11.

De La Torre, J. C. (2017). Are Major Dementias Triggered by Poor Blood Flow to the Brain? Theoretical Considerations. *Journal of Alzheimer's Disease*, 27(2), 1–19.

Libon, D. J., Price, C. C., Heilman, K. M. and Grossman, M. (2006). Alzheimer's 'other dementia.' *Cognitive and Behavioral Neurology*, 19(2), 112–116.

Liu, Q., Radwanski, R., Babadjouni, R., Patel, A., Hodis, D. M., Baumbacher, P., Zhao, Z., Zlokovic, B. and Mack, W. J. (2019). Experimental chronic cerebral hypoperfusion results in decreased pericyte coverage and increased blood-brain barrier permeability in the corpus callosum. *Journal of Cerebral Blood Flow & Metabolism*, 39(2), 340–250.

Manso, Y., Holland, P. R., Kitamura, A., Szymkowiak, S., Duncombe, J., Hennessy, E., Searcy, J. L., Marangoni, M., Randall, A. D., Brown, J. T., McColl, B. W. and Horsburgh, K. (2018). Minocycline reduces microgliosis and improves subcortical white matter function in a model of cerebral vascular disease. *Glia*, 66(1), 34–46.

Marchesi, C., Paradis, P. and Schiffrin, E. L. (2008). Role of the renin–angiotensin system in vascular inflammation. *Trends in Pharmacological Sciences*, 29(7), 367–374.

Martin, S. A. L., Jameson, C. H., Allan, S. M., Lawrence, C. B. and Luque, R. M. (2014). Maternal High-Fat Diet Worsens Memory Deficits in the Triple-Transgenic (3xTgAD) Mouse Model of Alzheimer's Disease. *PLoS ONE*, 9(6), e99226.

McColl, B. W., Carswell, H. V., McCulloch, J. and Horsburgh, K. (2004). Extension of cerebral hypoperfusion and ischaemic pathology beyond MCA territory after intraluminal filament occlusion in C57Bl/6J mice. *Brain Research*, 997(1), 15–23.

McQueen, J., Reimer, M. M., Holland, P. R., Manso, Y., McLaughlin, M., Fowler, J. H. and Horsburgh, K. (2014). Restoration of oligodendrocyte pools in a mouse model of chronic cerebral hypoperfusion. *PLoS ONE*, 9(2), e87227.

Merlini, M., Rafalski, V. A., Rios, P. E., Mucke, L. and Nelson, R. B. (2019). Fibrinogen Induces Microglia-Mediated Spine Elimination and Cognitive Impairment in an Alzheimer's Disease Model Genetic inhibition of fibrinogen-CD11b binding improves cognition in AD mice. *Neuron*, 101(1), 1099–1108.

Miners, J. S., Kehoe, P. G., Love, S., Zetterberg, H. and Blennow, K. (2019). CSF evidence of pericyte damage in Alzheimer's disease is associated with markers of blood-brain barrier dysfunction and disease pathology. *Alzheimer's Research & Therapy*, 11(1), 81.

Miners, J. S., Palmer, J. C. and Love, S. (2016). Pathophysiology of Hypoperfusion of the Precuneus in Early Alzheimer's Disease. *Brain Pathology*, 26(4), 533–541.

Miners, J. S., Schulz, I. and Love, S. (2018). Differing associations between Aβ accumulation, hypoperfusion, blood–brain barrier dysfunction and loss of PDGFRB pericyte marker in the precuneus and parietal white matter in Alzheimer's disease. *Journal of Cerebral Blood Flow & Metabolism*, 38(1), 103–115.

Nakaji, K., Ihara, M., Takahashi, C., Itohara, S., Noda, M., Takahashi, R. and Tomimoto, H. (2006). Matrix metalloproteinase-2 plays a critical role in the pathogenesis of white matter lesions after chronic cerebral hypoperfusion in rodents. *Stroke*, 37(11), 2816–2823.

Nishio, K., Ihara, M., Yamasaki, N., Kalaria, R. N., Maki, T., Fujita, Y., Ito, H., Oishi, N., Fukuyama, H., Miyakawa, T., Takahashi, R. and Tomimoto, H. (2010). A mouse model characterizing features of vascular dementia with hippocampal atrophy. *Stroke*, 41(6), 1278–1284.

Nortley, R., Korte, N., Izquierdo, P., Hirunpattarasilp, C., Mishra, A., Jaunmuktane, Z., Kyrargyri, V., Pfeiffer, T., Khennouf, L., Madry, C., Gong, H., Richard-Loendt, A., Huang, W., Saito, T., Saido, T. C., Brandner, S., Sethi, H. and Attwell, D. (2019). Amyloid β oligomers constrict human capillaries in Alzheimer's disease via signaling to pericytes. *Science*, 365(6450), 1–11.

Petersen, M. A., Ryu, J. K. and Akassoglou, K. (2018). Fibrinogen in neurological diseases: Mechanisms, imaging and therapeutics. *Nature Reviews Neuroscience*, 19(5), 283–301.

Potter, G. M., Doubal, F. N., Jackson, C. A., Sudlow, C. L. M., Dennis, M. S. and Wardlaw, J. M. (2012). Lack of association of white matter lesions with ipsilateral carotid artery stenosis. *Cerebrovascular Diseases*, 33(4), 378–384.

Power, M. C., Mormino, E., Soldan, A., James, B. D., Yu, L., Armstrong, N. M., Bangen, K. J., Delano-Wood, L., Lamar, M., Lim, Y. Y., Nudelman, K., Zahodne, L., Gross, A. L., Mungas, D., Widaman, K. F. and Schneider, J. (2018). Combined neuropathological pathways account for age-related risk of dementia. *Annals of Neurology*, 84(1), 10–22.

Reimer, M. M., McQueen, J., Searcy, L., Scullion, G., Zonta, B., Desmazieres, A., Holland, P. R., Smith, J., Gliddon, C., Wood, E. R., Herzyk, P., Brophy, P. J., McCulloch, J. and Horsburgh, K. (2011). Rapid disruption of axon-glial integrity in response to mild cerebral hypoperfusion. *Journal of Neuroscience*, 31(49), 18185–18194.

Rey, S. and Semenza, G. L. (2010). Hypoxia-inducible factor-1-dependent mechanisms of vascularization and vascular remodelling. *Cardiovascular Research*, 86(2), 236–242.

Roberts, J. M., Maniskas, M. E. and Bix, G. J. (2018). Bilateral carotid artery stenosis causes unexpected early changes in brain extracellular matrix and blood-brain barrier integrity in mice. *PLoS ONE*, 13(4), e0195765.

Rosenberg, G. A. (2009). Inflammation and white matter damage in vascular cognitive impairment. *Stroke*, 40(3), 20–3.

Rosenberg, G. a, Sullivan, N. and Esiri, M. M. (2001). White matter damage is associated with matrix metalloproteinases in vascular dementia. *Stroke*, 32(5), 1162–8.

Saggu, R., Schumacher, T., Gerich, F., Rakers, C., Tai, K., Delekate, A. and Petzold, G. C. (2016). Astroglial NF-kB contributes to white matter damage and cognitive impairment in a mouse model of vascular dementia. *Acta neuropathologica communications*, 4(1), 76.

Sam, K., Crawley, A. P., Conklin, J., Poublanc, J., Sobczyk, O., Mandell, D. M., Venkatraghavan, L., Duffin, J., Fisher, J. A., Black, S. E. and Mikulis, D. J. (2016). Development of White Matter Hyperintensity Is Preceded by Reduced Cerebrovascular Reactivity. *Annals of Neurology*, 80(2), 277–285.

Sengillo, J. D., Winkler, E. A., Walker, C. T., Sullivan, J. S., Johnson, M. and Zlokovic, B. V. (2013). Deficiency in mural vascular cells coincides with blood-brain barrier disruption in alzheimer's disease. *Brain Pathology*, 23(3), 303–310.

Seo, J. H., Maki, T., Maeda, M., Miyamoto, N., Liang, A. C., Hayakawa, K., Pham, L.-D. D., Suwa, F., Taguchi, A., Matsuyama, T., Ihara, M., Kim, K.-W., Lo, E. H. and Arai, K. (2014). Oligodendrocyte Precursor Cells Support Blood-Brain Barrier Integrity via TGF-β Signaling. *PLoS ONE*, 9(7), e103174.

Seo, J. H., Miyamoto, N., Hayakawa, K., Pham, L. D. D., Maki, T., Ayata, C., Kim, K. W., Lo, E. H. and Arai, K. (2013). Oligodendrocyte precursors induce early blood-brain barrier opening after white matter injury. *Journal of Clinical Investigation*, 123(2), 782–786.

Shi, Y., Thrippleton, M. J., Makin, S. D., Marshall, I., Geerlings, M. I., de Craen, A. J. M. M., Van Buchem, M. A. and Wardlaw, J. M. (2016). Cerebral blood flow in small vessel disease: A systematic review and meta-analysis. *Journal of Cerebral Blood Flow & Metabolism*, 36(10), 1653–1667.

Shibata, M., Ohtani, R., Ihara, M. and Tomimoto, H. (2004). White Matter Lesions and Glial Activation in a Novel Mouse Model of Chronic Cerebral Hypoperfusion. *Stroke*, 35(11), 2598–2603.

Shibata, M., Yamasaki, N., Miyakawa, T., Kalaria, R. N., Fujita, Y., Ohtani, R., Ihara, M., Takahashi, R. and Tomimoto, H. (2007). Selective Impairment of Working Memory in a Mouse Model of Chronic Cerebral Hypoperfusion. *Stroke*, 38(10), 2826–2832.

Sigfridsson, E., Marangoni, M., Johnson, J. A., Hardingham, G. E., Fowler, J. H., Horsburgh, K. (2018). Astrocyte-specific overexpression of Nrf2 protects against optic tract damage and behavioural alterations in a mouse model of cerebral hypoperfusion. *Scientific Reports*, **8 (**12552) 1-14.

Simpson, J. E., Hosny, O., Wharton, S. B., Heath, P. R., Holden, H., Fernando, M. S., Matthews, F., Forster, G., O'Brien, J. T., Barber, R., Kalaria, R. N., Brayne, C., Shaw, P. J., Lewis, C. E., Ince, P. G. and Medical Research Council Cognitive Function and Ageing Study Neuropathology Group (2009). Microarray RNA expression analysis of cerebral white matter lesions reveals changes in multiple functional pathways. *Stroke*, 40(2), 369–75.

Simpson, J. E., Ince, P. G., Higham, C. E., Gelsthorpe, C. H., Fernando, M. S., Matthews, F., Forster, G., O'Brien, J. T., Barber, R., Kalaria, R. N., Brayne, C., Shaw, P. J., Stoeber, K., Williams, G. H., Lewis, C. E. and Wharton, S. B. (2007). Microglial activation in white matter lesions and nonlesional white matter of ageing brains. *Neuropathology and Applied Neurobiology*, 33(6), 670–683.

Skoog, I., Wallin, A., Fredman, P., Hesse, C., Aevarsson, O., Karlsson, I., Gottfries, C. G. and Blennow, K. (1998). A population study on blood-brain barrier function in 85-year-olds: Relation to Alzheimer's disease and vascular dementia. *Neurology*, 50(4), 966–971.

Sun, Y., Jin, K., Xie, L., Childs, J., Mao, X. O., Logvinova, A. and Greenberg, D. A. (2003). VEGF-induced neuroprotection, neurogenesis, and angiogenesis after focal cerebral ischemia. *Journal of Clinical Investigation*, 111(12), 1843–1851.

Taheri, S., Gasparovic, C., Huisa, B. N., Adair, J. C., Edmonds, E., Prestopnik, J., Grossetete, M., Shah, N. J., Wills, J., Qualls, C. and Rosenberg, G. A. (2011). Blood-brain barrier permeability abnormalities in vascular cognitive impairment. *Stroke*, 42(8), 2158–2163.

Thomas, T., Miners, S. and Love, S. (2015). Post-mortem assessment of hypoperfusion of cerebral cortex in Alzheimer's disease and vascular dementia. *Brain*, 138(4), 1059–1069.

Toledo, J. B., Arnold, S. E., Raible, K., Brettschneider, J., Xie, S. X., Grossman, M., Monsell, S. E., Kukull, W. A. and Trojanowski, J. Q. (2013). Contribution of cerebrovascular disease in autopsy confirmed neurodegenerative disease cases in the National Alzheimer's Coordinating Centre. *Brain*, 136(9), 2697–2706.

Tomimoto, H., Akiguchi, I., Wakita, H., Lin, J. X. and Budka, H. (2000). Cyclooxygenase-2 is induced in microglia during chronic cerebral ischemia in humans. *Acta neuropathologica*, 99(1), 26–30.

Wada, H. (1998). Blood-Brain Barrier Permeability of the Demented Elderly as Studied by Cerebrospinal Fluid-Serum Albumin Ratio. *Internal Medicine*, 37(6), 509–513.

Wakita, H., Tomimoto, H., Akiguchi, I. and Kimura, J. (1994). Glial activation and white matter changes in the rat brain induced by chronic cerebral hypoperfusion: an immunohistochemical study. *Acta neuropathologica*, 87(5), 484–92.

Wardlaw, J. M. J., Sandercock, P. P. A. G., Dennis, M. S. M. and Starr, J. (2003). Is Breakdown of the Blood-Brain Barrier Responsible for Lacunar Stroke, Leukoaraiosis, and Dementia? *Stroke*, 34(3), 806–812.

Wardlaw, J. M., Makin, S. J., Vald Es Hern Andez, M. C., Armitage, P. A., Heye, A. K., Chappell, F. M., Muñoz-Maniega, S., Sakka, E., Shuler, K., Dennis, M. S., Thrippleton, M. J., Valdés Hernández, M. C., Armitage, P. A., Heye, A. K., Chappell, F. M., Muñoz-Maniega, S., Sakka, E., Shuler, K., Dennis, M. S. and Thrippleton, M. J. (2017). Blood-brain barrier failure as a core mechanism in cerebral small vessel disease and dementia: evidence from a cohort study. *Alzheimer's & Dementia*, 13(6), 634–643.

Yata, K., Nishimura, Y., Unekawa, M., Tomita, Y., Suzuki, N., Tanaka, T., Mizoguchi, A. and Tomimoto, H. (2014). In Vivo Imaging of the Mouse Neurovascular Unit Under Chronic Cerebral Hypoperfusion. *Stroke*, 45(12), 3698–3703.

Yemisci, M., Gursoy-Ozdemir, Y., Vural, A., Can, A., Topalkara, K. and Dalkara, T. (2009). Pericyte contraction induced by oxidative-nitrative stress impairs capillary reflow despite successful opening of an occluded cerebral artery. *Nature Medicine*, 15(9), 1031–1037.

Yuan, B., Shi, H., Zheng, K., Su, Z., Su, H., Zhong, M., He, X., Zhou, C., Chen, H., Xiong, Q., Zhang, Y. and Yang, Z. (2017). MCP-1-mediated activation of microglia promotes white matter lesions and cognitive deficits by chronic cerebral hypoperfusion in mice. *Molecular and Cellular Neuroscience*, 78(1), 52–58.

Zhang, C. E., Wong, S. M., Uiterwijk, R., Backes, W. H., Jansen, J. F. A., Jeukens, C. R. L. P. N., van Oostenbrugge, R. J. and Staals, J. (2019). Blood–brain barrier leakage in relation to white matter hyperintensity volume and cognition in small vessel disease and normal aging. *Brain Imaging and Behavior*, 13(2), 389–395.

Zhang, Z. G., Zhang, L., Jiang, Q., Zhang, R., Davies, K., Powers, C., Van Bruggen, N. and Chopp, M. (2000). VEGF enhances angiogenesis and promotes blood-brain barrier leakage in the ischemic brain. *Journal of Clinical Investigation*, 106(7), 829–838.

Zlokovic, B. V. (2008). The Blood-Brain Barrier in Health and Chronic Neurodegenerative Disorders. *Neuron*, 57(2), 178–201.

Chapter 3. Stroke induces prolonged changes in lipid metabolism and body composition in mice

Stroke induces prolonged changes in lipid metabolism, the liver and body composition in mice

Michael J Haley[1], **Claire S White**[1], Daisy Roberts, Kelly O'Toole, Catriona J Cunningham, Jack Rivers-Auty, Conor O'Boyle, Conor Lane, Oliver Heaney, Stuart M Allan, Catherine B Lawrence

[1]**Contributed equally**

Faculty of Biology, Medicine and Health, Manchester Academic Health Science Centre, The University of Manchester, Manchester, M13 9PT, U.K.

Published manuscript: **doi:10.1007/s12975-019-00763-2**

3.1. Author contributions

CBL, MH and SA were involved in the conception of the study. CBL, MH, SA and CW were involved in the design of the study. MH performed all the surgeries and conducted neuroscore assessment. MRI imaging was performed by CW. Behavioural assessments (nest building, burrowing, open field and Ymaze) were performed by CW, DR, and KOT; and analysed by CW. ELISA analysis was performed by: CW, DR, KOT, CL and analysed by CW. Plasma lipid assays were performed and analysed by CW. Liver histology was conducted by COB and OH, and liver steatosis and damage scoring was performed by CBL. Plasma ALT assay was conducted and analysed by MH. MRes and BSc students (DR, KOT, CL, OH) were all trained and supervised by CW. Data analysis was performed by CW, CBL and MH. CBL, CW, MH and SA were involved in the interpretation of data. JRA assisted with the statistical analyses. CBL and MH drafted the manuscript with input from SA and CW. CBL and MH handled referee's comments with input from SA and CW.

3.2. Abstract

During recovery, stroke patients are at risk of developing long-term complications that impact quality of life, including changes in body weight and composition, depression and anxiety, as well as an increased risk of subsequent vascular events. The aetiologies and time-course of these post-stroke complications have not been extensively studied, and are poorly understood. Therefore, we assessed long-term changes in body composition, metabolic markers and behaviour after middle cerebral artery occlusion in mice. These outcomes were also studied in the context of obesity, a common stroke comorbidity proposed to protect against post-stroke weight loss in patients. We found that stroke induced long-term changes in body composition, characterised by a sustained loss of fat mass with a recovery of lean weight lost. These global changes in response to stroke were accompanied by an altered lipid profile (increased plasma free fatty acids and triglycerides) and increased adipokine release at 60 days. After stroke the liver also showed histological changes indicative of liver damage and a decrease in plasma alanine aminotransferase (ALT) was observed. Stroke induced depression and anxiety-like behaviours in mice, illustrated by deficits in exploration, nest building and burrowing behaviours. When initial infarct volumes were matched between mice with and without comorbid obesity, these outcomes were not drastically altered. Overall, we found that stroke induced long-term changes in depressive/anxiety-like behaviours, and changes in plasma lipids, adipokines and the liver that may impact negatively on future vascular health.

3.3. Introduction

Stroke is the leading cause of long-term disability in the UK, chiefly due to the devastating effects of ischaemic brain damage on the sensorimotor system. However, patients also develop other complications that have a negative impact on recovery and reduce their quality of life. In the days, weeks and months after stroke, patients are at increased risk of infections and develop complications such as changes in body weight and appetite, depression, fatigue, anxiety and/or cognitive impairment (Duncan et al., 2012; Ayerbe et al., 2013; Nakling et al., 2017; Shi et al., 2018). Stroke patients are also at an increased risk for future vascular events (Putaala et al., 2010; Boulanger et al., 2019). Very little is known about the underlying mechanisms involved in post-stroke complications but long-lasting changes in metabolism and energy balance are likely key (Scherbakov et al., 2019).

Weight loss in stroke patients is common and an important determinant of outcome (Jöonsson et al., 2008; Kim et al., 2015; Nii et al., 2016). During the acute phase of stroke, the nutritional status of patients worsens, resulting in malnutrition that interferes with the recovery of patients' activities of daily living (Desai and Amraotkar, 2019; Sato et al., 2019). Approximately 20% of surviving patients may then develop tissue wasting (cachexia), characterised by loss of lean and fat tissue, with these patients showing poor functional recovery compared to nutritionally healthy patients (Scherbakov et al., 2019). Patients at high risk of malnutrition also have a high risk of mortality at 6 months post-stroke (Gomes et al., 2016), and malnutrition and low body weight are both then risk factors for further stroke recurrence (Olsen et al., 2008; Doehner et al., 2013; Andersen and Olsen, 2015; Wang et al., 2015). The reasons why patients experience weight loss after stroke are not entirely clear, but are thought to include reduction in food intake and increased catabolic drive. Stroke in mice can induce an acute whole body metabolic response that involves changes in lipids and adipokines in the liver, adipose tissue and plasma and which could impact on energy balance and weight control (Haley et al., 2017). Adipokines such as resistin and adiponectin are released from adipose tissue and early changes in both are reported in mice after stroke, suggesting disturbances in metabolic status. Adiponectin, resistin and lipids have also been linked to increased stroke risk in people (Gairolla et al., 2017; Opatrilova et al., 2018). However, whether these acute changes in lipolysis and

adipokines seen in experimental stroke are long lasting is unknown, but prolonged alterations in these physiological systems could potentially impact future vascular health.

Conditions that affect metabolism, for example obesity and diabetes, increase the risk of stroke, and are thus common co-morbidities found in stroke patients (Ostwald et al., 2006; Karatepe et al., 2008; O'Donnell et al., 2010; Sandu et al., 2015). These conditions may also affect the recovery from stroke, for example obesity worsens acute experimental stroke outcome (McColl et al., 2009; Maysami et al., 2015; Haley and Lawrence, 2016, 2017). In contrast to clinical studies that monitor patient recovery over several months, most of these studies in comorbid animals have focused on acute timepoints (e.g. 24-72h). In fact, some clinical studies suggest obesity may actually be beneficial for stroke recovery, the so-called 'obesity paradox', which leads to reduced mortality in obese patients (Vemmos et al., 2011; Doehner et al., 2013). One proposed biological explanation for these epidemiological observations is that excess energy stores in obesity protect against post-stroke weight loss (Scherbakov et al., 2011), thus preventing the harmful effects of malnutrition on post-stroke recovery. However, whether obesity affects weight loss, lipids and adipokine release, and neurological recovery and behaviour after experimental stroke in the long-term is poorly understood.

The aims of this study were to: (i) establish the effect of experimental stroke on depressive- and anxiety-like behaviours; long-term secondary complications commonly reported in stroke patients, and (ii) assess if stroke-induced prolonged changes in weight loss, and adipokine and lipid status. Additionally, we determined the impact of obesity on these outcomes.

3.4. Materials and Methods

3.4.1. Animals

Male C57BL/6J mice (Envigo) were used for all studies. All animals were housed in individually ventilated cages in standard housing conditions (temperature 21 ± 2°C; humidity 55% ± 5%; 12-h light/12-h dark cycle), with access to food and water *ad libitum*. At 8 weeks of age, cages of mice were randomly assigned (using 'rand()' function of Microsoft Excel) to either a high-fat diet (named obese; 60% energy from fat, 58G9, Test Diets, supplied by IPS Product Supplies Ltd) or a low-fat diet (named control; 12% energy from fat, 58G7, Test Diets, IPS Product Supplies Ltd) for 26 weeks prior to surgery (Maysami et al., 2015). All experiments were conducted in accordance with the UK Animals (Scientific Procedures) Act 1986 and approved by the local Animal Welfare and Ethical Review Board, University of Manchester, UK. All reporting of animal experiments complied with the ARRIVE guidelines (Animal Research: Reporting in In Vivo Experiments) (Kilkenny et al., 2010).

3.4.2. Transient middle cerebral artery occlusion

Transient middle cerebral artery occlusion (MCAo) was used to induce focal ischaemia in the left cerebral hemisphere using a protocol adapted from Longa *et al* (1989). Anaesthesia was induced with 4% isoflurane and maintained with 1.5% (30% O_2 and 70% N_2O). Core body temperature was monitored using a rectal probe and maintained at 37 ± 0.5°C with a homeothermic blanket (Harvard Apparatus). The left carotid arteries were exposed and a silicone-coated filament (coating 210 µm in diameter and 4-5 mm length, Doccol) was introduced into the external carotid artery and advanced along the internal carotid artery until occluding the origin of the middle cerebral artery. Successful MCAo was confirmed by a reduction in cerebral blood flow of at least 80% as measured using laser-Doppler (Moor Instruments). High-fat diet (for 6 months) is known to worsen ischaemic damage in rodents after 30 min but not 20 min MCAo (Maysami et al., 2015). As the severity of many outcome measures (e.g. post-stroke behavioural deficits) are likely to correlate with infarct volume the greater ischaemic damage seen after 30 min MCAo in obese high-fat fed mice could be a potential confounding factor. Therefore, to produce a similar volume of ischaemic damage between diet groups, the MCA was occluded for 20 min in obese mice (n = 10) and 30 min in control mice (n = 19). To confirm that obese mice have poorer outcome,

as previously reported by Maysami *et al* (2012), a group of obese mice (*n* = 4) also underwent MCA for 30 min. After the respective occlusion times, the filament was removed to allow reperfusion and the wound sutured. Sham operated mice (*n* = 10/diet group) underwent the same procedure, however once the filament had been inserted and advanced to the MCA it was immediately withdrawn. As we aimed to match infarct volumes between diet groups, and did not have a pilot data for animals recovered to 60 days, we had no pilot data on which to base power calculations. Therefore, a standardized effect size was used for the power analysis, using a Cohen's d of 1.4. Using an alpha of 0.5 and a power of 0.8, we found 10 animals per group would be required. However, additional animals were used in anticipation of drop-out over the 60-day recovery period due to the large infarcts expected. Due to the obese phenotype, blinding could not be performed during surgery, but all subsequent analyses were performed blinded to diet and surgery. To facilitate nutrition for the first 2 days post-MCAo, all animals were given access to a soft chow diet (Special Diets Services, BK001 E), in addition to their respective control and high-fat diets. Deficits in sensorimotor function were assessed using a 28-point neuroscore on days 2, 7, 14 and 51 post-MCAo, modified from procedures described previously (Encarnacion et al., 2011) (full protocol described in Appendix 2).

Due to animals reaching humane endpoints for animal suffering (Percie du Sert et al., 2017), several animals were euthanised within 14 days of surgery, some of which were euthanised prior to undergoing magnetic resonance imaging (MRI) imaging; 8 control (of which 3 had no MRI scan on day 2), 5 obese mice (20 min MCAo) and 4 obese mice (30 min MCAo). One animal each from the control 30 min and obese 20 min groups were excluded due to no stroke. No deaths or complications occurred in sham-operated animals. Final numbers were control sham *n* = 10, control MCAo/stroke *n* = 10, obese sham *n* = 10 and obese MCAo/stroke (20 min) *n* = 4, and are detailed in the figure legends.

3.4.3. Quantification of infarct volume/oedema/brain atrophy

Infarct volume and oedema were quantified at 48 hours post-MCAo, and brain atrophy at day 50 post-surgery by MRI. Under isoflurane anaesthesia, MRI scans were taken with a 7T horizontal bore magnet (Agilent Technologies) interfaced to a BrukerAvance III console (Bruker Biospin) using a surface transmit-receive coil.

Coronal pilot images were acquired to determine the correct geometry and localise the brain (using a multi-scale gradient echo sequence). T2-weighted TurboRARE high resolution images were taken under the following parameters; matrix = 256 x 256, slice thickness = 1 mm, interslice distance = 1 mm, resolution=0.0156 cm/pixel, acquisition time = 5 min 51 sec. Infarct volume at 48 hours was calculated by measuring infarct area over 8 slices in ImageJ (NIH). Oedema was calculated as the percentage difference between the volumes of the ipsilateral and contralateral hemispheres. At day 50, atrophy was calculated as the percentage reduction in the volume of the ipsilateral hemisphere compared to the contralateral. Analyses of atrophy, infarct volume and oedema were all performed blinded to experimental groups by randomising file names.

3.4.4. Behavioural Phenotyping

Depressive-like behaviours were assessed in all mice using the burrowing and nest building tests. For all tests a baseline measurement (day 0) was taken prior to surgery. Locomotor activity and measures of anxiety were assessed using the open field test. White noise was played throughout the tests to minimise auditory cues, and all testing (except nest building) was conducted during the light phase.

3.4.5. Burrowing

Burrowing ability was assessed in all mice on days 0, 3, 14 and 30 as adapted from R Deacon (2006). Briefly, burrows were made from 20 cm piece of 68 mm diameter plastic downpipe with one end sealed, 2.5 cm machine screws were inserted at the other end to elevate the burrow 3 cm off the cage floor. Mice were habituated to the burrowing arena (an empty cage) for 30 min, before burrowing tubes, containing 700 g of gravel, were introduced and left for 1 h. After 1 hour burrows were removed and remaining gravel was weighed to calculate percentage burrowed.

3.4.6. Nest building

Nest building ability was assessed in all mice on days 0, 3, 7, 14 and 30. Mice were individually housed with 140 g of wood chippings and 20 g of sizzle nest building material equally distributed throughout the cage, and food weighed. Mice were left overnight and images were taken of the nests from above and of the sides to determine depth and all mice returned to home cages. Nests were scored based

on Deacon's standardized scale (Deacon, 2006), from 0-5. All images were blinded and scored by two independent markers, an average score was calculated and further analysed. The amount of food consumed (kCal) during the dark phase was also calculated.

3.4.7. Open field

On day 37 mice were placed individually into the centre of a square opaque perspex box (45 cm x 30 cm x 45 cm) and their behaviour recorded for 5 min. Apparatus was cleaned with 70% ethanol between mice. Video recordings were analysed with Stoelting ANY-maze v4.9 software and for assessment of locomotion/activity the total distance (m) moved, average speed (m/sec), duration (sec) of mobile episodes were measured. For assessment of anxiety the time (sec) spent at the sides of the arena was measured and % time spent at the sides calculated.

3.4.8. Body Composition analysis.

Body composition (adipose tissue and lean mass) was assessed by nuclear magnetic resonance imaging (EchoMRI, Echo Medical systems) at days 0, 1, 3, 5, 7, 10, 14, 21, 42 and 49. Total body weight of animals was taken prior to scanning. Net loss (g) in total body weight and adipose and lean mass was calculated from day 0 (prior to stroke) and area under the curve (g x days) for all timepoints.

3.4.9. Tissue preparation and histology

At day 60 post-surgery mice were terminally anaesthetised with 4-5% isoflurane (30% O_2 and 70% N_2O) and cardiac blood taken before transcardial perfusion with phosphate buffered saline (PBS). Plasma was obtained by centrifugation at 1200g for 10 min and epididymal fat removed and both were frozen and stored at -80^{o}C. Animals were then transcardially perfused with 4% paraformaldehyde (PFA) and the brain and liver were immerse fixed in PFA for 48 h. The brain was sliced into 2 mm thick sections using a metal brain matrix. Brain sections and the liver were embedded in paraffin wax using a Shadon Citadel 2000 tissue processor (Thermo Fisher Scientific) and subsequently sectioned into 5 µm sections using a Leica RM 2155 Microtome (Leica Microsystems Ltd) and mounted on SuperFrost Plus slides (Thermo Fisher Scientific). Brain and livers were deparaffinised in xylene (followed by ethanol), stained with haemotaoxylin and eosin and coverslipped using DPX

mounting medium (Thermo Fisher Scientific). Hepatic steatosis (fatty vacuolation due to accumulation of lipid) and hepatocyte injury (ballooning degeneration and/or pale to clear cytoplasm) were semi-quantitatively graded using the criteria adapted from that previously described by *Kleiner et al* (2005). For each parameter, six random fields of view were evaluated using ImageJ (NIH) by an experimenter blinded to the groups by randomising file names.

3.4.10. Adipokine analysis

Adipose tissue (from frozen epididymal fat) was homogenized in buffer (50 mM Tris-HCl, 150 mM NaCl, 5 mM $CaCl_2$ and 0.02% NaN_3) containing 1% Triton-X and protease inhibitor cocktail 1 (Calbiochem). 5 µL was added per mg of tissue sample (around 100 mg of tissue was used). Samples were then homogenised using a T-10 Basic ULTRA-TURRAX homogeniser (IKA), briefly sonicated on ice with a hand-held probe sonicator (IKA) and left on ice for 30 min. Samples were centrifuged at 14,000 g for 30 min (4˚C). Supernatant was decanted and stored at -20˚C. Resistin, adiponectin and leptin in adipose tissue supernatant and plasma were analysed by enzyme-linked immunosorbent assay (ELISA; R&D Systems, DY1069, DY1119, DY498) according to the manufacturer's instructions. Adipokine concentrations were determined by reference to the relevant standard curves. For adipose tissue protein concentration was assessed by a bicinchoninic protein assay (BCA; Pierce Biotechnology), and results expressed as pg or ng/mg protein. For plasma data are expressed as µg or ng/ml/g fat weight.

3.4.11. Lipid analysis and ALT assay

Plasma levels of free fatty acids (FFAs; Zen-Bio Inc) and triglycerides (BioVision Inc) were measured (in mmol/l) using the relative assays according to the manufacturer's instructions. Alanine aminotransferase (ALT) levels were measured in the plasma using a colorimetric activity assay kit (Cayman Chemical).

3.4.12. Data and statistical analyses

Data are presented as mean ± standard deviation (SD), unless indicated. Equal variance and normality were assessed with the Brown-Forsythe and Shapiro–Wilk test respectively and appropriate transformations were applied when necessary. For discrete data and data with non-normal distributions (neuroscore), generalised linear mixed modelling (GLMM) was used with mouse I.D. as the

random effect (Fournier et al., 2012; Bates et al., 2015; Skaug et al., 2016). The significance of inclusion of an independent variable or interaction terms were evaluated using log-likelihood ratio. Holm-Šidák post-hocs were then performed for pair-wise comparisons using the least square means (Lenth, 2016). Pearson residuals were evaluated graphically using predicted vs level plots. All analyses were performed using R (version 3.5.1). Linear mixed effects models were used to assess the effects of diet and stroke on depressive-like behaviour. The linear mixed model function “lme” (nlme v1.1-9) was used to estimate the effects of stroke and diet on outcome measures. All factors and interactions were modelled as fixed effects. A within-subject design with random intercepts and by-subject random slopes for all effects was used, aiming for a maximal random effects structure. Inclusion of fixed effect into the model were evaluated using the log-likelihood ratio test. Modelling was carried out using R (version 3.2.5). All other statistical analyses were performed using GraphPad Prism v6 (GraphPad Software Inc) using the appropriate tests (as detailed in the figure legends). p values < 0.05 were considered statistically significant.

3.5. Results

3.5.1. Obese mice with the same infarct volume showed no difference in acute outcome

Although obesity is a well-established risk factor for ischaemic stroke, it is more controversial as to whether obesity worsens outcome in patients. We have shown previously that with an occlusion time of 30 min, obesity (induced by high-fat feeding) increases ischaemic damage after experimental stroke in mice (Maysami et al., 2015) and here 30 min occlusion of the MCA also produced severe ischaemic damage and all mice (n = 4) had to be culled at day 2. To better model the clinical situation and avoid the confounding effect of differences in infarct volumes between groups, the MCA was occluded for 20 min in obese mice, compared to 30 min in control mice. There was no effect of sham surgery on survival in either diet group. There was no significant difference in survival between control mice undergoing a 30 min occlusion, and obese mice undergoing a 20 min occlusion (Fig. 3.1a). There was also no significant difference in infarct volume or stroke-induced oedema between groups as measured by MRI at day 2, either in all mice including those that died, or in survivors only (Fig. 3.1b,c).

MRI imaging at day 2 (Fig. 3.1d) showed large infarcts present in both the striatum and cortex, and in some cases extending into the hippocampus and thalamus. At day 50, areas of hyperintensity on MRI were present predominantly in the outer cortical regions. On histological examination these regions were cerebral spinal fluid- (CSF) filled cavities devoid of brain tissue. Ventricular enlargement and ipsilateral hemisphere atrophy were also observed in both control and obese stroked animals, with no significant in atrophy difference between groups (Fig. 3.1e).

Sensorimotor function was assessed longitudinally using neuroscore. Deficits in both groups were observed up to 51 days post-stroke compared to sham animals (Fig. 3.1f). A significant effect of day ($p < 0.001$) was observed after stroke in control and obese mice indicating functional improvement (a reduction in neuroscore) over time. There was no effect of diet on neuroscore, and no interaction effect between diet and day.

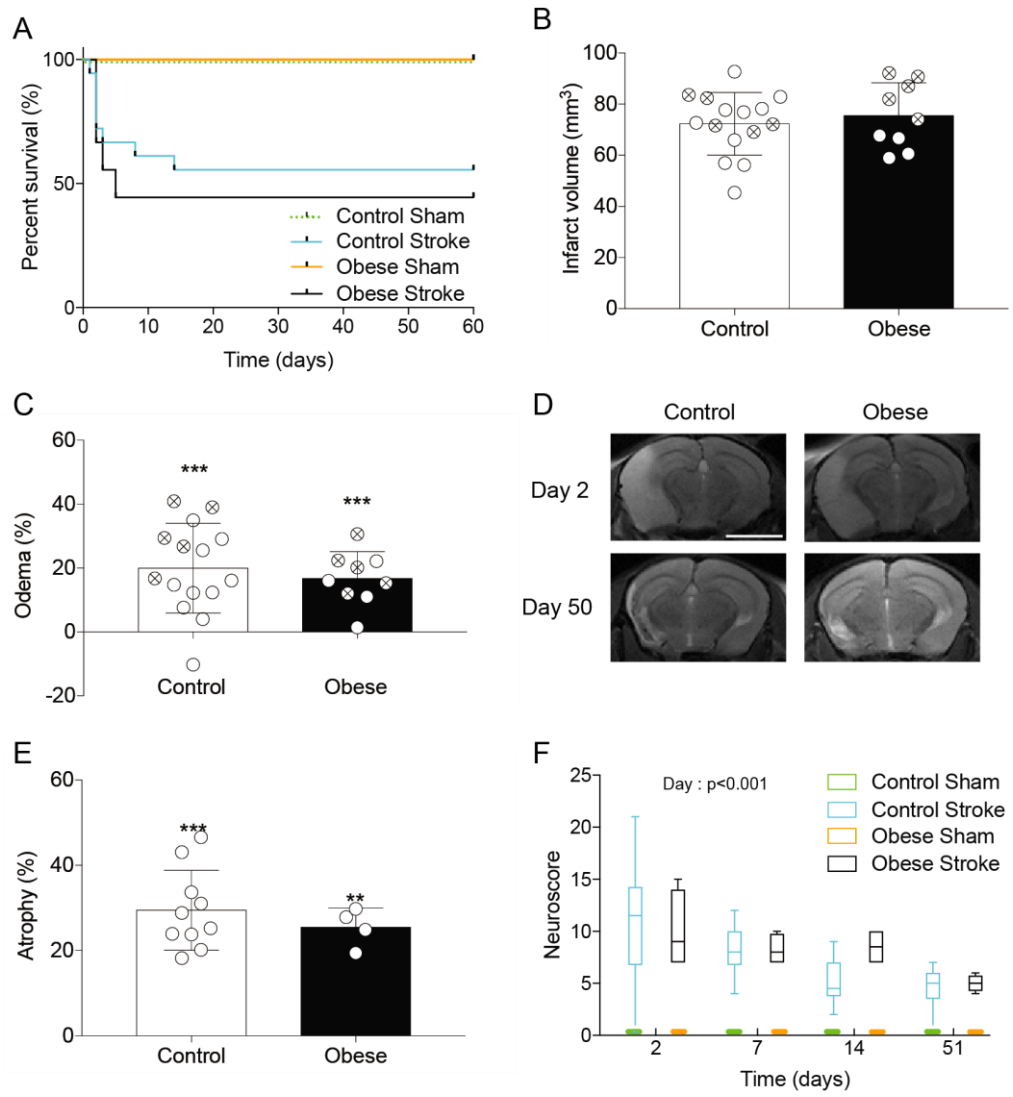

Figure 3.1 - Obese mice with the same infarct volume showed no difference in outcome.

C57BL/6J fed a control or high-fat (obese) diet for 6 months underwent middle cerebral artery occlusion (MCAo; 30 min for control, 20 min for obese). Percent survival over 60 days (**a**). MRI imaging (T2 Turborare) was performed on all mice at day 2, and in survivors at day 50. Infarct volume (**b**) and oedema (**c**) were quantified on day 2 using MRI images (crossed symbols represent mice culled prior to d 50). Representative MRI scans for both control and obese mice illustrating ischaemic damage on day 2 and ipsilateral hemisphere atrophy on day 50 (**d**). Representative images for both timepoints are from the same mouse (scale bar = 0.38 cm). Atrophy in ipsilateral hemisphere was measured at day 50 from MRI scans (**e**). Neuroscore was measured at days 2, 7, 14 and 51 after surgery to assess sensorimotor deficits (**f**). Data are presented as mean ± SD (**a, b, c, e**) or median and interquartile range (**f**). For (**b**) and (**c**) n = 9-15 and (**e**) and (**f**) n = 4-10. Data were assessed using (**a**) a Log-rank (Mantel-Cox) test, (**b**) unpaired t-test, (**c**) and (**e**) one-sample t test with hypothetical value of 0 within a group (where ***$p < 0.001$) and unpaired t-test between groups, (**f**) generalised linear mixed effects modelling followed by Holm-Šidák *post hoc* analysis.

3.5.2. Stroke disrupts spontaneous behaviours in mice

Both nest building and burrowing are behaviours engaged by healthy mice without training, and so the loss of these behaviours can be used as indication of depressive-like behaviour. Stroke induced deficits in both nest-building (Fig. 3.2a) and burrowing (Fig. 3.2b). The stroke-induced deficit in nest building was detectable up to 14 days post-stroke, with a maximal reduction seen at 3 days. Mixed linear model analysis identified a main effect of stroke (χ_1^2=7.076, $p < 0.008$), but no effect of diet, and no interaction between stroke and diet. Deficits in burrowing behaviour were observed at 3 days post-stroke compared to sham operated control mice. However, sham-operated obese mice also had significantly reduced burrowing behaviour at day 3. Mixed linear model analysis identified a main effect of both diet (χ_1^2=5.094, $p < 0.024$) and stroke (χ_1^2=4.563, $p < 0.033$). An interaction effect between stroke and diet was observed (χ_1^2=5.011, $p < 0.025$), and between stroke and day (χ_3^2=13.284, $p < 0.004$).

To determine if there were any changes in locomotion or anxiety-like behaviours, open field analysis was performed on day 37. No effect of diet or stroke was detected on the total distance travelled, average speed, or time mobile (Fig. 3.3a-c). A significant main effect of diet and stroke was observed on measures of anxiety (time spent in the sides of arena), with stroke increasing anxious behaviour (Fig. 3.3d). No interaction effect between diet and stroke was observed on any parameters assessed. To assess working memory the Y-maze test was performed at day 14 and 45. No memory impairment was observed after stroke in either control or obese mice compared to sham (Fig. 3.S1).

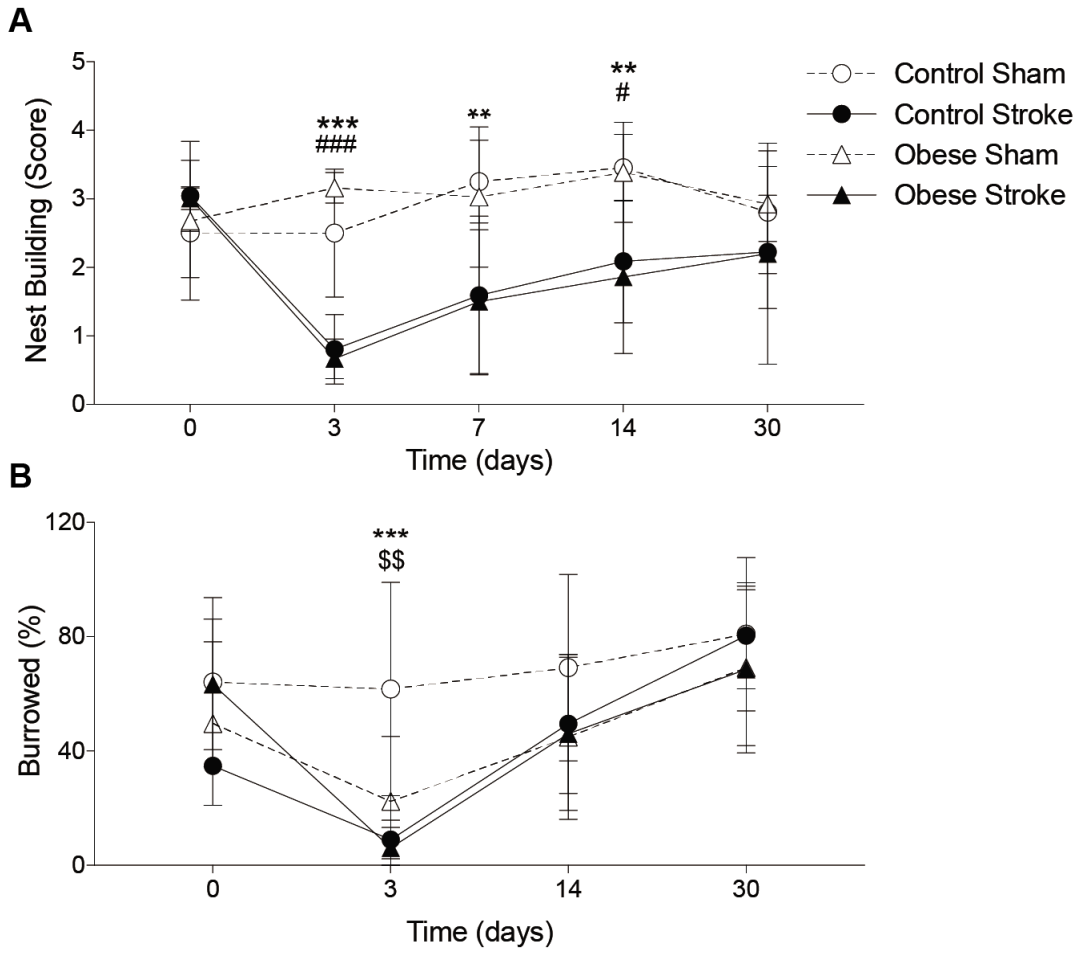

Figure 3.2 - Stroke induces prolonged depressive-like behaviours.
Depressive-like behaviours were assessed by nest building (a) and burrowing (b) on days: 0, 3, 7, 14 and 30 (not day 7 for burrowing) post-stroke. Impaired nest building behaviour in control and obese mice was observed up to 14 days after stroke, and at day 3 for burrowing, when obese sham mice also showed a deficit. Data are presented as mean ± SD (n = 4-10). $^{**}p < 0.01$ and $^{***}p < 0.001$ control sham versus control stroke; $^{\#}p < 0.05$ and $^{\#\#\#}p < 0.001$ obese sham versus obese stroke; $^{\$\$}p < 0.01$ control sham versus obese sham. Statistical analysis was performed using a linear mixed effects models followed by Šidák-Holmes *post hoc* analysis.

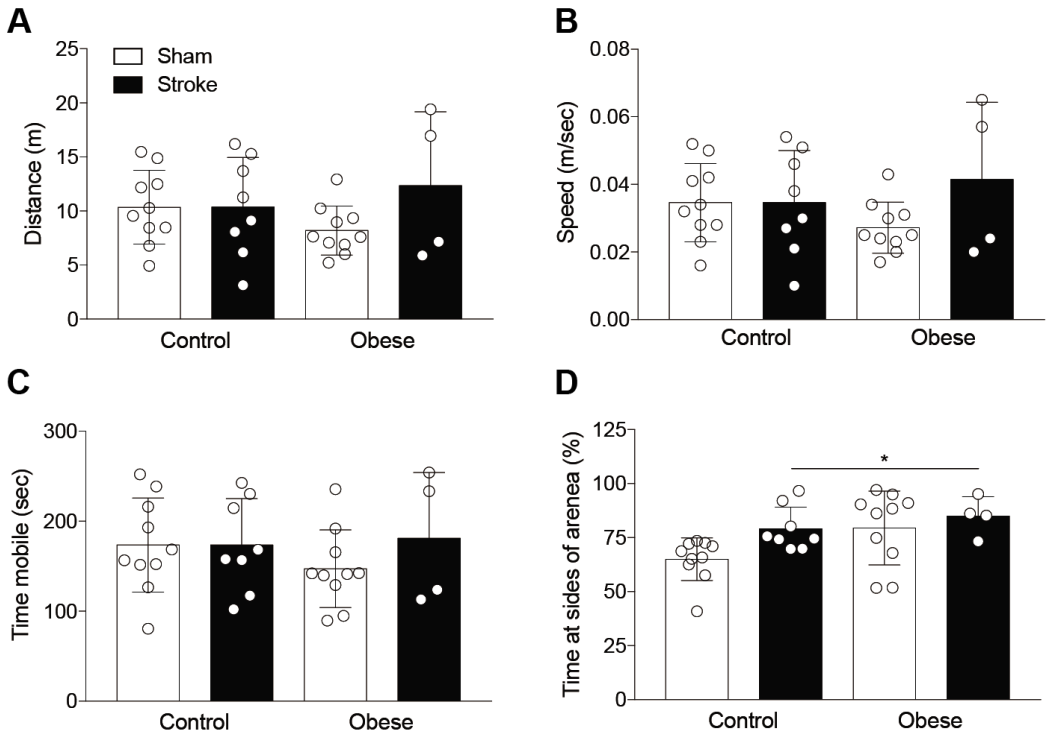

Figure 3.3 - Stroke induces behaviours indicative of anxiety.
Locomotor behaviour and measures of anxiety were assessed in the open field test on day 37 and expressed for locomotion as (**a**) total distance moved, (**b**) average speed, (**c**) time mobile, and for anxiety (**d**) percentage of time spent at sides of arena. An increase in the amount of time spent at the sides of the arena, indicating anxiety, was seen after stroke in control and obese mice and also in obese mice after sham surgery. Data are presented as mean ± SD (n = 4-10). *$p < 0.05$ for a main effect of stroke and diet. Statistical analysis was performed using a two-way ANOVA followed by Tukey's *post hoc* multiple comparisons test.

3.5.3. Greater and prolonged adipose tissue loss in obese mice after stroke

Before surgery (MCAo or sham), mice fed a high-fat diet had increased body weight and a higher percentage body fat but reduced lean mass (Table 3.1) compared to mice fed a control diet. After experimental stroke, both control and obese mice showed a prolonged loss of body weight compared to sham-operated mice (Fig. 3.4a,d, Table 3.1). However, body weight loss was significantly greater in obese mice. In both groups, post-stroke weight loss was primarily due to a reduction in adipose tissue mass, with obese mice losing significantly more adipose tissue (Fig. 3.4b,e). In comparison, lean mass reduced only transiently in both stroke groups, and the extent of the loss was similar between control and obese mice (Fig. 3.4c,f). In neither group did infarct volume correlate with weight loss (Fig. 3.4g). At day 14 when weight loss reached a nadir after stroke, overnight food intake was significantly greater compared to baseline (day 0) in both control-fed sham and stroke mice, but no difference was seen between day 0 and 14 in obese mice (Fig. 3.4h).

Table 3.1 - Body composition before and after stroke.

	Control		**Obese**	
	Sham	**Stroke**	**Sham**	**Stroke**
Initial				
Body weight	34.5 ± 5.8	34.0 ± 1.9	49.4 ± 1.7$^{###}$	50.1 ± 3.9$^{###}$
% fat	27.6 ± 13.2	28.5 ± 4.0	43.2 ± 2.2$^{###}$	43.1 ± 3.2$^{#}$
% lean	67.6 ± 12.2	67.3 ± 2.9	53.9 ± 2.2$^{###}$	52.6 ± 1.9$^{##}$
Final				
Body weight	35.4 ± 5.7	28.9 ± 1.5*	47.6 ± 4.4$^{###}$	34.9 ± 8.5***
% fat	27.7 ± 11.0	11.3 ± 5.0***	35.6 ± 5.3	19.5 ± 8.9**
% lean	70.9 ± 8.7	79.9 ± 8.7	61.3 ± 4.5$^{#}$	78.5 ± 9.3**

Mice were kept on a control diet or a high-fat diet (obese) for 6 months. Middle cerebral artery occlusion (MCAO; 30 min for control and 20 min for obese) to induce stroke, or sham surgery was performed. Body weight, and % fat and lean tissue were assessed before and at day 50 after surgery by EchoMRI. Data are shown as mean values ± S.D. (n = 4-10/group). Statistical analysis was performed using a two-way ANOVA followed by Tukey's *post hoc* multiple comparisons test. *p < 0.05, **p < 0.01, ***p < 0.001 versus surgery control on same diet and $^{#}p$ < 0.05, $^{##}p$ < 0.01, $^{###}p$ < 0.001 versus control diet for same surgery.

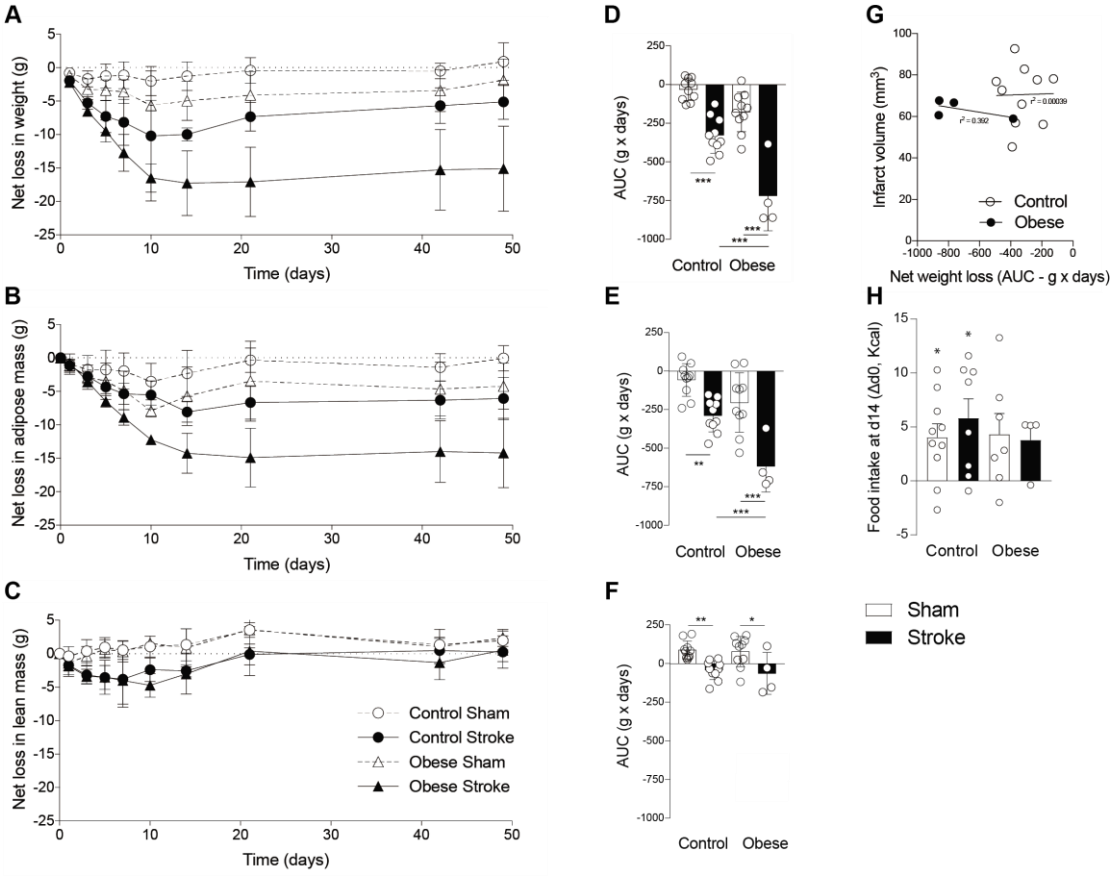

Figure 3.4 - Stroke induced a prolonged reduction in adipose tissue mass.
Net change in body weight (a), adipose/fat mass (b) and lean mass (c) in grams were measured at baseline and days 1, 3, 5, 7, 10, 14, 21, 42 and 49 after stroke. Fat and lean masses were determined by EchoMRI. Area under the curve was calculated for net change (d-f). A prolonged decrease in body weight due to loss of fat mass was observed in control and obese mice after stroke with greater loss in obese mice. Stroke induced a transient loss of lean mass in control and obese mice. No correlation was seen between body weight loss and infarct volume in control or obese mice (g). Overnight food intake on day 14 relative to food intake prior to surgery (day 0) (h) was significantly increased in control but not obese groups. Data are shown as mean values ± SD (n = 4-10/group). For AUC data, all groups were compared with a two-way ANOVA followed by Tukey's *post hoc* multiple comparisons test, where *$p < 0.05$, **$p < 0.01$, ***$p < 0.001$. Difference in food intake was compared to a hypothetical mean of 0 by one-sample t-test (where *$p < 0.05$). Correlation in (g) was performed using a linear regression.

3.5.4. Stroke induces a prolonged change in adipokine production

In mice fed a control diet, stroke induced significant alterations in adipokine production at 60 days post-stroke (Fig. 3.5). Resistin concentrations were significantly increased after stroke in the adipose tissue (Fig. 3.5a) and plasma (Fig. 3.5b), and adiponectin concentrations were increased in the plasma (Fig. 3.5c). Leptin concentrations were unaffected by stroke (Fig. 3.5c,f). The adipokine-response to stroke was similar in obese mice, though some differential effects were observed. For example, stroke did not induce a significant increase in resistin in the adipose tissue in obese mice. There was no significant correlation between the extent of weight loss and plasma adipokine levels after stroke in control or obese mice (adiponectin; control $r^2 = 0.09$, obese $r^2 = 0.32$: resistin; control $r^2 = 0.19$, obese $r^2 = 0.29$: leptin; control $r^2 = 0.0002$, obese $r^2 = 0.35$). Obesity by itself (in the absence of stroke) also affected adipokine production. Sham-operated obese mice had decreased resistin and adiponectin concentrations in the adipose tissue and plasma, and increased concentrations of leptin in adipose tissue.

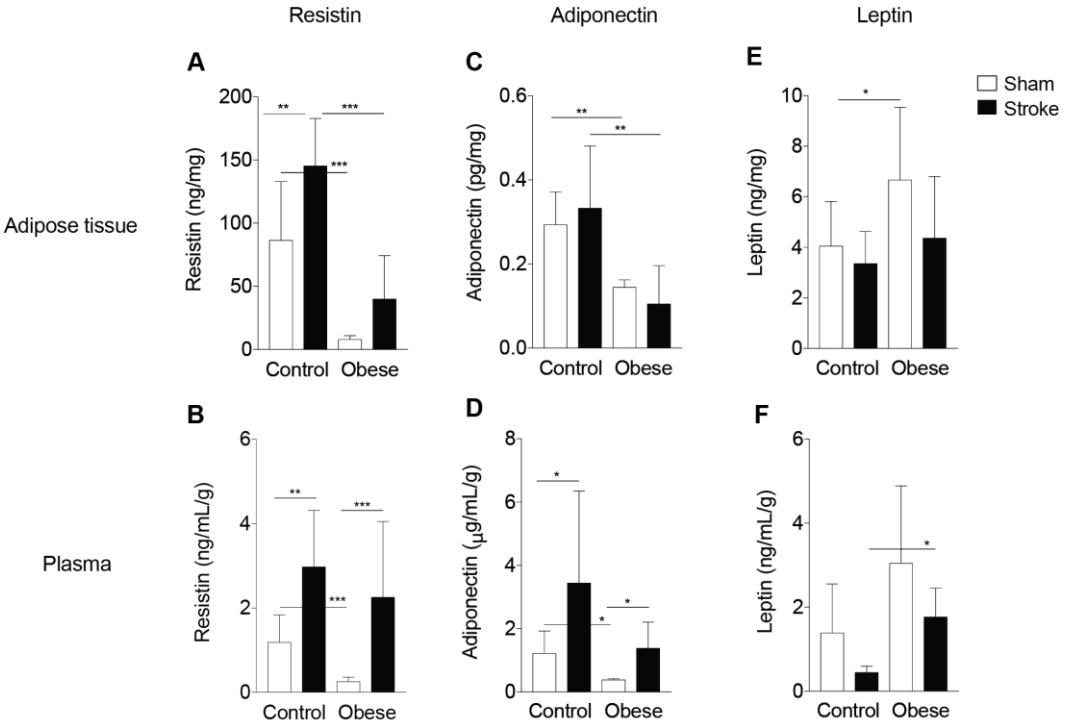

Figure 3.5 - Stroke induces a prolonged change in adipokine production.
White adipose tissue (epididymal, a,c,e) and plasma (b,d,f) was taken 60 days post-stroke and resistin (a-b), adiponectin (c-d) and leptin (e-f) levels assessed by ELISA. In control mice, stroke resulted in an increase in resistin in the adipose tissue and plasma, and an increase in plasma adiponectin. An increase in plasma resistin and adiponectin was also seen after stroke in obese mice. Adipose tissue concentrations were normalised to microgram of total protein from BCA assay and plasma concentrations normalised to total adipose mass. Data are presented as mean ± SD (n = 4-10). *p < 0.05, **p < 0.01 and ***p < 0.001. Statistical analysis was performed using two-way ANOVA followed by Tukey's *post hoc* multiple comparisons test.

3.5.5. Stroke induces a prolonged change in plasma lipids and induces liver function

In mice fed a control diet, at 60 days after stroke there was a significant increase in plasma free fatty acids and triglycerides (Fig. 3.6a,b). This effect was not seen in obese mice, though sham-operated obese mice had higher plasma triglycerides concentrations. In response to stroke in either control or obese mice there was no significant correlation between weight loss and plasma free fatty acids (control r^2 = 0.00002, obese r^2 = 0.26) or triglycerides (control r^2 = 0.05, obese r^2 = 0.19).

Increases in liver triglycerides have previously been reported 24 hours after stroke in mice. Livers were therefore taken at day 60 and assessed histologically. Liver steatosis was observed in sham-operated obese mice, though this effect was lost in obese mice undergoing experimental stroke (Fig. 3.6c,e). Stroke had no effect on liver steatosis in control-fed mice. Hepatocyte injury was also measured using a scoring system, with damaged hepatocytes being identified by their partial or complete loss of cytoplasm, and condensed or swollen nuclei (Fig. 3.6d,e). Stroke induced significant hepatocyte damage in mice fed a control diet, though significant hepatocyte damage was already observed in sham-operated obese mice, and so stroke did not further increase hepatocyte damage in obese mice. ALT was measured as an indicator of liver function and was lower in both control and obese mice after a stroke compared to sham groups (Fig. 3.6f).

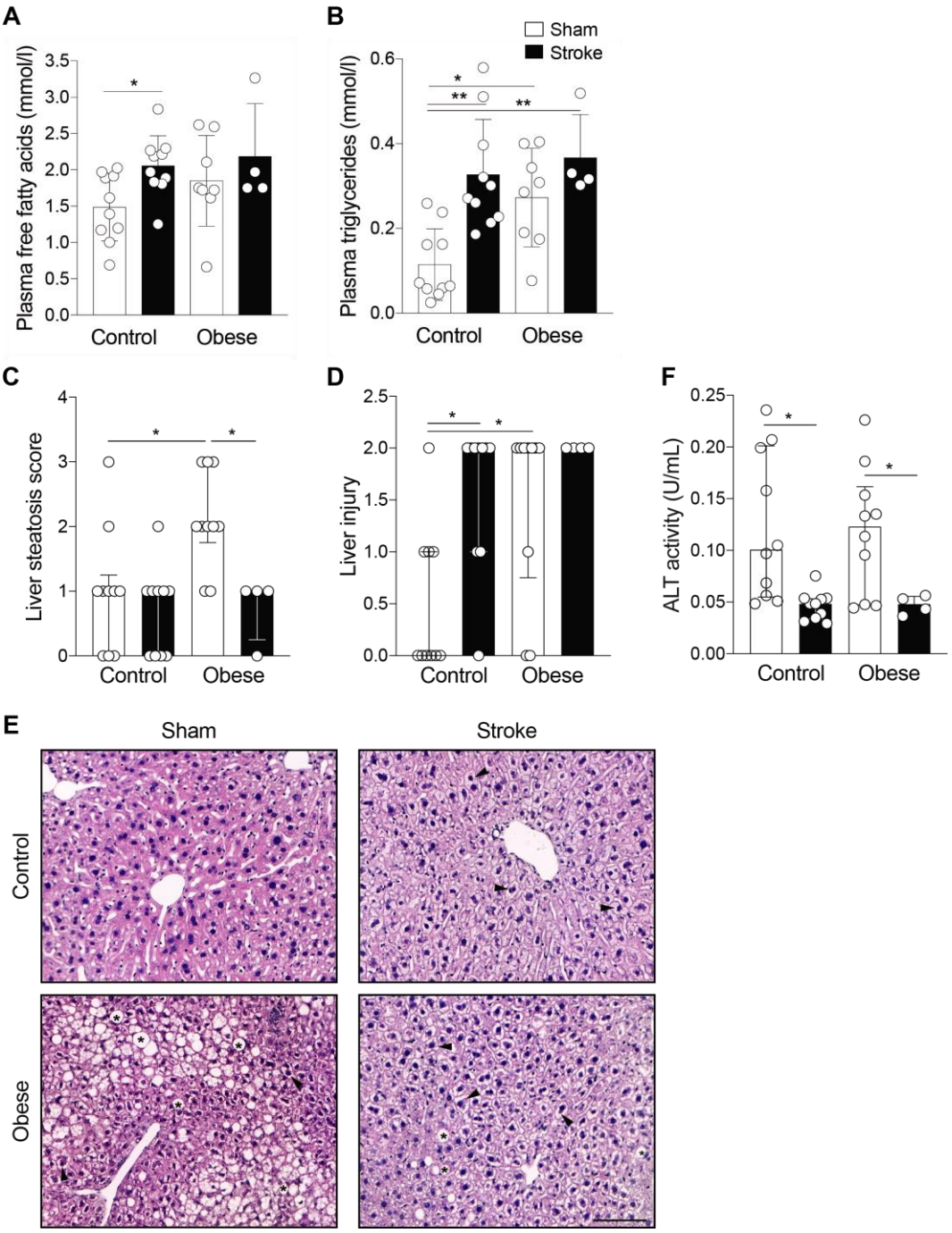
A
Plasma free fatty acids (mmol/l)
3.5
3.0
2.5
2.0
1.5
1.0
0.5
0.0
*
Control
Obese
B
Sham
Stroke
Plasma triglycerides (mmol/l)
0.6
0.4
0.2
0.0
*
**
**
Control
Obese
C
Liver steatosis score
4
3
2
1
0
*
*
Control
Obese
D
Liver injury
2.5
2.0
1.5
1.0
0.5
0.0
*
*
Control
Obese
F
ALT activity (U/mL)
0.25
0.20
0.15
0.10
0.05
0.00
*
*
Control
Obese
E
Sham
Stroke
Control
Obese

Figure 3.6 - Stroke induces a prolonged increase in plasma lipids and change in liver pathology and function.
At 60 day post-stroke, free fatty acids (a) and triglycerides (b) were assessed in the plasma. Liver steatosis and injury were assessed semi-quantitatively in tissue sections (c & d). Representative images of liver (e) showing steatosis (accumulation of fat) in obese mice (asterisks), and liver injury (ballooning of hepatocytes and/or pale to clear cytoplasm; arrow heads) in obese mice, and in control-fed mice. Scale bar 100µm. Plasma ALT levels (f). In control mice, stroke led to an increase in plasma free fatty acids and triglycerides, a decrease in ALT, and caused a change in liver pathology/injury. Raised triglycerides, liver injury and lower ALT were observed in obese mice after sham or stroke surgery, while liver steatosis seen in obese sham mice was reduced after stroke. Data are presented as mean ± SD (a, b, f) or median and interquartile range (c, d). (n = 4-10). *$p < 0.05$ and **$p < 0.01$. Statistical analysis was performed using two-way ANOVA followed by Tukey's *post hoc* multiple comparisons test for (a, b, f) and a non-parametric Kruskal-Wallis test followed by Dunn's test for multiple comparisons for (c, d).

3.6. Discussion

Here we monitored the long-term metabolic and behavioural effects of stroke, and the impact of the co-morbidity obesity and demonstrate in control male mice long-lasting changes that could indicate a risk for future vascular health.

Stroke patients commonly develop depression and anxiety, which are barriers to recovery and rehabilitation (Duncan et al., 2012; Ayerbe et al., 2013; Nakling et al., 2017). Here, experimental stroke in mice induced prolonged changes in behaviours that were measures of sickness behaviour, depression and anxiety. Both nest building and burrowing behaviours were disrupted, two tests that exploit natural rodent behaviours, which could also be surrogate markers for activities of daily living. Burrowing behaviour has classically been employed as a measure of sickness behaviour in mouse models of systemic inflammation and prion disease (Deacon et al., 2001; Teeling et al., 2007), but has also been suggested to measure attention and executive function (Deacon et al., 2008). Nest building, a complex goal-directed behaviour, has previously been used in models of schizophrenia to study negative symptoms including impaired attention (Takao et al., 2013; Pedersen et al., 2014). The reasons that patients develop depression are complex and poorly understood, though inflammation has been hypothesised to play a role (Becker, 2016). Inflammation is well understood to drive sickness behaviour in rodents, which seems phenotypically similar to depression, involving decreased concentration, fatigue and anhedonia (Maes et al., 2012). Prolonged anxiety was also seen after stroke, as mice spent more time at the sides of an open arena compared to the centre. It is unlikely that impairment in motor activity contributed solely to these behavioural changes (especially nest building and burrowing) after stroke as no changes in the distance moved or speed were observed in the open field test. Furthermore, we observed no deficits in nest building and burrowing at day 30 when there was still an impairment in sensorimotor function assessed using neuroscore. Some behaviours including burrowing have been proposed to be affected by repeated anaesthesia in healthy mice (Hohlbaum et al., 2017). However, in the latter study burrowing was assessed 30 min post-anaesthesia compared to at least 24 hours here. Burrowing was not impaired in control mice after sham surgery, thus making it unlikely that anaesthesia contributed to the burrowing deficits in the present study. Collectively therefore, by using these tests,

we have demonstrated that experimental stroke induced long-lasting changes in behaviour that were relevant to those seen in stroke patients.

Weight loss and malnutrition are frequently observed in patients with stroke, and are associated with poor outcome (Jöonsson et al., 2008; Kim et al., 2015; Nii et al., 2016; Scherbakov et al., 2019). It was originally thought that weight loss is due primarily to a reduction in lean mass, in particular muscle wasting (sarcopenia) (Scherbakov et al., 2015) but recent work also demonstrates loss of fat mass (Scherbakov et al., 2019). Weight loss and reduction in muscle mass (examined *ex vivo*) have also been reported in rodents up to 7 days after experimental stroke (Choe et al., 2004; Chang et al., 2010; Springer et al., 2014; Desgeorges et al., 2015). These changes in muscle mass appear to be transient as no differences were observed between 2-14 weeks (Ansved et al., 1996; Abo et al., 2004). Here, we comprehensively assessed the impact of stroke on body composition *in vivo* up to 49 days post-stroke, observing a prolonged reduction in body weight that was due to a loss of fat mass. Lean mass was also lost, but returned to pre-surgery levels by 21 days. The reason for this dramatic and prolonged weight loss after stroke is unclear and could involve several mechanisms, including reduced food intake and/or raised energy expenditure, possibly via the action of inflammatory mediators. Acute weight loss after experimental stroke can correlate positively with ischaemic damage (Scherbakov et al., 2011; Cai et al., 2015), although this correlation is not always observed (Haley et al., 2017). Here, the degree of weight loss over 49 days did not directly correlate with initial damage at 48 h, suggesting that post-stroke weight loss may be caused by factors secondary to the initial injury, and develop during recovery. Experimental models of stroke involving permanent external carotid ligation have been proposed to cause feeding difficulties that result in weight loss (Trueman et al., 2011; Trotman-Lucas et al., 2017). Although food intake is likely to be reduced in the initial few days after stroke, we observed that when weight loss was maximal (day 14), food intake was not different (in obese) or increased (in controls) compared to pre-surgery, which is in agreement with others showing no reduction in food intake 7 days after stroke in mice (Springer et al., 2014). Furthermore, weight loss was significantly less in sham-operated mice (compared to stroke) in which external carotid ligation was also performed.

The long-term reduction in body fat we observed after experimental stroke was also accompanied by changes in lipid metabolism. This effect was most pronounced in non-obese animals, which showed increases in plasma free fatty acids and triglycerides. Non-obese animals also had higher plasma concentrations of resistin and adiponectin after stroke. It is unlikely that weight loss alone caused these changes as there was no correlation between the severity of weight loss and plasma levels of these factors. In addition, healthy weight loss is typically associated with a reduction in plasma free fatty acids and triglycerides. Experimental stroke has been previously shown to acutely affect peripheral lipid metabolism, potentially through the release of inflammatory mediators that can promote a catabolic state (Haley et al., 2017), and can also exacerbate atherosclerosis (Roth et al., 2018). Together, these findings of lipid and adipokine disturbance here suggest that experimental stroke in non-obese mice resulted in long-lasting changes in metabolism, potentially originating in the adipose tissue. Changes in plasma adipokines and lipids in patients after stroke have been studied poorly, but a few studies report early increases in resistin and triglycerides (Kochanowski et al., 2012; Perovic et al., 2016, 2017). Whether these factors in patients are high prior to stroke, and/or if they remain elevated more chronically is unknown. Stroke patients are at an increased risk of future vascular events, but it is not fully understood why (Putaala et al., 2010; Boulanger et al., 2019). However, altered blood lipids (Yaghi and Elkind, 2015), increased plasma resistin (Opatrilova et al., 2018) and changes in adiponectin (Hao et al., 2013) have been reported as risk factors for stroke. Similarly, being underweight is a risk factor for stroke, and for poor stroke outcome (Olsen et al., 2008; Doehner et al., 2013; Andersen and Olsen, 2015; Wang et al., 2015). Therefore, prolonged weight loss after stroke may result in a lipid and adipokine profile that increases the risk of further vascular events.

After stroke, non-obese animals also showed prolonged liver histological changes suggestive of liver injury. Previous work has indicated liver damage and hepatocyte apoptosis after stroke in high-fat fed rats, but only an acute timepoint (24 h) was studied (Gong et al., 2012). Liver damage is also reported in other experimental models of injury including heart failure (Shaqura et al., 2017). Within in the first 24 hours after stroke in rodents an increase in chemokine and cytokine expression is observed in the liver, which is accompanied by infiltration of neutrophils that could

potentially initiate damage (Gong et al., 2012; Wang et al., 2014; Maysami et al., 2015; Haley et al., 2017). An increase in liver triglyceride content is also seen 24 hours after stroke in mice (Haley et al., 2017). It is not known if liver triglyceride levels are chronically elevated in the present study, but this is unlikely as there was no increase in liver steatosis after stroke when assessed histologically. Liver damage is usually accompanied by an increase in plasma ALT, and raised plasma ALT have been reported between 3-24 hours after stroke in rats (Yang et al., 2003; Wang et al., 2014). In contrast here, plasma ALT levels were lower 60 days after stroke compared to sham. However, low ALT blood levels have been shown to be a marker of frailty and be associated with increased risk of mortality and poorer long-term outcome in the middle-aged and elderly, and patients with ischaemic heart disease (Elinav et al., 2006; Ramaty et al., 2014; Ramati et al., 2015; Peltz-Sinvani et al., 2016; Edvardsson et al., 2018; Kogan et al., 2018). To our knowledge, chronic liver function has not been studied in ischaemic stroke patients, but liver disease is a co-morbidity and risk factor for stroke (Kim et al., 2017; Zhang et al., 2018) and lower ALT at admission is a predictor of poor outcome at 3 months (Gao et al., 2017). Thus overall, these data suggest that experimental stroke induced a prolonged change in liver function, but whether this has a long-term consequence on health remains to be determined.

Obese rodents have greater infarcts after experimental stroke (McColl et al., 2009; Maysami et al., 2015; Haley and Lawrence, 2017). As the extent of ischaemic damage is the most important determinant of acute sensory and motor outcomes, it is also likely a key determinant of the longer-term outcomes studied here. Therefore, to model the clinical situation in which obese patients often do not have worse initial ischaemic injury and outcome (Dehlendorff et al., 2014; Seet et al., 2014), we used different MCA occlusion times in our control and high-fat fed groups to match initial ischaemic damage. Indeed, there was no significant difference in infarct volume at 48 hours or long-term survival up to 60 days. Furthermore, there was also no influence of obesity on the extent of odema, brain atrophy, physical impairment (when assessed by neuroscore) or depressive and anxiety-like symptoms. In contrast to the experimental studies, some clinical studies report an ‘obesity paradox’ where obese stroke patients have reduced mortality and morbidity. A hypothesised biological explanation for the ‘obesity paradox’ is that the greater metabolic reserves found in obese stroke patients protect them from

severe weight loss, especially loss of lean tissue (Scherbakov et al., 2011; Haley and Lawrence, 2016). In the present study, we found that obese mice had a greater reduction in fat mass after stroke compared to control mice. This could be partly due to food intake, as food intake was not increased after stroke (at day 14) in obese mice, and without a positive calorie balance the lost weight will not be regained. Enhanced weight loss in obese mice may also be driven by inflammatory cytokines that promote an enhanced anorexic response and/or raised metabolic rate. Increases in inflammatory cytokines are observed in obese mice after stroke in the plasma, liver and adipose tissue (Maysami et al., 2015; Haley et al., 2017). Obese mice also show an enhanced anorectic response to lipopolysaccharide, which causes a greater and more prolonged reduction in food intake and body weight (Lawrence et al., 2012). Besides losing more adipose weight after stroke, obese mice showed an altered long-term disturbance in lipids and adipokines compared to control mice, likely as obesity *per se* resulted in metabolic abnormalities (e.g. increased plasma lipids), which were similar to those found after stroke in control mice. Together, these data suggest that obesity did not offer protection against weight loss after experimental stroke or affect long-term behavioural changes.

In summary, stroke patients commonly develop secondary complications in the weeks and months after stroke that negatively affect their recovery and quality of life. However, these complications are not well studied preclinically, and their mechanisms are poorly understood. Here, we identified new behavioural tools to assess secondary complications of stroke such as depression. We also were the first to observe long-term effects of stroke on metabolic markers. Specifically, our data demonstrate that in both obese and control mice, lean mass is only transiently reduced after stroke, whereas we observed a long-term effect on fat mass. This reduction in fat mass in control mice was accompanied by changes in adipokines and lipids, and potential changes in liver function. Future work should determine if these findings in male mice are also seen in females, and how they translate to stroke patients. However, these data suggest stroke causes a lasting effect on metabolism that could contribute to the increased risk of recurrent vascular events seen in stroke patients.

3.7. References

Abo, M., Miyano, S., Eun, S. S. and Yamauchi, H. (2004). Histochemical characterization of skeletal muscles in rats with photochemically-induced stroke. *Brain Injury*, 18(10), 1017–1024.

Andersen, K. K. and Olsen, T. S. (2015). The obesity paradox in stroke: Lower mortality and lower risk of readmission for recurrent stroke in obese stroke patients. *International Journal of Stroke*, 10(1), 99–104.

Ansved, T., Ohlsson, A. L., Jakobsson, F. and Johansson, B. B. (1996). Enzyme-histochemical and morphological characteristics of fast- and slow-twitch skeletal muscle after brain infarction in the rat. *Journal of the neurological sciences*, 144(1–2), 14–20.

Ayerbe, L., Ayis, S., Wolfe, C. D. A. and Rudd, A. G. (2013). Natural history, predictors and outcomes of depression after stroke: Systematic review and meta-analysis. *British Journal of Psychiatry*, 202(1), 14–21.

Bates, D., Mächler, M., Bolker, B. and Walker, S. (2015). Fitting Linear Mixed-Effects Models Using lme4. *Journal of Statistical Software*, 67(1), 1–48.

Becker, K. J. (2016). Inflammation and the Silent Sequelae of Stroke. *Neurotherapeutics*, 13(4), 801–810.

Boulanger, M., Li, L., Lyons, S., Lovett, N. G., Kubiak, M. M., Silver, L., Touzé, E. and Rothwell, P. M. (2019). Effect of coexisting vascular disease on long-term risk of recurrent events after TIA or stroke. *Neurology*, 93(7), e695–e707.

Cai, L., Geng, X., Hussain, M., Liu, Z., Gao, Z., Liu, S., Du, H., Ji, X. and Ding, Y. (2015). Weight loss: Indication of brain damage and effect of combined normobaric oxygen and ethanol therapy after stroke. *Neurological Research*, 37(5), 441–446.

Chang, H.-C., Yang, Y.-R., Wang, P. S., Kuo, C.-H. and Wang, R.-Y. (2010). Effects of insulin-like growth factor 1 on muscle atrophy and motor function in rats with brain ischemia. *The Chinese Journal of Physiology*, 53(5), 337–48.

Choe, M. A., Gyeong, J. A., Lee, Y. K., Ji, H. I., Choi-Kwon, S. and Heitkemper, M. (2004). Effect of inactivity and undernutrition after acute ischemic stroke in a rat hindlimb muscle model. *Nursing Research*, 53(5), 283–292.

Deacon, R. M. (2006). Assessing nest building in mice. *Nature Protocols*, 1(3), 1117–1119.

Deacon, R. M. J. (2006). Burrowing in rodents: a sensitive method for detecting behavioral dysfunction. *Nature Protocols*, 1(1), 118–121.

Deacon, R. M. J., Cholerton, L. L., Talbot, K., Nair-Roberts, R. G., Sanderson, D. J., Romberg, C., Koros, E., Bornemann, K. D. and Rawlins, J. N. P. (2008). Age-dependent and -independent behavioral deficits in Tg2576 mice. *Behavioural Brain Research*, 189(1), 126–138.

Deacon, R. M. J., Raley, J. M., Perry, V. H. and Rawlins, J. N. P. (2001). Burrowing into prion disease. *NeuroReport*, 12(9), 2053–2057.

Dehlendorff, C., Andersen, K. K. and Olsen, T. S. (2014). Body mass index and death by stroke no obesity paradox. *JAMA Neurology*, 71(8), 978–984.

Desai, R. and Amraotkar, A. R. (2019). Relationship of Malnutrition during Hospitalization with Functional Recovery and Postdischarge Destination in Elderly Stroke Patients. *Journal of Stroke and Cerebrovascular Diseases*, 28(12), 104347.

Desgeorges, M. M., Devillard, X., Toutain, J., Divoux, D., Castells, J., Bernaudin, M., Touzani, O. and Freyssenet, D. G. (2015). Molecular Mechanisms of Skeletal Muscle Atrophy in a Mouse Model of Cerebral Ischemia. *Stroke*, 46(6), 1673–1680.

Doehner, W., Schenkel, J., Anker, S. D., Springer, J. and Audebert, H. (2013). Overweight and obesity are associated with improved survival, functional outcome, and stroke recurrence after acute stroke or transient ischaemic attack: Observations from the tempis trial. *European Heart Journal*, 34(4), 268–277.

Duncan, F., Wu, S. and Mead, G. E. (2012). Frequency and natural history of fatigue after stroke: A systematic review of longitudinal studies. *Journal of Psychosomatic Research*, 73(1), 18–27.

Edvardsson, M., Sund-Levander, M., Milberg, A., Wressle, E., Marcusson, J. and Grodzinsky, E. (2018). Differences in levels of albumin, ALT, AST, γ-GT and creatinine in frail, moderately healthy and healthy elderly individuals. *Clinical Chemistry and Laboratory Medicine*, 56(3), 471–478.

Elinav, E., Ackerman, Z., Maaravi, Y., Ben-Dov, I. Z., Ein-Mor, E. and Stessman, J. (2006). Low alanine aminotransferase activity in older people is associated with greater long-term mortality. *Journal of the American Geriatrics Society*, 54(11), 1719–1724.

Encarnacion, A., Horie, N., Keren-Gill, H., Bliss, T. M., Steinberg, G. K. and Shamloo, M. (2011). Long-term behavioral assessment of function in an experimental model for ischemic stroke. *J Neurosci Methods*, 196(2), 247–257.

Fournier, D. A., Skaug, H. J., Ancheta, J., Ianelli, J., Magnusson, A., Maunder, M. N., Nielsen, A. and Sibert, J. (2012). AD Model Builder: Using automatic differentiation for statistical inference of highly parameterized complex nonlinear models. *Optimization Methods and Software*, 27(2), 233–249.

Gairolla, J., Kler, R., Modi, M. and Khurana, D. (2017). Leptin and adiponectin: Pathophysiological role and possible therapeutic target of inflammation in ischemic stroke. *Reviews in the Neurosciences*, 28(3), 295–306.

Gao, F., Chen, C., Lu, J., Zheng, J., Ma, X. C., Yuan, X. Y., Huo, K. and Han, J. F. (2017). De Ritis ratio (AST/ALT) as an independent predictor of poor outcome in patients with acute ischemic stroke. *Neuropsychiatric Disease and Treatment*, 13(1), 1551–1557.

Gomes, F., Emery, P. W. and Weekes, C. E. (2016). Risk of Malnutrition Is an Independent Predictor of Mortality, Length of Hospital Stay, and Hospitalization Costs in Stroke Patients. *Journal of Stroke and Cerebrovascular Diseases*, 25(4), 799–806.

Gong, W. H., Zheng, W. X., Wang, J., Chen, S. H., Pang, B., Hu, X. M. and Cao, X. L. (2012). Coexistence of hyperlipidemia and acute cerebral ischemia/reperfusion induces severe liver damage in a rat model. *World Journal of Gastroenterology*, 18(35), 4934–4943.

Haley, M. J. and Lawrence, C. B. (2016). Obesity and stroke: Can we translate from rodents to patients? *Journal of Cerebral Blood Flow & Metabolism*, 36(12), 2007–2021.

Haley, M. J. and Lawrence, C. B. (2017). The blood-brain barrier after stroke: Structural studies and the role of transcytotic vesicles. *Journal of Cerebral Blood Flow & Metabolism*, 37(2), 456–470.

Haley, M. J., Mullard, G., Hollywood, K. A., Cooper, G. J., Dunn, W. B. and Lawrence, C. B. (2017). Adipose tissue and metabolic and inflammatory responses to stroke are altered in obese mice. *Disease Models and Mechanisms*, 10(10), 1229–1243.

Hao, G., Li, W., Guo, R., Yang, J. G., Wang, Y., Tian, Y., Liu, M. Y., Peng, Y. G. and Wang, Z. W. (2013). Serum total adiponectin level and the risk of cardiovascular disease in general population: A meta-analysis of 17 prospective studies. *Atherosclerosis*, 228(1), 29–35.

Hohlbaum, K., Bert, B., Dietze, S., Palme, R., Fink, H. and Thöne-Reineke, C. (2017). Severity classification of repeated isoflurane anesthesia in C57BL/6JRj mice - Assessing the degree of distress. *PLoS ONE*, 12(6), e0179588.

Jöonsson, A. C., Lindgren, I., Norrving, B. and Lindgren, A. (2008). Weight loss after stroke: A population-based study from the Lund Stroke Register. *Stroke*, 39(3), 918–923.

Karatepe, A. G., Gunaydin, R., Kaya, T. and Turkmen, G. (2008). Comorbidity in patients after stroke: Impact on functional outcome. *Journal of Rehabilitation Medicine*, 40(10), 831–835.

Kilkenny, C., Browne, W. J., Cuthill, I. C., Emerson, M. and Altman, D. G. (2010). Improving Bioscience Research Reporting: The ARRIVE Guidelines for Reporting Animal Research. *PLoS Biology*, 8(6), e1000412.

Kim, S. U., Song, D., Heo, J. H., Yoo, J., Kim, B. K., Park, J. Y., Kim, D. Y., Ahn, S. H., Kim, K. J., Han, K. H. and Kim, Y. D. (2017). Liver fibrosis assessed with transient elastography is an independent risk factor for ischemic stroke. *Atherosclerosis*, 260(1), 156–162.

Kim, Y., Kim, C. K., Jung, S., Ko, S. B., Lee, S. H. and Yoon, B. W. (2015). Prognostic importance of weight change on short-term functional outcome in acute ischemic stroke. *International Journal of Stroke*, 10(100), 62–68.

Kleiner, D. E., Brunt, E. M., Van Natta, M., Behling, C., Contos, M. J., Cummings, O. W., Ferrell, L. D., Liu, Y. C., Torbenson, M. S., Unalp-Arida, A., Yeh, M., McCullough, A. J. and Sanyal, A. J. (2005). Design and validation of a histological scoring system for nonalcoholic fatty liver disease. *Hepatology*, 41(6), 1313–1321.

Knight, E. M., Martins, I. V. A. A., Gümüsgöz, S., Allan, S. M. and Lawrence, C. B. (2014). High-fat diet-induced memory impairment in triple-transgenic Alzheimer's disease (3xTgAD) mice isindependent of changes in amyloid and tau pathology. *Neurobiology of Aging*, 35(8), 1821–1832.

Kochanowski, J., Grudniak, M., Baranowska-Bik, A., Wolinska-Witort, E., Kalisz, M., Baranowska, B. and Bik, W. (2012). Resistin levels in women with ischemic stroke. *Neuro Endocrinology Letters*, 33(6), 603–7.

Kogan, M., Klempfner, R., Lotan, D., Wasserstrum, Y., Goldenberg, I. and Segal, G. (2018). Low ALT blood levels are associated with lower baseline fitness amongst participants of a cardiac rehabilitation program. *Journal of Exercise Science and Fitness*, 16(1), 1–4.

Lawrence, C. B., Brough, D. and Knight, E. M. (2012). Obese mice exhibit an altered behavioural and inflammatory response to lipopolysaccharide. *Disease Models & Mechanisms*, 5(5), 649–659.

Lenth, R. V. (2016). Least-Squares Means: The R Package lsmeans. *Journal of Statistical Software*, (69) 1.

Longa, E. Z., Weinstein, P. R., Carlson, S. and Cummins, R. (1989). Reversible middle cerebral artery occlusion without craniectomy in rats. *Stroke*, 20(1), 84–91.

Maes, M., Berk, M., Goehler, L., Song, C., Anderson, G., Gałecki, P. and Leonard, B. (2012). Depression and sickness behavior are Janus-faced responses to shared inflammatory pathways. *BMC Medicine*, 10(66), 1–19.

Maysami, S., Haley, M. J., Gorenkova, N., Krishnan, S., McColl, B. W. and Lawrence, C. B. (2015). Prolonged diet-induced obesity in mice modifies the inflammatory response and leads to worse outcome after stroke. *Journal of Neuroinflammation*, 12(1), 140.

Mccoll, B. W., Rose, N., Robson, F. H., Rothwell, N. J. and Lawrence, C. B. (2009). Increased brain microvascular MMP-9 and incidence of haemorrhagic transformation in obese mice after experimental stroke. *Journal of Cerebral Blood Flow & Metabolism*, 30(2), 267–272.

Nakling, A. E., Aarsland, D., Næss, H., Wollschlaeger, D., Fladby, T., Hofstad, H. and Wehling, E. (2017). Cognitive Deficits in Chronic Stroke Patients: Neuropsychological Assessment, Depression, and Self-Reports. *Dementia and Geriatric Cognitive Disorders Extra*, 7(2), 283–296.

Nii, M., Maeda, K., Wakabayashi, H., Nishioka, S. and Tanaka, A. (2016). Nutritional Improvement and Energy Intake Are Associated with Functional Recovery in Patients after Cerebrovascular Disorders. *Journal of Stroke and Cerebrovascular Diseases*, 25(1), 57–62.

O'Donnell, M. J., Denis, X., Liu, L., Zhang, H., Chin, S. L., Rao-Melacini, P., Rangarajan, S., Islam, S., Pais, P., McQueen, M. J., Mondo, C., Damasceno, A., Lopez-Jaramillo, P., Hankey, G. J., Dans, A. L., Yusoff, K., Truelsen, T., Diener, H. C., Sacco, R. L., Ryglewicz, D., Czlonkowska, A., Weimar, C., Wang, X. and Yusuf, S. (2010). Risk factors for ischaemic and intracerebral haemorrhagic stroke in 22 countries (the INTERSTROKE study): A case-control study. *The Lancet*, 376(9735), 112–123.

Olsen, T. S., Dehlendorff, C., Petersen, H. G. and Andersen, K. K. (2008). Body mass index and poststroke mortality. *Neuroepidemiology*, 30(2), 93–100.

Opatrilova, R., Caprnda, M., Kubatka, P., Valentova, V., Uramova, S., Nosal, V., Gaspar, L., Zachar, L., Mozos, I., Petrovic, D., Dragasek, J., Filipova, S., Büsselberg, D., Zulli, A., Rodrigo, L., Kruzliak, P. and Krasnik, V. (2018). Adipokines in neurovascular diseases. *Biomedicine and Pharmacotherapy*, 98(1), 424–432.

Ostwald, S. K., Wasserman, J. and Davis, S. (2006). Medications, comorbidities, and medical complications in stroke survivors: The cares study. *Rehabilitation Nursing*, 31(1), 10–14.

Pedersen, C. S., Sørensen, D. B., Parachikova, A. I. and Plath, N. (2014). PCP-induced deficits in murine nest building activity: Employment of an ethological rodent behavior to mimic negative-like symptoms of schizophrenia. *Behavioural Brain Research*, 273(1), 63–72.

Peltz-Sinvani, N., Klempfner, R., Ramaty, E., Sela, B. A., Goldenberg, I. and Segal, G. (2016). Low ALT Levels Independently Associated with 22-Year All-Cause Mortality Among Coronary Heart Disease Patients. *Journal of General Internal Medicine*, 31(2), 209–214.

Percie du Sert, N., Alfieri, A., Allan, S. M., Carswell, H. V. O., Deuchar, G. A., Farr, T. D., Flecknell, P., Gallagher, L., Gibson, C. L., Haley, M. J., Macleod, M. R., McColl, B. W., McCabe, C., Morancho, A., Moon, L. D. F., O'Neill, M. J., Pérez de Puig, I., Planas, A., Ragan, C. I., Rosell, A., Roy, L. A., Ryder, K. O., Simats, A., Sena, E. S., Sutherland, B. A., Tricklebank, M. D., Trueman, R. C., Whitfield, L., Wong, R. and Macrae, I. M. (2017). The IMPROVE Guidelines (Ischaemia Models: Procedural Refinements Of in Vivo Experiments). *Journal of Cerebral Blood Flow & Metabolism*, 37(11), 3488–3517.

Perovic, E., Mrdjen, A., Harapin, M., Kuna, A. T. and Simundic, A. M. (2017). Diagnostic and prognostic role of resistin and copeptin in acute ischemic stroke. *Topics in Stroke Rehabilitation*, 24(8), 614–618.

Perovic, E., Mrdjen, A., Harapin, M. and Simundic, A.-M. (2016). Short Term Changes of Serum Lipids in Acute Ischemic Stroke. *Clinical Laboratory*, 62(11), 2107–2113.

Putaala, J., Haapaniemi, E., Metso, A. J., Metso, T. M., Artto, V., Kaste, M. and Tatlisumak, T. (2010). Recurrent ischemic events in young adults after first-ever ischemic stroke. *Annals of Neurology*, 68(5), 661–671.

Ramati, E., Israel, A., Tal Kessler, Petz-Sinuani, N., Sela, B.-A., Idan Goren, Grinfeld, A., Lavi, B. and Segal, G. (2015). Low ALT activity amongst patients hospitalized in internal medicine wards is a widespread phenomenon associated with low vitamin B6 levels in their blood. *Harefuah*, 154(2), 89–93, 137.

Ramaty, E., Maor, E., Peltz-Sinvani, N., Brom, A., Grinfeld, A., Kivity, S., Segev, S., Sidi, Y., Kessler, T., Sela, B. A. and Segal, G. (2014). Low ALT blood levels predict long-term all-cause mortality among adults. A historical prospective cohort study. *European Journal of Internal Medicine*, 25(10), 919–921.

Roth, S., Singh, V., Tiedt, S., Schindler, L., Huber, G., Geerlof, A., Antoine, D. J., Anfray, A., Orset, C., Gauberti, M., Fournier, A., Holdt, L. M., Harris, H. E., Engelhardt, B., Bianchi, M. E., Vivien, D., Haffner, C., Bernhagen, J., Dichgans, M. and Liesz, A. (2018). Brain-released alarmins and stress response synergize in accelerating atherosclerosis progression after stroke. *Science Translational Medicine*, 10(432), 1–11.

Sandu, R. E., Buga, A. M., Uzoni, A., Petcu, E. B. and Popa-Wagner, A. (2015). Neuroinflammation and comorbidities are frequently ignored factors in CNS pathology. *Neural Regeneration Research*, 10(9), 1349–1355.

Sato, M., Ido, Y., Yoshimura, Y. and Mutai, H. (2019). Relationship of Malnutrition During Hospitalization With Functional Recovery and Postdischarge Destination in Elderly Stroke Patients. *Journal of Stroke and Cerebrovascular Diseases*, 28(7), 1866–1872.

Scherbakov, N., Dirnagl, U. and Doehner, W. (2011). Body weight after stroke lessons from the obesity paradox. *Stroke*, 42(12), 3646–3650.

Scherbakov, N., Pietrock, C., Sandek, A., Ebner, N., Valentova, M., Springer, J., Schefold, J. C., von Haehling, S., Anker, S. D., Norman, K., Haeusler, K. G. and Doehner, W. (2019). Body weight changes and incidence of cachexia after stroke. *Journal of Cachexia, Sarcopenia and Muscle*, 10(3), 611–620.

Scherbakov, N., Sandek, A. and Doehner, W. (2015). Stroke-Related Sarcopenia: Specific Characteristics. *Journal of the American Medical Directors Association*, 16(4), 272–276.

Seet, R. C. S., Zhang, Y., Wijdicks, E. F. M. and Rabinstein, A. A. (2014). Thrombolysis outcomes among obese and overweight stroke patients: An age- and national institutes of health stroke scale-matched comparison. *Journal of Stroke and Cerebrovascular Diseases*, 23(1), 1–6.

Shaqura, M., Mohamed, D. M., Aboryag, N. B., Bedewi, L., Dehe, L., Treskatsch, S., Shakibaei, M., Schäfer, M. and Mousa, S. A. (2017). Pathological alterations in liver injury following congestive heart failure induced by volume overload in rats. *PloS ONE*, 12(9), e0184161.

Shi, K., Wood, K., Shi, F. D., Wang, X. and Liu, Q. (2018). Stroke-induced immunosuppression and poststroke infection. *Stroke and Vascular Neurology*, 3(1), 34–41.

Skaug, H., Fournier, D., Bolker, B., Magnusson, A. and Nielsen, A. (2016). Generalized Linear Mixed Models using AD Model Builder using AD Model Builder. *R package version.*

Springer, J., Schust, S., Peske, K., Tschirner, A., Rex, A., Engel, O., Scherbakov, N., Meisel, A., Von Haehling, S., Boschmann, M., Anker, S. D., Dirnagl, U. and Doehner, W. (2014). Catabolic signaling and muscle wasting after acute ischemic stroke in mice: Indication for a stroke-specific sarcopenia. *Stroke*, 45(12), 3675–3683.

Takao, K., Kobayashi, K., Hagihara, H., Ohira, K., Shoji, H., Hattori, S., Koshimizu, H., Umemori, J., Toyama, K., Nakamura, H. K., Kuroiwa, M., Maeda, J., Atsuzawa, K., Esaki, K., Yamaguchi, S., Furuya, S., Takagi, T., Walton, N. M., Hayashi, N., Suzuki, H., Higuchi, M., Usuda, N., Suhara, T., Nishi, A., Matsumoto, M., Ishii, S. and Miyakawa, T. (2013). Deficiency of schnurri-2, an MHC enhancer binding protein, induces mild chronic inflammation in the brain and confers molecular, neuronal, and behavioral phenotypes related to schizophrenia. *Neuropsychopharmacology*, 38(8), 1409–1425.

Teeling, J. L., Felton, L. M., Deacon, R. M. J., Cunningham, C., Rawlins, J. N. P. and Perry, V. H. (2007). Sub-pyrogenic systemic inflammation impacts on brain and behavior, independent of cytokines. *Brain, Behavior, and Immunity*, 21(6), 836–850.

Trotman-Lucas, M., Kelly, M. E., Janus, J., Fern, R. and Gibson, C. L. (2017). An alternative surgical approach reduces variability following filament induction of experimental stroke in mice. *Disease Models & Mechanisms*, 10(7), 931–938.

Trueman, R. C., Harrison, D. J., Dwyer, D. M., Dunnett, S. B., Hoehn, M. and Farr, T. D. (2011). A Critical Re-Examination of the Intraluminal Filament MCAO Model: Impact of External Carotid Artery Transection. *Translational Stroke Research*, 2(4), 651–661.

Vemmos, K., Ntaios, G., Spengos, K., Savvari, P., Vemmou, A., Pappa, T., Manios, E., Georgiopoulos, G. and Alevizaki, M. (2011). Association between obesity and mortality after acute first-ever stroke: The obesity-stroke paradox. *Stroke*, 42(1), 30–36.

Wang, H. J., Si, Q. J., Shan, Z. L., Guo, Y. T., Lin, K., Zhao, X. N. and Wang, Y. T. (2015). Effects of body mass index on risks for ischemic stroke, thromboembolism, and mortality in Chinese atrial fibrillation patients: A single-center experience. *PLoS ONE*, 10(4), e0123516.

Wang, Y. Y., Lin, S. Y., Chuang, Y. H., Sheu, W. H. H., Tung, K. C. and Chen, C. J. (2014). Activation of hepatic inflammatory pathways by catecholamines is associated with hepatic insulin resistance in male ischemic stroke rats. *Endocrinology*, 155(4), 1235–1246.

Yaghi, S. and Elkind, M. S. V. (2015). Lipids and Cerebrovascular Disease: Research and Practice. *Stroke*, 46(11), 3322–3328.

Yang, X.-F., He, W., Lu, W.-H. and Zeng, F.-D. (2003). Effects of scutellarin on liver function after brain ischemia/reperfusion in rats. *Acta pharmacologica Sinica*, 24(11), 1118–24.

Zhang, X., Qi, X., Yoshida, E. M., Méndez-Sánchez, N., Hou, F., Deng, H., Wang, X., Qiu, J., He, C., Wang, S. and Guo, X. (2018). Ischemic stroke in liver cirrhosis: Epidemiology, risk factors, and in-hospital outcomes. *European Journal of Gastroenterology and Hepatology*, 30(2), 233–240.

3.8. Supplementary material

3.8.1. Y-maze spontaneous alternation test

To assess short-term working memory, the Y-maze spontaneous alternation test was performed as previously described by Knight *et al* (2014). Control and obese mice were assessed at day 0, and days 14 and 45 post-MCAo or sham surgery. Briefly, animals were placed in a white opaque Perspex maze with three arms (A, B and C) containing different visual cues and allowed to explore for 8 min before being returned to home cage. All tests were recorded by video and entries into arms were recorded (arm entries were defined as four paws crossing the threshold of a respective arm). Spontaneous alternation was defined as successive entry into three different arms. Subsequently, percent of correct alternation was calculated as the number of alternations divided by the number of arm entries minus two. The total number of moves was also recorded as an index of ambulatory activity. All videos were scored blinded by an independent observer.

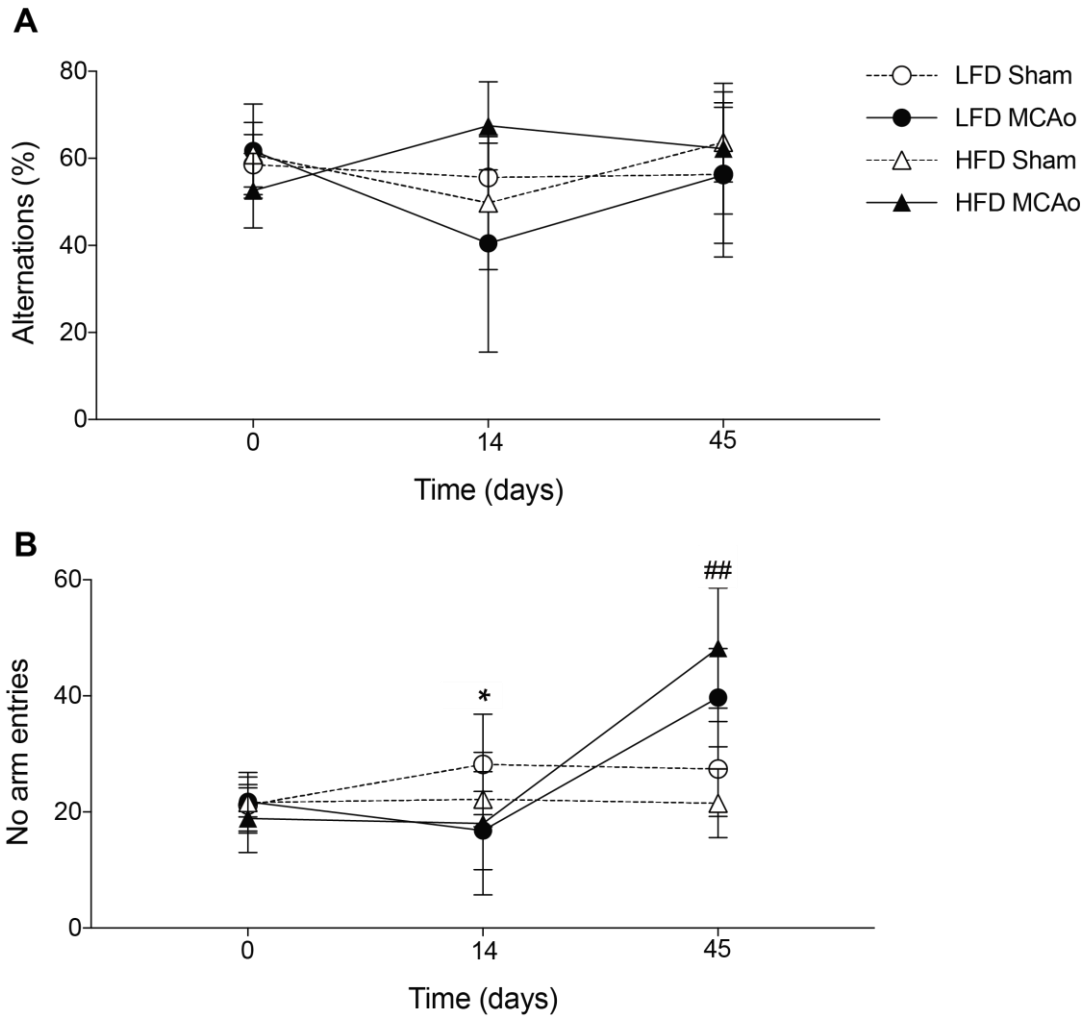

Figure 3.S1 - Stroke caused no impairment in memory.
C57BL/6J fed a control or high-fat (obese) diet for 6 months underwent middle cerebral artery occlusion (MCAo; 30 min for control, 20 min for obese). At day 0, 14 and 45 working memory was assessed using the spontaneous alternation Y-maze test and was calculated as the % alternation (a). Locomotor activity and motivation to perform the test was assessed by number of entries (b). No difference in memory was observed at any timepoint after stroke but a decrease in the number of arm entries was seen after stroke in control mice at day 14 and an increase in obese mice at day 45. Data are presented as mean ± SD (n = 4-10). *$p < 0.05$ control sham versus control stroke; $^{\#\#}p < 0.01$ obese sham versus obese stroke. Statistical analysis was performed using a linear mixed effects models followed by Šidák-Holmes *post hoc* analysis.

Chapter 4. High blood glucose worsens outcome after stroke through glycolytic-dependent production of IL-1β

High blood glucose worsens outcome after stroke through glycolytic-dependent production of IL-1β

Patrick Strangward[1*], **Claire S White**[1*], Jack Rivers-Auty[1, 2], Chris Hoyle[1], Stuart M Allan[1]

[*]**Contributed equally**

[1]Faculty of Biology, Medicine and Health, Manchester Academic Health Science Centre, The University of Manchester, Manchester, M13 9PT, UK.

[2]School of Medicine, College of Health and Medicine, University of Tasmania, Hobart, Tasmania, Australia.

Manuscript in preparation

4.1. Authors contributions

PS and CW were involved in the conception and design of the study. All *in vivo* studies were performed by PS, including leukocyte isolations and immunohistochemistry. All *in vitro* experiments were performed by CW. CH performed ELISAs for isolated leukocytes. RNA sequencing was performed by Genomics Facility and analysed by JRA. All other data analysis was performed by CW and PS. CW and PS were involved in the interpretation of data. CW drafted the manuscript with input from PS and SMA.

4.2. Abstract

High blood glucose (hyperglycaemia) levels are commonly observed in patients admitted to hospital for stroke and are associated with larger infarcts, increased mortality and worse recovery. The effects of hyperglycaemia on stroke outcomes are independent of other risk factors such as age, diabetes, and stroke severity. Similarly, in animal models of stroke, hyperglycaemia increases infarct volume and is associated with higher mortality. However, it is not clear how high blood glucose levels contribute to stroke damage. It is well known that inflammation exacerbates stroke damage. Specifically, stroke patients with high levels of interleukin (IL)-1 have worse recovery, and treatment with the natural antagonist, IL-1 receptor antagonist (IL-1RA), is associated with improved recovery in experimental models of stroke. In this study, we investigated whether blood glucose availability could regulate the IL-1β mediated inflammatory response post-stroke.

Using both cellular and experimental models of stroke, we show that hyperglycaemia exacerbates ischaemic brain injury by augmenting the post-stroke inflammatory response. Following activation from an inflammatory stimulus, proinflammatory macrophages switch their metabolic profile from oxidative phosphorylation to glycolysis, fuelling the production of proinflammatory mediators, including IL-1β. Consequently, increases in blood glucose enhance glycolysis-dependent macrophage activation after stroke and worsen ischaemic brain injury in mice which is ameliorated with 2-deoxyglucose (2DG), an inhibitor of glycolysis. As glucose metabolism is also essential for neuronal survival in ischaemic tissue, inhibition of glycolysis is not a viable therapeutic strategy. Therefore we investigated which metabolites downstream of glucose metabolism regulate IL-1β production. We identify pyruvate as an essential metabolite supporting IL-1β production, potentially via augmenting succinate accumulation. Ultimately, this study enhances our understanding of the relationship between blood glucose and inflammation, providing mechanistic insight into why hyperglycaemic patients have greater damage after stroke. This new understanding could aid the development of new therapeutic strategies for stroke patients.

4.3. Introduction

Hyperglycaemia has been reported in up to 60% of non-diabetic patients admitted to hospital for ischaemic stroke (Capes et al., 2001; Hjalmarsson et al., 2014), and is associated with larger infarct size and worse clinical outcomes, including increased mortality (Szczudlik et al., 2001; Dora et al., 2004; Kruyt et al., 2010). The effects of hyperglycaemia on stroke outcome are independent of other risk factors such as age, stroke severity, as well as diabetic status (Candelise et al., 1985; Cox and Lorains, 1986; Weir et al., 1997; Capes et al., 2001; Parsons et al., 2002; Baird et al., 2003; Saxena et al., 2016). Robust preclinical evidence support these findings, where hyperglycaemia exacerbates stroke damage in animal models of stroke (Kagansky et al., 2001). Insulin treatment to lower blood glucose was found to be neuroprotective in animal models of stroke (Bômont and MacKenzie, 1995). However, a large scale clinical trial, UK Glucose Insulin in Stroke Trial (GIST-UK), found no clinical benefit of lowering blood glucose levels with insulin post-stroke (Gray et al., 2007). Failure in this trial is likely to be due to the detrimental effects of hypoglycaemia, as neuronal viability is dependent on glucose availability, and lowering blood glucose post-stroke risks compromising neuronal survival (Piironen et al., 2012). Despite this, a strong association between poor outcomes and elevated blood glucose levels remains, and the mechanisms by which high blood glucose augments ischaemic brain damage have not yet been fully elucidated. Proposed mechanisms for how high blood glucose levels can aggravate damage include: (i) impairing vessel recanalisation by promoting coagulation (Stegenga et al., 2006; Vaidyula et al., 2006), (ii) decreasing cerebral reperfusion through inhibiting vasodilation (Williams et al., 1998), and (iii) increased reperfusion injury mediated by inflammation (Esposito et al., 2002).

Inflammation plays a critical and complex role in stroke pathophysiology, being involved in both the propagation and the resolution of damage. In particular, interleukin (IL)-1 mediated inflammation has been widely associated with worse outcome after stroke in rodents. Blocking IL-1 with the natural antagonist, IL-1 receptor antagonist (IL-1RA), was first demonstrated to be protective in ischaemic stroke in 1992 (Relton and Rothwell, 1992). Since then multiple studies have confirmed protective effects of IL-1RA in mice (McCann et al., 2016), including a multicentre preclinical trial (Maysami et al., 2016). Additionally, systemic administration of IL-1β was found to potentiate ischaemic stroke damage (McColl

et al., 2007). IL-1 production is rapidly induced following ischaemia, and has been shown to be produced predominantly from brain-resident macrophages, microglia (Amantea et al., 2010; Luheshi et al., 2011).

Proinflammatory activation of macrophages is coupled with cellular metabolic reprogramming which supports effector cell function. M1-like macrophages stimulated by lipopolysaccharide (LPS) and/or interferon-gamma (IFNγ) shift their metabolism from oxidative phosphorylation to glycolysis which supports the production of proinflammatory mediators, including IL-1β (Van den Bossche et al., 2017; Viola et al., 2019). Therefore, inhibiting glycolysis prevents macrophage activation and production of proinflammatory cytokines (Michl et al., 1976; Hamilton et al., 1986). Additionally, advances in the field of immunometabolism have revealed that alongside metabolic reprogramming to support cellular function, the accumulation of specific metabolites can act as signalling molecules which shape the immune response (O'Neill and Artyomov, 2019). Macrophages are extremely responsive to their microenvironments and nutrient availability can also directly affect metabolism and the immune response (Wei et al., 2017). Therefore, we hypothesised that hyperglycaemia (i.e. increased systemic glucose availability) could enhance glycolysis-dependent macrophage inflammatory responses after stroke.

In this study, we have attempted to reveal the mechanisms by which hyperglycaemia promotes inflammation and ischaemic damage following stroke. Using *in vitro* and *in vivo* models we show hyperglycaemia exacerbates ischaemic brain injury by augmenting the post-stroke inflammatory response. Increased glucose availability sustains glycolysis in macrophages and augments IL-1β production. Inhibition of glycolysis prevents IL-1β production and ameliorates stroke damage. However, as post-stroke glucose metabolism is also essential for neuronal survival, inhibition of glycolysis is unlikely to be a clinically viable therapeutic strategy. We identify pyruvate as an essential metabolite downstream of glycolysis that supports IL-1β production, potentially via succinate accumulation. Combined our results suggest that selective inhibition of glycolysis in immune cells will prevent post-stroke inflammation, whilst maintaining neuronal viability and may be a beneficial therapeutic strategy.

4.4. Materials and Methods

4.4.1. Materials

Pharmacological reagents were obtained from the following manufacturers: Sigma (D-Glucose, D-Mannitol, Lipopolysaccharides from Escherichia coli O26:B6 (LPS), Etoposide, 2-Deoxy-D-glucose, Oxamate, Sodium L-lactate, UK5099, Diethyl succinate (DS), Diethyl butylmalonate (DBM), β-Chloro-L-alanine); Tocris (GSK 2837808A); and Biolegend (IFNγ). Concentrations of drugs used are detailed in the figure legends. All other materials/reagents were obtained from Sigma unless otherwise stated.

4.4.2. Animals

Male C57BL/6J mice (Charles River) were used for stroke studies. All animals were housed in groups (2-5 per cage) in individually ventilated cages in standard housing conditions (temperature 21 ± 2°C; humidity 55% ± 5%; 12-hour light/12-hour dark cycle), with access to food and water *ad libitum*. All experiments were conducted in accordance with the UK Animals (Scientific Procedures) Act 1986 and approved by the Home Office under relevant personal and project licenses at The University of Manchester, Biological Sciences Facility. All reporting of animal experiments complied with the ARRIVE guidelines (Animal Research: Reporting in In Vivo Experiments) (Kilkenny et al., 2010).

4.4.3. Transient middle cerebral artery occlusion

Transient middle cerebral artery occlusion (MCAo) was used to induce focal ischaemia in the left cerebral hemisphere using a protocol adapted from Koizumi *et al* (1986). Anaesthesia was induced with 4% isoflurane and maintained with 1.5% (30% O_2 and 70% N_2O). Core body temperature was monitored using a rectal probe and maintained at 37 ± 0.5°C with a homeothermic blanket (Harvard Apparatus). The carotid arteries were exposed and a silicone-coated filament (coating 210 µm in diameter and 4-5 mm length, Doccol) was introduced into the common carotid artery and advanced along the internal carotid artery until occlusion of the origin of the MCA for 15 mins. At the start of surgery mice were given an interperitoneal (i.p.) injection of glucose (2.2 g/kg) or phosphate buffered saline (PBS). All pharmacological treatments: 2DG (2.2 g/kg), and UK5099 (10 mg/kg), were given i.p., at the same time as glucose injections. Animals were

numbered and then the treatments were randomly allocated using Excel's randbetween function. Treatments were coded by a third party to ensure all experiments were performed by an experimenter blinded to treatment groups. Blood glucose was measured before glucose treatment, and during occlusion using a SD CodeFree blood glucose meter (SD Biosensor). All animals were recovered for 24 hours and neurological dysfunction was assessed with a neurological score modified from a previously reported neuroscore (Bederson et al., 1986a). Animals with a neuroscore of <1 (e.g. barrel rolling, tonic clonic seizures, prone and not responsive to stimuli) were excluded. All animals were euthanised at 24 hours by terminal anesthesia (4-5% isoflurane, 30% O_2, and 70% N_2O) and transcardially perfused with PBS. All brains were taken for triphenyltetrazolium chloride (TTC) staining, leukocyte isolation, or immunostaining, details of final numbers of animals used for different analyses are summarised in Table 4.1.

Table 4.1 - Final group sizes for animals used for different analyses.

Experiment	Treatment	Analysis					
		IHC		TTC		Leukocyte Isolation	
		Final	**Died** *(Excluded)*	Final	**Died** *(Excluded)*	Final	**Died** *(Excluded)*
Glucose exacerbates lesion volume	PBS	11	**1**	8	**1** *(1)*	5	**2** *(1)*
	Glucose	7	**2** *(3)*	9	**1**	4	**3**
2DG blocks IL-1 production and reduces lesion volume	Glucose	-	-	8	**2**	7	**1**
	Glucose + 2DG	-	-	7	**2** *(1)*	6	2 *(1)*
UK5099 blocks IL-1 production and reduces lesion volume	Glucose	-	-	7	-	7	-
	Glucose + UK5099	-	-	7	-	6	**1**

4.4.4. Infarct quantification

To determine infarct volume, brains were cut into 1-mm thick coronal sections and stained with 2% TTC 24 hours post-stroke and fixed with 4% paraformaldehyde (PFA) for 30 min at room temperature (RT). Images were captured with a digital camera and infarct size was analysed using Image J (NIH). Infarct volume was calculated as: (contralateral hemisphere area – healthy area of ipsilateral hemisphere) x slice thickness x number of slices (Bederson et al., 1986b). All analysis was performed blinded to experimental groups by randomising file names.

4.4.5. Leukocyte isolation

Ipsilateral hemispheres were digested for 60 min at 37 °C with 50 U/mL Collagenase (Gibco, #17104-019), 0.5 U/mL Dispase II (Gibco, #17105-041) and 200 U/mL DNase I (Roche, #10104159001) in Hank's balanced-salt solution containing calcium and magnesium. The tissue was finely minced and myelin removed using a 32% isotonic percoll solution centrifuged at 2000 x*g* for 10 min at RT with brake on 2. Following single cell isolation red blood cells were lysed by 10 min incubation with BD Pharmlyse (BD Bioscience, #555899). Isolated leukocytes were subsequently lysed in NP-40 buffer supplemented with proteinase inhibitor cocktail (Calbiochem). Cell lysates were stored at -20 ˚C prior to biochemical analyses.

4.4.6. Tissue processing and Immunostaining

After PBS perfusion mice for immunostaining were further perfused with 4% PFA and brains were removed. Brains were further immerse fixed in PFA for 24 hours and gross sectioned into 3 mm thick sections using a metal brain matrix. All tissue was then embedded in paraffin wax using a Shadon Citadel 2000 tissue processor (Thermo Fisher Scientific), and subsequently sectioned at a thickness of 5 µm using a Leica RM 2155 Microtome (Leica Microsystems Ltd.), mounted onto SuperFrost© Plus slides (Thermo Fisher Scientific), and dried overnight. Slides were dewaxed and serially rehydrated in graded ethanol, followed by antigen retrieval with TrisEDTA (pH9) for 30 min at 95 °C, and left to cool for 20 min. Primary antibodies rabbit-anti-Iba1 (1:500, Abcam, #ab178846) and goat-anti-IL-1β (1:200, R&D systems, #A-401) were incubated overnight at 4 ˚C. Iba-1 was visualised using donkey-anti rabbit AF647 (Thermo Fisher Scientific). IL-1β was visualised using the Tyramide 555 SuperBoostTM (Thermo Fisher Scientific) as per manufacturer's instructions. Specificity controls were performed on additional sections with omission of the primary antibodies, and no staining was observed. Wash steps were performed throughout using wash buffer (0.1 % TWEEN20 in Tris-buffered saline) and all antibodies were diluted in 0.1% BSA TBST. Sections were sequentially rinsed in PBS and distilled water, dried overnight in the dark at room temperature and then coverslipped in ProLong Diamond anti-fade mountant (Thermo Fisher Scientific).

Images were collected on a Zeiss Axioimager.D2 or Olympus BX63 upright microscope and captured using a Coolsnap HQ2 camera (Photometrics) or DP80 camera (Olympus) through Micromanager software v1.4.23 or CellSens Dimensions V1.16 (Olympus). Specific band pass filter sets for were used to prevent bleed through from one channel to the next. Images were then processed and analysed using ImageJ (NIH). Six cortical and sub-cortical regions of interest (3 at Bregma −0.38 mm and 3 at Bregma −1.94 mm) spanning the MCA vascular territory were imaged and IL-1β^{+} Iba1^{+} cells were quantified in these regions using Image J (NIH). All analysis was performed blinded to experimental groups by randomising file names.

4.4.7. Cell culture

Primary bone marrow derived macrophages (BMDMs) were isolated from C57BL/6 (Charles River) mice as previously described (Trouplin et al., 2013). Harvested BMDMs were cultured in complete DMEM (supplemented with 10% heat-inactivated fetal bovine serum (FBS, Thermo Fisher Scientific) and 1% penicillin streptomycin (PenStrep)), and 33.3% L929-conditioned media for 7–10 days. After 7-10 days BMDMs were harvested and seeded in 48 well plates at 0.5 x 10^6 cells/well over night, and treated the next day.

Murine mixed glial cells were prepared from the brains of 2–4-day-old C57BL/6 mice of both sexes. Briefly, brains were dissected from pups and the meninges and cerebellum were then removed. The remaining tissue was homogenised in complete DMEM *via* repeated trituration. The resulting homogenate was centrifuged at 500 × *g* for 10 min and the pellet was resuspended in fresh culture medium. After five days, the cells were washed, and fresh medium was placed on the cells. The medium was replaced every two days. On day 12, the cells were seeded at 2 × 10^5 cells/mL in 24-well plates and incubated for a further two days prior to use. All cell cultures were incubated at 37 °C, 90% humidity, and 5% CO_2.

4.4.8. Glucose cell assays

Two main glucose containing media were used for cellular experiments: normal glucose DMEM (NormGlc), and high glucose DMEM (HighGlc) as described by Pavlou *et al* (2018). NormGlc is the low glucose (5.5 mM) DMEM (Thermo Fisher Scientific, #11885084), supplemented with 10% FBS and 1% PenStrep. HighGlc is NormGlc, supplemented with additional 25 mM glucose. BMDMs were changed into different glucose containing media and polarised into M1 with 50 ng/mL LPS + 100 ng/mL recombinant IFNγ for 24 hours and cell lysates and supernatants were collected and stored at -20 °C. Cells were lysed with lysis buffer (50 mM Tris/HCl, 150 mM NaCl, Triton 1% v/v, pH 7.3) containing protease inhibitor cocktail (Calbiochem).

For all drug treatments cells were pretreated with drugs for 3 hours in NormGlc media. Following pretreatment cells were M1 polarised with respective Glu containing media, and re-treated with drugs. Further adapted media used in experiments were: osmolarity control medium (Mannitol) and lactate enriched media. Osmolarity control medium (Mannitol) is NormGlc, supplemented with 25 mM Mannitol. Lactate enriched media is NormGlc, supplemented with additional 25 mM sodium L-lactate.

4.4.9. RNA seq

RNA was extracted using a PureLink RNA mini kit (Invitrogen). RNA-Seq analysis was performed. RNA samples were assessed for quality and integrity using a 2200 TapeStation (Agilent Technologies) according to the manufacturer's instructions. RNA-Seq libraries were generated using the TruSeq Stranded mRNA assay (Illumina, Inc.) according to the manufacturer's instructions. Briefly, poly-T, oligo-attached, magnetic beads were used to extract polyadenylated mRNA from 1 µg of total RNA. The mRNA was then fragmented using divalent cations under high temperature and then transcribed into first strand cDNA using random primers. Second strand cDNA was then synthesised using DNA polymerase I and RNase H, and a single "A" base addition was performed. Adapters were then ligated to the cDNA fragments and then purified and enriched by PCR to create the final cDNA library. Adapter indices were used to multiplex libraries, which were pooled prior to cluster generation using a cBot instrument. The loaded flow cell was then pair-end sequenced (101 + 101 cycles, plus indices) on an Illumina HiSeq4000 instrument. Demultiplexing of the output data (allowing one mismatch) and BCL-to-Fastq

conversion was performed with CASAVA 1.8.3. Sequencing quality for each sample was determined using the FastQC program. Low-quality sequence data were removed utilising the trimmomatic program. STAR v2.4.0 was utilised to map the trimmed sequence into the murine genome (mm10 genome with gencode M16 annotation). Raw counts for each sample were generated by the htseq-count program and subsequently normalised relative to respective library sizes using DESeq2 package for the R statistical program (Love et al., 2014). The DESeq2 program was additionally used to plot the PCA with all sample data to visualise different clusters at multiple levels that describes the maximum variance within the data set. Genes of interest were identified by pairwise comparisons. False discovery rate (FDR) adjusted p values were used to evaluate significance.

4.4.10. Functional and pathway enrichment analysis

Genes with an FDR-corrected p value of less than 0.01 were analysed for transcriptional regulation and cell pathway enrichment utilizing the enrichR package (Wajid Jawaid, 2019) to string search the Enrichr webserver: GO term, PANTHER and Transcriptional Regulatory Relationships Unraveled by Sentence-based Text mining (Han et al., 2018) datasets (Chen et al., 2013; Kuleshov et al., 2016) on R (R Core Team, 2017). Significant features ($p < 0.05$) were further probed by cluster analyses utilising Ward's minimum variance method of hierarchical clustering visualised using R package “pheatmaps (Kolde, 2015). Heatmap, PCA and volcano plots were generated using the R packages “pheatmaps”, R version 2.6.1 base and “ggplot2” (Wickham, 2016), respectively

4.4.11. Quantification of IL-1β, IL-6 and TNFα

IL-1β in cell lysates, and IL-6 and TNFα in supernatants were quantified by enzyme-linked immunosorbent assay (ELISA; #DY401; #DY406; #DY410; R&D Systems) according to manufacturer’s instructions.

IL-1β in cell lysates was further assayed by western blot. Samples were run on 10% SDS polyacrylamide gels and transferred at 15 V onto nitrocellulose membrane (Bio-Rad) using a Trans-Blot Turbo Transfer System (Bio-Rad) before blocking with 2.5% w/v bovine serum albumin (BSA) in phosphate-buffered saline, 1% Tween 20 (PBST) for 1 hour at RT. Membranes were washed and incubated

(4 °C) overnight in goat anti-mouse IL-1β (R&D Systems, #AF-401,) in PBST, 0.1% BSA. Following this, membranes were washed and incubated with rabbit anti-goat (Agilent, #P0160) in 2.5% BSA in PBST for 1 hour at RT. Membranes were washed and incubated in ECL Prime Western Blotting Detection Reagent (GE Life Sciences) before exposure with G:BOX (Syngene) and Genesys software. β-Actin was used as a loading control.

4.4.12. Quantification of lactate and succinate

Succinate was assessed in cell lysates by succinate assay kit (Abcam, #ab204718) according to manufacturer's instructions. Lactate was assessed in cell lysates and supernatants by lactate assay kit (Abcam, #ab65331) according to manufacturer's instructions.

4.4.13. Cell death and viability

Cell death was measured by assessing lactate dehydrogenase release using the CytoTox 96 Non-Radioactive Cytotoxicity Assay Kit (Promega, #G1780) according to manufacturer's instructions. Cell viability was assessed by CellTiter 96 Non-Radioactive Cell Proliferation Assay Kit (Promega, #G4000) according to the manufacturer's instructions. BMDMs were seeded in 96 well plates at 0.2 x 10^6 cells/well over night for CellTiter assay. Apoptotic cell death was assessed by western blot for cleaved caspase 3. Samples were run on 15% SDS polyacrylamide gels and transferred at 15 V onto nitrocellulose membrane (Bio-Rad) using a Trans-Blot Turbo Transfer System (Bio-Rad). Membranes were blocked with 2.5% w/v BSA in PBST for 1 hour at RT, washed and incubated (4 °C) overnight in rabbit anti-mouse caspase-3 (Cell Signalling Technology, #9662) in PBST, 2.5% BSA. Following this, membranes were washed and incubated with goat anti-rabbit (Agilent, #P0448,) in 2.5% BSA in PBST for 1 hour at RT. Membranes were washed and incubated in ECL Prime Western Blotting Detection Reagent (GE Life Sciences) before exposure with G:BOX (Syngene) and Genesys software. β-Actin was used as a loading control. A positive control of Etoposide (40 μM) treated cells was used for cleaved caspase-3.

4.4.14. Statistical analysis

Data collection and analysis was performed by experimenters in a blinded and randomised manner. Equal variance and normality were assessed with the Brown-Forsythe and Shapiro-Wilk test respectively and appropriate transformations were applied when necessary. Where appropriate, data are presented as: mean ± standard error (SEM); individual points plotted with best-fit linear regression and 95% confidence intervals; or median and interquartile range (IQ). Statistical analyses performed were: two-tailed unpaired *t*-tests; Welch's t-test; linear regression; one-way analysis of variance (ANOVA) with Dunnett's *post hoc* test; two-way ANOVA with Sidak's *posthoc* test; and Mann Whitney test. Statistical significance was accepted at $*p < 0.05$, $**p < 0.01$, $***p < 0.001$, and $****p < 0.0001$. All statistical analyses were performed using GraphPad Prism v8 (GraphPad Software Inc.), further details on statistical analyses used are stated in the figure legend.

4.5. Results

4.5.1. Elevated blood glucose promotes IL-1β production and ischaemic damage after stroke

To identify the effects of high extracellular glucose on macrophage function we performed RNA-seq on BMDMs cultured in either normal or high glucose containing media, in the presence or absence of an M1 stimulation for 24 hours. Unguided principal component analysis of the data identified as expected, M1 stimulation caused stark differences in cellular transcripts. Although glucose concentration did not alter the transcriptome of unstimulated macrophages, M1 stimulated cells cultured in high glucose had distinctly different transcripts (3337 differentially expressed genes) compared to cells cultured in normal glucose (*Fig. 4.1A*). Pathway enrichment analysis highlighted that M1 stimulated macrophages cultured in different glucose media possessed strikingly divergent nuclear factor kappa-light-chain-enhancer of activated B cells (NFκB)-dependent gene profiles (*Fig. 4.1B*). M1 stimulated cells which were cultured in high glucose had 40 NFκB-related genes downregulated, and 30 NFκB-related genes upregulated, compared to normal glucose. Notably, IL-1β expression was significantly increased in response to high glucose, but not other NFκB regulated proinflammatory cytokines, including IL-6 and TNFα.

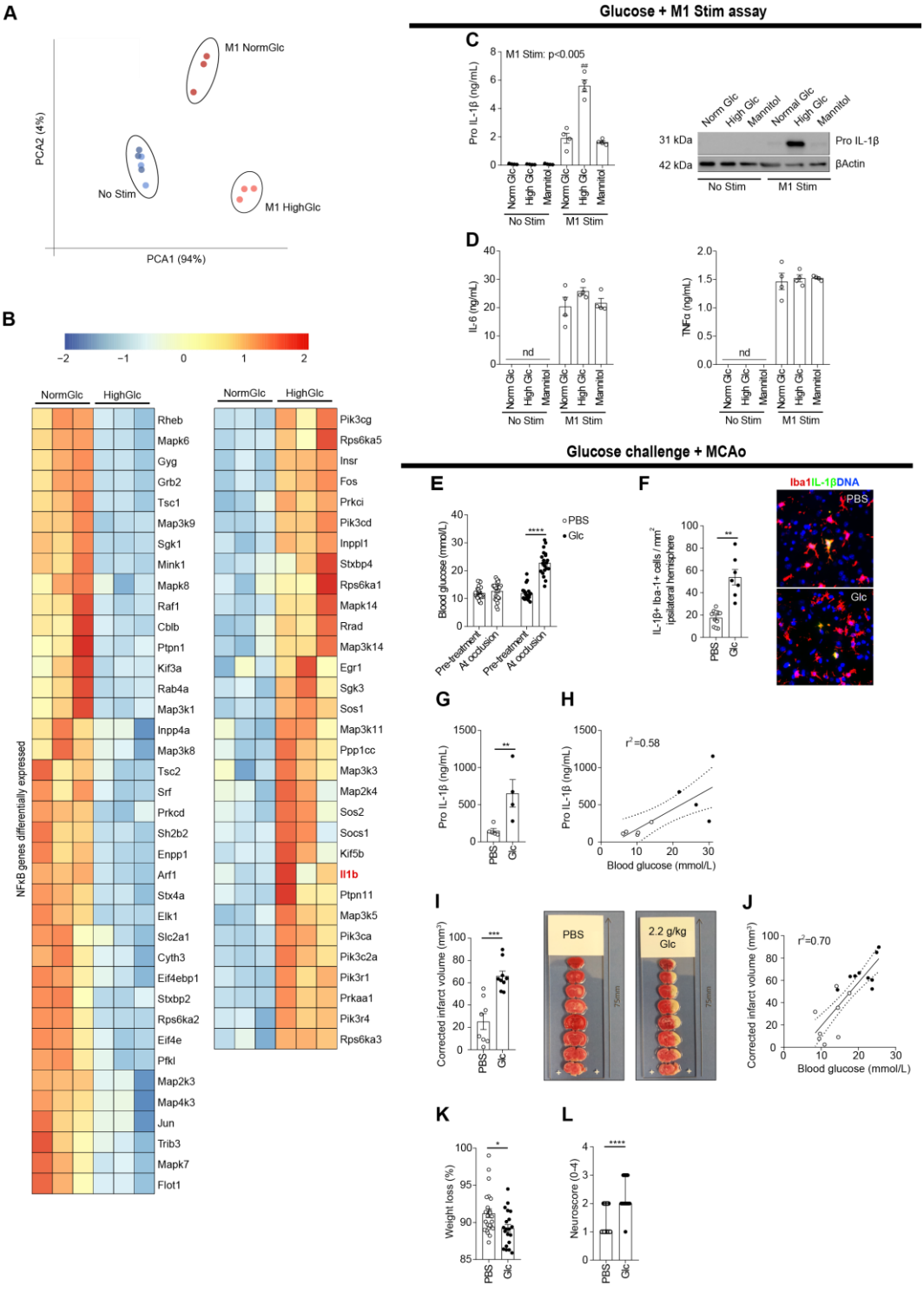
A
M1 NormGlc
No Stim
M1 HighGlc
PCA2 (4%)
PCA1 (94%)
B
NormGlc
HighGlc
NFκB genes differentially expressed
Rheb
Mapk6
Gyg
Grb2
Tsc1
Map3k9
Sgk1
Mink1
Mapk8
Raf1
Cblb
Ptpn1
Kif3a
Rab4a
Map3k1
Inpp4a
Map3k8
Tsc2
Srf
Prkcd
Sh2b2
Enpp1
Arf1
Stx4a
Elk1
Slc2a1
Cyth3
Eif4ebp1
Stxbp2
Rps6ka2
Eif4e
Pfkl
Map2k3
Map4k3
Jun
Trib3
Mapk7
Flot1
Pik3cg
Rps6ka5
Insr
Fos
Prkci
Pik3cd
Inppl1
Stxbp4
Rps6ka1
Mapk14
Rrad
Map3k14
Egr1
Sgk3
Sos1
Map3k11
Ppp1cc
Map3k3
Map2k4
Sos2
Socs1
Kif5b
Il1b
Ptpn11
Map3k5
Pik3ca
Pik3c2a
Pik3r1
Prkaa1
Pik3r4
Rps6ka3
Glucose + M1 Stim assay
C
M1 Stim: p<0.005
Pro IL-1β (ng/mL)
Norm Glc
High Glc
Mannitol
No Stim
M1 Stim
31 kDa
42 kDa
Pro IL-1β
βActin
D
IL-6 (ng/mL)
nd
TNFα (ng/mL)
Glucose challenge + MCAo
E
Blood glucose (mmol/L)
PBS
Glc
Pre-treatment
At occlusion
F
IL-1β+ Iba-1+ cells / mm²
ipsilateral hemisphere
Iba1 IL-1β DNA
G
Pro IL-1β (ng/mL)
H
r²=0.58
Blood glucose (mmol/L)
I
Corrected infarct volume (mm³)
2.2 g/kg Glc
J
r²=0.70
K
Weight loss (%)
L
Neuroscore (0-4)

Figure 4.1 - Elevated glucose levels promotes production of IL-1B, which exacerbates stroke damage.
BMDMs were treated with different glucose containing media: NormGlc (5.5 mM Glc) or HighGlc (30.5 mM Glc), in the presence or absence of an M1 stim (100 ng/mL IFNγ and 50 ng/mL LPS) for 24 hours and RNA was isolated and sequenced (**A-B,** n=3). Unguided principal component analysis cells (**A**), and heat maps of all significantly upregulated or downregulated genes downstream of NFκB activation (**B**). BMDMs were treated with different glucose containing media: NormGlc (5.5 mM Glc), HighGlc (30.5 mM Glc) or Mannitol (5.5 mM Glc + 25 mM mannitol), in the presence or absence of an M1 stim (100 ng/mL IFNγ and 50 ng/mL LPS) for 24 hours (**C-D**). Pro IL-1β was determined by ELISA and western blot (**C**), and IL-6 and TNFα in supernatants was determined by ELISA (**D**). Graphs are representative of two independent experiments, with four biological replicates (**C-D,** n=4). Mice were given 2.2 g/kg Glc, or PBS, by i.p. injection and a stroke was induced by MCAo (**E-L**). Blood glucose was assessed before Glc/PBS injection, and during MCA occlusion (**E**, n=44). Immunostaining for Iba1 and Pro IL-1β, representative images and quantification of $Iba1^{+}IL\text{-}1\beta^{+}$ cells in ipsilateral hemisphere 24 hours after MCAo (**F**, n=18). Leukocytes were isolated from the ipsilateral hemisphere and lysed. Pro IL-1β was determined by ELISA (**G**, n=9). Correlation between Pro IL-1β and blood glucose assessed (**H**). Infarct volume was assessed by TTC staining and representative images shown (**I**, n=17). Scale bar = 75 mm. Correlation between infarct volume and blood glucose assessed (**J**). Functional outcome was assessed by % weight loss (**K**, n=44) and neuroscore (**L**, n=44). Data are presented as mean ± SEM (**C, D, E, F, G, I, K**) or median and IQ (**L**). Solid lines indicate best-fit linear regression and the interrupted lines the 95% confidence intervals, r^2 values detailed in the figure, individual points represent separate animals (**H**, **J**). Data were assessed using: two-way ANOVA with Sidak's post hoc (**B**); one-way ANOVA with Dunnett's post hoc vs M1 Stim HighGlc (**D**); repeated two-way ANOVA with Sidak's post hoc (**E**); Welch's t test (**F, G, I, K**); Mann-Whitney test (**L**); and linear regression (**H**, **J**). ##p < 0.01 M1 Stim NormGlc vs High Glc, and M1 Stim Mannitol vs High Glc; *p < 0.05, **p < 0.01, ***p < 0.001, and ****p < 0.0001.

We next assessed whether glucose-dependent increases in IL-1β transcript were similarly observed at a protein level. As expected, M1 stimulation induced the production of NFκB regulated proteins: IL-1β, IL-6 and TNFα (*Fig. 4.1C-D*). M1 stimulated cells cultured in high glucose produced 3 fold more pro IL-1β compared to cells cultured in normal glucose (*Fig. 4.1C*), whilst glucose availability had no effect on IL-6 or TNFα production (*Fig. 4.1D*). Elevated production of IL-1β was not related to increased osmolarity as cells cultured in osmolarity matched media (Mannitol) produced similar levels of pro IL-1β to cells cultured in normal glucose (*Fig. 4.1C).* There was no cell death (pyroptosis or apoptosis) in response to M1 stim regardless of glucose concentration (*Fig. 4.S1*). To investigate whether glucose availability similarly regulates IL-1β production *in vivo*, mice were treated with glucose, or left untreated, prior to MCAo. Administration of glucose caused a 2 fold increase in blood glucose levels at the time of MCAo (*Fig. 4.1E*). Immunostaining for macrophage marker Iba1 and IL-1β revealed that the majority of IL-1β producing cells in the brain were $Iba1^+$ (microglia, monocyte-derived macrophages, or perivascular macrophages) 24 hours post-stroke (*Fig. 4.S2*). $IL\text{-}1\beta^+Iba1^+$ cells were found predominantly in the ipsilateral hemisphere, and often located in close proximity to blood vessels (*Fig. 4.S2*). Quantification of immunostaining identified a 3 fold increase in $IL\text{-}1\beta^+Iba1^+$ cells in the ipsilateral hemisphere of glucose treated mice, compared to untreated mice (*Fig. 4.1F*). These findings were confirmed using leukocyte isolations. 24 hours post-stroke leukocytes were isolated from ipsilateral hemisphere and a 4 fold increase in production of pro IL-1β was identified in glucose treated mice, compared to untreated mice (*Fig. 4.1G*). Moreover, the levels of pro IL-1β significantly correlated with blood glucose (*Fig. 4.1H*). Consistent with a substantial increase in IL-1β, glucose treated mice had 3 fold increased infarct volume compared to untreated mice (*Fig. 4.1I*), and a significant correlation between infarct volume and blood glucose was found (*Fig. 4.1J*). Indeed, glucose treated mice had a worse functional outcome with increased weight loss (*Fig. 4.1K*), and a higher neuroscore (*Fig. 4.1L*) compared to untreated mice. These results indicate that increased glucose availability enhances IL-1β production which is associated with worse outcomes after stroke.

4.5.2. Elevated blood glucose promotes IL-1β production and ischaemic damage via a glycolysis-dependent mechanism after stroke

Proinflammatory M1 polarisation in macrophages depends on a switch from oxidative phosphorylation to glycolysis (Viola et al., 2019). Hence, we hypothesised that high glucose levels may promote elevated production of IL-1β by augmenting glycolysis. To investigate this, we treated M1-stimulated BMDMs with the glucose analogue 2-deoxy glucose (2DG) (*Fig. 4.2A*). As expected, 2DG dose-dependently inhibited pro IL-1β production in M1 stimulated BMDMs cultured in high glucose (*Fig. 4.2B*). 2DG modestly inhibited IL-6 production but had no effect on TNFα (*Fig. 4.2C*). We next assessed whether 2DG could similarly selectively inhibit IL-1β production in brain resident macrophages. Pro IL-1β production, but not IL-6 or TNFα, was elevated in M1-stimulated mixed glial cultures cultured in high glucose, compared to glial cells cultured in normal glucose (*Fig. 4.S3A*). 2DG blocked the production of pro IL-1β production and IL-6, but increased TNFα production (*Fig. 4.S3B*).

To investigate whether 2DG similarly inhibited IL-1β production *in vivo*, mice were treated with glucose or glucose and 2DG combined prior to MCAo. Blood glucose levels at the point of MCAo occlusion were similar in mice treated with glucose or glucose and 2DG (*Fig. 4.2D*). Glucose and 2DG treatment decreased pro IL-1β production 3 fold in isolated leukocytes, compared to glucose treatment alone (*Fig. 4.2E*), and the correlation between pro IL-1β and blood glucose was lost in 2DG treated mice (*Fig. 4.2F*). Consistent with a substantial decrease in intracerebral IL-1β, there was a 3 fold reduction in infarct volume in glucose and 2DG treated mice compared to mice treated with glucose alone (*Fig. 4.2G*). In addition there was no correlation between pro IL-1β and blood glucose in 2DG-treated mice. 2DG treatment also improved functional outcome (*Fig. 4.2J*), but there was no significant effect on weight loss (*Fig. 4.2I*). These results suggest that increased glucose availability drives IL-1β production by glycolysis-dependent mechanisms.

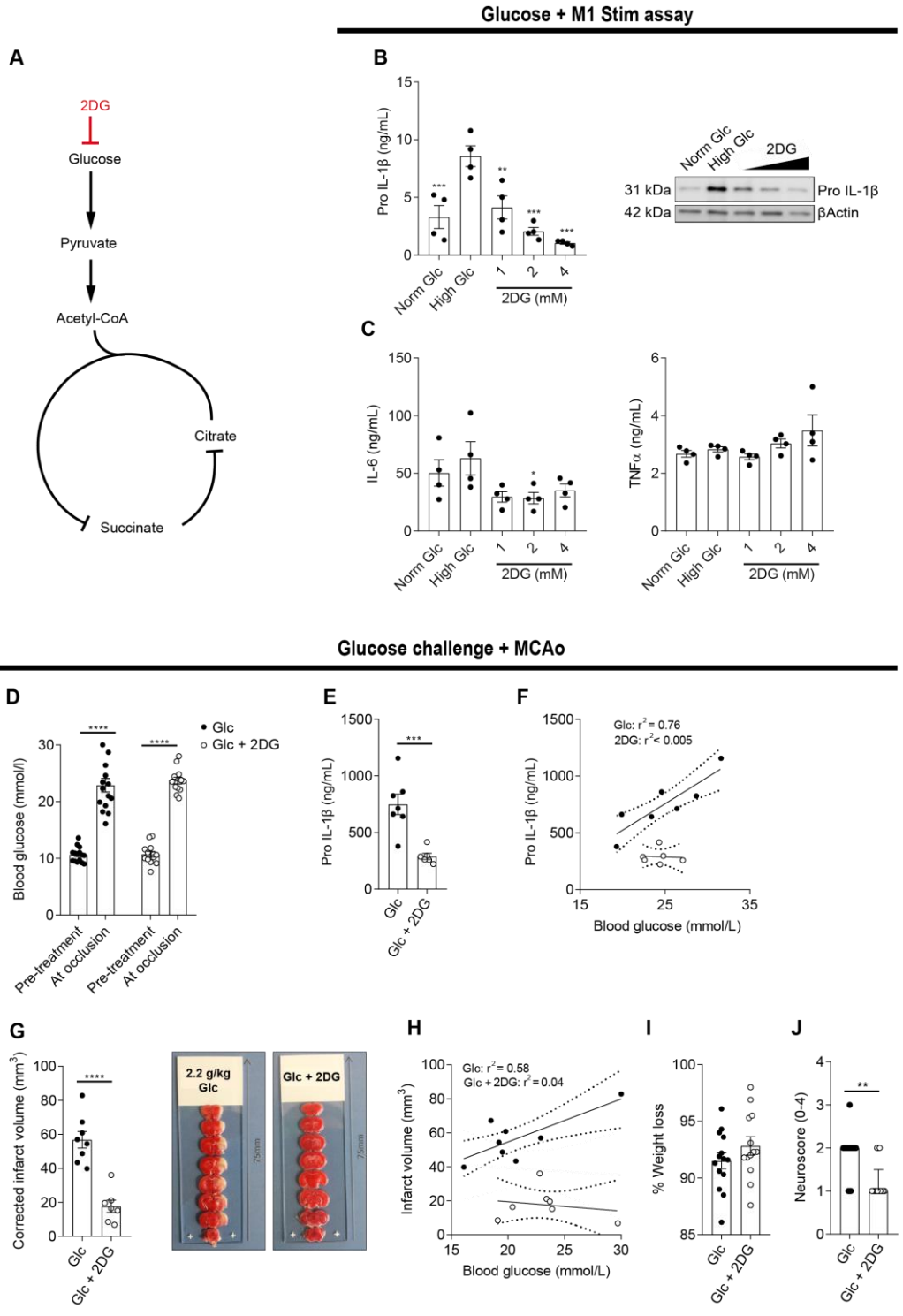
Glucose + M1 Stim assay
A
2DG
Glucose
Pyruvate
Acetyl-CoA
Citrate
Succinate
B
Pro IL-1β (ng/mL)
Norm Glc
High Glc
2DG (mM)
Norm Glc
High Glc
2DG
31 kDa
42 kDa
Pro IL-1β
βActin
C
IL-6 (ng/mL)
TNFα (ng/mL)
Glucose challenge + MCAo
D
Glc
Glc + 2DG
Blood glucose (mmol/l)
Pre-treatment
At occlusion
E
Pro IL-1β (ng/mL)
F
Glc: r² = 0.76
2DG: r² < 0.005
Blood glucose (mmol/L)
G
Corrected infarct volume (mm³)
2.2 g/kg Glc
Glc + 2DG
H
Glc: r² = 0.58
Glc + 2DG: r² = 0.04
Infarct volume (mm³)
I
% Weight loss
J
Neuroscore (0-4)

Figure 4.2 - Glycolysis is required for production of IL-1β, and exacerbates stroke damage.

Schematic diagram highlighting 2DG inhibits glycolysis (A). BMDMs were pretreated with increasing concentrations of 2DG (1 mM, 2 mM and 4 mM) for 3 hours, and then challenged with different M1 stimulated (100 ng/mL IFNγ and 50 ng/mL LPS) glucose containing medias (NormGlc 5.5 mM Glc, HighGlc 30.5 mM Glc) for 24 hours (B-C). Pro IL-1β was determined by ELISA and western blot (B), and IL-6 and TNFα in supernatants was determined by ELISA (C). Graphs are representative of one independent experiment, with four biological replicates (B-C, n=4). Mice were given 2.2 g/kg Glc i.p, followed by a further injection of either 2DG (2.2 g/kg) or PBS, and a stroke was induced by MCAo (D-J). Blood glucose was assessed before Glc injection, and during MCA occlusion (D, n=28). Leukocytes were isolated from the ipsilateral hemisphere and lysed. Pro IL-1β was determined by ELISA (E, n=13). Correlation between Pro IL-1β and blood glucose assessed (F). Infarct volume was assessed by TTC staining and representative images shown (G, n=15). Scale bar = 75 mm. Correlation between infarct volume and blood glucose assessed (H). Functional outcome was assessed by % weight loss (I, n=27) and neurological dysfunction (J, n=28). Data are presented as mean ± SEM (B, C, D, E, G, I) or median and IQ (J). Solid lines indicate best-fit linear regression and the interrupted lines the 95% confidence intervals, r^2 values detailed in the figure, individual points represent separate animals (F, H). Data were assessed using: one-way ANOVA with Dunnett's post hoc vs High Glc (B-C); repeated two-way ANOVA with Sidak's post hoc (D); Welch's t test (E, G, I); Mann-Whitney test (J); and linear regression (F, H). *$p < 0.05$, **$p < 0.01$, ***$p < 0.001$, and ****$p < 0.0001$.

4.5.3. Elevated blood glucose promotes IL-1β production and ischaemic damage via a mitochondrial pyruvate carrier-dependent mechanism after stroke

We next aimed to investigate which metabolites downstream of glycolysis regulated IL-1β production. The principal metabolite produced by glycolysis is pyruvate (*Fig. 4.3A*). Oxamate (40 mM), an analogue of pyruvate, significantly inhibited production of IL-1β and IL-6, but not TNFα, in M1 stimulated BMDMs cultured in high glucose (*Fig. 4.3B-C*). Oxamate at higher doses induced a global reduction in cytokine production, alongside reduced β-Actin intensity, which is indicative of reduced cell viability (*Fig. 4.3B-C*).

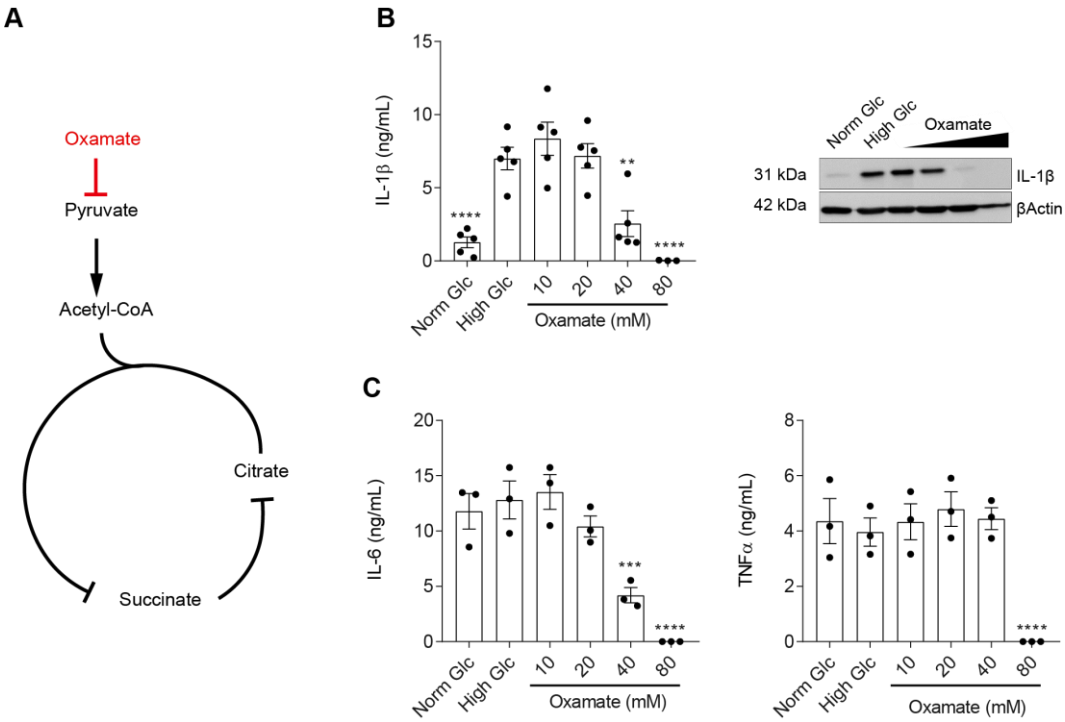

Figure 4.3 - Pyruvate metabolism is essential for production of IL-1β.
Schematic diagram illustrating inhibition of pyruvate metabolism by oxamate (A). BMDMs were pre-treated with increasing concentrations of oxamate (10 mM, 20 mM, 40 and 80 mM) for 3 hours, and then challenged with respective M1 stimulated (100 ng/mL IFNγ and 50 ng/mL LPS) glucose containing medias (NormGlc 5.5 mM, HighGlc 30.5 mM) for 24 hours (B-C). Pro IL-1β was determined by ELISA and western blot (B), and IL-6 and TNFα in supernatants was determined by ELISA (C). Graphs are representative of two independent experiment, with five biological replicates (B, n=5), or one independent experiment, with 3 biological replicates (C, n=3). Data are presented as mean ± SEM. Data was assessed with one-way ANOVA with Dunnett's post hoc vs High Glc. **p < 0.01, ***p < 0.001, and ****p < 0.0001 PBS vs Glc.

Once glucose is metabolised to pyruvate there are 3 major metabolic fates, we therefore investigated which of these fates is essential for IL-1β production. The conversion of pyruvate to lactate by lactate dehydrogenase (LDH_A) is a hallmark of aerobic glycolysis (*Fig. 4.4A*). As expected, intracellular lactate production was significantly increased in M1 stimulated BMDMs cultured in high glucose, compared to cells cultured in normal glucose (*Fig. 4.4B*). The LDH_A inhibitor, GSK 2837808A, significantly reduced lactate production at 100 μM (*Fig. 4.4C*), but also inhibited IL-1β, IL-6 and TNFα production, and reduced β-Actin intensity (*Fig. 4.4D-E*). Cell viability was assessed by MTT assay, and a significant reduction in cell viability was determined at 100 μM GSK 2837808A (*Fig. 4.4F*), suggesting lactate production is required for macrophage viability. As conversion of pyruvate to lactate appeared essential for macrophage viability following M1 stimulation, we used an alternate approach to investigate whether lactate is acting as an immunoregulatory signalling molecule promoting IL-1β production. M1 stimulated BMDMs were cultured in normal glucose, high glucose, or normal glucose and high lactate. Intracellular lactate was significantly increased in cells cultured with lactate enriched media (*Fig. 4.4G*), but there was no increase in pro IL-1β, compared to cells cultured in normal glucose (*Fig. 4.4F*). Combined, our results suggest that pyruvate conversion to lactate is essential to maintain cell viability, but lactate itself is not an immunometabolite regulating IL-1β. Pyruvate may also be converted to α-ketoglutarate and alanine via alanine aminotransferase (ALT) (*Fig. 4.4I*). However, increasing doses of the ALT inhibitor β-chloro-L-alanine had no effect on IL-1β, IL-6, or TNFα production (*Fig. 4.4J&K*). These results indicate that conversion of pyruvate to lactate, or α-ketoglutarate does not regulate IL-1β production.

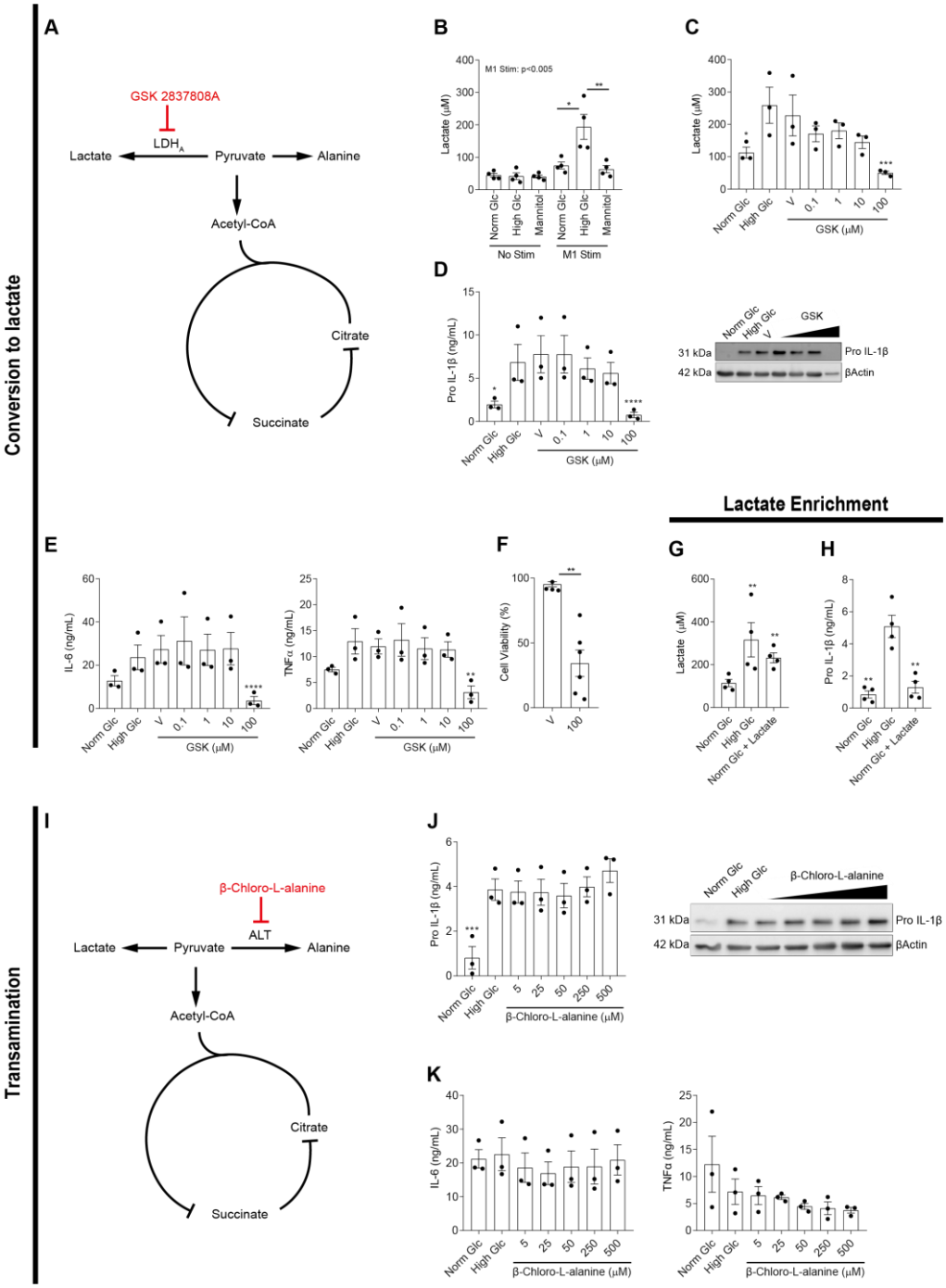
Conversion to lactate
A
GSK 2837808A
LDH$_A$
Lactate
Pyruvate
Alanine
Acetyl-CoA
Citrate
Succinate
B
M1 Stim: p<0.005
Lactate (μM)
Norm Glc
High Glc
Mannitol
No Stim
M1 Stim
C
GSK (μM)
D
Pro IL-1β (ng/mL)
31 kDa
42 kDa
Pro IL-1β
βActin
Lactate Enrichment
E
IL-6 (ng/mL)
TNFα (ng/mL)
F
Cell Viability (%)
G
Norm Glc + Lactate
H
Transamination
I
β-Chloro-L-alanine
ALT
J
β-Chloro-L-alanine (μM)
K

Figure 4.4 - Conversion of pyruvate to lactate, or α-Ketoglutarate, is not essential for production of IL-1β.
Schematic diagram illustrating the metabolic fates of pyruvate (A). BMDMs were treated with different glucose containing media: NormGlc (5.5 mM Glc), HighGlc (30.5 mM Glc) or Mannitol (5.5 mM Glc + 25 mM mannitol), in the presence or absence of an M1 stim (100 ng/mL IFNγ and 50 ng/mL LPS) for 24 hours, and intracellular lactate was determined (B). BMDMs were pretreated with increasing concentrations of GSK 2837808A (0.1, 1, 10, and 100 μM, vehicle used is DMSO) for 3 hours, and then challenged with respective M1 stimulated (100 ng/mL IFNγ and 50 ng/mL LPS) glucose containing medias (NormGlc 5.5 mM, HighGlc 30.5 mM) for 24 hours (C-E). Intracellular lactate (C), pro IL-1β (D), and IL-6 and TNFα was determined (E). Cell viability was assessed by MTT (F). BMDMs were treated with lactate enriched media (5.5 mM Glc + 25 mM Lactate) and intracellular lactate (G) and pro IL-1β was determined (H). BMDMs were pretreated with increasing concentrations of β-Chloro-L-alanine (5, 25, 50, 250, 500 μM) for 3 hours, and then challenged with respective M1 stimulated (100 ng/mL IFNγ and 50 ng/mL LPS) glucose containing medias (NormGlc 5.5 mM, HighGlc 30.5 mM) for 24 hours (I-J). Pro IL-1β was determined by ELISA and western blot (I), and IL-6 and TNFα in supernatants was determined by ELISA (J). Graphs are representative of two independent experiment (B-J, n=3-6), or one independent experiment, with 3 biological replicates (C, n=3). Data are presented as mean ± SEM. Data were assessed with: two-way ANOVA with Tukey's post hoc (B); one-way ANOVA with Dunnett's post hoc vs HighGlc (C-E, H, J-K); one-way ANOVA with Dunnett's post hoc vs NormGlc (G); and Kruskal-Wallis with Dunn's post hoc (F). *$p < 0.05$, **$p < 0.01$, ***$p < 0.001$, and ****$p< 0.0001$.

Pyruvate can also be transported to mitochondria, to support the tricarboxylic acid (TCA) cycle (*Fig. 4.5A*). To determine whether transport of pyruvate to the mitochondria is important for IL-1β production, we treated M1 stimulated BMDMs cultured in high glucose with increasing doses of the mitochondrial pyruvate carrier inhibitor, UK5099. UK5099 inhibited IL-1β production in a dose-dependent fashion (*Fig. 4.5B*), weakly inhibited IL-6, but did not affect TNFα, (*Fig. 4.5C*). To investigate whether UK5099 similarly inhibited IL-1β production *in vivo*, mice were treated with glucose or glucose and UK5099 combined prior to MCAo. Blood glucose levels at the point of MCAo occlusion were not significantly altered between mice treated with glucose or glucose and UK5099 (*Fig. 4.5D*). UK5099 decreased pro IL-1β production in isolated leukocytes compared to untreated mice (*Fig. 4.5E*), and there was no correlation between pro IL-1β and blood glucose in UK5099 treated mice (*Fig. 4.5F*). Similarly, there was a significant reduction in infarct volume in UK5099 treated mice (*Fig. 4.5G*), and an improved neuroscore (*Fig, 5.5H*), but no difference in weight loss between UK5099 and untreated mice (*Fig. 4.5I*). These results suggest that transport of pyruvate from the cytosol to the mitochondria and entry into the TCA is essential for IL-1β production.

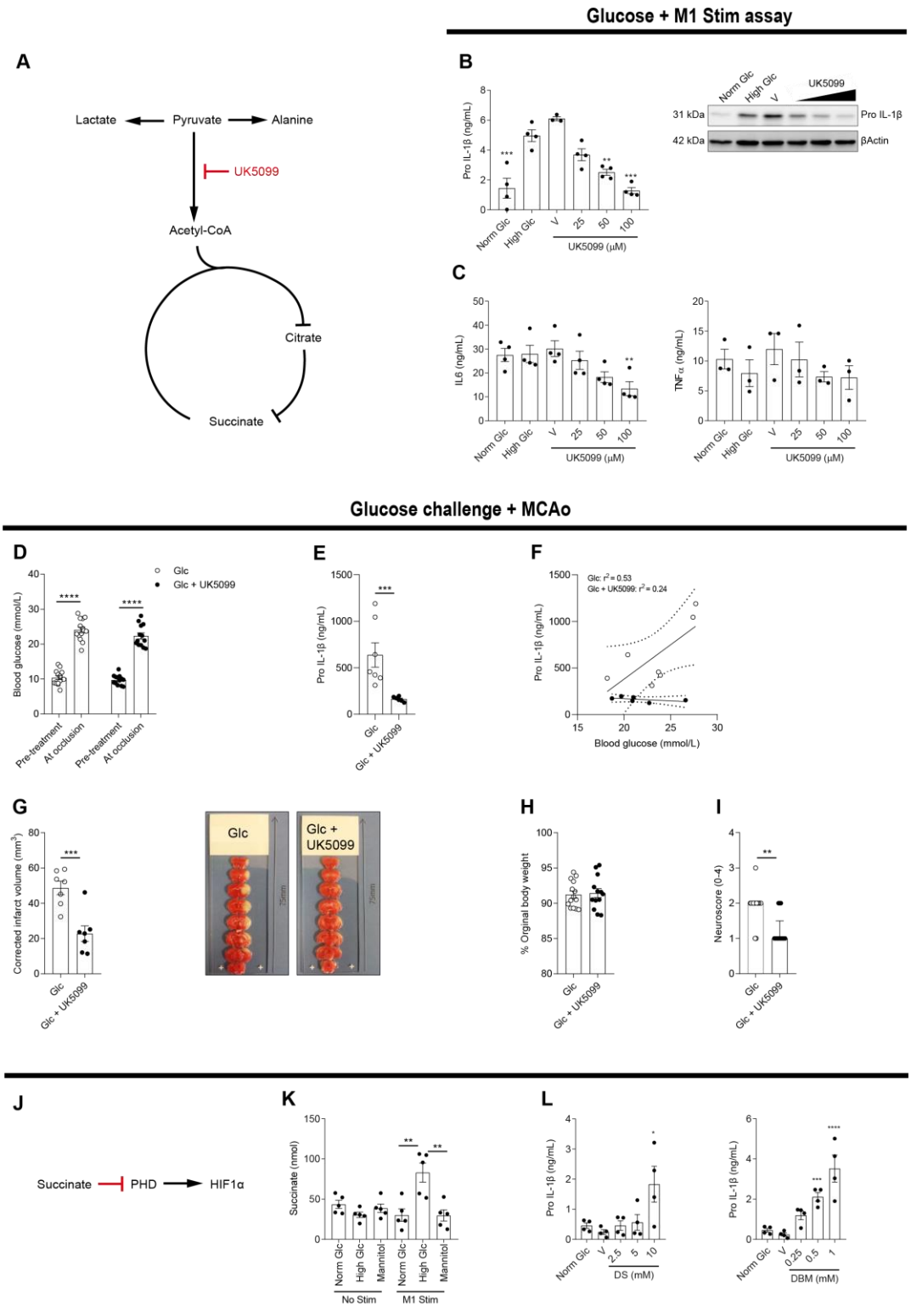
Glucose + M1 Stim assay
A
Lactate
Pyruvate
Alanine
UK5099
Acetyl-CoA
Citrate
Succinate
B
Pro IL-1β (ng/mL)
Norm Glc
High Glc
V
25
50
100
UK5099 (μM)
Norm Glc
High Glc
V
UK5099
31 kDa
42 kDa
Pro IL-1β
βActin
C
IL6 (ng/mL)
TNFα (ng/mL)
Glucose challenge + MCAo
D
Blood glucose (mmol/L)
Glc
Glc + UK5099
Pre-treatment
At occlusion
E
Pro IL-1β (ng/mL)
F
Glc: r² = 0.53
Glc + UK5099: r² = 0.24
Pro IL-1β (ng/mL)
Blood glucose (mmol/L)
G
Corrected infarct volume (mm³)
Glc
Glc + UK5099
H
% Orginal body weight
I
Neuroscore (0-4)
J
Succinate
PHD
HIF1α
K
Succinate (nmol)
Mannitol
No Stim
M1 Stim
L
Pro IL-1β (ng/mL)
DS (mM)
DBM (mM)

Figure 4.5 - Entry into TCA and succinate accumulation required for production of IL-1β, and blocking TCA entry is neuroprotective.
Schematic diagram illustrating UK5099 inhibits pyruvate entry into mitochondria and TCA (A). BMDMs were pretreated with increasing concentrations of UK5099 (25, 50, 100 μM, vehicle used is DMSO) for 3 hours, and then challenged with different M1 stimulated (100 ng/mL IFNγ and 50 ng/mL LPS) glucose containing medias (NormGlc 5.5 mM Glc, HighGlc 30.5 mM Glc) for 24 hours (B-C). Pro IL-1β was determined by ELISA and western blot (B), and IL-6 and TNFα in supernatants was determined by ELISA (C). Graphs are representative of one independent experiment (B-C, n=3-4). Mice were given 2.2 g/kg Glc i.p, followed by a further injection of either UK5099 (10 mg/kg) or PBS, and a stroke was induce by MCAo (D-J). Blood glucose was assessed before Glc injection, and during MCA occlusion (D, n=27). Leukocytes were isolated from the ipsilateral hemisphere and lysed. Pro IL-1β was determined by ELISA (E, n=13). Correlation between Pro IL-1β and blood glucose assessed (F). Infarct volume was assessed by TTC staining and representative images shown (G, n=14). Scale bar = 75 mm. Functional outcome was assessed by % weight loss (H, n=27) and neurological dysfunction (I, n=27). Schematic to show succinate accumulation inhibits prolyl-hydroxylase (PHD) enzymes which continually degrade HIF-1α, resulting in HIF-1α stabilisation (J). BMDMs were treated with different glucose containing media in the presence or absence of an M1 stim for 24 hours, and intracellular succinate was determined (K). BMDMs were pretreated with increasing concentrations of diethyl succinate (2.5, 5, 10 mM, vehicle used is DMSO), or diethyl butylmalonate (0.25, 0.5, 1 mM, vehicle used is DMSO) for 3 hours, and then challenged with different M1 stimulated in NormGlc for 24 hours (L). Pro IL-1β was determined by ELISA. Graphs are representative of two independent experiment (B-C, n=4-5). Data are presented as mean ± SEM (B, C, D, E, G, H, K, L) or median and IQ (I). Solid lines indicate best-fit linear regression and the interrupted lines the 95% confidence intervals, r^2 values detailed in the figure, individual points represent separate animals (F). Data were assessed using: one-way ANOVA with Dunnett's post hoc vs vehicle (B-C); one-way ANOVA with Dunnett's post hoc vs NormGlc (L); repeated two-way ANOVA with Sidak's post hoc (D); Welch's t test (E, G, H); Mann-Whitney test (I), linear regression (F) and two-way ANOVA with Tukey's post hoc (K). *$p < 0.05$, **$p < 0.01$, ***$p < 0.001$, and ****$p < 0.0001$.

As our data indicated that transport of pyruvate to the mitochondria is required for IL-1β production, we hypothesised that glucose availability may regulate the accumulation of a specific TCA cycle intermediate that could drive IL-1β production. Studies have shown that the TCA cycle intermediate succinate accumulates in M1 stimulated macrophages and supports IL-1β production (Tannahill et al., 2013). We therefore assessed succinate levels in M1 stimulated BMDMs cultured in normal or high glucose. We found that M1 stimulated BMDMs cultured in high glucose have significantly elevated succinate, compared to cells cultured in normal glucose (*Fig. 4.5K*). Moreover, in normal glucose media, elevating intracellular succinate with either cell permeable succinate (DS) or, an inhibitor of succinate dehydrogenase (SDH) (DBM), is sufficient drive the production of pro IL-1β in M1 stimulated BMDMs (*Fig. 4.5L*). Thus, our results indicate that glucose potentially regulates IL-1β production via succinate accumulation.

4.6. Discussion

Epidemiological evidence has shown a strong association between high blood glucose levels and worse outcomes after stroke (Kruyt et al., 2010; Hjalmarsson et al., 2014). However, the mechanisms by which high glucose exacerbates stroke damage are not well-understood. Here we present data indicating that hyperglycaemia may promote worse outcomes after stroke through metabolic reprogramming of brain-associated macrophages, and identify increased expression of IL-1β as a critical mediator of poor stroke outcomes.

Using RNA seq analysis we identified that elevated extracellular glucose levels caused stark differences in cellular transcripts. Pathway analysis further identified that specific NFκB regulated genes were differentially expressed in BMDMs in response to high glucose, which is consistent with previous findings where high glucose activates NFκB in vascular smooth muscle cells (Yerneni et al., 1999), pericytes (Romeo et al., 2002) and endothelial cells (Pieper and Riaz-ul-Haq, 1997; Ramana et al., 2004). Interestingly, IL-1β was significantly upregulated, but not other proinflammatory cytokines. Increased infarct volume in response to hyperglycaemia has been well-reported in preclinical models of stroke (Kruyt et al., 2010; MacDougall and Muir, 2011), which has been recapitulated in the current study. Here our data suggests that increased glucose availability supports IL-1β production which is associated with worse outcomes. Epidemiological studies have also shown an association between diabetes and Alzheimer's disease (AD) (Biessels et al., 2006), and HbA1c, a sensitive marker of chronic hyperglycaemia, was predictive of memory loss in both diabetic, and non-diabetic patients (Marden et al., 2017). Importantly, AD has been shown to have a strong neuroinflammatory component, and NLRP3-dependent production of IL-1β has been associated with AD pathology and cognitive decline (Heneka et al., 2013; Daniels et al., 2016), which may be exacerbated in the context of hyperglycaemia. Interestingly, a neuropathological investigation of regional AD pathology (amyloid plaques and neurofibrillary tangles) found no association with either diabetic status or HbA1c. They did, however, find a strong association between diabetic status and HbA1c on cerebrovascular pathology, such as subcortical infarcts (Pruzin et al., 2017). These results demonstrate that hyperglycaemia has prominent effects at the vasculature which may be the link between diabetes and AD.

It has been well described that macrophage polarisation to an M1-like inflammatory state is associated with metabolic shift from oxidative phosphorylation to glycolysis, which supports ATP generation and production of cytokines (Viola et al., 2019). Inhibiting glycolysis with 2DG specifically inhibited the production of IL-1β in high glucose conditions, confirming that glycolysis is required for IL-1β production (Tannahill et al., 2013). Next we recapitulated these findings *in vivo*, showing that 2DG blocks leukocyte production of IL-1β and is associated with better outcomes, which has also been previously found in rodent models of stroke (Combs et al., 1986; Yu and Mattson, 1999; Wei et al., 2003). A previous preclinical study has also directly implicated glucose metabolism as key pathological process which shapes immune cell function after stroke, and influences outcomes. Khan *et al* (2016) proposed that hyperglycaemia exacerbates stroke damage via the production of specific glucose metabolites, α-dicarbonyls, which prevent M2 polarisation of infiltrating monocytes. The protective role of infiltrating monocytes in the resolution of stroke pathology has been previously demonstrated in ischaemic stroke (Gliem et al., 2016), and in haemorrhagic stroke (Barrington *et al*, unpublished). We propose glucose metabolism enhances an M1 phenotype, rather than preventing M2 polarisation. Whilst we report these effects at 24 hours, Khan *et al* (2016) report their effects at 48 hours after stroke. Therefore at acute timepoints (24 hours) increased glucose metabolism could drive lL-1β production, contributing to the subsequent production of α-dicarbonyls which may also inhibit M2 polarisation of infiltrating monocytes at later timepoints (48 hours).

Immunostaining analysis identified IL-1β production from predominantly $Iba1^+$ cells which could be either microglia, perivascular macrophages, or monocyte-derived macrophages. In addition, high extracellular glucose potentiated the production of IL-1β in M1 stimulated mixed glial cultures (exclusively astrocytes and microglia), we hypothesise that the potentiated IL-1β response is predominantly mediated by brain-resident macrophages, microglia. Although astrocytes have been demonstrated to produce IL-1β (Choi et al., 2014) their capacity to produce IL-1β is limited compared to microglia, and microglial production of IL-1β has been well-described in different diseases (Liu and Quan, 2018). Immunostaining also identified $Iba1^+IL\text{-}1\beta^+$ cells clustered around blood vessels. This is in agreement with previous studies that have shown IL-1β to signal via interleukin-1 receptor 1 (IL-1R1) at the cerebrovasculature. This is evidenced by the fact that the

conditional deletion of IL-1R1 in brain endothelial cells caused a significant reduction in infarct volume and immune cell infiltration after MCAo (Liu et al., 2019; Wong et al., 2019)

Despite metabolic changes being well-described in peripheral immune cells, less is known about how metabolism shapes microglial function. Like macrophages, microglial activation has also been associated with a shift from oxidative phosphorylation to glycolysis and the production of inflammatory cytokines (Lynch, 2019). This has been demonstrated in response to LPS (Volobouéva et al., 2013; Orihuela et al., 2016) and LPS + IFNγ (Gimeno-Bayón et al., 2014) by other groups, and here we also recapitulate these findings with mixed glial cultures. Macrophage polarisation and metabolic reprogramming has been well-described in response to pathogen associated molecular patterns, such as LPS (Tannahill et al., 2013; Palsson-McDermott et al., 2015) and IFNγ (Wang et al., 2018), however until recently metabolic changes in response to DAMPs had not been shown. Di Gioia *et al* (2019) demonstrated the specific upregulation of proIL-1β in response to LPS and oxidised phospholipids, demonstrating that DAMPs can influence metabolic changes and alter immune responses. Oxidised phospholipids play a role in the formation of atherosclerotic plaques and Di Gioia *et al* (2019) demonstrate in animal models of atherosclerosis and clinically, that oxidised phospholipids contribute to a hyperinflammatory state. These findings are of direct clinical relevance in the context of stroke as 23% of all ischaemic strokes are of atherosclerotic aetiology (Adams et al., 1993), thus exposure to oxidised phospholipids may also be causing immune cell metabolic reprogramming which can shape stroke outcomes. Here we show elevated extracellular glucose acting as a DAMP to regulate immunometabolism and augmenting an inflammatory response. Interestingly, metabolic reprogramming of microglia has been also demonstrated in response to LPS + amyloid-β (Rubio-Araiz et al., 2018), and amyloid-β alone (Baik et al., 2019), establishing amyloid-β and another DAMP-like molecule which can induce metabolic changes, and implicating that immunometabolic changes may also be important in AD pathophysiology.

Ultimately, targeting glycolysis is therapeutically not a viable strategy as modulating a metabolic system which is shared by all cell types will have deleterious effects. Additionally, clinical trials using insulin to lower glucose did not

show any benefit (Gray et al., 2007), and it is likely that a therapeutic approach to inhibit glycolysis would fail for the same reasons. Blood glucose concentrations and stroke outcomes follow a U-shaped curve, and both hypoglycaemia and hyperglycaemia are associated with poorer clinical outcomes (Piironen et al., 2012). Whilst we propose that glucose potentiates post-stroke inflammation, it is also critical for neuronal survival. Consequently, a beneficial therapeutic strategy should selectively inhibit immune cell polarisation, whilst not compromising neuronal survival. Therefore, we sought to identify a key metabolite downstream of glucose metabolism which regulates IL-1β production in myeloid cells as a potential therapeutic target.

The final metabolite produced in glycolysis is pyruvate, which using an analogue of pyruvate, oxamate, we showed to be essential in regulating IL-1β production. Pyruvate is a versatile metabolite, with multiple metabolic fates: (i) conversion to lactate, (ii) transamination, and (iii) entry into the TCA. We investigated each of these fates to determine which is essential for regulating IL-1β production. First, we inhibited the conversion of pyruvate to lactate with the LDH_A inhibitor GSK 2837808A. An hallmark of M1 polarisation is the production of lactate, commonly referred to as the Warburg effect (Warburg, 1956; Palsson-McDermott and O'Neill, 2013), which was augmented when extracellular glucose availability was increased. Until recently lactate had largely been known as a metabolic by-product, however recently it has been demonstrated to act as a signalling molecule to shape immune cell function. Zhang *et al* (2019) show that the production of lactate from M1 stimulated macrophages increases histone lactylation, which promotes the expression of M2-like genes, coining this homeostatic process as the "lactate clock". Earlier research demonstrated that lactic acid produced from tumor cells can stabilise hypoxia-inducible factor (HIF)-1α, and upregulate the expression of vascular endothelial growth factor (Colegio et al., 2014). We demonstrate a maximal dose of GSK 2837808A inhibits lactate production, despite previously stated IC_{50} values to inhibit lactate production in cancer cell lines being significantly lower (Billiard et al., 2013). At a dose that inhibits lactate production we have a pan inhibition of cytokines, which we attribute to a loss in cell viability. Interestingly, oxamate is also a non-competitive inhibitor of LDH_A and at high concentrations we observe pan inhibition of cytokines, and a reduction in β-Actin intensity. Combined these results suggest that lactate is required for cell viability. During the conversion

of pyruvate to lactate NAD^+ is generated, which is required to sustain glycolysis and energy production, therefore inhibiting NAD^+ recycling may lead to an energy deficit and a subsequent reduction in cell viability. However, when enriching media with an equivalent concentration of lactate to glucose, lactate does not augment IL-1β production suggesting lactate is not an IL-1β-related immunometabolite.

These results have distinct clinical relevance as lactate accumulation has been proposed to contribute increased brain damage due to production of lactic acid and a subsequent decreased in pH (Rehncrona and Kågström, 1983; Katsura et al., 1992), and hyperglycaemia correlates positively with increased cerebral lactate after stroke (Parsons et al., 2002). However a decrease in pH during glycolysis has been demonstrated to be due to the release of H^+ ions during ATP hydrolysis and not lactic acid production (Zilva, 1978), and lactate administration is neuroprotective (Berthet et al., 2009), rebutting the notion that lactate accumulation is detrimental. Another important consideration in the context of stroke is the proposed role of lactate as an alternative energy source for neurons from the astrocyte-neuron lactate shuttle, further supporting the requirement of lactate production (Cater et al., 2003; Tang, 2018).

The second fate of pyruvate we investigated was transamination to α-ketoglutarate, mediated by ALT. Inhibition of ALT had no effect on IL-1β production, implicating transamination as a non-essential pathway in regulating IL-1β production. The final fate of pyruvate we investigated was the entry into the TCA. Using the mitochondrial transporter inhibitor, UK5099, we selectively inhibited IL-1β production and improved stroke outcomes, which is in agreement with previous studies that have shown pyruvate transport into the mitochondria is essential for regulating M1 polarisation and cytokine production (Meiser et al., 2016). The accumulation of the TCA intermediate succinate, has been well described to drive the production of IL-1β through stabilising HIF-1α and directly upregulating IL-1β expression (Tannahill et al., 2013). Succinate has been shown to stabilise HIF-1α expression via two distinct mechanisms. Firstly, accumulation in the mitochondria results in transport to the cytosol where it can inhibit prolyl-hydroxylase enzymes which degrade HIF-1α during normoxia (Tannahill et al., 2013). Secondly, the oxidation of succinate via SDH generates ROS production which also stabilises HIF-1α expression (Mills et al., 2016). Here we show high

extracellular glucose levels potentiated succinate accumulation, whilst increasing concentrations of cell permeable succinate, DS, or an inhibitor of SDH which degrades succinate, DBM, is sufficient to increases pro IL-1β production. Therefore, our results suggest that pyruvate metabolism and entry into the TCA supports succinate accumulation.

An importance consideration not addressed in this study is how pyruvate supports succinate accumulation. Following M1 polarisation the TCA cycle is interrupted and citrate and succinate accumulate (Viola et al., 2019). Due to these two breaks in the TCA, there is an incomplete flow of metabolites, and pyruvate entry into the TCA cannot directly support succinate accumulation. Tannahill *et al* (2013) proposed that glutaminolysis to generate α-ketoglutarate is the principle mechanism of succinate anaplerosis, and to a lesser extent, the gamma aminobutyric acid (GABA) shunt. However, a large metabolic and transcriptomic study demonstrated that glutamine deprivation affects M2 polarisation but not M1 polarisation (Jha et al., 2015), suggesting an unidentified pathway supports succinate accumulation. Therefore, further investigation to identify how pyruvate supports succinate accumulation may reveal a novel immunometabolic pathway and novel therapeutic targets to prevent IL-1β production.

In conclusion, we show hyperglycaemia exacerbates ischaemic brain injury by augmenting the post-stroke inflammatory response, via glycolysis-dependent production of IL-1β in macrophages. Glucose is serving two masters post-stroke, maintaining neuronal survival, whilst sustaining glycolysis dependent production of IL-1β production in macrophages. We identified pyruvate as a metabolite downstream of glycolysis which is essential for regulating IL-1β, and suggest pyruvate supports succinate accumulation. However, how pyruvate supports succinate accumulation is yet to be identified. Combined these results provides a mechanistic insight to why hyperglycaemic patients have greater damage after stroke, and may contribute to the development of new therapeutic strategies.

4.7. References

Adams, H. P., Bendixen, B. H., Kappelle, L. J., Biller, J., Love, B. B., Gordon, D. L. and Marsh, E. E. (1993). Classification of subtype of acute ischemic stroke definitions for use in a multicenter clinical trial. *Stroke*, 24(1), 35–41.

Amantea, D., Bagetta, G., Tassorelli, C., Mercuri, N. B. and Corasaniti, M. T. (2010). Identification of distinct cellular pools of interleukin-1β during the evolution of the neuroinflammatory response induced by transient middle cerebral artery occlusion in the brain of rat. *Brain Research*, 1313(1), 259–269.

Baik, S. H., Kang, S., Lee, W., Choi, H., Chung, S. and Kim, J.-I. (2019). A Breakdown in Metabolic Reprogramming Causes Microglia Dysfunction in Alzheimer's Disease. *Cell Metabolism*, (30) 493–507.

Baird, T. A., Parsons, M. W., Phan, T., Phanh, T., Butcher, K. S., Desmond, P. M., Tress, B. M., Colman, P. G., Chambers, B. R. and Davis, S. M. (2003). Persistent poststroke hyperglycemia is independently associated with infarct expansion and worse clinical outcome. *Stroke*, 34(9), 2208–14.

Bederson, Joshua B, Pitts, L. H., Germano, S. M., Nishimura, M. C., Davis, R. L. and Bartkowski, H. M. (1986b). Evaluation of 2, 3, 5-triphenyltetrazolium chloride as a stain for detection and quantification of experimental cerebral infarction in rats. *Stroke*, 17(6), 1304–1308.

Bederson, J B, Pitts, L. H., Tsuji, M., Nishimura, M. C., Davis, R. L. and Bartkowski, H. (1986a). Rat middle cerebral artery occlusion: Evaluation of the model and development of a neurologic examination. *Stroke*, 17(3), 472–476.

Berthet, C., Lei, H., Thevenet, J., Gruetter, R., Magistretti, P. J. and Hirt, L. (2009). Neuroprotective role of lactate after cerebral ischemia. *Journal of Cerebral Bloodflow & Metabolism*, 29(11), 1780–9.

Biessels, G. J., Staekenborg, S., Brunner, E., Brayne, C. and Scheltens, P. (2006). Risk of dementia in diabetes mellitus: A systematic review. *Lancet Neurology*, 5(1), 64–74.

Billiard, J., Dennison, J. B., Briand, J., Annan, R. S., Chai, D., Colón, M., Dodson, C. S., Gilbert, S. A., Greshock, J., Jing, J., Lu, H., McSurdy-Freed, J. E., Orband-Miller, L. A., Mills, G. B., Quinn, C. J., Schneck, J. L., Scott, G. F., Shaw, A. N., Waitt, G. M., Wooster, R. F. and Duffy, K. J. (2013). Quinoline 3-sulfonamides inhibit lactate dehydrogenase A and reverse aerobic glycolysis in cancer cells. *Cancer & Metabolism*, 19(1), 2–17.

Bômont, L. and MacKenzie, E. T. (1995). Neuroprotection after focal cerebral ischaemia in hyperglycaemic and diabetic rats. *Neuroscience Letters*, 197(1), 53–56.

Van den Bossche, J., O'Neill, L. A. and Menon, D. (2017). Macrophage Immunometabolism: Where Are We (Going)? *Trends in Immunology*, 38(6), 395–406.

Candelise, L., Landi, G., Orazio, E. N. and Boccardi, E. (1985). Prognostic Significance of Hyperglycemia in Acute Stroke. *Archives of Neurology*, 42(7), 661–663.

Capes, S. E., Hunt, D., Malmberg, K., Pathak, P. and Gerstein, H. C. (2001). Stress hyperglycemia and prognosis of stroke in nondiabetic and diabetic patients: A systematic overview. *Stroke*, 32(10), 2426–2432.

Cater, H. L., Chandratheva, A., Benham, C. D., Morrison, B. and Sundstrom, L. E. (2003). Lactate and glucose as energy substrates during, and after, oxygen deprivation in rat hippocampal acute and cultured slices. *Journal of Neurochemistry*, 87(6), 1381–1390.

Chen, E. Y., Tan, C. M., Kou, Y., Duan, Q., Wang, Z., Meirelles, G. V., Clark, N. R. and Ma'ayan, A. (2013). Enrichr: Interactive and collaborative HTML5 gene list enrichment analysis tool. *BMC Bioinformatics*, 14(1), 128.

Choi, S. S., Lee, H. J., Lim, I., Satoh, J. I. and Kim, S. U. (2014). Human astrocytes: Secretome profiles of cytokines and chemokines. *PLoS ONE*, 9(4), e92325.

Colegio, O. R., Chu, N. Q., Szabo, A. L., Chu, T., Rhebergen, A. M., Jairam, V., Cyrus, N., Brokowski, C. E., Eisenbarth, S. C., Phillips, G. M., Cline, G. W., Phillips, A. J. and Medzhitov, R. (2014). Functional polarization of tumour-associated macrophages by tumour-derived lactic acid. *Nature*, 513(7519), 559–563.

Combs, D. J., Reuland, D. S., Martin, D. B., Zelenock, G. B. and D'Alecy, L. G. (1986). Glycolytic inhibition by 2-deoxyglucose reduces hyperglycemia-associated mortality and morbidity in the ischemic rat. *Stroke*, 17(5), 989–994.

Cox, N. H. and Lorains, J. W. (1986). The prognostic value of blood glucose and glycosylated haemoglobin estimation in patients with stroke. *Postgraduate Medical Journal*, 62(723), 7–10.

Daniels, M. J. D., Rivers-Auty, J., Schilling, T., Spencer, N. G., Watremez, W., Fasolino, V., Booth, S. J., White, C. S., Baldwin, A. G., Freeman, S., Wong, R., Latta, C., Yu, S., Jackson, J., Fischer, N., Koziel, V., Pillot, T., Bagnall, J., Allan, S. M., Paszek, P., Galea, J., Harte, M. K., Eder, C., Lawrence, C. B. and Brough, D. (2016). Fenamate NSAIDs inhibit the NLRP3 inflammasome and protect against Alzheimer's disease in rodent models. *Nature Communications*, 7(12504), 1–10.

Dora, B., Mihçi, E., Eser, A., Özdemir, C., Çakir, M., Balci, M. K. and Balkan, S. (2004). Prolonged hyperglycemia in the early subacute period after cerebral infarction: Effects on short term prognosis. *Acta Neurologica Belgica*, 104(2), 64–67.

Esposito, K., Nappo, F., Marfella, R., Giugliano, G., Giugliano, F., Ciotola, M., Quagliaro, L., Ceriello, A. and Giugliano, D. (2002). Inflammatory cytokine concentrations are acutely increased by hyperglycemia in humans: Role of oxidative stress. *Circulation*, 106(16), 2067–2072.

Gimeno-Bayón, J., López-López, A., Rodríguez, M. J. and Mahy, N. (2014). Glucose pathways adaptation supports acquisition of activated microglia phenotype. *Journal of Neuroscience Research*, 92(6), 723–731.

Di Gioia, M., Spreafico, R., Springstead, J. R., Mendelson, M. M., Joehanes, R., Levy, D. and Zanoni, I. (2019). Endogenous oxidized phospholipids reprogram cellular metabolism and boost hyperinflammation. *Nature Immunology*, 21(1), 42–53.

Gliem, M., Schwaninger, M. and Jander, S. (2016). Protective features of peripheral monocytes/macrophages in stroke. *Biochimica et Biophysica Acta*, 1862(3), 329–338.

Gray, C. S., Hildreth, A. J., Sandercock, P. A., O'Connell, J. E., Johnston, D. E., Cartlidge, N. E., Bamford, J. M., James, O. F. and Alberti, K. G. M. (2007). Glucose-potassium-insulin infusions in the management of post-stroke hyperglycaemia: the UK Glucose Insulin in Stroke Trial (GIST-UK). *Lancet Neurology*, 6(5), 397–406.

Hamilton, J. A., Vairo, G. and Lingelbach, S. R. (1986). CSF-1 stimulates glucose uptake in murine bone marrow-derived macrophages. *Biochemical and Biophysical Research Communications*, 138(1), 445–454.

Han, H., Cho, J. W., Lee, Sangyoung, Yun, A., Kim, H., Bae, D., Yang, S., Kim, C. Y., Lee, M., Kim, E., Lee, Sungho, Kang, B., Jeong, D., Kim, Y., Jeon, H. N., Jung, H., Nam, S., Chung, M., Kim, J. H. and Lee, I. (2018). TRRUST v2: An expanded reference database of human and mouse transcriptional regulatory interactions. *Nucleic Acids Research*, 46(1), 380–386.

Heneka, M. T., Kummer, M. P., Stutz, A., Delekate, A., Schwartz, S., Vieira-Saecker, A., Griep, A., Axt, D., Remus, A., Tzeng, T.-C., Gelpi, E., Halle, A., Korte, M., Latz, E. and Golenbock, D. T. (2013). NLRP3 is activated in Alzheimer's disease and contributes to pathology in APP/PS1 mice. *Nature*, 493(7434), 674–8.

Hjalmarsson, C., Manhem, K., Bokemark, L. and Andersson, B. (2014). The Role of Prestroke Glycemic Control on Severity and Outcome of Acute Ischemic Stroke. *Stroke Research and Treatment*, 2014(694569), 1–6.

Jha, A. K., Huang, S. C. C., Sergushichev, A., Lampropoulou, V., Ivanova, Y., Loginicheva, E., Chmielewski, K., Stewart, K. M., Ashall, J., Everts, B., Pearce, E. J., Driggers, E. M. and Artyomov, M. N. (2015). Network integration of parallel metabolic and transcriptional data reveals metabolic modules that regulate macrophage polarization. *Immunity*, 42(3), 419–430.

Kagansky, N., Levy, S. and Knobler, H. (2001). The role of hyperglycemia in acute stroke. *Archives of Neurology*, 58(8), 1209–1212.

Katsura, K., Asplund, B., Ekholm, A. and Siesjö, B. K. (1992). Extra- and Intracellular pH in the Brain During Ischaemia, Related to Tissue Lactate Content in Normo-and Hypercapnic rats. *European Journal of Neuroscience*, 4(2), 166–176.

Khan, M. A., Schultz, S., Othman, A., Fleming, T., Lebrón-Galán, R., Rades, D., Clemente, D., Nawroth, P. P. and Schwaninger, M. (2016). Hyperglycemia in stroke impairs polarization of monocytes/macrophages to a protective noninflammatory cell type. *Journal of Neuroscience*, 36(36), 9313–9325.

Kilkenny, C., Browne, W. J., Cuthill, I. C., Emerson, M. and Altman, D. G. (2010). Improving Bioscience Research Reporting: The ARRIVE Guidelines for Reporting Animal Research. *PLoS Biology*, 8(6), e1000412.

Koizumi, J., Yoshida, Y., Nakazawa, T. and Ooneda, G. (1986). Experimental studies of ischemic brain edema. *Nosotchu*, 8(1), 1–8.

Kolde, R. (2015). pheatmap : Pretty Heatmaps. *R package version 1.0.8*.

Kruyt, N. D., Biessels, G. J., Devries, J. H. and Roos, Y. B. (2010). Hyperglycemia in acute ischemic stroke: Pathophysiology and clinical management. *Nature Reviews Neurology*, 6(3), 145–155.

Kuleshov, M. V, Jones, M. R., Rouillard, A. D., Fernandez, N. F., Duan, Q., Wang, Z., Koplev, S., Jenkins, S. L., Jagodnik, K. M., Lachmann, A., McDermott, M. G., Monteiro, C. D., Gundersen, G. W. and Ma'ayan, A. (2016). Enrichr: a comprehensive gene set enrichment analysis web server 2016 update. *Nucleic acids research*, 44(1), 90–97.

Liu, X., Nemeth, D. P., McKim, D. B., Zhu, L., DiSabato, D. J., Berdysz, O., Gorantla, G., Oliver, B., Witcher, K. G., Wang, Y., Negray, C. E., Vegesna, R. S., Sheridan, J. F., Godbout, J. P., Robson, M. J., Blakely, R. D., Popovich, P. G., Bilbo, S. D. and Quan, N. (2019). Cell-Type-Specific Interleukin 1 Receptor 1 Signaling in the Brain Regulates Distinct Neuroimmune Activities. *Immunity*, 50(2), 317–333.

Liu, X. and Quan, N. (2018). Microglia and CNS interleukin-1: Beyond immunological concepts. *Frontiers in Neurology*, 9 8.

Love, M. I., Huber, W. and Anders, S. (2014). Moderated estimation of fold change and dispersion for RNA-seq data with DESeq2. *Genome Biology*, 15(12), 1–21.

Luheshi, N. M., Kovács, K. J., Lopez-Castejon, G., Brough, D. and Denes, A. (2011). Interleukin-1α expression precedes IL-1β after ischemic brain injury and is localised to areas of focal neuronal loss and penumbral tissues. *Journal of Neuroinflammation*, 8(186), 1–5.

Lynch, M. A. (2019). Can the emerging field of immunometabolism provide insights into neuroinflammation? *Progress in Neurobiology*, 184(1), 101719.

MacDougall, N. J. J. and Muir, K. W. (2011). Hyperglycaemia and infarct size in animal models of middle cerebral artery occlusion: Systematic review and meta-analysis. *Journal of Cerebral Blood Flow & Metabolism*, 31(3), 807–818.

Marden, J. R., Mayeda, E. R., Tchetgen Tchetgen, E. J., Kawachi, I. and Glymour, M. M. (2017). High Hemoglobin A1c and Diabetes Predict Memory Decline in the Health and Retirement Study. *Alzheimer Disease and Associated Disorders*, 31(1), 48–54.

Maysami, S., Wong, R., Pradillo, J. M., Denes, A., Dhungana, H., Malm, T., Koistinaho, J., Orset, C., Rahman, M., Rubio, M., Schwaninger, M., Vivien, D., Bath, P. M., Rothwell, N. J. and Allan, S. M. (2016). A cross-laboratory preclinical study on the effectiveness of interleukin-1 receptor antagonist in stroke. *Journal of Cerebral Blood Flow & Metabolism*, 36(3), 596–605.

McCann, S. K., Cramond, F., Macleod, M. R. and Sena, E. S. (2016). Systematic Review and Meta-Analysis of the Efficacy of Interleukin-1 Receptor Antagonist in Animal Models of Stroke: an Update. *Translational Stroke Research*, 7(5), 395–406.

McColl, B. W., Rothwell, N. J. and Allan, S. M. (2007). Systemic inflammatory stimulus potentiates the acute phase and CXC chemokine responses to experimental stroke and exacerbates brain damage via interleukin-1- and neutrophil-dependent mechanisms. *Journal of Neuroscience*, 27(16), 4403–4412.

Meiser, J., Krämer, L., Sapcariu, S. C., Battello, N., Ghelfi, J., D'Herouel, A. F., Skupin, A. and Hiller, K. (2016). Pro-inflammatory Macrophages Sustain Pyruvate Oxidation through Pyruvate Dehydrogenase for the Synthesis of Itaconate and to Enable Cytokine Expression. *The Journal of Biological Chemistry*, 291(8), 3932–3946.

Michl, J., Ohlbaum, D. J. and Silverstein, S. C. (1976). 2-Deoxyglucose selectively inhibits fc and complement receptor-mediated phagocytosis in mouse peritoneal macrophages: Description of the inhibitory effect. *Journal of Experimental Medicine*, 144(6), 1465–1483.

Mills, E. L., Kelly, B., Logan, A., Costa, A. S. H. H., Varma, M., Bryant, C. E., Tourlomousis, P., Däbritz, J. H. M., Gottlieb, E., Latorre, I., Corr, S. C., McManus, G., Ryan, D., Jacobs, H. T., Szibor, M., Xavier, R. J., Braun, T., Frezza, C., Murphy, M. P. and O'Neill, L. A. (2016). Succinate Dehydrogenase Supports Metabolic Repurposing of Mitochondria to Drive Inflammatory Macrophages. *Cell*, 167(2), 457–470.

O'Neill, L. A. J. and Artyomov, M. N. (2019). Itaconate: the poster child of metabolic reprogramming in macrophage function. *Nature Reviews Immunology*, 19(5), 273–281.

Orihuela, R., McPherson, C. A. and Harry, G. J. (2016). Microglial M1/M2 polarization and metabolic states. *British Journal of Pharmacology*, 173(4), 649–665.

Palsson-McDermott, E. M., Curtis, A. M., Goel, G., Lauterbach, M. A. R., Sheedy, F. J., Gleeson, L. E., van den Bosch, M. W. M., Quinn, S. R., Domingo-Fernandez, R., Johnston, D. G. W., Jiang, J., Israelsen, W. J., Keane, J., Thomas, C., Clish, C., Vander Heiden, M., Xavier, R. J. and O'Neill, L. A. J. (2015). Pyruvate Kinase M2 Regulates Hif-1α Activity and IL-1β Induction and Is a Critical Determinant of the Warburg Effect in LPS-Activated Macrophages. *Cell Metabolism*, 21(1), 65–80.

Palsson-McDermott, E. M. and O'Neill, L. A. J. (2013). The Warburg effect then and now: From cancer to inflammatory diseases. *BioEssays*, 35(11), 965–973.

Parsons, M. W., Barber, P. A., Desmond, P. M., Baird, T. A., Darby, D. G., Byrnes, G., Tress, B. M. and Davis, S. M. (2002). Acute hyperglycemia adversely affects stroke outcome: A magnetic resonance imaging and spectroscopy study. *Annals of Neurology*, 52(1), 20–28.

Pavlou, S., Lindsay, J., Ingram, R., Xu, H. and Chen, M. (2018). Sustained high glucose exposure sensitizes macrophage responses to cytokine stimuli but reduces their phagocytic activity. *BMC Immunology*, 19(24), 1–13.

Pieper, G. M. and Riaz-ul-Haq, J. (1997). Activation of Nuclear Factor-κB in Cultured Endothelial Cells by Increased Glucose Concentration: Prevention by Calphostin C. *Journal of Cardiovascular Pharmacology*, 30(4), 528–532.

Piironen, K., Putaala, J., Rosso, C. and Samson, Y. (2012). Glucose and acute stroke: evidence for an interlude. *Stroke*, 43(3), 898–902.

Pruzin, J. J., Schneider, J. A., Capuano, A. W., Leurgans, S. E., Barnes, L. L., Ahima, R. S., Arnold, S. E., Bennett, D. A. and Arvanitakis, Z. (2017). Diabetes, Hemoglobin A1C, and Regional Alzheimer's Disease and Infarct Pathology HHS Public Access. *Alzheimer Dis Assoc Disord*, 31(1), 41–47.

R Core Team (2017). R: a language and environment for statistical computing. *R Foundation for Statistical Computing*.

Ramana, K. V., Friedrich, B., Srivastava, S., Bhatnagar, A. and Srivastava, S. K. (2004). Activation of nulcear factor-κB by hyperglycemia in vascular smooth muscle cells is regulated by aldose reductase. *Diabetes*, 53(11), 2910–2920.

Rehncrona, S. and Kågström, E. (1983). Tissue lactic acidosis and ischemic brain damage. *American Journal of Emergency Medicine*, 1(2), 168–174.

Relton, J. K. and Rothwell, N. J. (1992). Interleukin-1 receptor antagonist inhibits ischaemic and excitotoxic neuronal damage in the rat. *Brain Research Bulletin*, 29(2), 243–246.

Romeo, G., Liu, W. H., Asnaghi, V., Kern, T. S. and Lorenzi, M. (2002). Activation of nuclear factor-κB induced by diabetes and high glucose regulates a proapoptotic program in retinal pericytes. *Diabetes*, 51(7), 2241–2248.

Rubio-Araiz, A., Finucane, O. M., Keogh, S. and Lynch, M. A. (2018). Anti-TLR2 antibody triggers oxidative phosphorylation in microglia and increases phagocytosis of β-amyloid. *Journal of Neuroinflammation*, 15(1), 247.

Saxena, A., Anderson, C. S., Wang, X., Sato, S., Arima, H., Chan, E., Munoz-Venturelli, P., Delcourt, C., Robinson, T., Stapf, C., Lavados, P. M., Wang, J., Neal, B., Chalmers, J. and Heeley, E. (2016). Prognostic Significance of Hyperglycemia in Acute Intracerebral Hemorrhage: The INTERACT2 Study. *Stroke*, 47(3), 682–688.

Stegenga, M. E., Van Der Crabben, S. N., Levi, M., De Vos, A. F., Tanck, M. W., Sauerwein, H. P. and Van Der Poll, T. (2006). Hyperglycemia stimulates coagulation, whereas hyperinsulinemia impairs fibrinolysis in healthy humans. *Diabetes*, 55(6), 1807–1812.

Szczudlik, A., Slowik, A., Turaj, W., Wyrwicz-Petkow, U., Pera, J., Dziedzic, T., Trabka-Janik, E. and Iskra, T. (2001). Transient hyperglycemia in ischemic stroke patients. *Journal of the Neurological Sciences*, 189(1), 105–111.

Tang, B. L. (2018). Brain activity-induced neuronal glucose uptake/glycolysis: Is the lactate shuttle not required? *Brain Research Bulletin*, 137(1), 225–228.

Tannahill, G. M., Curtis, A. M., Adamik, J., Palsson-McDermott, E. M., McGettrick, A. F., Goel, G., Frezza, C., Bernard, N. J., Kelly, B., Foley, N. H., Zheng, L., Gardet, A., Tong, Z., Jany, S. S., Corr, S. C., Haneklaus, M., Caffrey, B. E., Pierce, K., Walmsley, S., Beasley, F. C., Cummins, E., Nizet, V., Whyte, M., Taylor, C. T., Lin, H., Masters, S. L., Gottlieb, E., Kelly, V. P., Clish, C., Auron, P. E., Xavier, R. J. and O'Neill, L. A. J. (2013). Succinate is an inflammatory signal that induces IL-1β through HIF-1α. *Nature*, 496(7444), 238–42.

Trouplin, V., Boucherit, N., Gorvel, L., Conti, F., Mottola, G. and Ghigo, E. (2013). Bone marrow-derived macrophage production. *Journal of Visualized Experiments*, (81) e50966.

Vaidyula, V. R., Rao, A. K., Mozzoli, M., Homko, C., Cheung, P. and Boden, G. (2006). Effects of hyperglycemia and hyperinsulinemia on circulating tissue factor procoagulant activity and platelet CD40 ligand. *Diabetes*, 55(1), 202–8.

Viola, A., Munari, F., Sánchez-Rodríguez, R., Scolaro, T. and Castegna, A. (2019). The metabolic signature of macrophage responses. *Frontiers in Immunology*, 10(1), 1462.

Volobоueva, L. A., Emery, J. F., Sun, X. and Giffard, R. G. (2013). Inflammatory response of microglial BV-2 cells includes a glycolytic shift and is modulated by mitochondrial glucose-regulated protein 75/mortalin. *FEBS Letters*, 587(6), 756–762.

Wajid Jawaid (2019). *enrichR: An R interface to the Enrichr database*. [Online] [Accessed on 18th March 2020] https://cran.r-project.org/web/packages/enrichR/vignettes/enrichR.html.

Wang, F., Zhang, S., Jeon, R., Vuckovic, I., Jiang, X., Lerman, A., Folmes, C. D., Dzeja, P. D. and Herrmann, J. (2018). Interferon Gamma Induces Reversible Metabolic Reprogramming of M1 Macrophages to Sustain Cell Viability and Pro-Inflammatory Activity. *EBioMedicine*, (30) 303–316.

Warburg, O. (1956). On the Origin of Cancer Cells. *Science,* 123(3191), 309–314.

Wei, J., Cohen, D. M. and Quast, M. J. (2003). Effects of 2-Deoxy-D-glucose on focal cerebral ischemia in hyperglycemic rats. *Journal of Cerebral Blood Flow & Metabolism*, 23(5), 556–564.

Wei, J., Raynor, J., Nguyen, T. L. M. and Chi, H. (2017). Nutrient and metabolic sensing in T cell responses. *Frontiers in Immunology*, (8) 247.

Weir, C. J., Murray, G. D., Dyker, A. G. and Lees, K. R. (1997). Is hyperglycaemia an independent predictor of poor outcome after acute stroke? Results of a long term follow up study. *BMJ*, 314(7090), 1303.

Wickham, H. (2016). *Ggplot2 : elegant graphics for data analysis*.

Williams, S. B., Goldfine, A. B., Timimi, F. K., Ting, H. H., Roddy, M. A., Simonson, D. C. and Creager, M. A. (1998). Acute hyperglycemia attenuates endothelium-dependent vasodilation in humans in vivo. *Circulation*, 97(17), 1695–1701.

Wong, R., Lénárt, N., Hill, L., Toms, L., Coutts, G., Martinecz, B., Császár, E., Nyiri, G., Papaemmanouil, A., Waisman, A., Müller, W., Schwaninger, M., Rothwell, N., Francis, S., Pinteaux, E., Denés, A. and Allan, S. M. (2019). Interleukin-1 mediates ischaemic brain injury via distinct actions on endothelial cells and cholinergic neurons. *Brain, Behavior, and Immunity*, 76(1), 126–138.

Yerneni, K. K. V., Bai, W., Khan, B. V., Medford, R. M. and Natarajan, R. (1999). Hyperglycemia-induced activation of nuclear transcription factor κB in vascular smooth muscle cells. *Diabetes*, 48(4), 855–864.

Yu, Z. F. and Mattson, M. P. (1999). Dietary restriction and 2-deoxyglucose administration reduce focal ischemic brain damage and improve behavioral outcome: Evidence for a preconditioning mechanism. *Journal of Neuroscience Research*, 57(6), 830–839.

Zhang, D., Tang, Z., Huang, H., Zhou, G., Cui, C., Weng, Y., Liu, W., Kim, S., Lee, S., Perez-Neut, M., Ding, J., Czyz, D., Hu, R., Ye, Z., He, M., Zheng, Y. G., Shuman, H. A., Dai, L., Ren, B., Roeder, R. G., Becker, L. and Zhao, Y. (2019). Metabolic regulation of gene expression by histone lactylation. *Nature*, (574) October, 575–580.

Zilva, J. F. (1978). The origin of the acidosis in hyperlactataemia. *Annals of Clinical Biochemistry*, 15(1), 40–43.

4.8. Supplementary material

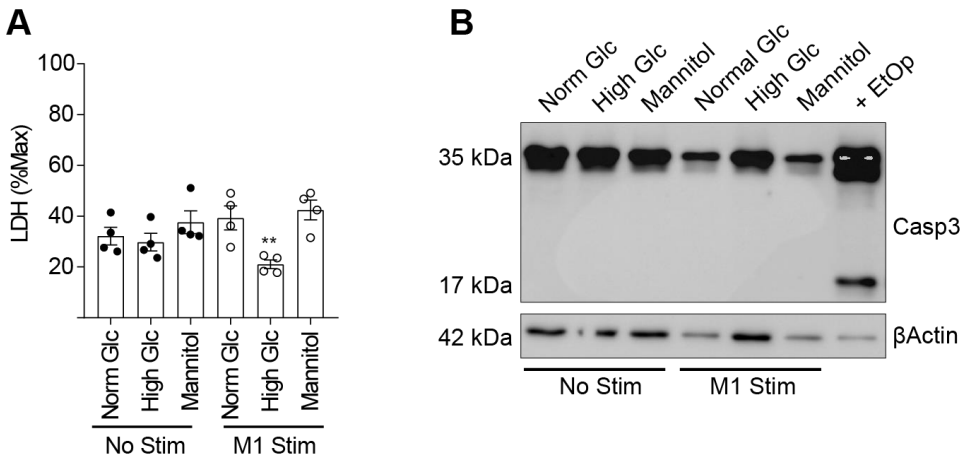

Figure 4.S1 – Glucose and M1 challenge does not cause cell death in BMDMs.
BMDMs were treated with different glucose containing media: NormGlc (5.5 mM Glc), HighGlc (30.5 mM Glc) or Mannitol (5.5 mM Glc + 25 mM mannitol), in the presence or absence of an M1 stim (100 ng/mL IFNγ and 50 ng/mL LPS) for 24 hours (A-B). Pyroptotic cell death was assessed by LDH release (A, n=4), and apoptotic death was assessed by western blot for cleaved Casp3 (B). A positive control for cleaved Casp3 was run alongside samples, where mixed glial cultures were been treated with EtOp (40 µg/mL). Data are presented as mean ± SEM. Data were assessed with two-way ANOVA with Tukey's *post hoc* (A) , $^{**}p < 0.01$ M1 Stim Norm Glc vs High Glc and M1 Stim Mannitol vs High Glc.

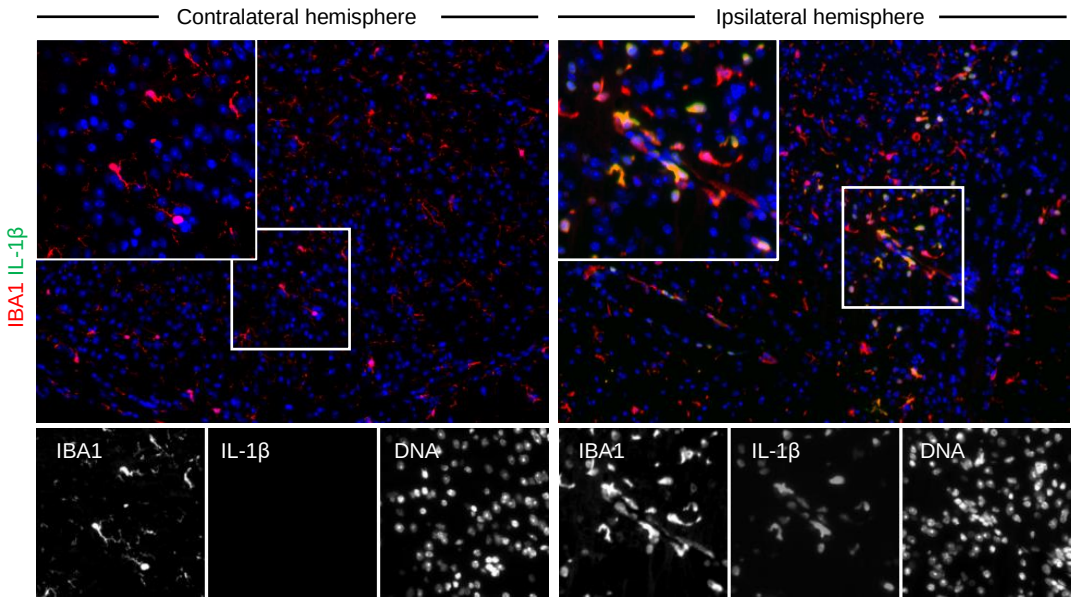

Figure 4.S2 – IL-1β production after MCAo is predominantly from Iba1⁺ cells.
Mice were given 2.2 g/kg Glc, or PBS, by i.p. injection and a stroke was induce by MCAo. Representative images show immunostaining for Iba1, pro IL-1β, and DNA in the contralateral and ipsilateral hemisphere (n=18).

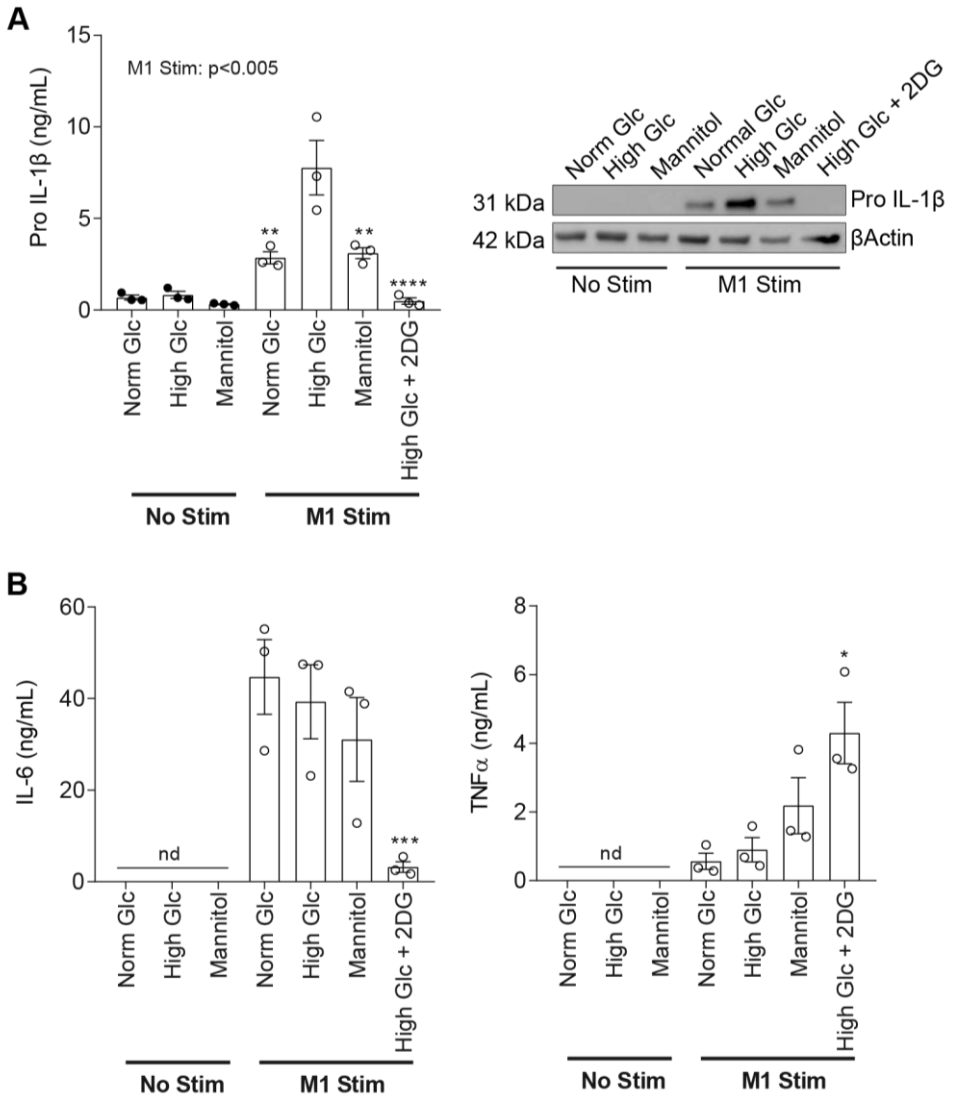

Figure 4.S3 – Elevated glucose drives production of IL-1β in brain specific cell types, which is dependent of glycolysis.
Murine mixed glia were pretreated with 2DG (2mM) for 3 hours, and then challenged with respective M1 stimulated (100 ng/mL IFNγ and 50 ng/mL LPS) glucose containing medias (NormGlc 5.5 mM, HighGlc 30.5 mM) for 24 hours (A-B). Pro IL-1β was determined by ELISA and western blot (A), and IL-6 and TNFα in supernatants was determined by ELISA (B). Graphs are representative of one independent experiment, with three biological replicates (B-C, n=3). Data are presented as mean ± SEM. Data was assessed using: two-way ANOVA with Tukey's post hoc (A); one-way ANOVA with Dunnett's post hoc (B). *p < 0.05, **p < 0.01, ***p < 0.001, and ****p < 0.0001 vs M1 stim High Glc.

Chapter 5. General Discussion

5.1. Summary

Cerebral ischaemia can occur in response to a transient focal cessation or chronic global reduction in blood flow to the brain, both of which have potentially detrimental consequences and central roles in the pathology of stroke and SVD. A number of modifiable risk factors, such as diet, have been shown to exacerbate ischaemic damage. Here, we investigated global and focal ischaemic pathology in murine models, and how obesity and hyperglycaemia modulates the response to neuropathology.

The overarching aim of this thesis was to investigate how diet influences inflammatory responses and the subsequent neuropathological and functional outcomes after global and focal cerebral ischaemia. Within this overall aim, we set out to address three specific objectives:

1. **Develop and characterise the BCAS model of global cerebral hypoperfusion, which will be used for the first time at the University of Manchester.**

2. **Investigate how obesity regulates inflammatory responses and long-term functional outcomes in mice following experimental stroke.**

3. **Determine how hyperglycaemia regulates inflammatory responses and neuropathological outcome in mice following experimental stroke.**

In Chapter 2, we aimed to establish a mouse model of hypoperfusion, BCAS. The BCAS model was first established in 2004, and has been widely published since then, producing a modest reduction in CBF, and distinct vascular and white matter pathologies in mice (Shibata et al., 2004). In this study, we showed a sustained reduction in CBF, but we did not observe a concomitant reduction in tissue oxygenation or altered ischaemic pathology. We hypothesise that the reduction in CBF was not severe enough and/or there was sufficient compensatory collateral flow; this meant that the critical threshold required to induce the neuropathological and cognitive changes previously observed in murine models was not reached. In subsequent chapters, we therefore employed the well-established MCAo model of

transient focal ischaemia, to investigate how different dietary states can affect post-ischaemic inflammatory responses and ischaemic injury.

In Chapter 3, we investigated long-term outcomes after stroke, focusing on clinically relevant outcomes. We found that stroke induced long-term changes in depressive and anxiety-like behaviours and a sustained loss in adipose mass. We also found an altered lipid profile, increased adipokine release, and increased liver damage, which are indicative of an increased risk of subsequent vascular events. Additionally, we assessed these outcomes in obese mice to determine what effect obesity has on long-term outcomes after stroke. We corroborated previous findings that obese mice have increased lesion volume and higher mortality after MCAo (Maysami et al., 2015). In light of this, we took a novel approach to equalise lesion volumes with different occlusion times; therefore, any changes in outcomes can be attributed to the effects of obesity, rather than increased damage. Obese mice, with equivalent lesion volumes, had long-term changes in depressive and anxiety-like behaviours, but these changes did not differ from normal-fed mice. Obese mice did have a greater reduction in adipose mass, compared to normal-fed mice; however, this was not accompanied by pronounced changes in adipokine release, lipid profile and liver damage.

In Chapter 4, we investigated the effect of hyperglycaemia on inflammatory stroke pathology. Hyperglycaemia is commonly observed in patients admitted to hospital for stroke and is associated with larger infarcts, increased mortality and poorer clinical outcomes. These effects are independent of other risk factors such as age, diabetes, and stroke severity. However, it is unclear how blood glucose exacerbates ischaemic injury. Here, we show that following stroke, macrophage/microglial cells undergo extensive metabolic reprogramming to support an inflammatory phenotype, which is characterised by enhanced IL-1β production. Moreover, production of IL-1β was dependent on glycolysis. However, as inhibiting glycolysis is not a clinically viable therapeutic methodology, we sought to identify key metabolites downstream of glycolysis regulating IL-1β production, in a bid to discover potential targets. We identified that pyruvate metabolism and entry into the TCA cycle is required for IL-1β production, where it likely supports succinate accumulation.

5.2. Experimental considerations and future directions

5.2.1. Refinement of the BCAS model

The main finding of Chapter 2 was that there were no major pathological changes in the brain in response to BCAS-induced chronic hypoperfusion. Despite a sustained reduction in CBF at 3 months, tissue oxygenation was not affected at this timepoint. Consequently, ischaemia-related pathology such as BBB breakdown and neuroinflammation did not occur. To determine tissue oxygenation, we used clinically validated markers of tissue oxygenation, MAG:PLP and VEGF, which were assessed for the first time in the BCAS model in this study. We did not see a significant change in these markers and suggest that the lack of effect is due to CBF not being sufficiently reduced. To further validate MAG:PLP and VEGF as markers of ischaemia in mouse tissue we could: (i) assess MAG:PLP and VEGF acutely in more severe model of ischaemia, e.g. MCAo or 2VO, or (ii) assess changes at Day 1 in the BCAS model when maximal reduction in CBF is observed. Following validation of MAG:PLP and VEGF as relevant markers of ischaemia in mouse tissue, we could re-assess these markers in an optimised model of BCAS and evaluate the translatability of the model.

With respect to the validity of the BCAS model, there are several experimental considerations to ensure that sufficient pathological hypoperfusion occurs and subsequent ischaemia achieved. The first option is to decrease the diameter of the coil, furthering restricting CBF. In an early paper characterising the BCAS model, the authors used 4 different diameters of coils: 0.16, 0.18, 0.20 and 0.22 mm, with the 0.16 mm coil being associated with more severe CBF reduction, higher mortality and grey matter damage (Shibata et al., 2004). Indeed, other research groups employing this model have experienced issues with modest reductions in CBF using 0.18 mm coils, and have consequently switched to tighter coils. A further experimental consideration which may have impacted our results is the inherent biological variability within groups. It is well described that C57BL/6 mice have large variations in the anatomy of the Circle of Willis and this anatomical diversity may account for the variability in our data (McColl et al., 2004). To account for this in future experiments, we could incorporate strict exclusion criteria such as: (i) a minimum reduction in CBF at Day 1, (ii) pre-selecting animals with suitable vasculature by MRI before BCAS surgery, or (iii) assessment of posterior communicating arteries post-mortem by carbon black ink perfusion.

In Chapters 3 and 4, we showed how dietary influences, obesity and hyperglycaemia, modulate outcomes after transient ischaemia. To our knowledge, there have not been any studies that have investigated these co-morbidities in the context of the BCAS model. Thus, it would be interesting to conduct experiments investigating obesity and hyperglycaemia in the context of chronic global hypoperfusion, to draw comparisons between the pathology in focal and global ischaemia. Additionally, Chapter 4 investigated immunometabolic changes after ischaemic stroke, but very little is known about metabolic changes in response to global ischaemia, and it would therefore be of interest to investigate the role of immunometabolism in the BCAS model.

5.2.2. Investigating long-term vascular risk after stroke and the obesity paradox

In chapter 3, we identified that normal-fed mice had an altered lipid, adipokine and ALT profile, and this was indicative of poor vascular health, and risk of future vascular events. Indeed, in humans, the risk of recurrent vascular events, such as secondary stroke or myocardial infarction, is high for many years after the initial stroke (Putaala et al., 2010). A recent preclinical study also indicated that experimental stroke induces profound effects on vascular health through enhanced atherosclerotic mechanisms (Roth et al., 2018). In this study, the authors showed that 1 month after stroke, mice had increased aortic plaque burden, which was mediated via HMGB1 release and activation of endothelial cells. In our study, incorporation of *en face* vessel staining to characterise plaque burden would have been beneficial to determine if the poor vascular risk profile translates into a pathological manifestation. Further long-term studies to investigate recurrent cardiovascular events after stroke are required to confirm these findings.

To investigate how obesity effects long-term changes after stroke, we also used mice that had been fed a high-fat diet for 6 months. We confirmed previous reports demonstrating that obesity is associated with increased mortality at acute timepoints after MCAo (Maysami et al., 2015). Consequently, we took a novel approach to use different MCA occlusion times to equalise lesion volumes. This approach allowed us to assess the effect of obesity on long-term outcomes, independent of lesion volume. We found obesity did not affect anxiety and

depressive behaviours post-stroke, compared to normal-fed mice. This contradicts the obesity hypothesis that suggests that obese patients have better outcomes after stroke due to increased energy stores which protect from weight loss (Vemmos et al., 2011; Doehner et al., 2013). Here, despite finding obese mice to have an enhanced/exaggerated reduction in post-stroke adipose loss, long-term outcomes did not differ from control-fed mice. However, the major limitation of these findings is the low sample size (n = 4), and as such, these results would need to be verified in a larger cohort. Alongside obesity being associated with worse short-term outcomes in experimental models of stroke, acute high-fat feeding (3 days) is also associated with worse outcomes after MCAo. Haley *et al* (2019) identified that acute high-fat feeding causes distinct disruptions in glucose homeostasis, highlighting an important link between high-fat and high-glucose diets on outcomes after stroke.

5.2.3. Immunometabolism shaping stroke outcomes

In Chapter 4, we propose that glycolytic flux, following M1-like polarisation, regulates post-stroke IL-1β production. In the context of hyperglycaemia, there is increased substrate availability that drives glycolytic flux and IL-1β production, which proposes a mechanistic insight into why hyperglycaemia may be associated with larger infarcts after stroke. Here, we demonstrate glycolytic flux via a number of different parameters, increased lactate production, succinate accumulation and pro IL-1β production. The gold standard assessment of metabolic fluxes is performed using the Seahorse analyser to determine oxygen consumption rate (OCR) and extracellular acidification rate (ECAR); future work including these analyses would help to build on the metabolic characterisations described here.

Data in Chapter 4 show that hyperglycaemia results in potentiated pro IL-1β production, and subsequent increased lesion volume following stroke. However, a major caveat is that we have not yet validated the directionality of this relationship. It is plausible that hyperglycaemia exacerbates neuronal damage via an IL-1β-independent mechanism, and increased damage causes increased IL-1β production. To address these concerns, future experiments using IL-1RA or IL-1β$^{-/-}$ mice would verify the directionality of hyperglycaemia and IL-1β, and confirm our hypothesis that IL-1β is a major driver of ischaemic damage. A further assumption of this study is that IL-1β production is driven by HIF-1α stabilisation, which has

previously been shown to bind to the IL-1β promotor and upregulate expression (Tannahill et al., 2013). However, we do not directly show HIF-1α stabilisation by conventional immunoblotting techniques, due to technical difficulties with rapid HIF-1α degradation in normoxic conditions. Useful future experiments could incorporate a CXCR3 HIF-1α$^{-/-}$ mouse line to establish the role HIF-1α in regulating IL-1β. These mice could be used for both BMDM isolations to directly implicate HIF-1α in IL-1β production, and also *in vivo* experiments to directly assess the relative contribution of macrophage/microglia IL-1β production in stroke damage.

We identify pyruvate as an essential metabolite for IL-1β production, potentially by supporting succinate accumulation. Tannahill *et al* (2013) proposed that glutaminolysis is the principle mechanism of succinate anaplerosis. Glutaminolysis is a two-step process that converts glutamine to glutamate and glutamate to α-ketoglutarate, which supports the anaplerosis of succinate in the TCA. However, our data indicate glucose-derived pyruvate as the critical intermediate, rather than glutamine, supporting succinate-dependent IL-1β production. In agreement, a recent 'omics' study identified that glutamine deprivation affects M2 polarisation but not M1 polarisation, suggesting an unidentified pathway which supports succinate accumulation (Jha et al., 2015). Future experiments should utilise isotope-labelled mass spectrometry approaches to identify whether glucose or glutamine is the crucial carbon source for succinate, and/or whether this relationship is altered depending on relative substrate availability.

Another consideration of this study is the issue of translatability from mice to humans. Currently all experimental work has been conducted in mouse tissue, and concerns have been raised about the differences in mouse and human cellular metabolism. Vijayan *et al* (2019) proposed that human macrophage stimulated with LPS are reliant on OXPHOS, in contrast to the glycolysis reliance observed in murine macrophages. However, when Wang *et al* (2018) stimulated human monocytes and macrophages with IFNγ, they showed that these cells express IL-1β in a glycolysis-dependent manner. Future studies should utilise human isolated macrophages to validate our findings in mice of a glucose-dependent hyperinflammatory phenotype. Additionally, there may be utility in employing clinical datasets and historical plasma samples to assess the relationships

between blood glucose, specific plasma metabolites (e.g. succinate/lactate, IL-1β), and stroke severity/outcomes.

5.3. Translational and clinical considerations

5.3.1. Dietary interventions for age-related diseases

It is well described that modifiable risk factors are associated with poor vascular health and the development of ischaemia-related diseases, such as stroke and dementia. It has been estimated that approximately 35% of dementia cases worldwide can be attributed to modifiable risk factors: poor education in early life, midlife hypertension, obesity, diabetes, smoking, physical inactivity, depression, social isolation and hearing loss (Livingston et al., 2017). Given that these risk factors can be modulated by lifestyle changes, a number of RCTs are ongoing to investigate the effects of lifestyle-based preventions on the development of dementia (Ngandu et al., 2015; van Charante et al., 2016; Andrieu et al., 2017; Rosenberg et al., 2019). To date, three large European multi-domain lifestyle-based prevention studies have been completed: FINGER, the French Multidomain Alzheimer Preventive Trial (MAPT), and the Dutch Prevention of Dementia by Intensive Vascular Care (PreDIVA) study. All 3 studies have shown promising results, and the FINGER trial met its primary outcome showing a 25% improvement in cognitive performance in patients with a high dementia risk score. Whilst MAPT and PreDIVA did not meet their primary outcomes, they showed promising results in cognitive improvement in subgroup analyses. The FINGER trial implemented multidomain interventions which consisted of dietary counselling, exercise, cognitive training, and social activities, and interventions were tailored to individuals and their risk profiles. The use of multidomain approaches clearly illustrates the importance of lifestyle choices, such as diet, on vascular health. However, the relative contribution of diet on disease outcomes cannot be determined in these multidomain studies. RCTs that focus primarily on dietary intervention and cognition, such as the Mediterranean diet (Martínez-Lapiscina et al., 2013; Tussing-Humphreys et al., 2017), Dietary Approaches to Stop Hypertension (DASH) and Mediterranean-DASH Intervention for Neurodegenerative Delay (MIND) diets (van den Brink et al., 2019), omega-3 rich diets (Cole et al., 2009), and ketogenic diets (Neth et al., 2020) have reported positive effects on cognition.

In order to inform and shape studies in humans, preclinical research is essential for gaining mechanistic insight into the role of diet in the development of neurological and cerebrovascular diseases. A seminal preclinical study identified how salt-rich diets contribute to cognitive dysfunction. Faraco *et al* (2018) demonstrated that dietary salt reduces CBF and promotes cognitive decline, via a novel TH17 gut-brain axis affecting endothelial cell function. The authors show that cognitive decline is independent of hypoperfusion but dependent on endothelial nitric oxide dysfunction, and this promotes tau phosphorylation and subsequent neurodegeneration (Faraco et al., 2019). Another important study provided mechanistic insight into how a western diet has long lasting effects on our immune response. Christ et al (2018) showed that a diet rich in saturated fats and refined sugars can prime monocytes for an augmented IL-1β response to future inflammatory signals, and may contribute to the aetiology of atherosclerosis. Ultimately, an improved understanding of how dietary influences contribute to and shape disease outcomes is essential for educating individuals about healthy lifestyle choices. It is plausible that improved education in western countries may be partly responsible for the decreasing prevalence of dementia (Wu et al., 2017), in contrast to countries such as China (Chan et al., 2013) and Japan (Dodge et al., 2012), where the rates of obesity and diabetes are increasing (Loef and Walach, 2013).

Combined evidence from clinical and preclinical studies demonstrates that different dietary states can have profound impacts on disease outcomes, such as stroke and dementia. Increased public awareness and improved education, as well as enhanced regulatory measures, such as stricter manufacturing regulations for sugar content in processed foods (Feigin and Krishnamurthi, 2016), should be used together to limit the exposure to potentially harmful dietary components. Moreover, the introduction of aversion strategies, such as taxation, may also be a viable in alleviating disease burden (Wilson, 2004; Asaria et al., 2007; Briggs et al., 2013).

5.3.2. Metabolic changes in dementia

In Chapter 4, we found that hyperglycaemia had profound effects in the context of stroke, but the effects of hyperglycaemia were not considered in the context of chronic hypoperfusion and dementia. Contrastingly, glucose hypometabolism has been associated with development of AD. A recent study highlighted the genetic variant apolipoprotein E (APOE) 2 allele is protective against the development of AD, and is associated with increased glucose metabolism in the brain (Wu et al., 2018). Conversely, the APOE4 allele is associated with an increased risk of AD and decreased brain glucose metabolism. Moreover, AD brains have been shown to have decreased expression of glucose transporters and are associated with decreased glycolytic flux (An et al., 2018). As such, there have been different therapeutic approaches to regulate glucose levels in AD patients, such as insulin and the GLP-1 analogue, liraglutide, with some success (Kuehn, 2019). In our study, we showed that increased glucose metabolism is pro-inflammatory, and as neuroinflammation is associated with AD progression and poorer outcomes (Heneka et al., 2015), this may indicate that increasing glucose metabolism in AD may have harmful inflammatory side-effects.

5.3.3. Clinical considerations for immunometabolism therapeutic strategies

Chapter 4 suggests that targeting molecular components involved in immunometabolism may be beneficial in the treatment of stroke. However, this raises concerns about off-target effects, as metabolic programming is fundamental to all cell types. However, despite these concerns, immunometabolic strategies have been employed for many years in the treatment of cancer, thus proving the feasibility of these types of treatments. The success of these treatments in the cancer field is based upon the amplified metabolic demands of tumour cells compared to that of surrounding tissue, which makes them more sensitive to anti-metabolic drugs. For example, anti-folate drugs capitalise on cancer cells' increased proliferative capacities, by inhibiting one-carbon transfer reaction which is required for nucleotide synthesis (Newman and Maddocks, 2017). In our work, we identified a distinctly different metabolic phenotype of myeloid cells to other tissue types, creating an anti-metabolite therapeutic window. A possible advantage of using metabolic approaches in inflammatory disorders over cancer is that the endpoints are far less destructive. Specifically, cancer treatments are designed to

kill cancerous cells, whereas anti-metabolite drugs for inflammatory diseases are designed to reshape cellular function. Therefore, in treating these conditions, a potentially lower dose could be administered with less harmful side-effects than would be needed in the context of cancer (Mazumdar et al., 2020).

We acknowledge that any approach that systemically targets glucose metabolism is likely to fail in the clinical setting, due to its importance in many biological processes and more specifically in the context of stroke, its critical role in neuronal survival and brain repair. We therefore attempted to identify specific metabolites downstream of glycolysis that regulate IL-1β production. We found that pyruvate metabolism is essential for IL-1β production, and supports succinate accumulation; however, we have not fully elucidated the pathways which may identify novel therapeutic targets. Another consideration is the use of the diabetes drug, metformin. Metformin has been shown to inhibit glycolysis specifically in immune cells, and could be repurposed for acute stroke treatment to selectively inhibit M1 polarisation in immune cells (Caslin et al., 2018).

An immunometabolic approach to prevent post-stroke inflammation would need to be time-dependent, targeting pro-inflammatory myeloid cells in the acute period after stroke. Therapies designed for acute timepoints after stroke are difficult to implement, due to lengthy admission times and the requirement for ischaemic stroke confirmation. However, an advantage of this therapeutic strategy is that at-risk sub-groups of patients may be stratified for different treatment regimens based on their blood glucose measurements, and provide a more patient-specific approach. Additional clinical concerns may arise through the inhibition of IL-1β, as this has been associated with an increased risk of fatal sepsis (Ridker et al., 2017).

5.4. Final conclusions

It is well known that a balanced and healthy diet can guard against many diseases, and alteration of diet has the potential to mitigate or exacerbate certain pathological disease features. In the context of ischaemia, it well known that poor diet exacerbates outcomes. This thesis investigates in detail how obesity and hyperglycaemia affect outcomes after transient ischaemia. We found that obesity is associated with increased acute mortality, but does not exacerbate long-term outcomes when lesion volumes are equal between groups. Hyperglycaemia has profound effects on innate immunity, sustaining glycolytic flux and IL-1β production. SVD is a growing global burden and a major contributor to dementia, whereby extensive microvascular disease can result in chronic hypoperfusion and global ischaemia. Indeed, poor diet is a risk factor for dementia and has been shown to exacerbate disease. Lifestyle-based prevention RCTs show benefit in targeting modifiable risk factors to improve vascular health and to improve the rate of cognitive decline. Therefore, future preclinical studies are required in order to gain a mechanistic insight to how diet affects chronic hypoperfusion.

Importantly, unlike genetics and age, diet is a modifiable risk factor. A better understanding of how diet modulates cerebrovascular disease will help to educate and inform public health policies (such as the sugar tax) that promote healthier lifestyle choices. However, as lifestyle-based treatments are commonly fraught with low compliance rates, it is important to also continue gaining better mechanistic insights into how specific dietary states influence ischaemic outcomes; this research will help identify new therapeutic targets and novel pharmacological treatments that may help in reducing disease burden.

Bibliography

Abdelaziz, D. H., Amr, K. and Amer, A. O. (2010). Nlrc4/Ipaf/CLAN/CARD12: more than a flagellin sensor. *The international journal of biochemistry & cell biology*, 42(6), 789–91.

Abrahám, H. and Lázár, G. (2000). Early microglial reaction following mild forebrain ischemia induced by common carotid artery occlusion in rats. *Brain research*, 862(1–2), 63–73.

Adams, H. P., Bendixen, B. H., Kappelle, L. J., Biller, J., Love, B. B., Gordon, D. L. and Marsh, E. E. (1993). Classification of subtype of acute ischemic stroke definitions for use in a multicenter clinical trial. *Stroke*, 24(1), 35–41.

Afonina, I. S., Müller, C., Martin, S. J. and Beyaert, R. (2015). Proteolytic Processing of Interleukin-1 Family Cytokines: Variations on a Common Theme. *Immunity*, 42(6), 991–1004.

Akiguchi, I., Tomimoto, H., Suenaga, T., Wakita, H. and Budka, H. (1997). Alterations in Glia and Axons in the Brains of Binswanger's Disease Patients. *Stroke*, 28(7), 1423–1429.

Alber, J., Alladi, S., Bae, H. J., Barton, D. A., Beckett, L. A., Bell, J. M., Berman, S. E., Biessels, G. J., Black, S. E., Bos, I., Bowman, G. L., Brai, E., Brickman, A. M., Callahan, B. L., Corriveau, R. A., Fossati, S., Gottesman, R. F., Gustafson, D. R., Hachinski, V., Hayden, K. M., Helman, A. M., Hughes, T. M., Isaacs, J. D., Jefferson, A. L., Johnson, S. C., Kapasi, A., Kern, S., Kwon, J. C., Kukolja, J., Lee, A., Lockhart, S. N., Murray, A., Osborn, K. E., Power, M. C., Price, B. R., Rhodius-Meester, H. F. M., Rondeau, J. A., Rosen, A. C., Rosene, D. L., Schneider, J. A., Scholtzova, H., Shaaban, C. E., Silva, N. C. B. S., Snyder, H. M., Swardfager, W., Troen, A. M., van Veluw, S. J., Vemuri, P., Wallin, A., Wellington, C., Wilcock, D. M., Xie, S. X. and Hainsworth, A. H. (2019). White matter hyperintensities in vascular contributions to cognitive impairment and dementia (VCID): Knowledge gaps and opportunities. *Alzheimer's and Dementia: Translational Research and Clinical Interventions*, (5) 107–117.

Albers, G. W., Marks, M. P., Kemp, S., Christensen, S., Tsai, J. P., Ortega-Gutierrez, S., McTaggart, R. A., Torbey, M. T., Kim-Tenser, M., Leslie-Mazwi, T., Sarraj, A., Kasner, S. E., Ansari, S. A., Yeatts, S. D., Hamilton, S., Mlynash, M., Heit, J. J., Zaharchuk, G., Kim, S., Carrozzella, J., Palesch, Y. Y., Demchuk, A. M., Bammer, R., Lavori, P. W., Broderick, J. P. and Lansberg, M. G. (2018). Thrombectomy for stroke at 6 to 16 hours with selection by perfusion imaging. *New England Journal of Medicine*, 378(8), 708–18.

Alonso, D. and Nungester, W. J. (1956). Comparative study of host resistance of guinea pigs and rats v. the effect of pneumococcal products on glycolysis and oxygen uptake by polymorphonuclear leucocytes. *Journal of Infectious Diseases*, 99(2), 174–181.

Alosco, M. L., Spitznagel, M. B., Raz, N., Cohen, R., Sweet, L. H., Colbert, L. H., Josephson, R., van Dulmen, M., Hughes, J., Rosneck, J. and Gunstad, J. (2012). Obesity Interacts with Cerebral Hypoperfusion to Exacerbate Cognitive Impairment in Older Adults with Heart Failure. *Cerebrovascular Diseases Extra*, 2(1), 88–98.

An, Y., Varma, V. R., Varma, S., Casanova, R., Dammer, E., Pletnikova, O., Chia, C. W., Egan, J. M., Ferrucci, L., Troncoso, J., Levey, A. I., Lah, J., Seyfried, N. T., Legido-Quigley, C., O'Brien, R. and Thambisetty, M. (2018). Evidence for brain glucose dysregulation in Alzheimer's disease. *Alzheimer's and Dementia*, 14(3), 318–329.

Andrieu, S., Guyonnet, S., Coley, N., Cantet, C., Bonnefoy, M., Bordes, S., Bories, L., Cufi, M. N., Dantoine, T., Dartigues, J. F., Desclaux, F., Gabelle, A., Gasnier, Y., Pesce, A., Sudres, K., Touchon, J., Robert, P., Rouaud, O., Legrand, P., Payoux, P., Caubere, J. P., Weiner, M., Carrié, I., Ousset, P. J. and Vellas, B. (2017). Effect of long-term omega 3 polyunsaturated fatty acid supplementation with or without multidomain intervention on cognitive function in elderly adults with memory complaints (MAPT): a randomised, placebo-controlled trial. *The Lancet Neurology*, 16(5), 377–389.

Appel, L. J., Frohlich, E. D., Hall, J. E., Pearson, T. A., Sacco, R. L., Seals, D. R., Sacks, F. M., Smith, S. C., Vafiadis, D. K. and Van Horn, L. V (2011). The importance of population-wide sodium reduction as a means to prevent cardiovascular disease and stroke: a call to action from the American Heart Association. *Circulation*, 123(10), 1138–43.

Appelros, P., Stegmayr, B. and Terent, A. (2009). Sex differences in stroke epidemiology: A systematic review. *Stroke*, 40(4), 1082–1090.

Arakawa, S., Wright, P. M., Koga, M., Phan, T. G., Reutens, D. C., Lim, I., Gunawan, M. R., Ma, H., Perera, N., Ly, J., Zavala, J., Fitt, G. and Donnan, G. A. (2006). Ischemic thresholds for gray and white matter: a diffusion and perfusion magnetic resonance study. *Stroke*, 37(5), 1211–6.

Arend, W. P., Malyak, M., Guthridge, C. J. and Gabay, C. (1998). Interleukin-1 receptor antagonist: Role in Biology. *Annual Review of Immunology*, 16(1), 27–55.

Arvanitakis, Z., Leurgans, S. E., Wang, Z., Wilson, R. S., Bennett, D. A. and Schneider, J. A. (2011). Cerebral amyloid angiopathy pathology and cognitive domains in older persons. *Annals of Neurology*, 69(2), 320–327.

Asaria, P., Chisholm, D., Mathers, C., Ezzati, M. and Beaglehole, R. (2007). Chronic disease prevention: health effects and financial costs of strategies to reduce salt intake and control tobacco use. *Lancet*, 370(9604), 2044–2053.

Baik, S. H., Kang, S., Lee, W., Choi, H., Chung, S. and Kim, J.-I. (2019). A Breakdown in Metabolic Reprogramming Causes Microglia Dysfunction in Alzheimer's Disease. *Cell Metabolism*, (30) 493–507.

Banerjee, G., Carare, R., Cordonnier, C., Greenberg, S. M., Schneider, J. A., Smith, E. E., Van Buchem, M., Van Der Grond, J., Verbeek, M. M. and Werring, D. J. (2017). The increasing impact of cerebral amyloid angiopathy: Essential new insights for clinical practice. *Journal of Neurology, Neurosurgery and Psychiatry*, 88(11), 982–994.

Banwell, V., Sena, E. S. and Macleod, M. R. (2009). Systematic Review and Stratified Meta-analysis of the Efficacy of Interleukin-1 Receptor Antagonist in Animal Models of Stroke. *Journal of Stroke and Cerebrovascular Diseases*, 18(4), 269–276.

Barrington, J., Lemarchand, E. and Allan, S. M. (2017). A brain in flame; do inflammasomes and pyroptosis influence stroke pathology? *Brain pathology*, 27(2), 205–212.

Bentzon, J. F., Otsuka, F., Virmani, R. and Falk, E. (2014). Mechanisms of plaque formation and rupture. *Circulation Research*, 114(12), 1852–1866.

Bergsbaken, T., Fink, S. L. and Cookson, B. T. (2009). Pyroptosis: Host cell death and inflammation. *Nature Reviews Microbiology*, 7(2), 99–109.

Best, J. G., Bell, R., Haque, M., Chandratheva, A. and Werring, D. J. (2019). Atrial fibrillation and stroke: A practical guide. *Practical Neurology*, 19(3), 208–224.

Blüher, M. (2019). Obesity: global epidemiology and pathogenesis. *Nature Reviews Endocrinology*, 15(5), 288–298.

Bodhankar, S., Chen, Y., Vandenbark, A. A., Murphy, S. J. and Offner, H. (2013). IL-10-producing B-cells limit CNS inflammation and infarct volume in experimental stroke. *Metabolic Brain Disease*, 28(3), 375–386.

Van den Bossche, J., O'Neill, L. A. and Menon, D. (2017). Macrophage Immunometabolism: Where Are We (Going)? *Trends in Immunology*, 38(6), 395–406.

Boutin, H., LeFeuvre, R. A., Horai, R., Asano, M., Iwakura, Y. and Rothwell, N. J. (2001). Role of IL-1α and IL-1β in ischemic brain damage. *Journal of Neuroscience*, 21(15), 5528–5534.

Boyden, E. D. and Dietrich, W. F. (2006). Nalp1b controls mouse macrophage susceptibility to anthrax lethal toxin. *Nature genetics*, 38(2), 240–4.

Briggs, A. D. M., Mytton, O. T., Kehlbacher, A., Tiffin, R., Rayner, M. and Scarborough, P. (2013). Overall and income specific effect on prevalence of overweight and obesity of 20% sugar sweetened drink tax in UK: Econometric and comparative risk assessment modelling study. *British Medical Journal*, 347(1), 6189.

Broughton, B. R. S., Reutens, D. C. and Sobey, C. G. (2009). Apoptotic mechanisms after cerebral ischemia. *Stroke*, 40(5), e331-9.

Buck, B. H., Liebeskind, D. S., Saver, J. L., Bang, O. Y., Yun, S. W., Starkman, S., Ali, L. K., Kim, D., Villablanca, J. P., Salamon, N., Razinia, T. and Ovbiagele, B. (2008). Early neutrophilia is associated with volume of ischemic tissue in acute stroke. *Stroke*, 39(2), 355–360.

Bürckstümmer, T., Baumann, C., Blüml, S., Dixit, E., Dürnberger, G., Jahn, H., Planyavsky, M., Bilban, M., Colinge, J., Bennett, K. L. and Superti-Furga, G. (2009). An orthogonal proteomic-genomic screen identifies AIM2 as a cytoplasmic DNA sensor for the inflammasome. *Nature Immunology*, 10(3), 266–272.

Cammer, W., Bloom, B. R., Norton, W. T. and Gordon, S. (1978). Degradation of basic protein in myelin by neutral proteases secreted by stimulated macrophages: A possible mechanism of inflammatory demyelination. *Proceedings of the National Academy of Sciences of the United States of America*, 75(3), 1554–1558.

Campbell, B. C. V., De Silva, D. A., Macleod, M. R., Coutts, S. B., Schwamm, L. H., Davis, S. M. and Donnan, G. A. (2019). Ischaemic stroke. *Nature Reviews Disease Primers*, 5(1), 1–22.

Carmo, M. R. S., Simões, A. P., Fonteles, A. A., Souza, C. M., Cunha, R. A. and Andrade, G. M. (2014). ATP P2Y1 receptors control cognitive deficits and neurotoxicity but not glial modifications induced by brain ischemia in mice. *European Journal of Neuroscience*, 39(4), 614–622.

Caslin, H. L., Taruselli, M. T., Haque, T., Pondicherry, N., Baldwin, E. A., Barnstein, B. O. and Ryan, J. J. (2018). Inhibiting Glycolysis and ATP Production Attenuates IL-33-Mediated Mast Cell Function and Peritonitis. *Frontiers in immunology*, 9(1), 3026.

Caso, J. R., Pradillo, J. M., Hurtado, O., Lorenzo, P., Moro, M. A. and Lizasoain, I. (2007). Toll-like receptor 4 is involved in brain damage and inflammation after experimental stroke. *Circulation*, 115(12), 1599–1608.

Castellano, J. M., Sanz, G., Peñalvo, J. L., Bansilal, S., Fernández-Ortiz, A., Alvarez, L., Guzmán, L., Linares, J. C., García, F., D'Aniello, F., Arnáiz, J. A., Varea, S., Martínez, F., Lorenzatti, A., Imaz, I., Sánchez-Gómez, L. M., Roncaglioni, M. C., Baviera, M., Smith, S. C., Taubert, K., Pocock, S., Brotons, C., Farko, M. E. and Fuster, V. (2014). A polypill strategy to improve adherence. *Journal of the American College of Cardiology*, 64(20), 2071–2082.

Chabriat, H., Pappata, S., Ostergaard, L., Clark, C. A., Pachot-Clouard, M., Vahedi, K., Jobert, A., Le Bihan, D. and Bousser, M. G. (2000). Cerebral hemodynamics in CADASIL before and after acetazolamide challenge assessed with MRI bolus tracking. *Stroke*, 31(8), 1904–1912.

Chamorro, Á., Meisel, A., Planas, A. M., Urra, X., van de Beek, D. and Veltkamp, R. (2012). The immunology of acute stroke. *Nature Reviews Neurology*, 8(7), 401–410.

Chan, K. Y., Wu, J. J., Liu, L., Theodoratou, E., Car, J., Middleton, L., Russ, T. C., Deary, I. J., Campbell, H., Wang, W. and Rudan, I. (2013). Epidemiology of alzheimer's disease and other forms of dementia in China, 1990-2010: A systematic review and analysis. *The Lancet*, 381(9882), 2016–2023.

Chandler, S., Coates, R., Gearing, A., Lury, J., Wells, G. and Bone, E. (1995). Matrix metalloproteinases degrade myelin basic protein. *Neuroscience letters*, 201(3), 223–6.

van Charante, E. P. M., Richard, E., Eurelings, L. S., van Dalen, J. W., Ligthart, S. A., van Bussel, E. F., Hoevenaar-Blom, M. P., Vermeulen, M. and van Gool, W. A. (2016). Effectiveness of a 6-year multidomain vascular care intervention to prevent dementia (preDIVA): a cluster-randomised controlled trial. *The Lancet*, 388(10046), 797–805.

Chow, J. C., Young, D. W., Golenbock, D. T., Christ, W. J. and Gusovsky, F. (1999). Toll-like Receptor-4 Mediates Lipopolysaccharide-induced Signal Transduction. *Journal of Biological Chemistry*, 274(16), 10689–10692.

Christ, A., Günther, P., Lauterbach, M. A. R., Duewell, P., Biswas, D., Pelka, K., Scholz, C. J., Oosting, M., Haendler, K., Baßler, K., Klee, K., Schulte-Schrepping, J., Ulas, T., Moorlag, S. J. C. F. M., Kumar, V., Park, M. H., Joosten, L. A. B., Groh, L. A., Riksen, N. P., Espevik, T., Schlitzer, A., Li, Y., Fitzgerald, M. L., Netea, M. G., Schultze, J. L. and Latz, E. (2018). Western Diet Triggers NLRP3-Dependent Innate Immune Reprogramming. *Cell*, 172(1–2), 162–175.

Chu, H. X., Broughton, B. R. S., Ah Kim, H., Lee, S., Drummond, G. R. and Sobey, C. G. (2015). Evidence That Ly6Chi Monocytes Are Protective in Acute Ischemic Stroke by Promoting M2 Macrophage Polarization. *Stroke*, 46(7), 1929–1937.

Chu, H. X., Kim, H. A., Lee, S., Moore, J. P., Chan, C. T., Vinh, A., Gelderblom, M., Arumugam, T. V., Broughton, B. R., Drummond, G. R. and Sobey, C. G. (2014). Immune cell infiltration in malignant middle cerebral artery infarction: Comparison with transient cerebral ischemia. *Journal of Cerebral Blood Flow & Metabolism*, 34(3), 450–459.

Ciacciarelli, A., Sette, G., Giubilei, F. and Orzi, F. (2020). Chronic cerebral hypoperfusion: An undefined, relevant entity. *Journal of Clinical Neuroscience*, 73(1), 8–12.

Claxton, A., Baker, L. D., Wilkinson, C. W., Trittschuh, E. H., Chapman, D., Watson, G. S., Cholerton, B., Plymate, S. R., Arbuckle, M. and Craft, S. (2013). Sex and ApoE genotype differences in treatment response to two doses of intranasal insulin in adults with mild cognitive impairment or alzheimer's disease. *Journal of Alzheimer's Disease*, 35(4), 789–797.

Cole, G. M., Ma, Q. L. and Frautschy, S. A. (2009). Omega-3 fatty acids and dementia. *Prostaglandins Leukotrienes and Essential Fatty Acids*, 81(3), 213–221.

Colotta, F., Re, F., Muzio, M., Bertini, R., Polentarutti, N., Sironi, M., Giri, J. G., Dower, S. K., Sims, J. E. and Mantovani, A. (1993). Interleukin-1 type II receptor: A decoy target for IL-1 that is regulated by IL-4. *Science*, 261(5120), 472–475.

Coltman, R., Spain, A., Tsenkina, Y., Fowler, J. H., Smith, J., Scullion, G., Allerhand, M., Scott, F., Kalaria, R. N., Ihara, M., Daumas, S., Deary, I. J., Wood, E., McCulloch, J. and Horsburgh, K. (2011). Selective white matter pathology induces a specific impairment in spatial working memory. *Neurobiology of Aging*, 32(12), 7–12.

Corcoran, S. E. and O'Neill, L. A. J. (2016). HIF1α and metabolic reprogramming in inflammation. *Journal of Clinical Investigation*, 126(10), 3699–3707.

Cordes, T., Wallace, M., Michelucci, A., Divakaruni, A. S., Sapcariu, S. C., Sousa, C., Koseki, H., Cabrales, P., Murphy, A. N., Hiller, K. and Metallo, C. M. (2016). Immunoresponsive gene 1 and itaconate inhibit succinate dehydrogenase to modulate intracellular succinate levels. *Journal of Biological Chemistry*, 291(27), 14274–14284.

Coutts, S. B. (2017). Diagnosis and Management of Transient Ischemic Attack. *CONTINUUM Lifelong Learning in Neurology*, 23(1), 82–92.

Coutts, S. B., Berge, E., Campbell, B. C. V., Muir, K. W. and Parsons, M. W. (2018). Tenecteplase for the treatment of acute ischemic stroke: A review of completed and ongoing randomized controlled trials. *International Journal of Stroke*, 13(9), 885–892.

Creager, M. A., Lüscher, T. F., Cosentino, F. and Beckman, J. A. (2003). Diabetes and Vascular Disease. Pathophysiology, Clinical Consequences, and Medical Therapy: Part I. *Circulation*, 108(12), 1527–1532.

Dalekos, G. N., Elisaf, M., Bairaktari, E., Tsolas, O. and Siamopoulos, K. C. (1997). Increased serum levels of interleukin-1beta in the systemic circulation of patients with essential hypertension: additional risk factor for atherogenesis in hypertensive patients? *The Journal of laboratory and clinical medicine*, 129(3), 300–8.

Van Dalen, J. W., Mutsaerts, H. J. M. M., Nederveen, A. J., Vrenken, H., Steenwijk, M. D., Caan, M. W. A., Majoie, C. B. L. M., Van Gool, W. A. and Richard, E. (2016). White matter hyperintensity volume and cerebral perfusion in older individuals with hypertension using arterial spin-labeling. *American Journal of Neuroradiology*, 37(10), 1824–1830.

Ten Dam, V. H., Van Den Heuvel, D. M. J., Van Buchem, M. A., Westendorp, R. G. J., Bollen, E. L. E. M., Ford, I., De Craen, A. J. M. and Blauw, G. J. (2005). Effect of pravastatin on cerebral infarcts and white matter lesions. *Neurology*, 64(10), 1807–1809.

DeFronzo, R. A., Ferrannini, E., Groop, L., Henry, R. R., Herman, W. H., Holst, J. J., Hu, F. B., Kahn, C. R., Raz, I., Shulman, G. I., Simonson, D. C., Testa, M. A. and Weiss, R. (2015). Type 2 diabetes mellitus. *Nature Reviews Disease Primers*, 1(1), 1–22.

Denes, A., Coutts, G., Lénárt, N., Cruickshank, S. M., Pelegrin, P., Skinner, J., Rothwell, N., Allan, S. M. and Brough, D. (2015). AIM2 and NLRC4 inflammasomes contribute with ASC to acute brain injury independently of NLRP3. *Proceedings of the National Academy of Sciences of the United States of America*, 112(13), 4050–4055.

Denes, A., Lopez-Castejon, G. and Brough, D. (2012). Caspase-1: is IL-1 just the tip of the ICEberg? *Cell death & disease*, 3(1), e338.

Dichgans, M. and Leys, D. (2017). Vascular Cognitive Impairment. *Circulation Research*, 120(3), 573–591.

Dinarello, C. A. (2009). Immunological and Inflammatory Functions of the Interleukin-1 Family. *Annual Review of Immunology*, 27(1), 519–550.

Dinarello, C. A. (2018). Overview of the IL-1 family in innate inflammation and acquired immunity. *Immunological Reviews*, 281(1), 8–27.

Dinarello, C. A., Ikejima, T., Warner, S. J., Orencole, S. F., Lonnemann, G., Cannon, J. G. and Libby, P. (1987). Interleukin 1 induces interleukin 1. I. Induction of circulating interleukin 1 in rabbits in vivo and in human mononuclear cells in vitro. *Journal of Immunology*, 139(6), 1902–10.

Ding, E. L. and Mozaffarian, D. (2006). Optimal Dietary Habits for the Prevention of Stroke. *Seminars in Neurology*, 26(1), 011–023.

Dirnagl, U., Iadecola, C. and Moskowitz, M. A. (1999). Pathobiology of ischaemic stroke: An integrated view. *Trends in Neurosciences*, 22(9), 391–397.

Dobbs, R., Sawers, C., Thompson, F., Manyika, J., Woetzel, J., Child, P., McKenna, S. and Spatharou, A. (2014). *How the world could better fight obesity*. [Online] [Accessed on 20th February 2020] https://www.mckinsey.com/industries/healthcare-systems-and-services/our-insights/how-the-world-could-better-fight-obesity.

Dodge, H. H., Buracchio, T. J., Fisher, G. G., Kiyohara, Y., Meguro, K., Tanizaki, Y. and Kaye, J. A. (2012). Trends in the prevalence of dementia in Japan. *International Journal of Alzheimer's Disease*, 2012(1), 956354.

Doehner, W., Schenkel, J., Anker, S. D., Springer, J. and Audebert, H. (2013). Overweight and obesity are associated with improved survival, functional outcome, and stroke recurrence after acute stroke or transient ischaemic attack: Observations from the tempis trial. *European Heart Journal*, 34(4), 268–277.

Donath, M. Y. (2014). Targeting inflammation in the treatment of type 2 diabetes: time to start. *Nature reviews. Drug discovery*, 13(6), 465–76.

Dörffel, Y., Lätsch, C., Stuhlmüller, B., Schreiber, S., Scholze, S., Burmester, G. R. and Scholze, J. (1999). Preactivated Peripheral Blood Monocytes in Patients With Essential Hypertension. *Hypertension*, 1(34), 113–117.

Doyle, A. G., Herbein, G., Montaner, L. J., Minty, A. J., Caput, D., Ferrara, P. and Gordon, S. (1994). Interleukin-13 alters the activation state of murine macrophages in vitro: Comparison with interleukin-4 and interferon-γ. *European Journal of Immunology*, 24(6), 1441–1445.

Doyle, K. P. and Buckwalter, M. S. (2017). Does B lymphocyte-mediated autoimmunity contribute to post-stroke dementia? *Brain, Behavior, and Immunity*, (64) 1–8.

Duering, M., Righart, R., Wollenweber, F. A., Zietemann, V., Gesierich, B. and Dichgans, M. (2015). Acute infarcts cause focal thinning in remote cortex via degeneration of connecting fiber tracts. *Neurology*, 84(16), 1685–1692.

Duewell, P., Kono, H., Rayner, K. J., Sirois, C. M., Vladimer, G., Bauernfeind, F. G., Abela, G. S., Franchi, L., Nuñez, G., Schnurr, M., Espevik, T., Lien, E., Fitzgerald, K. A., Rock, K. L., Moore, K. J., Wright, S. D., Hornung, V. and Latz, E. (2010). NLRP3 inflammasomes are required for atherogenesis and activated by cholesterol crystals. *Nature*, 464(7293), 1357–1361.

Dufouil, C., Chalmers, J., Coskun, O., Besançon, V., Bousser, M.-G., Guillon, P., MacMahon, S., Mazoyer, B., Neal, B., Woodward, M., Tzourio-Mazoyer, N., Tzourio, C. and PROGRESS MRI Substudy Investigators (2005). Effects of blood pressure lowering on cerebral white matter hyperintensities in patients with stroke: the PROGRESS (Perindopril Protection Against Recurrent Stroke Study) Magnetic Resonance Imaging Substudy. *Circulation*, 112(11), 1644–50.

Ebinger, M., Winter, B., Wendt, M., Weber, J. E., Waldschmidt, C., Rozanski, M., Kunz, A., Koch, P., Kellner, P. A., Gierhake, D., Villringer, K., Fiebach, J. B., Grittner, U., Hartmann, A., Mackert, B. M., Endres, M. and Audebert, H. J. (2014). Effect of the use of ambulance-based thrombolysis on time to thrombolysis in acute ischemic stroke: A randomized clinical trial. *JAMA - Journal of the American Medical Association*, 311(16), 1622–1631.

Eltzschig, H. K. and Eckle, T. (2011). Ischemia and reperfusion-from mechanism to translation. *Nature Medicine*, 17(11), 1391–1401.

Emberson, J., Lees, K. R., Lyden, P., Blackwell, L., Albers, G., Bluhmki, E., Brott, T., Cohen, G., Davis, S., Donnan, G., Grotta, J., Howard, G., Kaste, M., Koga, M., Von Kummer, R., Lansberg, M., Lindley, R. I., Murray, G., Olivot, J. M., Parsons, M., Tilley, B., Toni, D., Toyoda, K., Wahlgren, N., Wardlaw, J., Whiteley, W., Del Zoppo, G. J., Baigent, C., Sandercock, P. and Hacke, W. (2014). Effect of treatment delay, age, and stroke severity on the effects of intravenous thrombolysis with alteplase for acute ischaemic stroke: A meta-analysis of individual patient data from randomised trials. *The Lancet*, 384(9958), 1929–1935.

Emsley, H. C. A., Smith, C. J., Georgiou, R. F., Vail, A., Hopkins, S. J., Rothwell, N. J. and Tyrrell, P. J. (2005). A randomised phase II study of interleukin-1 receptor antagonist in acute stroke patients. *Journal of Neurology, Neurosurgery and Psychiatry*, 76(10), 1366–1372.

Engelhardt, B. and Sorokin, L. (2009). The blood-brain and the blood-cerebrospinal fluid barriers: Function and dysfunction. *Seminars in Immunopathology*, 31(4), 497–511.

Faraco, G., Brea, D., Garcia-Bonilla, L., Wang, G., Racchumi, G., Chang, H., Buendia, I., Santisteban, M. M., Segarra, S. G., Koizumi, K., Sugiyama, Y., Murphy, M., Voss, H., Anrather, J. and Iadecola, C. (2018). Dietary salt promotes neurovascular and cognitive dysfunction through a gut-initiated TH17 response. *Nature Neuroscience*, 21(2), 240–249.

Faraco, G., Hochrainer, K., Segarra, S. G., Schaeffer, S., Santisteban, M. M., Menon, A., Jiang, H., Holtzman, D. M., Anrather, J. and Iadecola, C. (2019). Dietary salt promotes cognitive impairment through tau phosphorylation. *Nature*, 574(7780), 686–690.

Farkas, E., Donka, G., de Vos, R. A. I., Mihály, A., Bari, F. and Luiten, P. G. M. (2004). Experimental cerebral hypoperfusion induces white matter injury and microglial activation in the rat brain. *Acta Neuropathologica*, 108(1), 57–64.

Farkas, E., Luiten, P. G. M. and Bari, F. (2007). Permanent, bilateral common carotid artery occlusion in the rat: A model for chronic cerebral hypoperfusion-related neurodegenerative diseases. *Brain Research Reviews*, 54(1), 162–180.

Farrall, A. J. and Wardlaw, J. M. (2009). Blood-brain barrier: Ageing and microvascular disease - systematic review and meta-analysis. *Neurobiology of Aging*, 30(3), 337–352.

Fearon, W. F. and Fearon, D. T. (2008). Inflammation and Cardiovascular Disease. *Circulation*, 117(20), 2577–2579.

Feigin, V. L. and Krishnamurthi, R. (2016). Stroke is largely preventable across the globe: where to next? *The Lancet*, 388(10046), 733–734.

Feng, Q., Fan, S., Wu, Y., Zhou, D., Zhao, R., Liu, M. and Song, Y. (2018). Adherence to the dietary approaches to stop hypertension diet and risk of stroke: A meta-analysis of prospective studies. *Medicine*, 97(38), e12450.

Fernandes-Alnemri, T., Wu, J., Yu, J.-W., Datta, P., Miller, B., Jankowski, W., Rosenberg, S., Zhang, J. and Alnemri, E. S. (2007). The pyroptosome: a supramolecular assembly of ASC dimers mediating inflammatory cell death via caspase-1 activation. *Cell death and differentiation*, 14(9), 1590–604.

Fernando, M. S., Simpson, J. E., Matthews, F., Brayne, C., Lewis, C. E., Barber, R., Kalaria, R. N., Forster, G., Esteves, F., Wharton, S. B., Shaw, P. J., O'Brien, J. T., Ince, P. G. and MRC Cognitive Function and Ageing Neuropathology Study Group (2006). White Matter Lesions in an Unselected Cohort of the Elderly: Molecular Pathology Suggests Origin From Chronic Hypoperfusion Injury. *Stroke*, 37(6), 1391–1398.

Feuerstein, G. Z. and Chavez, J. (2009). Translational medicine for stroke drug discovery the pharmaceutical industry perspective. *Stroke*, 40(3), 121–5.

Fisher, C. M. (1982). Lacunar strokes and infarcts: A review. *Neurology*, 32(8), 871–876.

Freeman, L. C. and Ting, J. P. Y. (2016). The pathogenic role of the inflammasome in neurodegenerative diseases. *Journal of Neurochemistry*, 136(1), 29–38.

Freemerman, A. J., Johnson, A. R., Sacks, G. N., Milner, J. J., Kirk, E. L., Troester, M. A., Macintyre, A. N., Goraksha-Hicks, P., Rathmell, J. C. and Makowski, L. (2014). Metabolic reprogramming of macrophages: Glucose transporter 1 (GLUT1)-mediated glucose metabolism drives a proinflammatory phenotype. *Journal of Biological Chemistry*, 289(11), 7884–7896.

Frondelius, K., Borg, M., Ericson, U., Borné, Y., Melander, O. and Sonestedt, E. (2017). Lifestyle and dietary determinants of serum apolipoprotein A1 and apolipoprotein B concentrations: Cross-sectional analyses within a Swedish Cohort of 24,984 individuals. *Nutrients*, 9(3), 211.

Fukatsu, T., Miyake-Takagi, K., Nagakura, A., Omino, K., Okuyama, N., Ando, T., Takagi, N., Furuya, Y. and Takeo, S. (2002). Effects of nefiracetam on spatial memory function and acetylcholine and GABA metabolism in microsphere-embolized rats. *European Journal of Pharmacology*, 453(1), 59–67.

Fukutake, T. (2011). Cerebral autosomal recessive arteriopathy with subcortical infarcts and leukoencephalopathy (CARASIL): From discovery to gene identification. *Journal of Stroke and Cerebrovascular Diseases*, 20(2), 85–93.

Furman, D., Chang, J., Lartigue, L., Bolen, C. R., Haddad, F., Gaudilliere, B., Ganio, E. A., Gabriela K Fragiadakis, M. H. S., Douchet, I., Daburon, S., Moreau, J.-F., Nolan, G. P., Blanco, P., Déchanet-Merville, J., Dekker, C. L., Jojic, V., Kuo, C. J., Davis, M. M. and Faustin, B. (2017). Expression of specific inflammasome gene modules stratifies older individuals into two extreme clinical and immunological states. *Nature Medicine*, 23(2), 174–184.

Garcia, J. H., Liu, K. F. and Relton, J. K. (1995). Interleukin-1 receptor antagonist decreases the number of necrotic neurons in rats with middle cerebral artery occlusion. *American Journal of Pathology*, 147(5), 1477–1486.

Garlanda, C., Dinarello, C. A. and Mantovani, A. (2013). The Interleukin-1 Family: Back to the Future. *Immunity*, 39(6), 1003–1018.

GBD 2016 Stroke Collaborators (2016). Global and regional effects of potentially modifiable risk factors associated with acute stroke in 32 countries (INTERSTROKE): a case-control study. *The Lancet*, 388(10046), 761–775.

GBD 2016 Stroke Collaborators (2019). Global, regional, and national burden of stroke, 1990–2016: a systematic analysis for the Global Burden of Disease Study 2016. *The Lancet Neurology*, 18(5), 439–458.

Gimeno-Bayón, J., López-López, A., Rodríguez, M. J. and Mahy, N. (2014). Glucose pathways adaptation supports acquisition of activated microglia phenotype. *Journal of Neuroscience Research*, 92(6), 723–731.

Goldberg, E. L. and Dixit, V. D. (2015). Drivers of age-related inflammation and strategies for healthspan extension. *Immunological Reviews*, 265(1), 63–74.

Gordon, S., Plüddemann, A. and Martinez Estrada, F. (2014). Macrophage heterogeneity in tissues: Phenotypic diversity and functions. *Immunological Reviews*, 262(1), 36–55.

Goyal, M., Menon, B. K., Van Zwam, W. H., Dippel, D. W. J., Mitchell, P. J., Demchuk, A. M., Dávalos, A., Majoie, C. B. L. M., Van Der Lugt, A., De Miquel, M. A., Donnan, G. A., Roos, Y. B. W. E. M., Bonafe, A., Jahan, R., Diener, H. C., Van Den Berg, L. A., Levy, E. I., Berkhemer, O. A., Pereira, V. M., Rempel, J., Millán, M., Davis, S. M., Roy, D., Thornton, J., Román, L. S., Ribó, M., Beumer, D., Stouch, B., Brown, S., Campbell, B. C. V., Van Oostenbrugge, R. J., Saver, J. L., Hill, M. D. and Jovin, T. G. (2016). Endovascular thrombectomy after large-vessel ischaemic stroke: A meta-analysis of individual patient data from five randomised trials. *The Lancet*, 387(10029), 1723–1731.

Hainsworth, A. H., Minett, T., Andoh, J., Forster, G., Bhide, I., Barrick, T. R., Elderfield, K., Jeevahan, J., Markus, H. S. and Bridges, L. R. (2017). Neuropathology of white matter lesions, blood-brain barrier dysfunction, and dementia. *Stroke*, 48(10), 2799–2804.

Haley, M. J., Krishnan, S., Burrows, D., de Hoog, L., Thakrar, J., Schiessl, I., Allan, S. M. and Lawrence, C. B. (2019). Acute high-fat feeding leads to disruptions in glucose homeostasis and worsens stroke outcome. *Journal of Cerebral Blood Flow and Metabolism*, 39(6), 1026–1037.

Hamilton, J. A., Vairo, G. and Lingelbach, S. R. (1986). CSF-1 stimulates glucose uptake in murine bone marrow-derived macrophages. *Biochemical and Biophysical Research Communications*, 138(1), 445–454.

Hara, H., Friedlander, R. M., Gagliardini, V., Ayata, C., Fink, K., Huang, Z., Shimizu-Sasamata, M., Yuan, J. and Moskowitz, M. A. (1997). Inhibition of interleukin 1β converting enzyme family proteases reduces ischemic and excitotoxic neuronal damage. *Proceedings of the National Academy of Sciences of the United States of America*, 94(5), 2007–2012.

Hattori, Y., Enmi, J., Iguchi, S., Saito, S., Yamamoto, Y., Tsuji, M., Nagatsuka, K., Kalaria, R. N., Iida, H. and Ihara, M. (2016). Gradual Carotid Artery Stenosis in Mice Closely Replicates Hypoperfusive Vascular Dementia in Humans. *Journal of the American Heart Association*, 5(2), e002757.

Hattori, Y., Enmi, J., Kitamura, A., Yamamoto, Y., Saito, S., Takahashi, Y., Iguchi, S., Tsuji, M., Yamahara, K., Nagatsuka, K., Iida, H. and Ihara, M. (2015). A novel mouse model of subcortical infarcts with dementia. *The Journal of Neuroscience*, 35(9), 3915–3928.

Hattori, Y., Kitamura, A., Nagatsuka, K. and Ihara, M. (2014). A Novel Mouse Model of Ischemic Carotid Artery Disease. *PLoS ONE*, 9(6), e100257.

Hayes, J. D. and Dinkova-Kostova, A. T. (2014). The Nrf2 regulatory network provides an interface between redox and intermediary metabolism. *Trends in Biochemical Sciences*, 39(4), 199–218.

He, F. J. and MacGregor, G. A. (2002). Effect of modest salt reduction on blood pressure: A meta-analysis of randomized trials. Implications for public health. *Journal of Human Hypertension*, 16(11), 761–770.

Heneka, M. T., Carson, M. J., Khoury, J. El, Landreth, G. E., Brosseron, F., Feinstein, D. L., Jacobs, A. H., Wyss-Coray, T., Vitorica, J., Ransohoff, R. M., Herrup, K., Frautschy, S. A., Finsen, B., Brown, G. C., Verkhratsky, A., Yamanaka, K., Koistinaho, J., Latz, E., Halle, A., Petzold, G. C., Town, T., Morgan, D., Shinohara, M. L., Perry, V. H., Holmes, C., Bazan, N. G., Brooks, D. J., Hunot, S., Joseph, B., Deigendesch, N., Garaschuk, O., Boddeke, E., Dinarello, C. A., Breitner, J. C., Cole, G. M., Golenbock, D. T. and Kummer, M. P. (2015). Neuroinflammation in Alzheimer's disease. *The Lancet Neurology*, 14(4), 388–405.

Heneka, M. T., Kummer, M. P. and Latz, E. (2014). Innate immune activation in neurodegenerative disease. *Nature Reviews Immunology*, 14(7), 463.

Heneka, M. T., Kummer, M. P., Stutz, A., Delekate, A., Schwartz, S., Vieira-Saecker, A., Griep, A., Axt, D., Remus, A., Tzeng, T.-C., Gelpi, E., Halle, A., Korte, M., Latz, E. and Golenbock, D. T. (2013). NLRP3 is activated in Alzheimer's disease and contributes to pathology in APP/PS1 mice. *Nature*, 493(7434), 674–8.

Hewitt, J., Castilla Guerra, L., Fernández-Moreno, M. D. C. and Sierra, C. (2012). Diabetes and stroke prevention: A review. *Stroke Research and Treatment*, 2012(1), 673187.

Heye, A. K., Thrippleton, M. J., Chappell, F. M., Valdés Hernández, M. del C., Armitage, P. A., Makin, S. D., Maniega, S. M., Sakka, E., Flatman, P. W., Dennis, M. S. and Wardlaw, J. M. (2016). Blood pressure and sodium: association with MRI markers in cerebral small vessel disease. *Journal of Cerebral Blood Flow & Metabolism*, 36(1), 264–74.

Holland, P. R., Searcy, J. L., Salvadores, N., Scullion, G., Chen, G., Lawson, G., Scott, F., Bastin, M. E., Ihara, M., Kalaria, R., Wood, E. R., Smith, C., Wardlaw, J. M. and Horsburgh, K. (2015). Gliovascular disruption and cognitive deficits in a mouse model with features of small vessel disease. *Journal of Cerebral Blood Flow & Metabolism*, 35(10), 1005–1014.

Holland, R., McIntosh, A. L., Finucane, O. M., Mela, V., Rubio-Araiz, A., Timmons, G., McCarthy, S. A., Gun'ko, Y. K. and Lynch, M. A. (2018). Inflammatory microglia are glycolytic and iron retentive and typify the microglia in APP/PS1 mice. *Brain, Behavior, and Immunity*, (68) 183–196.

Holmstedt, C. A., Turan, T. N. and Chimowitz, M. I. (2013). Atherosclerotic intracranial arterial stenosis: Risk factors, diagnosis, and treatment. *The Lancet Neurology*, 12(11), 1106–1114.

Horecký, J., Bačiak, L., Kašparová, S., Pacheco, G., Aliev, G. and Vančová, O. (2009). Minimally invasive surgical approach for three-vessel occlusion as a model of vascular dementia in the rat-brain bioenergetics assay. *Journal of the Neurological Sciences*, 283(1–2), 178–181.

Hou, X., Liang, X., Chen, J.-F. and Zheng, J. (2015). Ecto-5′-nucleotidase (CD73) is involved in chronic cerebral hypoperfusion-induced white matter lesions and cognitive impairment by regulating glial cell activation and pro-inflammatory cytokines. *Neuroscience*, 297(1), 118–126.

Huang, S. C. C., Everts, B., Ivanova, Y., O'Sullivan, D., Nascimento, M., Smith, A. M., Beatty, W., Love-Gregory, L., Lam, W. Y., O'Neill, C. M., Yan, C., Du, H., Abumrad, N. A., Urban, J. F., Artyomov, M. N., Pearce, E. L. and Pearce, E. J. (2014). Cell-intrinsic lysosomal lipolysis is essential for alternative activation of macrophages. *Nature Immunology*, 15(9), 846–855.

Huisa, B. N., Caprihan, A., Thompson, J., Prestopnik, J., Qualls, C. R. and Rosenberg, G. A. (2015). Long-Term Blood-Brain Barrier Permeability Changes in Binswanger Disease. *Stroke*, 46(9), 2413–2418.

Iadecola, C. and Anrather, J. (2011). The immunology of stroke: From mechanisms to translation. *Nature Medicine*, 17(7), 796–808.

Ihara, M. and Tomimoto, H. (2011). Lessons from a Mouse Model Characterizing Features of Vascular Cognitive Impairment with White Matter Changes. *Journal of Aging Research*, 2011(1), 978761.

Ihara, M. and Yamamoto, Y. (2016). Emerging Evidence for Pathogenesis of Sporadic Cerebral Small Vessel Disease. *Stroke*, 47(2), 554–60.

Infantino, V., Convertini, P., Cucci, L., Panaro, M. A., Di Noia, M. A., Calvello, R., Palmieri, F. and Iacobazzi, V. (2011). The mitochondrial citrate carrier: A new player in inflammation. *Biochemical Journal*, 438(3), 433–436.

Ismael, S., Zhao, L., Nasoohi, S. and Ishrat, T. (2018). Inhibition of the NLRP3-inflammasome as a potential approach for neuroprotection after stroke. *Scientific Reports*, 8(1), 1–9.

IST-3 collaborative group (2015). Association between brain imaging signs, early and late outcomes, and response to intravenous alteplase after acute ischaemic stroke in the third International Stroke Trial (IST-3): secondary analysis of a randomised controlled trial. *The Lancet Neurology*, 14(5), 485–496.

Jha, A. K., Huang, S. C. C., Sergushichev, A., Lampropoulou, V., Ivanova, Y., Loginicheva, E., Chmielewski, K., Stewart, K. M., Ashall, J., Everts, B., Pearce, E. J., Driggers, E. M. and Artyomov, M. N. (2015). Network integration of parallel metabolic and transcriptional data reveals metabolic modules that regulate macrophage polarization. *Immunity*, 42(3), 419–430.

Jiang, H., Shi, H., Sun, M., Wang, Y., Meng, Q., Guo, P., Cao, Y., Chen, J., Gao, X., Li, E. and Liu, J. (2016). PFKFB3-Driven Macrophage Glycolytic Metabolism Is a Crucial Component of Innate Antiviral Defense. *The Journal of Immunology*, 197(7), 2880–2890.

Jickling, G. C., Liu, D., Ander, B. P., Stamova, B., Zhan, X. and Sharp, F. R. (2015). Targeting neutrophils in ischemic stroke: translational insights from experimental studies. *Journal of Cerebral Bood Flow & Metabolism*, 35(6), 888–901.

Jiwa, N. S., Garrard, P. and Hainsworth, A. H. (2010). Experimental models of vascular dementia and vascular cognitive impairment: A systematic review. *Journal of Neurochemistry*, 115(4), 814–828.

De Jong, G. I., Farkas, E., Stienstra, C. M., Plass, J. R. M., Keijser, J. N., De La Torre, J. C. and Luiten, P. G. M. (1999). Cerebral hypoperfusion yields capillary damage in the hippocampal CA1 area that correlates with spatial memory impairment. *Neuroscience*, 91(1), 203–210.

Joutel, A. and Chabriat, H. (2017). Pathogenesis of white matter changes in cerebral small vessel diseases: Beyond vessel-intrinsic mechanisms. *Clinical Science*, 131(8), 635–651.

Joutel, A., Corpechot, C., Ducros, A., Vahedi, K., Chabriat, H., Mouton, P., Alamowitch, S., Domenga, V., Cécillion, M., Marechal, E., Maciazek, J., Vayssiere, C., Cruaud, C., Cabanis, E. A., Ruchoux, M. M., Weissenbach, J., Bach, J. F., Bousser, M. G. and Tournier-Lasserve, E. (1996). Notch3 mutations in CADASIL, a hereditary adult-onset condition causing stroke and dementia. *Nature*, 383(6602), 707–710.

Kamel, H., Okin, P. M., Elkind, M. S. V. and Iadecola, C. (2016). Atrial Fibrillation and Mechanisms of Stroke. *Stroke*, 47(3), 895–900.

Karatas, H., Erdener, S. E., Gursoy-Ozdemir, Y., Gurer, G., Soylemezoglu, F., Dunn, A. K. and Dalkara, T. (2011). Thrombotic distal middle cerebral artery occlusion produced by topical FeCl3 application: A novel model suitable for intravital microscopy and thrombolysis studies. *Journal of Cerebral Blood Flow & Metabolism*, 31(6), 1452–1460.

Khare, S., Dorfleutner, A., Bryan, N. B., Yun, C., Radian, A. D., de Almeida, L., Rojanasakul, Y. and Stehlik, C. (2012). An NLRP7-containing inflammasome mediates recognition of microbial lipopeptides in human macrophages. *Immunity*, 36(3), 464–76.

Kim, B., Lee, Y., Kim, E., Kwak, A., Ryoo, S., Bae, S. H., Azam, T., Kim, S. and Dinarello, C. A. (2013). The interleukin-1α precursor is biologically active and is likely a key alarmin in the IL-1 family of cytokines. *Frontiers in Immunology*, 4(391), 1–9.

Kim, J. S., Kim, Y.-J., Ahn, S.-H. and Kim, B. J. (2018). Location of cerebral atherosclerosis: Why is there a difference between East and West? *International Journal of Stroke*, 13(1), 35–46.

Kitamura, A., Fujita, Y., Oishi, N., Kalaria, R. N., Washida, K., Maki, T., Okamoto, Y., Hase, Y., Yamada, M., Takahashi, J., Ito, H., Tomimoto, H., Fukuyama, H., Takahashi, R. and Ihara, M. (2012). Selective white matter abnormalities in a novel rat model of vascular dementia. *Neurobiology of Aging*, 33(5), e25-35.

Kitamura, A., Saito, S., Maki, T., Oishi, N., Ayaki, T., Hattori, Y., Yamamoto, Y., Urushitani, M., Kalaria, R. N., Fukuyama, H., Horsburgh, K., Takahashi, R. and Ihara, M. (2016). Gradual cerebral hypoperfusion in spontaneously hypertensive rats induces slowly evolving white matter abnormalities and impairs working memory. *Journal of Cerebral Blood Flow & Metabolism*, 36(9), 1592–1602.

Kivimäki, M., Luukkonen, R., Batty, G. D., Ferrie, J. E., Pentti, J., Nyberg, S. T., Shipley, M. J., Alfredsson, L., Fransson, E. I., Goldberg, M., Knutsson, A., Koskenvuo, M., Kuosma, E., Nordin, M., Suominen, S. B., Theorell, T., Vuoksimaa, E., Westerholm, P., Westerlund, H., Zins, M., Kivipelto, M., Vahtera, J., Kaprio, J., Singh-Manoux, A. and Jokela, M. (2018). Body mass index and risk of dementia: Analysis of individual-level data from 1.3 million individuals. *Alzheimer's and Dementia*, 14(5), 601–609.

Kivipelto, M., Mangialasche, F. and Ngandu, T. (2018). World Wide Fingers will advance dementia prevention. *The Lancet Neurology*, 17(1), 27.

Knight, E. M., Martins, I. V. A. A., Gümüsgöz, S., Allan, S. M. and Lawrence, C. B. (2014). High-fat diet-induced memory impairment in triple-transgenic Alzheimer's disease (3xTgAD) mice isindependent of changes in amyloid and tau pathology. *Neurobiology of Aging*, 35(8), 1821–1832.

Kobayashi, E. H., Suzuki, T., Funayama, R., Nagashima, T., Hayashi, M., Sekine, H., Tanaka, N., Moriguchi, T., Motohashi, H., Nakayama, K. and Yamamoto, M. (2016). Nrf2 suppresses macrophage inflammatory response by blocking proinflammatory cytokine transcription. *Nature Communications*, 7(1), 1–14.

Koizumi, J., Yoshida, Y., Nakazawa, T. and Ooneda, G. (1986). Experimental studies of ischemic brain edema. *Nosotchu*, 8(1), 1–8.

Kolodny, E., Fellgiebel, A., Hilz, M. J., Sims, K., Caruso, P., Phan, T. G., Politei, J., Manara, R. and Burlina, A. (2015). Cerebrovascular involvement in fabry disease: Current status of knowledge. *Stroke*, 46(1), 302–313.

Kostura, M. J., Tocci, M. J., Limjuco, G., Chin, J., Cameron, P., Hillman, A. G., Chartrain, N. A. and Schmidt, J. A. (1989). Identification of a monocyte specific pre-interleukin 1β convertase activity. *Proceedings of the National Academy of Sciences of the United States of America*, 86(14), 5227–5231.

Kruyt, N. D., Biessels, G. J., Devries, J. H. and Roos, Y. B. (2010). Hyperglycemia in acute ischemic stroke: Pathophysiology and clinical management. *Nature Reviews Neurology*, 6(3), 145–155.

Kuehn, B. M. (2019). In Alzheimer Research, Glucose Metabolism Moves to Center Stage. *JAMA - Journal of the American Medical Association*, 323(4), 297–299.

Kuida, K., Lippke, J. A., Ku, G., Harding, M. W., Livingston, D. J., Su, M. S. S. and Flavell, R. A. (1995). Altered cytokine export and apoptosis in mice deficient in interleukin-1β converting enzyme. *Science*, 267(5206), 2000–2003.

Kunnas, T., Määttä, K. and Nikkari, S. T. (2015). NLR family pyrin domain containing 3 (NLRP3) inflammasome gene polymorphism rs7512998 (C>T) predicts aging-related increase of blood pressure, the TAMRISK study. *Immunity & Ageing*, 12(19), 1–5.

De La Torre, J. C. and Fortin, T. (1994). A chronic physiological rat model of dementia. *Behavioural Brain Research*, 63(1), 35–40.

Labat-gest, V. and Tomasi, S. (2013). Photothrombotic ischemia: a minimally invasive and reproducible photochemical cortical lesion model for mouse stroke studies. *Journal of Visualized Experiments*, 76(1), 50370.

Lamkanfi, M. and Dixit, V. M. M. (2014). Mechanisms and Functions of Inflammasome. *Cell*, 157(5), 1013–1022.

Lampropoulou, V., Sergushichev, A., Bambouskova, M., Nair, S., Vincent, E. E., Loginicheva, E., Cervantes-Barragan, L., Ma, X., Huang, S. C. C., Griss, T., Weinheimer, C. J., Khader, S., Randolph, G. J., Pearce, E. J., Jones, R. G., Diwan, A., Diamond, M. S. and Artyomov, M. N. (2016). Itaconate Links Inhibition of Succinate Dehydrogenase with Macrophage Metabolic Remodeling and Regulation of Inflammation. *Cell Metabolism*, 24(1), 158–166.

Lanfranconi, S. and Markus, H. S. (2010). COL4A1 mutations as a monogenic cause of cerebral small vessel disease: a systematic review. *Stroke*, 41(8), e513-8.

Langhorne, P. (1997). Collaborative systematic review of the randomised trials of organised inpatient (stroke unit) care after stroke. *British Medical Journal*, 314(7088), 1151–1159.

Latz, E., Xiao, T. S. and Stutz, A. (2013). Activation and regulation of the inflammasomes. *Nature Reviews Immunology*, 13(6), 397–411.

Lehnardt, S., Lehmann, S., Kaul, D., Tschimmel, K., Hoffmann, O., Cho, S., Krueger, C., Nitsch, R., Meisel, A. and Weber, J. R. (2007). Toll-like receptor 2 mediates CNS injury in focal cerebral ischemia. *Journal of Neuroimmunology*, 190(1), 28–33.

Van Leijsen, E. M. C., Bergkamp, M. I., Van Uden, I. W. M., Ghafoorian, M., Van Der Holst, H. M., Norris, D. G., Platel, B., Tuladhar, A. M. and De Leeuw, F. E. (2018). Progression of white matter hyperintensities preceded by heterogeneous decline of microstructural integrity. *Stroke*, 49(6), 1386–1393.

Lemarchand, E., Barrington, J., Chenery, A., Haley, M., Coutts, G., Allen, J. E., Allan, S. M. and Brough, D. (2019). Extent of Ischemic Brain Injury After Thrombotic Stroke Is Independent of the NLRP3 (NACHT, LRR and PYD Domains-Containing Protein 3) Inflammasome. *Stroke*, 50(5), 1232–1239.

Lénárt, N., Brough, D. and Dénes, Á. (2016). Inflammasomes link vascular disease with neuroinflammation and brain disorders. *Journal of Cerebral Blood Flow & Metabolism*, 36(10), 1668–1685.

Ley, S. H., Hamdy, O., Mohan, V. and Hu, F. B. (2014). Prevention and management of type 2 diabetes: Dietary components and nutritional strategies. *The Lancet*, 383(9933), 1999–2007.

Li, P., Allen, H., Banerjee, S., Franklin, S., Herzog, L., Johnston, C., McDowell, J., Paskind, M., Rodman, L., Salfeld, J., Towne, E., Tracey, D., Wardwell, S., Wei, F. Y., Wong, W., Kamen, R. and Seshadri, T. (1995). Mice deficient in IL-1β-converting enzyme are defective in production of mature IL-1β and resistant to endotoxic shock. *Cell*, 80(3), 401–411.

Libermann, T. A. and Baltimore, D. (1990). Activation of interleukin-6 gene expression through the NF-kappa B transcription factor. *Molecular and Cellular Biology*, 10(5), 2327–2334.

Liesz, A., Suri-Payer, E., Veltkamp, C., Doerr, H., Sommer, C., Rivest, S., Giese, T. and Veltkamp, R. (2009). Regulatory T cells are key cerebroprotective immunomodulators in acute experimental stroke. *Nature Medicine*, 15(2), 192–199.

Lipton, P. (1999). Ischemic cell death in brain neurons. *Physiological Reviews*, 79(4), 1431–1568.

Liu, L. and Chan, C. (2014). IPAF inflammasome is involved in interleukin-1β production from astrocytes, induced by palmitate; implications for Alzheimer's Disease. *Neurobiology of aging*, 35(2), 309–21.

Liu, X., Nemeth, D. P., McKim, D. B., Zhu, L., DiSabato, D. J., Berdysz, O., Gorantla, G., Oliver, B., Witcher, K. G., Wang, Y., Negray, C. E., Vegesna, R. S., Sheridan, J. F., Godbout, J. P., Robson, M. J., Blakely, R. D., Popovich, P. G., Bilbo, S. D. and Quan, N. (2019). Cell-Type-Specific Interleukin 1 Receptor 1 Signaling in the Brain Regulates Distinct Neuroimmune Activities. *Immunity*, 50(2), 317–333.

Livingston, G., Sommerlad, A., Orgeta, V., Costafreda, S. G., Huntley, J., Ames, D., Ballard, C., Banerjee, S., Burns, A., Cohen-Mansfield, J., Cooper, C., Fox, N., Gitlin, L. N., Howard, R., Kales, H. C., Larson, E. B., Ritchie, K., Rockwood, K., Sampson, E. L., Samus, Q., Schneider, L. S., Selbæk, G., Teri, L. and Mukadam, N. (2017). Dementia prevention, intervention, and care. *The Lancet*, 390(10113), 2673–2734.

Llovera, G., Roth, S., Plesnila, N., Veltkamp, R. and Liesz, A. (2014). Modeling stroke in mice: Permanent coagulation of the distal middle cerebral artery. *Journal of Visualized Experiments*, 89(1), e51729.

Loddick, S. A. and Rothwell, N. J. (1996). Neuroprotective effects of human recombinant interleukin-1 receptor antagonist in focal cerebral ischaemia in the rat. *Journal of Cerebral Blood Flow & Metabolism*, 16(5), 932–40.

Loef, M. and Walach, H. (2013). Midlife obesity and dementia: Meta-analysis and adjusted forecast of dementia prevalence in the United States and China. *Obesity*, 21(1), E51-5.

Longa, E. Z., Weinstein, P. R., Carlson, S. and Cummins, R. (1989). Reversible middle cerebral artery occlusion without craniectomy in rats. *Stroke*, 20(1), 84–91.

Lopez-Castejon, G. and Brough, D. (2011). Understanding the mechanism of IL-1β secretion. *Cytokine & growth factor reviews*, 22(4), 189–95.

Low, A., Mak, E., Rowe, J. B., Markus, H. S. and O'Brien, J. T. (2019). Inflammation and cerebral small vessel disease: A systematic review. *Ageing Research Reviews*, 53(100916), 1–28.

Lynch, M. A. (2019). Can the emerging field of immunometabolism provide insights into neuroinflammation? *Progress in Neurobiology*, 184(1), 101719.

Ma, J., Zhang, J., Hou, W. W., Wu, X. H., Liao, R. J., Chen, Y., Wang, Z., Zhang, X. N., Zhang, L. S., Zhou, Y. D., Chen, Z. and Hu, W. W. (2015). Early treatment of minocycline alleviates white matter and cognitive impairments after chronic cerebral hypoperfusion. *Scientific Reports*, 5(12079), 1–14.

MacRae, I. (2011). Preclinical stroke research - Advantages and disadvantages of the most common rodent models of focal ischaemia. *British Journal of Pharmacology*, 164(4), 1062–1078.

Madigan, J. B., Wilcock, D. M. and Hainsworth, A. H. (2016). Vascular Contributions to Cognitive Impairment and Dementia. *Stroke*, 47(7), 1953–1959.

Magistretti, P. J. and Allaman, I. (2015). Review A Cellular Perspective on Brain Energy Metabolism and Functional Imaging. *Neuron*, 86(4), 883–901.

Mantovani, A., Biswas, S. K., Galdiero, M. R., Sica, A. and Locati, M. (2013). Macrophage plasticity and polarization in tissue repair and remodelling. *Journal of Pathology*, 229(2), 176–185.

Mantovani, A., Dinarello, C. A., Molgora, M. and Garlanda, C. (2019). Interleukin-1 and Related Cytokines in the Regulation of Inflammation and Immunity. *Immunity*, 50(4), 778–795.

Martin, R. L., Lloyd, H. G. E. and Cowan, A. I. (1994). The early events of oxygen and glucose deprivation: setting the scene for neuronal death? *Trends in Neurosciences*, 17(6), 251–257.

Martínez-Lapiscina, E. H., Clavero, P., Toledo, E., Estruch, R., Salas-Salvadó, J., San Julián, B., Sanchez-Tainta, A., Ros, E., Valls-Pedret, C. and Martinez-Gonzalez, M. Á. (2013). Mediterranean diet improves cognition: The PREDIMED-NAVARRA randomised trial. *Journal of Neurology, Neurosurgery and Psychiatry*, 84(12), 1318–1325.

Martinez, F. O. and Gordon, S. (2014). The M1 and M2 paradigm of macrophage activation: Time for reassessment. *F1000Prime Reports*, 6(13), 6–13.

Marulanda-Londoño, E. and Chaturvedi, S. (2016). Stroke due to large vessel atherosclerosis: Five new things. *Neurology: Clinical Practice*, 6(3), 252.

Maysami, S., Haley, M. J., Gorenkova, N., Krishnan, S., McColl, B. W. and Lawrence, C. B. (2015). Prolonged diet-induced obesity in mice modifies the inflammatory response and leads to worse outcome after stroke. *Journal of Neuroinflammation*, 12(1), 140.

Maysami, S., Wong, R., Pradillo, J. M., Denes, A., Dhungana, H., Malm, T., Koistinaho, J., Orset, C., Rahman, M., Rubio, M., Schwaninger, M., Vivien, D., Bath, P. M., Rothwell, N. J. and Allan, S. M. (2016). A cross-laboratory preclinical study on the effectiveness of interleukin-1 receptor antagonist in stroke. *Journal of Cerebral Blood Flow & Metabolism*, 36(3), 596–605.

Mazumdar, C., Driggers, E. M. and Turka, L. A. (2020). The Untapped Opportunity and Challenge of Immunometabolism: A New Paradigm for Drug Discovery. *Cell Metabolism*, 31(1), 26–34.

McCann, S. K., Cramond, F., Macleod, M. R. and Sena, E. S. (2016). Systematic Review and Meta-Analysis of the Efficacy of Interleukin-1 Receptor Antagonist in Animal Models of Stroke: an Update. *Translational Stroke Research*, 7(5), 395–406.

McColl, B. W., Carswell, H. V., McCulloch, J. and Horsburgh, K. (2004). Extension of cerebral hypoperfusion and ischaemic pathology beyond MCA territory after intraluminal filament occlusion in C57Bl/6J mice. *Brain Research*, 997(1), 15–23.

Mccoll, B. W., Rose, N., Robson, F. H., Rothwell, N. J. and Lawrence, C. B. (2009). Increased brain microvascular MMP-9 and incidence of haemorrhagic transformation in obese mice after experimental stroke. *Journal of Cerebral Blood Flow & Metabolism*, 30(2), 267–272.

McColl, B. W., Rothwell, N. J. and Allan, S. M. (2007). Systemic inflammatory stimulus potentiates the acute phase and CXC chemokine responses to experimental stroke and exacerbates brain damage via interleukin-1- and neutrophil-dependent mechanisms. *Journal of Neuroscience*, 27(16), 4403–4412.

McMeekin, P., White, P., James, M. A., Price, C. I., Flynn, D. and Ford, G. A. (2017). Estimating the number of UK stroke patients eligible for endovascular thrombectomy. *European Stroke Journal*, 2(4), 319–326.

Mertens, M. and Singh, J. A. (2009). Anakinra for rheumatoid arthritis: A systematic review. *Journal of Rheumatology*, 36(6), 1118–1125.

Michl, J., Ohlbaum, D. J. and Silverstein, S. C. (1976). 2-Deoxyglucose selectively inhibits fc and complement receptor-mediated phagocytosis in mouse peritoneal macrophages: Description of the inhibitory effect. *Journal of Experimental Medicine*, 144(6), 1465–1483.

Millet, P., Vachharajani, V., McPhail, L., Yoza, B. and McCall, C. E. (2016). GAPDH Binding to TNF-α mRNA Contributes to Posttranscriptional Repression in Monocytes: A Novel Mechanism of Communication between Inflammation and Metabolism. *The Journal of Immunology*, 196(6), 2541–2551.

Mills, E. L., Kelly, B., Logan, A., Costa, A. S. H. H., Varma, M., Bryant, C. E., Tourlomousis, P., Däbritz, J. H. M., Gottlieb, E., Latorre, I., Corr, S. C., McManus, G., Ryan, D., Jacobs, H. T., Szibor, M., Xavier, R. J., Braun, T., Frezza, C., Murphy, M. P. and O'Neill, L. A. (2016). Succinate Dehydrogenase Supports Metabolic Repurposing of Mitochondria to Drive Inflammatory Macrophages. *Cell*, 167(2), 457–470.

Mills, E. L., Ryan, D. G., Prag, H. A., Dikovskaya, D., Menon, D., Zaslona, Z., Jedrychowski, M. P., Costa, A. S. H. H., Higgins, M., Hams, E., Szpyt, J., Runtsch, M. C., King, M. S., McGouran, J. F., Fischer, R., Kessler, B. M., McGettrick, A. F., Hughes, M. M., Carroll, R. G., Booty, L. M., Knatko, E. V., Meakin, P. J., Ashford, M. L. J. J., Modis, L. K., Brunori, G., Sévin, D. C., Fallon, P. G., Caldwell, S. T., Kunji, E. R. S. S., Chouchani, E. T., Frezza, C., Dinkova-Kostova, A. T., Hartley, R. C., Murphy, M. P., O'Neill, L. A. and O'Neill, L. A. (2018). Itaconate is an anti-inflammatory metabolite that activates Nrf2 via alkylation of KEAP1. *Nature*, 556(7699), 113–117.

Miró-Mur, F., Pérez-de-Puig, I., Ferrer-Ferrer, M., Urra, X., Justicia, C., Chamorro, A. and Planas, A. M. (2016). Immature monocytes recruited to the ischemic mouse brain differentiate into macrophages with features of alternative activation. *Brain, Behavior, and Immunity*, (53) 18–33.

Miyake, K., Takeo, S. and Kaijihara, H. (1993). Sustained decrease in brain regional blood flow after microsphere embolism in rats. *Stroke*, 24(3), 415–420.

Mohamed, I. N., Hafez, S. S., Fairaq, A., Ergul, A., Imig, J. D. and El-Remessy, A. B. (2014). Thioredoxin-interacting protein is required for endothelial NLRP3 inflammasome activation and cell death in a rat model of high-fat diet. *Diabetologia*, 57(2), 413–23.

Morris, M. C., Tangney, C. C., Wang, Y., Sacks, F. M., Barnes, L. L., Bennett, D. A. and Aggarwal, N. T. (2015). MIND diet slows cognitive decline with aging. *Alzheimer's and Dementia*, 11(9), 1015–1022.

Mosley, B., Dower, S. K., Gillis, S. and Cosman, D. (1987). Determination of the minimum polypeptide lengths of the functionally active sites of human interleukins 1α and 1β. *Proceedings of the National Academy of Sciences of the United States of America*, 84(13), 4572–4576.

Mracsko, E., Liesz, A., Stojanovic, A., Lou, W. P. K., Osswald, M., Zhou, W., Karcher, S., Winkler, F., Martin-Villalba, A., Cerwenka, A. and Veltkamp, R. (2014). Antigen dependently activated cluster of differentiation 8-positive T cells cause perforin-mediated neurotoxicity in experimental stroke. *Journal of Neuroscience*, 34(50), 16784–16795.

Muchada, M., Rodriguez-Luna, D., Pagola, J., Flores, A., Sanjuan, E., Meler, P., Boned, S., Alvarez-Sabin, J., Ribo, M., Molina, C. A. and Rubiera, M. (2014). Impact of time to treatment on tissue-type plasminogen activator-induced recanalization in acute ischemic stroke. *Stroke*, 45(9), 2734–2738.

Muñoz Maniega, S., Chappell, F. M., Valdés Hernández, M. C., Armitage, P. A., Makin, S. D., Heye, A. K., Thrippleton, M. J., Sakka, E., Shuler, K., Dennis, M. S. and Wardlaw, J. M. (2017). Integrity of normal-appearing white matter: Influence of age, visible lesion burden and hypertension in patients with small-vessel disease. *Journal of Cerebral Blood Flow & Metabolism*, 37(2), 644–656.

Murthy, P., Durco, F., Miller-Ocuin, J. L., Takedai, T., Shankar, S., Liang, X., Liu, X., Cui, X., Sachdev, U., Rath, D., Lotze, M. T., Zeh, H. J., Gawaz, M., Weber, A. N. and Vogel, S. (2017). The NLRP3 inflammasome and bruton's tyrosine kinase in platelets co-regulate platelet activation, aggregation, and in vitro thrombus formation. *Biochemical and Biophysical Research Communications*, 483(1), 230–236.

Nawashiro, H., Martin, D. and Hallenbeck, J. M. (1997). Neuroprotective effects of TNF binding protein in focal cerebral ischemia. *Brain Research*, 778(2), 265–271.

Neth, B. J., Mintz, A., Whitlow, C., Jung, Y., Solingapuram Sai, K., Register, T. C., Kellar, D., Lockhart, S. N., Hoscheidt, S., Maldjian, J., Heslegrave, A. J., Blennow, K., Cunnane, S. C., Castellano, C. A., Zetterberg, H. and Craft, S. (2020). Modified ketogenic diet is associated with improved cerebrospinal fluid biomarker profile, cerebral perfusion, and cerebral ketone body uptake in older adults at risk for Alzheimer's disease: a pilot study. *Neurobiology of Aging*, (86) 54–63.

Neumann, J., Riek-Burchardt, M., Herz, J., Doeppner, T. R., König, R., Hütten, H., Etemire, E., Männ, L., Klingberg, A., Fischer, T., Görtler, M. W., Heinze, H. J., Reichardt, P., Schraven, B., Hermann, D. M., Reymann, K. G. and Gunzer, M. (2015). Very-late-antigen-4 (VLA-4)-mediated brain invasion by neutrophils leads to interactions with microglia, increased ischemic injury and impaired behavior in experimental stroke. *Acta Neuropathologica*, 129(2), 259–277.

Newman, A. C. and Maddocks, O. D. K. (2017). One-carbon metabolism in cancer. *British Journal of Cancer*, 116(12), 1499–1504.

Newsholme, P., Curi, R., Gordon, S. and Newsholme, E. A. (1986). Metabolism of glucose, glutamine, long-chain fatty acids and ketone bodies by murine macrophages. *Biochemical Journal*, 239(1), 121–125.

Ng, Y. S., Stein, J., Ning, M. M. and Black-Schaffer, R. M. (2007). Comparison of clinical characteristics and functional outcomes of ischemic stroke in different vascular territories. *Stroke*, 38(8), 2309–2314.

Ngandu, T., Lehtisalo, J., Solomon, A., Levälahti, E., Ahtiluoto, S., Antikainen, R., Bäckman, L., Hänninen, T., Jula, A., Laatikainen, T., Lindström, J., Mangialasche, F., Paajanen, T., Pajala, S., Peltonen, M., Rauramaa, R., Stigsdotter-Neely, A., Strandberg, T., Tuomilehto, J., Soininen, H. and Kivipelto, M. (2015). A 2 year multidomain intervention of diet, exercise, cognitive training, and vascular risk monitoring versus control to prevent cognitive decline in at-risk elderly people (FINGER): A randomised controlled trial. *The Lancet*, 385(9984), 2255–2263.

Nishino, A., Tajima, Y., Takuwa, H., Masamoto, K., Taniguchi, J., Wakizaka, H., Kokuryo, D., Urushihata, T., Aoki, I., Kanno, I., Tomita, Y., Suzuki, N., Ikoma, Y. and Ito, H. (2016). Long-term effects of cerebral hypoperfusion on neural density and function using misery perfusion animal model. *Scientific Reports*, 6(25072), 1–8.

Nishio, K., Ihara, M., Yamasaki, N., Kalaria, R. N., Maki, T., Fujita, Y., Ito, H., Oishi, N., Fukuyama, H., Miyakawa, T., Takahashi, R. and Tomimoto, H. (2010). A mouse model characterizing features of vascular dementia with hippocampal atrophy. *Stroke*, 41(6), 1278–1284.

Nogueira, R. G., Jadhav, A. P., Haussen, D. C., Bonafe, A., Budzik, R. F., Bhuva, P., Yavagal, D. R., Ribo, M., Cognard, C., Hanel, R. A., Sila, C. A., Hassan, A. E., Millan, M., Levy, E. I., Mitchell, P., Chen, M., English, J. D., Shah, Q. A., Silver, F. L., Pereira, V. M., Mehta, B. P., Baxter, B. W., Abraham, M. G., Cardona, P., Veznedaroglu, E., Hellinger, F. R., Feng, L., Kirmani, J. F., Lopes, D. K., Jankowitz, B. T., Frankel, M. R., Costalat, V., Vora, N. A., Yoo, A. J., Malik, A. M., Furlan, A. J., Rubiera, M., Aghaebrahim, A., Olivot, J. M., Tekle, W. G., Shields, R., Graves, T., Lewis, R. J., Smith, W. S., Liebeskind, D. S., Saver, J. L. and Jovin, T. G. (2018). Thrombectomy 6 to 24 hours after stroke with a mismatch between deficit and infarct. *New England Journal of Medicine*, 378(1), 11–21.

Nyberg, S. T., Batty, G. D., Pentti, J., Virtanen, M., Alfredsson, L., Fransson, E. I., Goldberg, M., Heikkilä, K., Jokela, M., Knutsson, A., Koskenvuo, M., Lallukka, T., Leineweber, C., Lindbohm, J. V., Madsen, I. E. H., Magnusson Hanson, L. L., Nordin, M., Oksanen, T., Pietiläinen, O., Rahkonen, O., Rugulies, R., Shipley, M. J., Stenholm, S., Suominen, S., Theorell, T., Vahtera, J., Westerholm, P. J. M., Westerlund, H., Zins, M., Hamer, M., Singh-Manoux, A., Bell, J. A., Ferrie, J. E. and Kivimäki, M. (2018). Obesity and loss of disease-free years owing to major non-communicable diseases: a multicohort study. *The Lancet Public Health*, 3(10), e490–e497.

O'Brien, J. T. and Thomas, A. (2015). Vascular dementia. *The Lancet* 1698–1706.

O'Donnell, M. J., Denis, X., Liu, L., Zhang, H., Chin, S. L., Rao-Melacini, P., Rangarajan, S., Islam, S., Pais, P., McQueen, M. J., Mondo, C., Damasceno, A., Lopez-Jaramillo, P., Hankey, G. J., Dans, A. L., Yusoff, K., Truelsen, T., Diener, H. C., Sacco, R. L., Ryglewicz, D., Czlonkowska, A., Weimar, C., Wang, X. and Yusuf, S. (2010). Risk factors for ischaemic and intracerebral haemorrhagic stroke in 22 countries (the INTERSTROKE study): A case-control study. *The Lancet*, 376(9735), 112–123.

O'Neill, L. A. J. and Artyomov, M. N. (2019). Itaconate: the poster child of metabolic reprogramming in macrophage function. *Nature Reviews Immunology*, 19(5), 273–281.

O'Neill, L. A. J. J., Kishton, R. J. and Rathmell, J. (2016). A guide to immunometabolism for immunologists. *Nature Reviews Immunology*, 16(9), 553–565.

Omi, T., Kumada, M., Kamesaki, T., Okuda, H., Munkhtulga, L., Yanagisawa, Y., Utsumi, N., Gotoh, T., Hata, A., Soma, M., Umemura, S., Ogihara, T., Takahashi, N., Tabara, Y., Shimada, K., Mano, H., Kajii, E., Miki, T. and Iwamoto, S. (2006). An intronic variable number of tandem repeat polymorphisms of the cold-induced autoinflammatory syndrome 1 (CIAS1) gene modifies gene expression and is associated with essential hypertension. *European Journal of Human Genetics*, 14(12), 1295–1305.

Orihuela, R., McPherson, C. A. and Harry, G. J. (2016). Microglial M1/M2 polarization and metabolic states. *British Journal of Pharmacology*, 173(4), 649–665.

Orset, C., Macrez, R., Young, A. R., Panthou, D., Angles-Cano, E., Maubert, E., Agin, V. and Vivien, D. (2007). Mouse model of in situ thromboembolic stroke and reperfusion. *Stroke*, 38(10), 2771–2778.

Ortega, S. B., Torres, V. O., Latchney, S. E., Whoolery, C. W., Noorbhai, I. Z., Poinsatte, K., Selvaraj, U. M., Benson, M. A., Meeuwissen, A. J. M., Plautz, E. J., Kong, X., Ramirez, D. M., Ajay, A. D., Meeks, J. P., Goldberg, M. P., Monson, N. L., Eisch, A. J. and Stowe, A. M. (2020). B cells migrate into remote brain areas and support neurogenesis and functional recovery after focal stroke in mice. *Proceedings of the National Academy of Sciences*, 117(9), 4983–4993.

Otori, T., Katsumata, T., Muramatsu, H., Kashiwagi, F., Katayama, Y. and Terashi, A. (2003). Long-term measurement of cerebral blood flow and metabolism in a rat chronic hypoperfusion model. *Clinical and experimental pharmacology & physiology*, 30(4), 266–272.

Palsson-McDermott, E. M., Curtis, A. M., Goel, G., Lauterbach, M. A. R., Sheedy, F. J., Gleeson, L. E., van den Bosch, M. W. M., Quinn, S. R., Domingo-Fernandez, R., Johnston, D. G. W., Jiang, J., Israelsen, W. J., Keane, J., Thomas, C., Clish, C., Vander Heiden, M., Xavier, R. J. and O'Neill, L. A. J. (2015). Pyruvate Kinase M2 Regulates Hif-1α Activity and IL-1β Induction and Is a Critical Determinant of the Warburg Effect in LPS-Activated Macrophages. *Cell Metabolism*, 21(1), 65–80.

Pantoni, L., Blomberg, M., Jonsson, M., Al., E., Al., E., Study, for the A. S. P., Group, for the G.-I.-26 S., Group, Q. of C. O. in R. I. W. and Al., E. (2010). Cerebral small vessel disease: from pathogenesis and clinical characteristics to therapeutic challenges. *Lancet Neurology*, 9(7), 689–701.

Pappas, B. A., De La Torre, J. C., Davidson, C. M., Keyes, M. T. and Fortin, T. (1996). Chronic reduction of cerebral blood flow in the adult rat: Late-emerging CA1 cell loss and memory dysfunction. *Brain Research*, 708(1), 50–58.

Park, J. H., Hong, J. H., Lee, S. W., Ji, H. D., Jung, J. A., Yoon, K. W., Lee, J. I., Won, K. S., Song, B. Il and Kim, H. W. (2019). The effect of chronic cerebral hypoperfusion on the pathology of Alzheimer's disease: A positron emission tomography study in rats. *Scientific Reports*, 9(1), 1–9.

Pearce, E. L. (2010). Metabolism in T cell activation and differentiation. *Current Opinion in Immunology*, 22(3), 314–320.

Pendlebury, S. T. and Rothwell, P. M. (2019). Incidence and prevalence of dementia associated with transient ischaemic attack and stroke: analysis of the population-based Oxford Vascular Study. *The Lancet Neurology*, 18(3), 248–258.

Perego, C., Fumagalli, S., Zanier, E. R., Carlino, E., Panini, N., Erba, E. and De Simoni, M. G. (2016). Macrophages are essential for maintaining a M2 protective response early after ischemic brain injury. *Neurobiology of Disease*, (96) 284–293.

Petersen, M. A., Ryu, J. K. and Akassoglou, K. (2018). Fibrinogen in neurological diseases: Mechanisms, imaging and therapeutics. *Nature Reviews Neuroscience*, 19(5), 283–301.

Planas, A. M. (2018). Role of Immune Cells Migrating to the Ischemic Brain. *Stroke*, 49(9), 2261–2267.

Plaschke, K., Yun, S. W., Martin, E., Hoyer, S. and Bardenheuer, H. J. (1999). Interrelation between cerebral energy metabolism and behaviour in a rat model of permanent brain vessel occlusion. *Brain Research*, 830(2), 320–9.

Pollock, A., St George, B., Fenton, M. and Firkins, L. (2012). Top ten research priorities relating to life after stroke. *The Lancet Neurology*, 11(3), 209.

Potter, G. M., Doubal, F. N., Jackson, C. A., Sudlow, C. L. M., Dennis, M. S. and Wardlaw, J. M. (2012). Lack of association of white matter lesions with ipsilateral carotid artery stenosis. *Cerebrovascular Diseases*, 33(4), 378–384.

Power, M. C., Mormino, E., Soldan, A., James, B. D., Yu, L., Armstrong, N. M., Bangen, K. J., Delano-Wood, L., Lamar, M., Lim, Y. Y., Nudelman, K., Zahodne, L., Gross, A. L., Mungas, D., Widaman, K. F. and Schneider, J. (2018). Combined neuropathological pathways account for age-related risk of dementia. *Annals of Neurology*, 84(1), 10–22.

Powers, W. J., Rabinstein, A. A., Ackerson, T., Adeoye, O. M., Bambakidis, N. C., Becker, K., Biller, J., Brown, M., Demaerschalk, B. M., Hoh, B., Jauch, E. C., Kidwell, C. S., Leslie-Mazwi, T. M., Ovbiagele, B., Scott, P. A., Sheth, K. N., Southerland, A. M., Summers, D. V. and Tirschwell, D. L. (2018). 2018 Guidelines for the Early Management of Patients With Acute Ischemic Stroke: A Guideline for Healthcare Professionals From the American Heart Association/American Stroke Association. *Stroke*, 49(3), e46–e110.

Proell, M., Gerlic, M., Mace, P. D., Reed, J. C. and Riedl, S. J. (2013). The CARD plays a critical role in ASC foci formation and inflammasome signalling. *The Biochemical Journal*, 449(3), 613–21.

Putaala, J., Haapaniemi, E., Metso, A. J., Metso, T. M., Artto, V., Kaste, M. and Tatlisumak, T. (2010). Recurrent ischemic events in young adults after first-ever ischemic stroke. *Annals of Neurology*, 68(5), 661–671.

Rabuffetti, M., Sciorati, C., Tarozzo, G., Clementi, E., Manfredi, A. A. and Beltramo, M. (2000). Inhibition of caspase-1-like activity by Ac-Tyr-Val-Ala-Asp-chloromethyl ketone induces long-lasting neuroprotection in cerebral ischemia through apoptosis reduction and decrease of proinflammatory cytokines. *Journal of Neuroscience*, 20(12), 4398–4404.

Rajaṁaki, K., Lappalainen, J., Öörni, K., Välimäki, E., Matikainen, S., Kovanen, P. T. and Kari, E. K. (2010). Cholesterol crystals activate the NLRP3 inflammasome in human macrophages: A novel link between cholesterol metabolism and inflammation. *PLoS ONE*, 5(7), e11765.

Rajani, R. M. and Williams, A. (2017). Endothelial cell–oligodendrocyte interactions in small vessel disease and aging. *Clinical Science*, 131(5), 369–379.

Rapp, J. H., Pan, X. M., Neumann, M., Hong, M., Hollenbeck, K. and Liu, J. (2008). Microemboli composed of cholesterol crystals disrupt the blood-brain barrier and reduce cognition. *Stroke*, 39(8), 2354–2361.

Rees, K., Dyakova, M., Ward, K., Thorogood, M. and Brunner, E. (2013). Dietary advice for reducing cardiovascular risk. *Cochrane Database of Systematic Reviews*, (12).

Relton, J. K. and Rothwell, N. J. (1992). Interleukin-1 receptor antagonist inhibits ischaemic and excitotoxic neuronal damage in the rat. *Brain Research Bulletin*, 29(2), 243–246.

Ridker, P. M., Everett, B. M., Thuren, T., MacFadyen, J. G., Chang, W. H., Ballantyne, C., Fonseca, F., Nicolau, J., Koenig, W., Anker, S. D., Kastelein, J. J. P., Cornel, J. H., Pais, P., Pella, D., Genest, J., Cifkova, R., Lorenzatti, A., Forster, T., Kobalava, Z., Vida-Simiti, L., Flather, M., Shimokawa, H., Ogawa, H., Dellborg, M., Rossi, P. R. F., Troquay, R. P. T., Libby, P. and Glynn, R. J. (2017). Antiinflammatory therapy with canakinumab for atherosclerotic disease. *New England Journal of Medicine*, 377(12), 1119–1131.

Rocha, V. Z. and Libby, P. (2009). Obesity, inflammation, and atherosclerosis. *Nature Reviews Cardiology*, 6(6), 399–409.

Román, G. C. and Benavente, O. (2004). The neuropathology of vascular dementia. *Seminars in Cerebrovascular Diseases and Stroke*, 4(2), 87–96.

Rose, G., Stamler, J., Stamler, R., Elliott, P., Marmot, M., Pyorala, K., Kesteloot, H., Joossens, J., Hansson, L., Mancia, G., Dyer, A., Kromhout, D., Laaser, U. and Sans, S. (1988). Intersalt: An international study of electrolyte excretion and blood pressure. Results for 24 hour urinary sodium and potassium excretion. *British Medical Journal*, 297(6644), 319–328.

Rosenberg, A., Mangialasche, F., Ngandu, T., Solomon, A. and Kivipelto, M. (2019). Multidomain Interventions to Prevent Cognitive Impairment, Alzheimer's Disease, and Dementia: From FINGER to World-Wide FINGERS. *The Journal of Prevention of Alzheimer's Disease*, 10(432), 1–8.

Rosenberg, G. A. (2009). Inflammation and white matter damage in vascular cognitive impairment. *Stroke*, 40(3), 20–3.

Ross, J., Brough, D., Gibson, R. M., Loddick, S. A. and Rothwell, N. J. (2007). A selective, non-peptide caspase-1 inhibitor, VRT-018858, markedly reduces brain damage induced by transient ischemia in the rat. *Neuropharmacology*, 53(5), 638–642.

Roth, S., Singh, V., Tiedt, S., Schindler, L., Huber, G., Geerlof, A., Antoine, D. J., Anfray, A., Orset, C., Gauberti, M., Fournier, A., Holdt, L. M., Harris, H. E., Engelhardt, B., Bianchi, M. E., Vivien, D.,

Haffner, C., Bernhagen, J., Dichgans, M. and Liesz, A. (2018). Brain-released alarmins and stress response synergize in accelerating atherosclerosis progression after stroke. *Science Translational Medicine*, 10(432), 1–11.

Rubio-Araiz, A., Finucane, O. M., Keogh, S. and Lynch, M. A. (2018). Anti-TLR2 antibody triggers oxidative phosphorylation in microglia and increases phagocytosis of β-amyloid. *Journal of Neuroinflammation*, 15(1), 247.

Ryan, C. L., Doucette, T. A., Gill, D. A., Langdon, K. D., Liu, Y., Perry, M. A. and Tasker, R. A. (2006). An improved post-operative care protocol allows detection of long-term functional deficits following MCAo surgery in rats. *Journal of Neuroscience Methods*, 154(1), 30–37.

Sacks, F. M., Svetkey, L. P., Vollmer, W. M., Appel, L. J., Bray, G. A., Harsha, D., Obarzanek, E., Conlin, P. R., Miller, E. R., Simons-Morton, D. G., Karanja, N., Lin, P. H., Aickin, M., Most-Windhauser, M. M., Moore, T. J., Proschan, M. A. and Cutler, J. A. (2001). Effects on blood pressure of reduced dietary sodium and the dietary approaches to stop hypertension (dash) diet. *New England Journal of Medicine*, 344(1), 3–10.

Saggu, R., Schumacher, T., Gerich, F., Rakers, C., Tai, K., Delekate, A. and Petzold, G. C. (2016). Astroglial NF-kB contributes to white matter damage and cognitive impairment in a mouse model of vascular dementia. *Acta Neuropathologica Communications*, 4(1), 76.

Sam, K., Crawley, A. P., Poublanc, J., Conklin, J., Sobczyk, O., Mandell, D. M., Duffin, J., Venkatraghavan, L., Fisher, J. A., Black, S. E. and Mikulis, D. J. (2016). Vascular dysfunction in leukoaraiosis. *American Journal of Neuroradiology*, 37(12), 2258–2264.

Saresella, M., La Rosa, F., Piancone, F., Zoppis, M., Marventano, I., Calabrese, E., Rainone, V., Nemni, R., Mancuso, R. and Clerici, M. (2016). The NLRP3 and NLRP1 inflammasomes are activated in Alzheimer's disease. *Molecular Neurodegeneration*, 11(23), 1–14.

Sarti, C., Pantoni, L., Bartolini, L. and Inzitari, D. (2002). Persistent impairment of gait performances and working memory after bilateral common carotid artery occlusion in the adult Wistar rat. *Behavioural Brain Research*, 136(1), 13–20.

Schmidt-Kastner, R., Aguirre-Chen, C., Saul, I., Yick, L., Hamasaki, D., Busto, R. and Ginsberg, M. D. (2005). Astrocytes react to oligemia in the forebrain induced by chronic bilateral common carotid artery occlusion in rats. *Brain Research*, 1052(1), 28–39.

Schroder, K. and Tschopp, J. (2010). The Inflammasomes. *Cell*, 140(6), 821–832.

Semba, H., Takeda, N., Isagawa, T., Sugiura, Y., Honda, K., Wake, M., Miyazawa, H., Yamaguchi, Y., Miura, M., Jenkins, D. M. R., Choi, H., Kim, J. W., Asagiri, M., Cowburn, A. S., Abe, H., Soma, K., Koyama, K., Katoh, M., Sayama, K., Goda, N., Johnson, R. S., Manabe, I., Nagai, R. and Komuro, I. (2016). HIF-1α-PDK1 axis-induced active glycolysis plays an essential role in macrophage migratory capacity. *Nature Communications*, 7(1), 1–10.

Seo, J. H., Miyamoto, N., Hayakawa, K., Pham, L. D. D., Maki, T., Ayata, C., Kim, K. W., Lo, E. H. and Arai, K. (2013). Oligodendrocyte precursors induce early blood-brain barrier opening after white matter injury. *Journal of Clinical Investigation*, 123(2), 782–786.

Shi, J., Zhao, Y., Wang, K., Shi, X., Wang, Y., Huang, H., Zhuang, Y., Cai, T., Wang, F. and Shao, F. (2015). Cleavage of GSDMD by inflammatory caspases determines pyroptotic cell death. *Nature*, 526(7575), 660–665.

Shi, Y., Thrippleton, M. J., Makin, S. D., Marshall, I., Geerlings, M. I., de Craen, A. J. M. M., Van Buchem, M. A. and Wardlaw, J. M. (2016). Cerebral blood flow in small vessel disease: A systematic review and meta-analysis. *Journal of Cerebral Blood Flow & Metabolism*, 36(10), 1653–1667.

Shibata, M., Ohtani, R., Ihara, M. and Tomimoto, H. (2004). White Matter Lesions and Glial Activation in a Novel Mouse Model of Chronic Cerebral Hypoperfusion. *Stroke*, 35(11), 2598–2603.

Shibata, M., Yamasaki, N., Miyakawa, T., Kalaria, R. N., Fujita, Y., Ohtani, R., Ihara, M., Takahashi, R. and Tomimoto, H. (2007). Selective Impairment of Working Memory in a Mouse Model of Chronic Cerebral Hypoperfusion. *Stroke*, 38(10), 2826–2832.

Shichita, T., Sugiyama, Y., Ooboshi, H., Sugimori, H., Nakagawa, R., Takada, I., Iwaki, T., Okada, Y., Iida, M., Cua, D. J., Iwakura, Y. and Yoshimura, A. (2009). Pivotal role of cerebral interleukin-17-producing T cells in the delayed phase of ischemic brain injury. *Nature Medicine*, 15(8), 946–950.

Sims, J. E. and Smith, D. E. (2010). The IL-1 family: Regulators of immunity. *Nature Reviews Immunology*, 10(2), 89–102.

Smith, C. J., Hulme, S., Vail, A., Heal, C., Parry-Jones, A. R., Scarth, S., Hopkins, K., Hoadley, M., Allan, S. M., Rothwell, N. J., Hopkins, S. J. and Tyrrell, P. J. (2018). SCIL-STROKE (subcutaneous interleukin-1 receptor antagonist in ischemic stroke): A randomized controlled phase 2 trial. *Stroke*, 49(5), 1210–1216.

Smith, E. E. and Eichler, F. (2006). Cerebral amyloid angiopathy and lobar intracerebral hemorrhage. *Archives of Neurology*, 63(1), 148–151.

Sobowale, O. A., Parry-Jones, A. R., Smith, C. J., Tyrrell, P. J., Rothwell, N. J. and Allan, S. M. (2016). Interleukin-1 in Stroke: From Bench to Bedside. *Stroke*, 47(8), 2160–2167.

Solak, Y., Afsar, B., Vaziri, N. D., Aslan, G., Yalcin, C. E., Covic, A. and Kanbay, M. (2016). Hypertension as an autoimmune and inflammatory disease. *Hypertension Research*, 39(8), 567–73.

Stamler, J., Rose, G., Stamler, R., Elliott, P., Dyer, A. and Marmot, M. (1989). INTERSALT study findings. Public health and medical care implications. *Hypertension*, 14(5), 570–7.

Stein, M., Keshav, S., Harris, N. and Gordon, S. (1992). Interleukin 4 potently enhances murine macrophage mannose receptor activity: A marker of alternative immunologic macrophage activation. *Journal of Experimental Medicine*, 176(1), 287–292.

Stoll, G. and Nieswandt, B. (2019). Thrombo-inflammation in acute ischaemic stroke — implications for treatment. *Nature Reviews Neurology*, 15(8), 473–481.

Strazzullo, P., D'Elia, L., Kandala, N. B. and Cappuccio, F. P. (2009). Salt intake, stroke, and cardiovascular disease: Meta-analysis of prospective studies. *British Medical Journal*, 339(7733), 1296.

Strelko, C. L., Lu, W., Dufort, F. J., Seyfried, T. N., Chiles, T. C., Rabinowitz, J. D. and Roberts, M. F. (2011). Itaconic acid is a mammalian metabolite induced during macrophage activation. *Journal of the American Chemical Society*, 133(41), 16386–16389.

Stroke Association (2015). *Current, future and avoidable costs of stroke in the UK*. Stroke Association. [Online] [Accessed on 14th February 2020] https://doi.org/10.1093/ageing/afz162/5679684.

Tan, Z., Xie, N., Cui, H., Moellering, D. R., Abraham, E., Thannickal, V. J. and Liu, G. (2015). Pyruvate Dehydrogenase Kinase 1 Participates in Macrophage Polarization via Regulating Glucose Metabolism. *The Journal of Immunology*, 194(12), 6082–6089.

Tannahill, G. M., Curtis, A. M., Adamik, J., Palsson-McDermott, E. M., McGettrick, A. F., Goel, G., Frezza, C., Bernard, N. J., Kelly, B., Foley, N. H., Zheng, L., Gardet, A., Tong, Z., Jany, S. S., Corr, S. C., Haneklaus, M., Caffrey, B. E., Pierce, K., Walmsley, S., Beasley, F. C., Cummins, E., Nizet, V., Whyte, M., Taylor, C. T., Lin, H., Masters, S. L., Gottlieb, E., Kelly, V. P., Clish, C., Auron, P. E., Xavier, R. J. and O'Neill, L. A. J. (2013). Succinate is an inflammatory signal that induces IL-1β through HIF-1α. *Nature*, 496(7444), 238–42.

Tanswell, P., Modi, N., Combs, D. and Danays, T. (2002). Pharmacokinetics and pharmacodynamics of tenecteplase in fibrinolytic therapy of acute myocardial infarction. *Clinical Pharmacokinetics*, 41(15), 1229–1245.

Taylor, R. C., Cullen, S. P. and Martin, S. J. (2008). Apoptosis: Controlled demolition at the cellular level. *Nature Reviews Molecular Cell Biology*, 9(3), 231–241.

Toledo, J. B., Arnold, S. E., Raible, K., Brettschneider, J., Xie, S. X., Grossman, M., Monsell, S. E., Kukull, W. A. and Trojanowski, J. Q. (2013). Contribution of cerebrovascular disease in autopsy confirmed neurodegenerative disease cases in the National Alzheimer's Coordinating Centre. *Brain*, 136(9), 2697–2706.

Tomimoto, H., Akiguchi, I., Wakita, H., Lin, J. X. and Budka, H. (2000). Cyclooxygenase-2 is induced in microglia during chronic cerebral ischemia in humans. *Acta Neuropathologica*, 99(1), 26–30.

Tomimoto, H., Ihara, M., Wakita, H., Ohtani, R., Lin, J. X., Akiguchi, I., Kinoshita, M. and Shibasaki, H. (2003). Chronic cerebral hypoperfusion induces white matter lesions and loss of oligodendroglia with DNA fragmentation in the rat. *Acta Neuropathologica*, 106(6), 527–534.

Tussing-Humphreys, L., Lamar, M., Blumenthal, J. A., Babyak, M., Fantuzzi, G., Blumstein, L., Schiffer, L. and Fitzgibbon, M. L. (2017). Building research in diet and cognition: The BRIDGE randomized controlled trial. *Contemporary Clinical Trials*, 59(1), 87–97.

van den Brink, A. C., Brouwer-Brolsma, E. M., Berendsen, A. A. M. and van de Rest, O. (2019). The Mediterranean, Dietary Approaches to Stop Hypertension (DASH), and Mediterranean-DASH Intervention for Neurodegenerative Delay (MIND) Diets Are Associated with Less Cognitive Decline and a Lower Risk of Alzheimer's Disease—A Review. *Advances in Nutrition*, 10(6), 1040–1065.

Vemmos, K., Ntaios, G., Spengos, K., Savvari, P., Vemmou, A., Pappa, T., Manios, E., Georgiopoulos, G. and Alevizaki, M. (2011). Association between obesity and mortality after acute first-ever stroke: The obesity-stroke paradox. *Stroke*, 42(1), 30–36.

Vicente, É., Degerone, D., Bohn, L., Scornavaca, F., Pimentel, A., Leite, M. C., Swarowsky, A., Rodrigues, L., Nardin, P., Vieira de Almeida, L. M., Gottfried, C., Souza, D. O., Netto, C. A. and Gonçalves, C. A. (2009). Astroglial and cognitive effects of chronic cerebral hypoperfusion in the rat. *Brain Research*, 1251(1), 204–212.

Vijayan, V., Pradhan, P., Braud, L., Fuchs, H. R., Gueler, F., Motterlini, R., Foresti, R. and Immenschuh, S. (2019). Human and murine macrophages exhibit differential metabolic responses to lipopolysaccharide - A divergent role for glycolysis. *Redox Biology*, 22(1), 101147.

Viola, A., Munari, F., Sánchez-Rodríguez, R., Scolaro, T. and Castegna, A. (2019). The metabolic signature of macrophage responses. *Frontiers in Immunology*, 10(1), 1462.

Vitkovic, L., Bockaert, J. and Jacque, C. (2001). 'Inflammatory' Cytokines: Neuromodulators in Normal Brain? *Journal of Neurochemistry*, 74(2), 457–471.

Voloboueva, L. A., Emery, J. F., Sun, X. and Giffard, R. G. (2013). Inflammatory response of microglial BV-2 cells includes a glycolytic shift and is modulated by mitochondrial glucose-regulated protein 75/mortalin. *FEBS Letters*, 587(6), 756–762.

Vyas, V. and Lambiase, P. (2019). Obesity and atrial fibrillation: Epidemiology, pathophysiology and novel therapeutic opportunities. *Arrhythmia and Electrophysiology Review*, 8(1), 28–36.

Wakita, H., Tomimoto, H., Akiguchi, I. and Kimura, J. (1994). Glial activation and white matter changes in the rat brain induced by chronic cerebral hypoperfusion: an immunohistochemical study. *Acta Neuropathologica*, 87(5), 484–92.

Wakita, H., Tomimoto, H., Akiguchi, I. and Kimura, J. (1995). Protective Effect of Cyclosporin A on White Matter Changes in the Rat Brain After Chronic Cerebral Hypoperfusion. *Stroke*, 26(8), 1415–1422.

Wang, F., Geng, X., Tao, H. Y. and Cheng, Y. (2010). The restoration after repetitive transcranial magnetic stimulation treatment on cognitive ability of vascular dementia rats and its impacts on synaptic plasticity in hippocampal CA1 area. *J Mol Neurosci*, 41(1), 145–155.

Wang, F., Zhang, S., Jeon, R., Vuckovic, I., Jiang, X., Lerman, A., Folmes, C. D., Dzeja, P. D. and Herrmann, J. (2018). Interferon Gamma Induces Reversible Metabolic Reprogramming of M1 Macrophages to Sustain Cell Viability and Pro-Inflammatory Activity. *EBioMedicine*, (30) 303–316.

Warburg, O. (1956). On the Origin of Cancer Cells. *Science,* 123(3191), 309–314.

Wardlaw, J. M. J., Sandercock, P. P. A. G., Dennis, M. S. M. and Starr, J. (2003). Is Breakdown of the Blood-Brain Barrier Responsible for Lacunar Stroke, Leukoaraiosis, and Dementia? *Stroke*, 34(3), 806–812.

Wardlaw, J. M., Makin, S. J., Vald Es Hern Andez, M. C., Armitage, P. A., Heye, A. K., Chappell, F. M., Muñoz-Maniega, S., Sakka, E., Shuler, K., Dennis, M. S., Thrippleton, M. J., Valdés Hernández, M. C., Armitage, P. A., Heye, A. K., Chappell, F. M., Muñoz-Maniega, S., Sakka, E., Shuler, K., Dennis, M. S. and Thrippleton, M. J. (2017). Blood-brain barrier failure as a core mechanism in cerebral small vessel disease and dementia: evidence from a cohort study. *Alzheimer's & Dementia*, 13(6), 634–643.

Wardlaw, J. M., Smith, C. and Dichgans, M. (2013). Mechanisms of sporadic cerebral small vessel disease: Insights from neuroimaging. *The Lancet Neurology*, 12(5), 483–497.

Wardlaw, J. M., Smith, C. and Dichgans, M. (2019). Small vessel disease: mechanisms and clinical implications. *Lancet Neurology*, 18(7), 684–96.

Weber, A., Wasiliew, P. and Kracht, M. (2010). Interleukin-1 (IL-1) pathway. *Science Signaling*, 3(105), 1–6.

Weber, R., Weimar, C., Blatchford, J., Hermansson, K., Wanke, I., Möller-Hartmann, C., Gizewski, E. R., Forsting, M., Demchuk, A. M., Sacco, R. L., Saver, J. L., Warach, S., Diener, H.-C., Diehl, A. and PRoFESS Imaging Substudy Group (2012). Telmisartan on top of antihypertensive treatment does not prevent progression of cerebral white matter lesions in the prevention regimen for effectively avoiding second strokes (PRoFESS) MRI substudy. *Stroke*, 43(9), 2336–42.

Werring, D. J. (2018). CT scanning to diagnose CAA: back to the future? *The Lancet Neurology*, 17(3), 197–198.

White, C. S., Lawrence, C. B., Brough, D. and Rivers-Auty, J. (2017). Inflammasomes as therapeutic targets for Alzheimer's disease. *Brain pathology*, 27(2), 223–234.

Willette, A. A., Bendlin, B. B., Starks, E. J., Birdsill, A. C., Johnson, S. C., Christian, B. T., Okonkwo, O. C., La Rue, A., Hermann, B. P., Koscik, R. L., Jonaitis, E. M., Sager, M. A. and Asthana, S. (2015). Association of insulin resistance with cerebral glucose uptake in late middle-aged adults at risk for Alzheimer disease. *JAMA Neurology*, 72(9), 1013–1020.

Williamson, J. D., Pajewski, N. M., Auchus, A. P., Bryan, R. N., Chelune, G., Cheung, A. K., Cleveland, M. L., Coker, L. H., Crowe, M. G., Cushman, W. C., Cutler, J. A., Davatzikos, C., Desiderio, L., Erus, G., Fine, L. J., Gaussoin, S. A., Harris, D., Hsieh, M. K., Johnson, K. C., Kimmel, P. L., Tamura, M. K., Launer, L. J., Lerner, A. J., Lewis, C. E., Martindale-Adams, J., Moy, C. S., Nasrallah, I. M., Nichols, L. O., Oparil, S., Ogrocki, P. K., Rahman, M., Rapp, S. R., Reboussin, D. M., Rocco, M. V., Sachs, B. C., Sink, K. M., Still, C. H., Supiano, M. A., Snyder, J. K., Wadley, V. G., Walker, J., Weiner, D. E., Whelton, P. K., Wilson, V. M., Woolard, N., Wright, J. T. and Wright, C. B. (2019). Effect of Intensive vs Standard Blood Pressure Control on Probable Dementia: A Randomized Clinical Trial. *JAMA - Journal of the American Medical Association*, 321(6), 553–561.

Wilson, N. (2004). Salt tax could reduce population's salt intake . *British Medical Journal*, 329(7471), 918.

Wolf, P. A., D'Agostino, R. B., O'Neal, M. A., Sytkowski, P., Kase, C. S., Belanger, A. J. and Kannel, W. B. (1992). Secular trends in stroke incidence and mortality: The framingham study. *Stroke*, 23(11), 1551–1555.

Wong, R., Lénárt, N., Hill, L., Toms, L., Coutts, G., Martinecz, B., Császár, E., Nyiri, G., Papaemmanouil, A., Waisman, A., Müller, W., Schwaninger, M., Rothwell, N., Francis, S., Pinteaux, E., Denés, A. and Allan, S. M. (2019). Interleukin-1 mediates ischaemic brain injury via distinct actions on endothelial cells and cholinergic neurons. *Brain, Behavior, and Immunity*, 76(1), 126–138.

Wu, L., Zhang, X. and Zhao, L. (2018). Human apoe isoforms differentially modulate brain glucose and ketone body metabolism: Implications for Alzheimer's disease risk reduction and early intervention. *Journal of Neuroscience*, 38(30), 6665–6681.

Wu, Y. T., Beiser, A. S., Breteler, M. M. B., Fratiglioni, L., Helmer, C., Hendrie, H. C., Honda, H., Ikram, M. A., Langa, K. M., Lobo, A., Matthews, F. E., Ohara, T., Pérès, K., Qiu, C., Seshadri, S., Sjölund, B. M., Skoog, I. and Brayne, C. (2017). The changing prevalence and incidence of dementia over time-current evidence. *Nature Reviews Neurology*, 13(6), 327–339.

Yamasaki, Y., Matsuura, N., Shozuhara, H., Onodera, H., Itoyama, Y. and Kogure, K. (1995). Interleukin-1 as a pathogenetic mediator of ischemic brain damage in rats. *Stroke*, 26(4), 676–680.

Yang, F., Wang, Z., Wei, X., Han, H., Meng, X., Zhang, Y., Shi, W., Li, F., Xin, T., Pang, Q. and Yi, F. (2014). NLRP3 deficiency ameliorates neurovascular damage in experimental ischemic stroke. *Journal of Cerebral Blood Flow & Metabolism*, 34(4), 660–7.

Ye, X., Shen, T., Hu, J., Zhang, L., Zhang, Y., Bao, L., Cui, C., Jin, G., Zan, K., Zhang, Z., Yang, X., Shi, H., Zu, J., Yu, M., Song, C., Wang, Y., Qi, S. and Cui, G. (2017). Purinergic 2X7 receptor/NLRP3 pathway triggers neuronal apoptosis after ischemic stroke in the mouse. *Experimental Neurology*, 292(1), 46–55.

Yemisci, M., Gursoy-Ozdemir, Y., Vural, A., Can, A., Topalkara, K. and Dalkara, T. (2009). Pericyte contraction induced by oxidative-nitrative stress impairs capillary reflow despite successful opening of an occluded cerebral artery. *Nature Medicine*, 15(9), 1031–1037.

Yoshizaki, K., Adachi, K., Kataoka, S., Watanabe, A., Tabira, T., Takahashi, K. and Wakita, H. (2008). Chronic cerebral hypoperfusion induced by right unilateral common carotid artery occlusion causes delayed white matter lesions and cognitive impairment in adult mice. *Experimental Neurology*, 210(2), 585–591.

Youm, Y.-H., Grant, R. W., McCabe, L. R., Albarado, D. C., Nguyen, K. Y., Ravussin, A., Pistell, P., Newman, S., Carter, R., Laque, A., Münzberg, H., Rosen, C. J., Ingram, D. K., Salbaum, J. M. and Dixit, V. D. (2013). Canonical Nlrp3 Inflammasome Links Systemic Low-Grade Inflammation to Functional Decline in Aging. *Cell Metabolism*, 18(4), 519–532.

Yusuf, P. S., Hawken, S., Ôunpuu, S., Dans, T., Avezum, A., Lanas, F., McQueen, M., Budaj, A., Pais, P., Varigos, J. and Lisheng, L. (2004). Effect of potentially modifiable risk factors associated with myocardial infarction in 52 countries (the INTERHEART study): Case-control study. *Lancet*, 364(9438), 937–952.

Zhang, H. A., Gao, M., Chen, B., Shi, L., Wang, Q., Yu, X., Xuan, Z., Gao, L. and Du, G. (2013). Evaluation of hippocampal injury and cognitive function induced by embolization in the rat brain. *Anatomical Record*, 296(8), 1207–1214.

Zhang, S., Weinberg, S., DeBerge, M., Gainullina, A., Schipma, M., Kinchen, J. M., Ben-Sahra, I., Gius, D. R., Yvan-Charvet, L., Chandel, N. S., Schumacker, P. T. and Thorp, E. B. (2019). Efferocytosis Fuels Requirements of Fatty Acid Oxidation and the Electron Transport Chain to Polarize Macrophages for Tissue Repair. *Cell Metabolism*, 29(2), 443–456.

Zhao, N., Liu, C. C., Van Ingelgom, A. J., Martens, Y. A., Linares, C., Knight, J. A., Painter, M. M., Sullivan, P. M. and Bu, G. (2017). Apolipoprotein E4 Impairs Neuronal Insulin Signaling by Trapping Insulin Receptor in the Endosomes. *Neuron*, 96(1), 115–129.

Zhao, X., Gu, C., Yan, C., Zhang, X., Li, Y., Wang, L., Ren, L., Zhang, Y., Peng, J., Zhu, Z. and Han, Y. (2016). NALP3-Inflammasome-Related Gene Polymorphisms in Patients with Prehypertension and Coronary Atherosclerosis. *BioMed Research International*, 2016(7395627), 1–6.

Zhou, Yiting, Zhang, J., Wang, L., Chen, Y., Wan, Y., He, Y., Jiang, L., Ma, J., Liao, R., Zhang, X., Shi, L., Qin, Z., Zhou, Yudong, Chen, Z. and Hu, W. (2017). Interleukin-1β impedes oligodendrocyte progenitor cell recruitment and white matter repair following chronic cerebral hypoperfusion. *Brain, Behavior, and Immunity*, 60(1), 93–105.

Zuloaga, K. L., Zhang, W., Yeiser, L. A., Stewart, B., Kukino, A., Nie, X., Roese, N. E., Grafe, M. R., Pike, M. M., Raber, J. and Alkayed, N. J. (2015). Neurobehavioral and Imaging Correlates of Hippocampal Atrophy in a Mouse Model of Vascular Cognitive Impairment. *Translational Stroke Research*, 6(5), 390–398.

Appendix 1

Extended immunohistochemistry protocol

Extended IHC protocol used in Chapter 2 and Chapter 4. For specific details on antibodies used and concentrations please see respective methods sections.

1. **Dewax and rehydrate:** xylene 1 (5 min); xylene 2 (5 min); 100% EtOH (3 min); 100% EtOH (3 min); 90% EtOH (3 min), dH_2O
2. **Antigen retrieval:** Tris EDTA (pH9) at 95 °C for 30 min
3. Cool for 20 mins
4. Wash with dH_2O and load slides in sequencer cassettes
5. Wash x3 with 0.1 % TWEEN20 in Tris-buffered saline (TBST)
6. Add 1° Ab for 1 hour at RT or, at 4 °C overnight. Ab were diluted in 0.1% BSA TBST.
7. Wash x3 TBST
8. Add 2° biotinylated Ab for 1 hour at RT. Ab were diluted in 0.1% BSA TBST.
9. Wash x3 TBST
10. Prepare ABC-AP kit according to manufacturer's instructions and incubate with slide for 30 min at RT
11. Wash x3 TBST
12. Prepare Vector Red Substrate according to manufacturer's instructions and incubate with slide for 30 min at RT, in the dark
13. Wash x3 TBST
14. **Counterstain:** Running dH_2O (2 min); Heamatoxlyin (45 sec); Running dH_2O (2 min); Scott's water (10 dips); Running dH_2O (2 min); 90% EtOH (2 dips); 100% EtOH (10 dips); 100% EtOH (30 sec); Xylene
15. Apply DPX and secure coverslip. Leave to air dry overnight

Appendix 2

28 point neuroscore protocol

In Chapter 3 deficits in sensorimotor function were assessed using a 28-point neuroscore modified from procedures described previously by Encarnacion *et al.* (2011). See below for full details on 28 point scoring system used.

	0	1	2	3	4
(1) Body symmetry (open bench top)	Normal	Slight asymmetry	Moderate asymmetry	Prominent asymmetry	Extreme asymmetry
(2) Gait (open bench top)	Normal	Stiff, inflexible	Limping	Trembling, drifting, falling	Does not walk
(3) Climbing (gripping surface, 45° angle)	Normal	Climbs with strain, limb weakness present	Holds onto slope, does not slip or climb	Slides down slope, unsuccessful effort to prevent slope	Slides Immediately, no effort to prevent fall
(4) Circling behaviour (open bench top)	Not Present	Predominantly one-sided turns	Circles to one side (not constantly)	Circles constantly to one side	Pivoting, swaying or no movement
(5) Front limb symmetry (mouse suspended by its tail)	Normal	Light asymmetry	Marked asymmetry	Prominent asymmetry	Slight asymmetry, no body/limb movement
(6) Compulsory circling (front limbs on bench, rear suspended by tail)	Not Present	Tendency to turn to one side	Circles to one side	Pivots to one side sluggishly	Does not advance
(7) Whisker response (light touch from behind)	Symmetrical Response	Light asymmetry	Prominent asymmetry	Absent response ipsilaterally, diminished contralaterally	Absent proprioceptive response bilaterally

Appendix 3

Tables of reagents

Table A3.1 - Summary of reagents used for experiments in Chapter 2.

Reagent type	Designation	Catalogue #	Identifiers	Additional
Strain, strain background (Mus musculus)	C57BL/6 (B6) mice		Charles River	
Chemical compound, drug	PFA	#P6148	Sigma Aldrich	
Chemical compound, drug	PBS	#D8537	Sigma Aldrich	
Chemical compound, drug	SDS	#62862	Sigma Aldrich	
Chemical compound, drug	Phenylmethylsulfonyl fluoride	#P7626	Sigma Aldrich	
Chemical compound, drug	Aprotinin	#A6279	Sigma Aldrich	
Antibody	Biotinylated goat anti-rabbit IgG	#BA-1000	Vector Laboratories	IHC: (1/200)
Antibody	Mouse anti-Iba1 (rabbit monoclonal)	#ab178846	Abcam	IHC: (1/1000)
Antibody	Mouse anti-GFAP (rabbit monoclonal)	#ab68428	Abcam	IHC: (1/1000)
Commercial assay or kit	PLP ELISA	#OKEH05831	Aviva Biosystems	
Commercial assay or kit	VEGF ELISA	#DY493-05	R&D systems	
Commercial assay or kit	Fibrinogen ELISA	#SEA193Mu	Cloud Clone	
Commercial assay or kit	PDGFRB ELISA	#OKEH03442	Aviva Biosystems	
Commercial assay or kit	GFAP ELISA	#SEA068Mu	Cloud Clone	
Commercial assay or kit	CD11b ELISA	#MBS934157	My Biosource	
Commercial assay or kit	ABC-Alyakine Phosphatase	#AK-5000	Vector Laboratories	
Commercial assay or kit	Vector Red Substrate Kit	#SK-5100	Vector Laboratories	
Software, algorithm	MoorFLPI software		Moor Instruments Ltd	
Software, algorithm	QuPath		University of Edinburgh	
Software, algorithm	GraphPad Prism		GraphPad Software Inc	v8

Table A3.2 - Summary of reagents used for experiments in Chapter 3.

Reagent type	Designation	Catalogue #	Identifiers	Additional
Strain, strain background (Mus musculus)	C57BL/6 (B6) mice		Envigo	
Animal Diet	60% energy from fat	Cat. #58G9	Test Diets	
Animal Diet	12% energy from fat	Cat. #58G7	Test Diets	
Chemical compound, drug	PFA	Cat. #P6148	Sigma Aldrich	
Chemical compound, drug	Triton X	Cat. #T8787	Sigma Aldrich	
Chemical compound, drug	Protease Inhibitor Cocktail Set I	Cat. #539131	Calbiochem	
Chemical compound, drug	DPX mounting medium	Cat. #6522	Sigma Aldrich	
Chemical compound, drug	PBS	Cat. #D8537	Sigma Aldrich	
Commercial assay or kit	ALT assay	Cat. #700260	Cayman Chemical	
Commercial assay or kit	FFA assay	Cat. #CA-31	Zen-Bio Inc	
Commercial assay or kit	BCA Protein Assay Kit	Cat. #23225	Pierce Biotechnology	
Commercial assay or kit	Resistin ELISA	Cat. #DY1359	R&D Systems	
Commercial assay or kit	Adiponectin ELISA	Cat. #DY1119	R&D Systems	
Commercial assay or kit	Leptin ELISA	Cat. #DY398	R&D Systems	
Software, algorithm	ANY-maze		Stoelting	v4.9
Software, algorithm	Image J			
Software, algorithm	GraphPad Prism		GraphPad Software Inc	v6
Software, algorithm	R		RStudio, Inc	

Table A3.3 - Summary of reagents used for experiments in Chapter 4.

Reagent type	Designation	Catalogue #	Identifiers	Additional
Strain, strain background (Mus musculus)	C57BL/6 (B6) mice		Charles River	
Chemical compound, drug	Low Glucose DMEM	11885084	Thermo Fisher Scientific	5.5 mM
Chemical compound, drug	High Glucose DMEM	D6429	Sigma	
Chemical compound, drug	Fetal Bovine Serum	10500064	Thermo Fisher Scientific	
Chemical compound, drug	PBS	D8537	Sigma Aldrich	
Chemical compound, drug	Penicillin Streptomycin	P0781	Sigma Aldrich	
Chemical compound, drug	Glucose	G8270	Sigma Aldrich	*In vitro*: 25 mM *In vivo*: 2.2 g/kg
Chemical compound, drug	2DG	D8375	Sigma Aldrich	*In vitro:* 1, 2, 4 mM *In vivo:* 2.2 g/kg
Chemical compound, drug	Mannitol	M4125	Sigma Aldrich	25 mM
Chemical compound, drug	DMSO	D2650	Sigma Aldrich	
Chemical compound, drug	Oxamate	O2751	Sigma Aldrich	10, 20, 40 mM
Chemical compound, drug	UK5099	PZ0160	Sigma Aldrich	*In vitro*: Vehicle DMSO; 25, 50, 100 µM *In vivo:* 10 mg/kg
Chemical compound, drug	Sodium L-lactate	L7022	Sigma Aldrich	25 mM
Chemical compound, drug	GSK 2837808A	5189	Tocris	Vehicle DMSO; 0.1, 1, 10, 100 µM
Chemical compound, drug	Etoposide	E1383	Sigma Aldrich	40 µM
Chemical compound, drug	Diethyl succinate	112402	Sigma Aldrich	Vehicle DMSO; 2.5, 5, 10 mM
Chemical compound, drug	Diethyl butylmalonate	112038	Sigma	Vehicle DMSO; 0.25, 0.5, 1 mM
Chemical compound, drug	β-Chloro-L-alanine hydrochloride	C9033	Sigma Aldrich	Vehicle PBS; 5, 25, 50, 250, 500 µM
Chemical compound, drug	Bovine Serum Albumin	A9647	Sigma Aldrich	
Chemical compound, drug	Tween 20	P9416	Sigma Aldrich	
Chemical compound, drug	Protease Inhibitor Cocktail Set I	539131	Calbiochem	

Reagent type	Designation	Catalogue #	Identifiers	Additional
Chemical compound, drug	Lipopolysaccharides from *Escherichia coli* O26:B6	L2654	Sigma Aldrich	50 ng/mL
Chemical compound, drug	TTC	T8877	Sigma Aldrich	2%
Chemical compound, drug	Collagenase	17104-019	Thermo Fisher Scientific	50 U mL^{-1}
Chemical compound, drug	Dispase II	17105-041	Thermo Fisher Scientific	0.5 U mL^{-1}
Chemical compound, drug	DNase I	10104159001	Roche	200 U mL^{-1}
Chemical compound, drug	Percoll	P4937	Sigma	
Chemical compound, drug	BD Pharmlyse	555899	BD Bioscience	
Chemical compound, drug	NP40 Cell Lysis Buffer	FNN0021	Thermo Fisher Scientific	
Peptide, recombinate protein	Recombinant Mouse IFN-γ	575306	Biolegend	100 ng/mL
Antibody	Mouse anti-IL-1β (goat polyclonal)	AF-401	R&D Systems	WB: (1/800) IHC: (1:200)
Antibody	Mouse anti-caspase-3 (rabbit monoclonal)	9662	Cell Signalling Technology	WB: (1/1000)
Antibody	Goat anti-IgG (rabbit polyclonal)	P0160	Agilent	WB: (1/1000)
Antibody	Rabbit anti-IgG (rabbit polyclonal)	P0448	Agilent	WB: (1/1000)
Antibody	HRP Bactin	ab49900	Abcam	WB: (1/50 000)
Antibody	Mouse anti-Iba1 (rabbit polyclonal)	ab178846	Abcam	IHC: (1/500)
Antibody	anti-rabbit AF647 (donkey polyclonal)	A32795	Thermo Fisher Scientific	
Commercial assay or kit	Lactate Kit	ab65331	Abcam	
Commercial assay or kit	ECL Prime Western Blotting Detection Reagent	GERPN2232	GE Healthcare	
Commercial assay or kit	PureLink™ RNA Mini Kit	12183025	Invitrogen	
Commercial assay or kit	PureLink™ DNase Set	10207483	Invitrogen	
Commercial assay or kit	Succinate Kit	ab204718	Abcam	
Commercial assay or kit	CytoTox 96 Non-Radioactive Cytotoxicity Assay Kit	G1780	Promega	
Commercial assay or kit	CellTiter 96 Non-Radioactive Cell Proliferation Assay Kit	G4000	Promega	
Commercial assay or kit	IL-1β ELISA	DY401	R&D Systems	

Reagent type	Designation	Catalogue #	Identifiers	Additional
Commercial assay or kit	IL-6 ELISA	CDY406	R&D Systems	
Commercial assay or kit	TNFα ELISA	DY410	R&D Systems	
Commercial assay or kit	Tyramide 555 SuperBoostTM	B40936	Thermo Fisher Scientific	
Commercial assay or kit	ProLong Diamond anti-fade Mountant	P36970	Thermo Fisher Scientific	
Software, algorithm	Image J			
Software, algorithm	R		RStudio, Inc	
Software, algorithm	GraphPad Prism		GraphPad Software Inc	v8